Enhanced Limbic Network Excitation in the Pilocarpine Animal Model of Temporal Lobe Epilepsy

Philip Henry de Guzman

Degree of Doctor of Philosophy

Department of Neurology & Neurosurgery
McGill University
Montreal, Quebec, Canada
June, 2007

A thesis submitted to the faculty of Graduate Studies and Research in partial fulfillment of the requirements of the degree of Doctor of Philosophy.

Your file Votre référence
ISBN: 978-0-494-38578-4
Our file Notre référence
ISBN: 978-0-494-38578-4

DEDICATION

This thesis is dedicated to my nephew, Edward William Oliynyk, who was born two hours ago on the day this text was written.

ACKNOWLEDGEMENTS

I would like to thank my Ph.D. supervisor, Dr. Massimo Avoli, who provided me with encouragement and a creative working environment during my PhD studies. His scientific insight and approach nurtured my ability to effectively frame scientific problems and design experiments. These educational experiences help me realize which questions to ask and determine, not only, the solution but also the subsequent questions spawned from these answers.

I would definitely like to thank my friends and colleagues Dr. Yuji Inaba, Dr. Ruba Benini and Dr. Pieroangelo Ciefeli (the original pilocarpine team). This group dynamic provided an enjoyable and stimulating environment to work in.

I thank the newest recruits and alumni of the lab, Ms. Jessica Sudbury, Dr. Giulia Curia and Dr. Garbiella Panuccio. In addition, I express thanks to Mrs. Toula Popadopoulos for her secretarial assistance and for her patience in dealing with all of my incessant last minute requests.

I would like to give my appreciation to my Ph.D. advisory committee, Dr. David Ragsdale and Dr. Kresimir Krnjevic, who provided advice and assistance during the course of my graduate work.

Lastly, I would like to thank my parents and my sister and my closest of friends for their support and encouragement throughout the Ph.D. studies.

TABLE OF CONTENTS

DEDICATION ii
ACKNOWLEDGEMENTS iii
TABLE OF CONTENTS iv
LIST OF TABLES vii
LIST OF FIGURES viii
ABSTRACT ix
ABRÉGÉ x
CONTRIBUTION OF AUTHORS xii
Preface 1
0.1 Introduction 1
0.2 Research Rationale of Thesis 2
0.3 Human Temporal Lobe Epilepsy 4
0.3.1 Clinical definition of TLE 4
0.3.2 Histopathological features of TLE 5
0.4 GABA and Glutamate in TLE 6
0.4.1 Glutamatergic neurotransmission in TLE 6
0.4.2 NMDA receptor function in TLE 7
0.4.3 GABAergic neurotransmission in TLE 9
0.4.4 $GABA_A$ receptor mediated depolarization and the KCC2 11
0.5 Synchronous Network Epileptiform Discharges in TLE 12
0.5.1 Limbic seizure activity in human TLE 12
0.5.2 Synchronous network activity in acute *in vitro* seizure models 14
0.6 The Pilocarpine-Treated Animal Model of TLE 16
0.6.1 Pilocarpine induced limbic seizures 16
0.6.2 Network structural alterations and network hyperexcitability 17
0.7 The Role of the Subiculum in TLE 20
0.7.1 Anatomy 20
0.7.2 The epileptic subiculum 21
0.8 The Role of the Entorhinal Cortex in TLE 23
0.8.1 Anatomy 23
0.8.2 The epileptic entorhinal cortex 23
0.9 The Role of the Insular Cortex in TLE 26
0.9.1 Anatomy 26
0.9.2 The epileptic insular cortex 26
0.10.0 References: 29
Chapter 1: Subiculum Network Excitability is Increased in a Rodent Model of Temporal Lobe Epilepsy 46
1.0 Linking Text & Information About Publication 46
1.1 Abstract 46
1.2 Introduction 47
1.3 Methods 48
1.3.1 Preparation of pilocarpine treated rats 48
1.3.2 Electrophysiology procedures 49
1.3.3 Real-Time PCR 51
1.3.3 Histopathology procedures 52
1.3.4 Statistical method 54
1.4 Results 54
1.4.1 Unaltered intrinsic cellular properties in NEC and pilocarpine-treated subiculum 54
1.4.2 Activation of CA1 inputs demonstrates hyperexcitability within the epileptic subiculum 55
1.4.3 Subicular cells in pilocarpine-treated slices have a lower threshold to synaptic stimuli than in NEC tissue 56

1.4.4 Activation of EC layer III produces multiphasic activity in the pilocarpine-treated subiculum 57
1.4.5 Spontaneous synaptic activity in NEC and pilocarpine-treated subiculum 58
1.4.6 Reversal potential of 'monosynaptic' IPSPs in NEC and pilocarpine-treated subicular neurons 59
1.4.7 Reversal potential of 'monosynaptic' IPSPs generated by EC layer V neurons from NEC and pilocarpine-treated rats 60
1.4.8 Reduced KCC2 expression in the pilocarpine treated subiculum 60
1.4.9 Histopathological evaluation of neuronal damage 61
1.5 Discussion 63
1.5.1 Network hyperexcitability in the epileptic subiculum 63
1.5.2 Reduced GABAergic inhibition within the pilocarpine-treated subiculum 65
1.5.3 Structural changes in subicular and EC networks 66
1.6 Acknowledgements 68
1.7 References 70
1.8 Figures 75
Chapter 2: Network Hyperexcitability in the Deep Layers of the Pilocarpine-Treated Entorhinal Cortex 87
2.0 Linking Text & Information About Publication 87
2.1 Abstract 87
2.2 Introduction 88
2.3 Methods 89
2.3.1 Preparation of pilocarpine-treated rats 89
2.3.2 Electrophysiology procedures 90
2.3.3 Statistical methods 92
2.4 Results 92
2.4.1 Epileptiform activity is a hallmark of the pilocarpine-treated EC 92
2.4.2 Network interactions within the pilocarpine-treated EC 93
2.4.3 Firing properties of layer V lateral EC neurons in both NEC and pilocarpine-treated tissue 94
2.4.4 Intracellular characteristics of spontaneous and stimulus-induced events in NEC and pilocarpine-treated lateral EC neurons 94
2.4.5 Epileptiform activity in pilocarpine-treated EC persists during NMDA receptor antagonism but is abolished by a non-NMDA glutamatergic antagonist 96
2.4.6 Reduced GABAergic inhibition in the pilocarpine-treated EC 97
2.5 Discussion 97
2.5.1 Network hyperexcitability within the pilocarpine-treated EC 98
2.5.2 Reduced network inhibition in the pilocarpine-treated EC 100
2.5.3 Glutamatergic mechanisms in the pilocarpine-treated EC 101
2.6 Conclusions 102
2.7 Acknowledgements 103
2.8 References 104
2.9 Figures 109
Chapter 3: NMDA Receptor-Mediated Transmission Contributes to Network 'Hyperexcitability' in the Rat Insular Cortex 118
3.0 Linking Text & Information About Publication 118
3.1 Abstract 118
3.2 Introduction 119
3.3 Methods 120
3.4 Results 122
3.5 Discussion 124
3.6 Acknowledgements 126
3.7 References 127
Conclusion 132
0.1 Summary of Research Findings 132

0.2 Can the epileptic subiculum contribute to the amplification of limbic seizures?... 133
0.3 What are the additional factors that contribute to network hyperexcitability within the epileptic entorhinal cortex? ... 134
0.4 How can the insular cortex contribute to the generation of seizure activity? ... 135
0.5 Concluding remarks ... 136
0.6 References ... 138
APPENDIX A: Reprint of Chapter 1 and Waiver from Hippocampus ... 141
APPENDIX B: Reprint of Chapter 3 and Waiver from the European Journal of Neuroscience ... 142
APPENDIX C: Animal Subject Use Approval ... 143

LIST OF TABLES

Table 1-1: 86
Table 2-1: 117

LIST OF FIGURES

Figure 1-1:.....75
Figure 1-2:.....76
Figure 1-3:.....77
Figure 1-4:.....78
Figure 1-5:.....79
Figure 1-6:.....80
Figure 1-7:.....81
Figure 1-8:.....82
Figure 1-9:.....83
Figure 1-10:.....84
Figure 1-11:.....85

Figure 2-1:.....109
Figure 2-2:.....110
Figure 2-3:.....111
Figure 2-4:.....112
Figure 2-5:.....113
Figure 2-6:.....114
Figure 2-7:.....115
Figure 2-8:.....116

Figure 3-1:.....129
Figure 3-2:.....130
Figure 3-3:.....131

ABSTRACT

Through the use of chronic experimental animal models, the majority of *in vitro* investigations of temporal lobe epilepsy have demonstrated enhanced network activity within the subdivisions of the hippocampal formation. However, clinical evidence in combination with *in vivo* and *in vitro* studies indicates that structures external to the hippocampus contribute to the genesis of seizure activity. To address the effects of limbic network excitation, I have utilized combined hippocampal–entorhinal cortex brain slices from pilocarpine-treated rats that display chronic seizures.

My investigations have focused upon three structures, the subiculum, entorhinal cortex and the insular cortex. The experiments in the pilocarpine-treated subiculum demonstrated increased network excitability that was attributed to a more positive $GABA_A$ receptor mediated inhibitory post-synaptic potential (IPSP) reversal point coupled with a reduced IPSP peak conductance. Utilizing RT-PCR analysis and immunohistochemical staining we observed a decline in K^+-Cl^- cotransporter mRNA expression and a reduced number of parvalbumin-positive, presumptive inhibitory interneurons. My second project assessed the network hyperexcitability in layer V of the lateral entorhinal cortex. This is the first study to report spontaneous bursting, in the absence of epileptogenic agents, in the epileptic entorhinal cortex. We attributed this level of network excitation to reduced $GABA_A$ receptor mediated inhibition and increased synaptic sprouting. In the final project, we extended our slice preparation to include the insular cortex, a structure external to the temporal lobe. Our investigations identified a mechanism of NMDA receptor dependent synaptic bursting that masked $GABA_A$ receptor mediated conductances.

ABRÉGÉ

La majorité des études *in vitro* sur l'épilepsie du lobe temporal a démontré par l'utilisation de modèles animaux chroniques, une augmentation de l'activité de circuits dans les subdivisions de la formation de l'hippocampe. Pourtant, des observations cliniques et des études *in vivo* et *in vitro* indiquent que des structures à l'extérieur de l'hippocampe contribuent aussi à la genèse d'activité épileptique. Afin d'évaluer l'effet de l'excitation du système limbique sur l'épilepsie induite par la pilocarpine chez le rat, nous avons utilisé des coupes de cerveaux incluant à la fois l'hippocampe et le cortex entorhinal.

Á l'aide d 'expériences d'électrophysiologie, nous avons étudié 3 régions en particulier : le subiculum, le cortex entorhinal et le cortex insulaire. Dans les subiculi traités à la pilocarpine, nous avons pu observer une excitabilité accrue des circuits. Cette augmentation est due à une valeur plus positive d'inversion du potentiel post-synaptique inhibiteur (PPSI) des récepteurs $GABA_A$, ainsi qu'à une diminution de la conductance maximale des PPSI. Des études d'amplification par RT-PCR ont d'autre part révélé une diminution des niveaux d'ARN messagers encodant le co-transporteur à K+ et Cl-. De plus, nous avons observé une diminution du nombre de neurones inhibiteurs positifs pour la parvalbumine par analyses immunohistochimiques. Dans le second projet, nous avons étudié l'hyperexcitabilité des circuits de la couche V du cortex entorhinal latéral. Cette étude est la première à rapporter la présence de rafales d'activité spontanée en absence d'agents épileptogènes dans le cortex entorhinal épileptique. Nous avons attribué ce niveau d'excitation des circuits à une diminution de l'inhibition par les récepteurs $GABA_A$, de même qu'à une augmentation de l'arborisation synaptique. Pour le projet final, nous avons inclus le cortex insulaire, une structure externe au lobe temporal, dans nos

coupes. Nous avons identifié un mécanisme par lequel des rafales d'activité synaptique dépendantes des récepteurs NMDA masquent les conductances des récepteurs $GABA_A$

CONTRIBUTION OF AUTHORS

The research presented in this thesis is arranged into 3 main chapters, each of which represents original work that was published or is submitted for publication. The manuscripts for chapters 1, 2 and 3 were written collaboratively by Dr. Massimo Avoli and I.

Chapter 1:

de Guzman P, Inaba Y, Biagini G, Baldelli E, Mollinari C, Merlo D, and Avoli M (2006) Subiculum network excitability is increased in a rodent model of temporal lobe epilepsy. Hippocampus 16:843-60

Preparation of the pilocarpine-treated animals was performed through the efforts of Dr. Ruba Benini, Dr. Yuji Inaba and I. The electrophysiological experiments and analysis were executed by Dr. Yuji Inaba and I. Immunohistochemical data regarding staining of the K^+-Cl^- cotransporter (KCC2) and presynaptic synaptophysin, as well as, RT PCR experiments of the KCC2 were produced due to the efforts of our Italian collaborators at the Universita di Modena (Dr. Guiseppe Biagini and Enrica Baldelli) and at the Istituto Superiore di Sanita` (Dr. Cristiana Mollinari and Dr. Daniela Merlo).

In this manuscript we reported reduced network inhibition in the pilocarpine treated subiculum combined with an enhanced response to CA1 and lateral entorhinal cortex layer III inputs. We attribute this level of hyperexcitability to a more positive γ-aminobutyric acid $(GABA)_A$ receptor mediated reversal point due to a decreased expression of the KCC2. Additional alterations in the pilocaprine-treated subiculum consisted of increased synaptic sprouting combined with a reduction of subicular inhibitory interneurons.

Chapter 2:

Philip de Guzman, Yuji Inaba, Marco de Curtis and Massimo Avoli (2007) Network hyperexcitability within the deep layers of the pilocarpine treated entorhinal cortex. Journal of Neurophysiology (*submitted*)

Dr. Yuji Inaba assisted me in acquiring the electrophysiological data in epileptic and control tissue. To produce this paper, I generated the underlying concept of this project; I performed the data analysis, and the creation of the figures. Dr. Marco de Curtis provided additional insight in the creation of the manuscript.

In this project, we identified for the first time the presence of robust spontaneous network bursting within layer V of the pilocarpine treated lateral entorhinal cortex; these event demonstrated resistance to NMDA receptor blockade. This increased level of network excitation was accompanied by a reduced frequency and amplitude of spontaneous $GABA_A$ receptor mediated inhibitory post-synaptic potentials.

Chapter 3:

Inaba Y, de Guzman P and Avoli M (2006) NMDA receptor-mediated transmission contributes to network 'hyperexcitability' in the rat insular cortex. European Journal of Neuroscience 23:1071-1076

This manuscript is a co-first authorship as Dr. Yuji Inaba and I contributed equally to acquisition of electrophysiological data and experimental analysis. Utilizing a modified brain slice preparation that included the insular cortex we demonstrated spontaneous network bursting that was NMDA receptor

sensitive. Blockade of glutamatergic activity unmasked a $GABA_A$ receptor mediated response.

Preface

0.1 Introduction

Neuronal networks in structures of the limbic system such as the hippocampus, the amygdala as well as the entorhinal and perirhinal cortices are involved in the generation of seizure activity in patients presenting temporal lobe epilepsy (TLE). Associated with this disorder is a pattern of neuronal damage termed Ammon's horn sclerosis (Gloor 1991; Gloor 1997). Unfortunately, 30 to 40% of TLE patients ineffectively respond to antiepileptic medication, thereby affecting their quality of life (Kwan and Brodie 2000; Regesta and Tanganelli 1999). Consequently, it is necessary to further understand the pathophysiology of this disorder to assist in the development of more effective treatments.

Cellular, pharmacological and molecular investigations over the past few decades have contributed to identifying the mechanisms underlying epileptic syndromes (Delgado-Escueta et al. 1999). While these studies have led to an increased understanding of TLE, they have the limitation of being performed in *in vitro* isolated hippocampal slices. To minimize these limitations, researchers have adopted brain slice preparations that include more than one interconnected limbic structure (Jones and Lambert 1990a; b; Walther et al. 1986; Wilson et al. 1988). These studies have demonstrated that neuronal networks in extended slices of the limbic system produce electrographic waveforms that resemble limbic seizure activity in patients presenting TLE. Most of these investigations, however, occur in the presence of convulsive agents in control tissue.

Alternatively, researchers have adopted chronic experimental animal models such as pilocarpine injection to assess *in vitro* network excitability. To date, many

studies have centered upon the role of the dentate gyrus (DG), Cornu Ammonis 3(CA3) and CA1 within the epileptic hippocampus while few studies have addressed additional structures beyond Ammon's horn and the fascia dentata.

0.2 Research Rationale of Thesis

The aim of my Ph.D. investigations was to assess the network interactions and excitability beyond the hippocampal formation in pilocarpine-treated tissue. As such, I addressed the network hyperexcitability in the subiculum and entorhinal cortex (EC) in pilocarpine-treated animals. Further investigations extended to the insular cortex (IC), a structure that is neuroanatomically connected to the limbic system.

In chapter 1, my studies focused upon the role of the epileptic subiculum. Interestingly, despite its function as the primary hippocampal output it has received minimal attention. In the human epileptic subiculum, spontaneous network bursting was attributed to a more positive γ-aminobutyric acid $(GABA)_A$ receptor mediated reversal point (Cohen et al. 2002). Attempts to replicate these results in human epileptic tissue and chronic seizure models have failed (Wozny et al. 2003). Indeed, the hyperexcitability of the epileptic subiculum is contentious as additional studies report an increase or reduced number of intrinsically bursting neurons (Knopp et al. 2005; Wellmer et al. 2002). In my investigations, I assessed whether the pilocarpine-treated subicular network is altered through intrinsic or synaptically mediated mechanisms. In addition, I address subicular network interactions within limbic regions CA1 and lateral EC layer III.

My studies of the pilocarpine-treated EC are detailed in Chapter 2. The majority of investigations of the *in vitro* epileptic EC have often focused upon the utilization of convulsive agents or the superficial layers of the medial region. While

neuronal death is reported to occur in medial EC layers II/III (Du et al. 1995; Du et al. 1993), *in vitro* studies demonstrate that ictal discharges originate from the deep layers of the EC (Dickson and Alonso 1997; Lopantsev and Avoli 1998a; b). In over a decade, three studies have addressed the *in vitro* hyperexcitability of medial EC layer V in chronic seizure models (Fountain et al. 1998; Thompson et al. 2007; Yang et al. 2006). However, the lateral region of the EC has been overlooked. Studies in pilocarpine treated tissue indicate high levels of FOS immunoreactivity – indicative of network activation – during the chronic phase (Biagini et al. 2005). Moreover, an additional report indicates that ablation of the lateral EC controls seizure activity (Kopniczky et al. 2005). My investigations of epileptic lateral EC layer V addresses whether there are perturbations in network inhibition and excitation.

The final investigation of this Ph.D. thesis involves the IC. At present, the understanding of the IC has been limited to clinical reports in TLE and research in nociception. The clinical studies of Isnard et al., (2000), indicate that ictal events can originate from the IC or invade the IC from limbic regions. In line with this viewpoint, studies in coronal slices, following $GABA_A$ receptor blockade, suggest the insular and perirhinal cortices exhibit low seizure thresholds (Demir et al. 1998). In these particular studies, however, the lack of intracellular recordings makes it difficult to discern the synaptic mechanisms involved in the IC that could contribute to this result. To this end, I report the first intracellular and network electrophysiological characterization of the IC in control tissue, and its interaction with the perirhinal cortex.

0.3 Human Temporal Lobe Epilepsy

0.3.1 Clinical definition of TLE

Epilepsy affects 0.5 to 1% of the North American population (Theodore et al. 2006) and is ranked as the second most common neurological disorder. One of the more notorious epileptic subtypes is TLE. The initial insult, and development of TLE, has often been linked to brain injuries during early childhood; the events can range from birth traumas, hypoxia and toxin exposure (French et al. 1993; Mathern et al. 1995). Febrile seizures, another precipitating injury, have been linked with 2/3 of patients with TLE (Falconer 1971; French et al. 1993; VanLandingham et al. 1998). Subsequent to this neuronal insult, the patient enters a seizure free latent period. Unfortunately, during adolescence a subset of these individuals will experience recurrent non-provoked seizures.

Patients with epilepsy often experience auras prior to the onset of seizures (French et al. 1993). The aura is a simple partial seizure during which consciousness is maintained, and can serve as a warning for the individual. While no discernable outward behavioural response is observed during the aura, patients have described feelings of nausea, epigastric rising, fear, déjà vu or altered senses of olfaction (French et al. 1993; Mathern et al. 1995). Following this, patients with TLE often undergo complex partial seizures. This particular seizure results in impaired consciousness combined with repetitive motor movements (automatisms) such as lip smacking or swallowing; the duration can last from 30 seconds to 2 minutes.

The treatment of TLE can be achieved through antiepileptic medication or removal of epileptic tissue. Antiepileptic medication can stop or reduce seizure frequency; however, 30% of epileptic patients exhibit drug resistance (Kwan and Brodie 2000; Regesta and Tanganelli 1999). Alternatively, surgical resection of the

epileptic focus provides complete seizure relief in 80 to 90% of drug resistant TLE patients (Engel et al. 1997) and is demonstrated to be a more effective than longterm medication (Wiebe et al. 2001). Despite this outcome, clinicians still consider surgical intervention as the final option for intractable epilepsy (Engel 2001).

The development of drug resistant seizures is not well known. Pharmacoresistance is speculated to be a consequence of multifactorial events, involving a molecular alteration to drug targets or an upregulation of protein pumps in the blood brain barrier (Jandova et al. 2006; Remy and Beck 2006). What is intriguing, however, is the high correlation of drug resistant seizure patients and neuronal death within the hippocampal formation.

0.3.2 Histopathological features of TLE

Numerous studies have focused on the histochemical and structural alterations that occur in patients with TLE and in animal models simulating this disorder. In both instances, the brain often exhibits Ammon's horn sclerosis, which is believed to result from status epilepticus or prolonged febrile seizures in early childhood (Gloor 1997; Harvey 1999; Jackson et al. 1998; Lewis 1999; Wiebe et al. 2001). The histopathological hallmark of Ammon's horn sclerosis consists of a selective loss of neurons in the dentate hilus, hippocampal Cornu Ammonis 3 and 1 (CA3 and CA1, respectively) (Gloor 1997). In contrast, the dentate granule cells and area CA2 of the hippocampus as well as the subiculum remain unscathed (Gloor 1997). Additional limbic structures that are reported to exhibit neuronal death include layer III of the EC (Du et al. 1993) and the amygdala (Gloor 1997). In line with these observations, MRI analyses of patients with TLE have demonstrated volumetric reductions in the

aforementioned limbic structures (Bernasconi et al. 1999; Goncalves Pereira et al. 2005; Jutila et al. 2001; Salmenpera et al. 2000).

0.4 GABA and Glutamate in TLE

0.4.1 Glutamatergic neurotransmission in TLE

One of the factors associated with seizure events is the loss of network inhibition and enhanced network excitation. The two primary neurotransmitters involved in generating this synchronous network activity are the excitatory and inhibitory neurotransmitters glutamate and γ-aminobutyric acid (GABA), respectively. Glutamate specifically binds and activates the metabotropic and ionotropic glutamate receptors. The metabotropic glutamate receptor family consists of 8 receptor subtypes (mGlu1 to mGlu 8) that are divided into three groups. Group I (mGlu1 and mGlu5) is coupled to the intracellular phosphoinositide cascade whereas Groups II (mGlu2 and mGlu3) and III (MGlu4, mGlu6, mGlu7 and mGlu8) inhibit adenylate cyclase activity. These g-protein coupled receptors modulate slow synaptic transmission via intracellular signaling and secondary messengers. In contrast, rapid excitatory glutamatergic neurotransmission is mediated via three ionotropic excitatory amino acid receptor subtypes: N-methyl-D-aspartate (NMDA), α-amino-3-hydroxy-5-methyl-4-isoxazole propionate (AMPA) and kainate. The activation of the AMPA and kainate receptors produces a post-synaptic depolarization; subsequent binding of glycine or D-serine (Mothet et al., 2000) and glutamate relieves the voltage-gated Mg^{2+} blockade (Nowak et al., 1984) within the ionophore of the NMDA receptor followed by the influx of sodium and calcium. Persistent activation of the glutamate receptor subtypes, primarily the NMDA receptor, is one of the factors implicated in epileptogenesis and neuronal death.

The termination and prevention of increased extracellular glutamate is mediated through the excitatory amino acid transporter (EAAT) localized on neurons and glial cells; presently 5 mammalian isoforms (EAAT1- EAAT5) have been identified (Arriza et al. 1997; Arriza et al. 1994; Fairman et al. 1995; Shashidharan et al. 1994). EAAT function relies upon the extracellular ionic concentration gradient to promote glutamate uptake. In pathophysiological conditions such as stroke and TLE, alterations in membrane voltage and calcium concentration promote glumatergic efflux and the subsequent increase of extracellular glutamate (Rossi et al. 2000). These results are further supported with clinical evidence from epileptic patients, as increased extracellular glutamate is reported to occur prior and during seizures (During and Spencer 1993). This accumulation of extracellular glutamate would be consistent with the decreased transcription and expression of EAAT1 and EAAT2 in human sclerotic epileptic tissue (Proper et al. 2002); however, other studies have reported no differences in EAAT expression (Mathern et al. 1999; Tessler et al. 1999). Nevertheless, these data are contentious and they suggest that EAAT downregulation is a predisposition of brain structure (Tessler et al. 1999) or require extensive tissue damage (Proper et al. 2002). In either case, the accumulation of extracellular glutamate enhances limbic network excitation combined with the adverse effects of persistent NMDA receptor activation.

0.4.2 NMDA receptor function in TLE

Pharmacological antagonism of the NMDA receptor has been demonstrated to halt *in vivo* and *in vitro* seizure discharges (Dreier and Heinemann 1991; Holmes et al. 1992; Lopantsev and Avoli 1998a; Tortorella et al. 1997; Meldrum 1993). The importance of the NMDA receptor in epileptogenesis is further supported from the robust *in vitro*

discharges in hippocampal-parahippocampal slices under low Mg^{2+} conditions (Dreier and Heinemann 1991; Jones and Lambert 1990b; Walther et al. 1986; Wilson et al. 1988). This network synchronization promotes the propagation of *in vitro* epileptiform events across limbic structures (de Guzman et al. 2004) coupled with energy run down (Schuchmann et al. 1999) and altered GABAergic function (Rivera et al. 2004). These temporal changes within the hyperexcitable slice preparation are intriguing as recent investigations also indicate the susceptibility of the NMDA receptor.

The physiological impact of altered NMDA receptor subunits and its role in epilepsy has only recently been addressed. Tissue acquired from patients with cortical dysplasia (Andre et al. 2004) and epilepsy animal models (Bandyopadhyay and Hablitz 2006; Yang et al. 2006) indicate the increased functional expression of the NR2B subunit of the NMDA receptor. Interestingly, the NR2B subunit is predominant during early mammalian development but is reduced in expression and superseded by the NR2A subunit in adulthood (Monyer et al. 1994; Sheng et al. 1994). This suggests a possible developmental regression of the NMDA receptor in epileptic tissue or the consequence of chronic seizures. In epileptic neocortical tissue, application of specific NR2B receptor antagonists prevent the spread of epileptiform discharges (Bandyopadhyay and Hablitz 2006). These results contrast with investigations in the epileptic DG where NR2B antagonism did not prevent status epilepticus or mossy fibre sprouting (Chen et al. 2007). This conflict may be a result of the developmental time frame of the epileptic animals used, structural dependence or even, perhaps, the requirement of more extensive damage. The latter prospect may not necessarily be true as the epileptic EC undergoes minimal structural damage, yet it has been demonstrated to exhibit altered NR2B presynaptic function and increased glutamate release in layer V (Yang et al. 2006). Taken together, these

reports demonstrate the dynamics of the NMDA receptor and its crucial role in mediating seizure activity through glutamate interactions. The final contribution of the NMDA receptor, in stroke and epilepsy, is the calcium mediated downstream signalling pathways that initiate the parallel pathways of apoptosis (programmed cell death) and necrosis.

The excitotoxic glutamate cascade is a consequence of unregulated extracellular glutamate. Intracellular accumulation of calcium, via the NMDA receptor, activates pro-apoptotic factors and proteolytic enzymes which lead to cellular degradation and sequential caspase activation culminating in cell death (Charriaut-Marlangue et al. 1996; Liou et al. 2003). As such, apoptosis is an orchestrated sequence of intracellular and morphological events. The dying cell experiences nuclear and cytoplasmic condensation of the plasma membrane, and subsequently separates into membrane-enclosed structures termed apoptotic bodies. If apoptotic mechanisms cannot be completed as a result of energy depletion, necrosis occurs (Cereghetti and Scorrano 2006). This alternative mode of unorganized cellular death concludes with cellular swelling and inflammation. To this end, glutamate drives seizure activity and indirectly contributes to cellular death and the eventual structural reorganization of epileptic structures; however, the maintenance of these seizures still requires the necessary interplay with GABAergic networks.

0.4.3 GABAergic neurotransmission in TLE

The inhibitory actions of GABA operate through the binding of either ionotropic or metabotropic $GABA_A$ and $GABA_B$ receptors, respectively. The increased conductance and subsequent shunting effects are mediated through Cl^- influx of the $GABA_A$ receptor ionophore, while $GABA_B$ receptor intracellular signaling cascades promote

K^+ efflux. In contrast to $GABA_B$ receptor function, $GABA_A$ receptor activation generates two forms of network inhibition: phasic and tonic activity. The phasic activity of the pentameric $GABA_A$ receptor relies upon the properties of alpha, beta and gamma $GABA_A$ subunits; however, the presence of alpha 5 and delta subunits mediates tonic inhibition (Caraiscos et al. 2004; Nusser and Mody 2002).

In clinical and experimental conditions of TLE, alterations in $GABA_A$ receptor subunits reduce tonic inhibition (Glykys and Mody 2006; Houser and Esclapez 2003; Peng et al. 2004) and attenuate $GABA_A$ receptor affinity (Ragozzino et al. 2005); thereby, increasing excitatory neurotransmission (Olsen and Avoli, 1997; Avoli et al., 2000). The importance of the $GABA_A$ receptor in epilepsy is further illustrated from *in vivo* and *in vitro* experiments where application of $GABA_A$ receptor antagonists generate behavioural and electrographic seizures (Acharya and Katyare 2005; Jones and Lambert 1990a; b; Sierra-Paredes et al. 1998). Moreover, in the *in vitro* brain slice and whole brain preparations, $GABA_A$ receptor blockade facilitates the propagation of epileptiform discharges throughout the hippocampal and parahippocampal networks (D'Antuono et al. 2002; Federico and MacVicar 1996; Uva et al. 2005).

Increased significance of GABAergic signaling can be extrapolated from the 4-aminopyridine (4-AP) model of epilepsy, where $GABA_A$ receptor mediated potentials persist following glutamate receptor antagonism (Avoli et al. 1996; Perreault and Avoli 1992). These results indicate that synchronous network discharges require the conflicting interaction of GABA and glutamate; this is further illustrated with the simultaneous, yet interchangeable intracellular firing patterns of interneurons and pyramidal cells during epileptiform events (Ziburkus et al. 2006). Moreover, the

hyperpolarizing effects of GABA in physiological or pathophysiological conditions are not restricted to neuronal inhibition.

0.4.4 $GABA_A$ receptor mediated depolarization and the KCC2

Early in life, $GABA_A$ receptor activation produces excitation, an electrographic phenomenon referred to as giant depolarizing potentials (Ben-Ari et al. 1989; Khazipov et al. 2001). GABAergic depolarization is a consequence of increased intracellular Cl^- and subsequent $HCO3^-/Cl^-$ efflux (Dzhala et al. 2005). These depolarizing potentials become inhibitory during maturation and are indicated to be a result of Na^+-K^+-$2Cl^-$ (NCC1) downregulation and increased KCC2 expression (Rivera et al. 1999). Both proteins function as cotransporters, where KCC2 and NCC1 mediate the efflux and influx of Cl^-, respectively. Alternatively, the trophic effects of GABA and oxytocin may trigger the mammalian development of GABAergic inhibition (Represa and Ben-Ari 2005; Tyzio et al. 2006).

In adult mammalian tissue, the hyperpolarizing effects of $GABA_A$ are mediated in the neuronal cell body, but $GABA_A$ receptor activation at the apical dendrites results in neuronal depolarization (Gulledge and Stuart 2003). This paradoxical depolarizing event is thought to be a result of increased intracellular Cl^- and a more positive Cl^- reversal point. These results are however conflicting as KCC2 is reported to be dendritically localized (Gulyas et al. 2001) and would prevent intracellular Cl^- accumulation. Investigations of spike timing dependent plasticity in mature brain tissue also demonstrate KCC2 alterations and the subsequent effects of GABAergic depolarization (Woodin et al. 2003). While $GABA_A$ receptor mediated depolarization can occur within control, adult mammalian tissue, the excitatory effects of GABA have been identified in epileptic conditions (Benini and Avoli 2006; Cohen et al. 2002).

This observation of GABAergic plasticity within control tissue suggests the possibility that enhanced network excitation could promote similar results.

Investigations in epileptic tissue acquired from TLE patients (Cohen et al. 2002) and chronic seizure paradigms (Benini and Avoli 2006), report spontaneous network bursting and GABAergic depolarization. Utilizing *in vivo* and *in vitro* seizure models, KCC2 downregulation and the more positive $GABA_A$ receptor mediated reversal potential was attributed to brain-derived neurotrophic factor (BNDF) and TrkB receptor interactions (Rivera et al. 2002; Rivera et al. 2004). In contrast, *in vitro* studies in the pilocarpine-treated subiculum have demonstrated an unaltered $GABA_A$ receptor mediated reversal point (Wozny et al. 2003). Regardless, the flexibility of KCC2 expression appears to correlate with persistent epileptiform discharges. It is important to note, however, that the hyperpolarizing and depolarizing effects of GABA provide a shunting effect. Alterations in synaptic conductance will determine the impact of network inhibition. As such, GABAergic depolarization can provide the duplicitous action of shunting excitatory inputs, while facilitating distal excitatory inputs that coincide with the decaying inhibitory post-synaptic potential (Chen et al. 1996). Indeed, GABA and glutamate are two of the key neurotransmitters involved in TLE, both of which have been investigated through *in vitro* electrophysiological recordings in human epileptic tissue and animal seizure models.

0.5 Synchronous Network Epileptiform Discharges in TLE

0.5.1 Limbic seizure activity in human TLE

In vivo and in vitro electrophysiological studies in human epileptic limbic structures have demonstrated evidence of network reorganization and increased excitation. Most of these investigations have focused upon the epileptic hippocampal formation –

specifically the DG. However, more recent reports have addressed the epileptogenicity of CA1, the subiculum, and the EC.

The intrinsic firing properties and electrophysiological characteristics of neurons within the epileptic tissue are suggested to undergo alterations following epileptic events (Sanabria et al. 2001; Wellmer et al. 2002). However, the fundamental intrinsic electrophysiological properties (input resistance, action potential amplitude, resting membrane potential) and firing characteristics in human epileptic neurons do not substantially differ from animal brain tissue (Avoli and Olivier 1989; Isokawa et al. 1991; Schwartzkroin and Knowles 1984; Strowbridge et al. 1992); these similarities extend to the voltage-gated K^+ and Ca^{2+} currents in human epileptic granule cells (Beck et al. 1996; Beck et al. 1997; Schumacher et al. 1998). At present, the only intrinsic modification that has been electrophysiologically identified is an enhanced Na^+ current density (Reckziegel et al. 1998) and a lower Na^+ activation threshold (Vreugdenhil et al. 2004) in epileptic subicular neurons.

Compared to intrinsic properties, the alterations in human epileptic tissue are more evident at the synaptic level. The human epileptic DG exhibits enhanced NMDA receptor conductances (Masukawa et al. 1991; Urban et al. 1990), reduced $GABA_A$ receptor mediated inhibition (Masukawa et al. 1989) combined with an attenuated pathway specific inhibitory input (Uruno et al. 1994). Additional modifications of the dentate granule network include a sensitivity to extracellular potassium ($[K^+]_o$), particularly in sclerotic tissue (Gabriel et al. 2004). Interestingly, electrographic waveforms comprising transient tonic-clonic discharges required 10 mM $[K^+]_o$ in sclerotic tissue, whereas 12 mM $[K^+]_o$ produced similar waveforms in non sclerotic samples (Gabriel et al. 2004). In line with this viewpoint, studies report reduced $[K^+]_o$ buffering in the epileptic DG (Bordey and Spencer 2004), which was

also reported in epileptic CA1 (Kivi et al. 2000). Consequently, the increased $[K^+]_o$ coupled with reduced network inhibition, can lead to the generation of network synchronization and the recruitment of surrounding neuronal structures.

To date, most of the investigations in human epileptic tissue have often addressed one structure but not the interactions between structures. *In vivo* electrophysiological studies in the epileptic EC have indicated reciprocal network excitatory interactions with CA3 (Rutecki et al. 1989). Moreover, an *in vivo* study revealed significantly higher firing rates, burst propensity and large synchronous discharges in the epileptic EC, subiculum and hippocampal formation during slow wave sleep (Staba et al. 2002), which differed drastically when recordings were obtained from non-epileptic zones. The most recent *in vitro* study demonstrated GABAergic depolarizing effects and synchronous network bursting within the isolated epileptic subiculum (Cohen et al. 2002). Collectively, these investigations demonstrate alterations in specific limbic structures; unfortunately, the methods required to effectively characterize the interaction between these structural epileptic networks is limited. To this end, the *in vitro* slice preparation from animal brain tissue allows researchers to perform more invasive techniques and to assess detailed information on the cellular and pharmacological characteristics of limbic seizures.

0.5.2 Synchronous network activity in acute *in vitro* seizure models

The *in vitro* brain slice preparation allows the investigation of interconnected neuronal structures; however, spontaneous network bursting is a rare occurrence in isolated brain tissue (Kano et al. 2005). Application of convulsive agents provides a convenient and immediate solution to generate robust *in vitro* epileptiform events within neuronal tissue. Synchronous network discharges are the consequence of low Mg^{2+}, cholinergic agonists, $GABA_A$ receptor antagonism or the potassium A channel

blocker, 4-AP; the latter promotes the release of glutamatergic and GABAergic neurotransmission (Buckle and Haas 1982). All conditions generate distinctive electrographic wave forms that can exist in isolated structures or propagate to adjacent territories (Benini and Avoli 2005; de Guzman et al. 2004; Klueva et al. 2003; Nagao et al. 1996).

In the *in vitro* hippocampus, $GABA_A$ receptor blockade can generate rhythmic network bursts that propagate throughout the hippocampal trisynaptic loop (D'Antuono et al. 2005; Jones and Lambert 1990a; b; Uva et al. 2005). The distinguishing feature are the high frequency ripple oscillations exceeding 200 Hz, exclusive to the adult DG (D'Antuono et al. 2005); although, increased extracellular potassium in tissue acquired postnatal day 12-30 rats generate fast oscillatory ripple waveforms in CA3 (Dzhala and Staley 2004). Additional investigations within the hippocampal formation utilizing 4-AP, low Mg^{2+} or cholinergic activation generated brief synchronous discharges that did not display fast oscillatory ripple activity and were AMPA/Kainate receptor sensitive (Avoli et al. 1996; de Guzman et al. 2004; Dickson and Alonso 1997; Nagao et al. 1996).

Alternatively, in the presence of 4-AP, low Mg^{2+} or cholinergic agonists, parahippocampal (perirhinal and entorhinal cortices) structures demonstrate enhanced NMDA receptor-dependent epileptiform events, lasting several seconds, consisting of tonic and clonic components (Avoli et al. 1996; de Guzman et al. 2004; Dickson and Alonso 1997; Jones and Heinemann 1988; Nagao et al. 1996). This epileptiform discharge morphologically parallels the EEG ictal waveform that accompanies seizure activity *in vivo*, and thus will be referred to as the ictal discharge *(Chatrian et al. 1974).* Studies indicate that *in vitro* ictal bursts generate alternating sites of parahippocampal origin but most often initiate from the perirhinal cortex (de

Guzman et al. 2004; Klueva et al. 2003). In addition, application of these drugs promote theta oscillations within the ictal discharge (de Guzman et al. 2004; Dickson and Alonso 1997; Klueva et al. 2003), which is interesting as high oscillations are hypothesized to serve as markers of epileptogenic regions (Bragin et al. 2004).

The use of acute seizure models provide crucial insight in how a hyperexcitable network will function in isolation or during interaction with adjacent structures. The primary caveat, however, is that these pharmacological biases detract specific physiological activity from the network's natural state making it difficult to discern the perturbations present in epileptic tissue. This scenario is further complicated as control tissue is often investigated and does not exhibit the network alterations specific to TLE. To this end, investigations in chronic seizure models of TLE, such as the pilocarpine animal model can address these limitations.

0.6 The Pilocarpine-Treated Animal Model of TLE

0.6.1 Pilocarpine induced limbic seizures

The cholinergic muscarinic agonist, pilocarpine, injected intracranially or intraperitoneally generates behavioural and electrographic seizures (Lindekens et al. 2000; Smolders et al. 1997). Categorization of seizure activity is organized by the Racine seizure class; class I through class V seizures are respectively comprised of mouth and facial movements, head nodding, forelimb clonus, rearing, followed by rearing and falling (Racine 1972). Subsequent to prolonged intervals of class 4 or 5 seizures (exceeding 30 minutes) and post-ictal recovery, the animals enter a latent period. This time point is referred to as the latent phase, and mimics the clinical condition, due to the absence of seizure activity. The latent phase is a crucial time

point, as it provides the prospect of determining the cause and effect of chronic epileptic states. Approximately 3 or 4 weeks post status epilepticus, over 90% of animals will develop chronic seizures that persist throughout life (Cavalheiro et al. 1991; Priel et al. 1996).

The mechanisms underlying the cholinergic induction of motor seizures are multifactorial. Blockade of the K^+ mediated non inactivating M current promotes action potential spiking (Brown and Adams 1980), leading to enhanced excitatory neurotransmission (Martire et al. 2004) and increased network hyperexcitability. In line with this viewpoint, superfusion of pilocarpine in the *in vitro* EC generates NMDA receptor dependent ictal discharges (Nagao et al. 1996). This synaptic mechanism differs from the *in vitro* hippocampal formation as the epileptiform events are sensitive to AMPA/kainate receptors or GluR5 receptor antagonism (Clarke and Collingridge 2002; Nagao et al. 1996; Rutecki and Yang 1998). In addition, recent studies in the *in vitro* whole brain indicate that pilocarpine induced seizures necessitate a breached blood brain barrier (Marco de Curtis, personal communications), which agrees with the clinical observations in TLE patients (van Vliet et al. 2007).

0.6.2 Network structural alterations and network hyperexcitability

The network modifications following pilocarpine induced status epilepticus are demonstrated to occur prior to the development of chronic seizures. 24 hours post-status epilepticus, edema is reported within the amygdala, piriform and entorhinal cortices accompanied with neuronal loss (Roch et al. 2002). Within similar time frames, high levels of network activation - indicated by FOS immunoreactivity - are localized within limbic regions (CA3, CA1, the subiculum, the lateral EC and the DG) (Biagini et al. 2005). Further anatomical modifications occur within the chronic phase,

as MRI studies indicate volumetric reduction within the perirhinal, and piriform cortices, and hippocampus combined with gliosis (Niessen et al. 2005). Similar to the clinical scenario, the histopathological patterns in the pilocarpine model involve cellular loss within hippocampal CA1 and CA3, medial EC layer III, and the perirhinal cortex (Avoli et al. 2002; Covolan and Mello 2000; Du et al. 1995). Additional structures include the amygdala, piriform and insular cortices (Covolan and Mello 2000). However, unlike the aforementioned limbic regions, the alterations in the DG include not only cellular death but also neurogenesis of granule cells (Parent et al. 2006; Parent et al. 1998; Scharfman et al. 2000).

The functional alterations reported in the pilocarpine-treated DG involve newly developed granule cells, in the hilar region, innervated by mossy fibres (Feng et al. 2003; Parent et al. 1998; Scharfman et al. 1999; 2000; Scharfman et al. 2002; Williams et al. 2002). Enhanced excitatory neurotransmission is thought to be a consequence of mossy fibre sprouting as 500 new synapes per granule cell are estimated (Buckmaster et al. 2002). This increase in recurrent excitation is accompanied by reduced alpha 1 and increased alpha 4 $GABA_A$ subunits, which may potentiate epileptiform activity through enhanced $GABA_A$ receptor sensitivity to Zn^{2+} (Gibbs et al. 1997). At the synaptic level, the excitatory network of the DG can be inhibited or enhanced through neuropeptide Y (NPY) (Tu et al. 2005) or BDNF-trkB receptor activation, respectively (Scharfman et al. 1999). These findings are intriguing, as reduced NPY1R expression would trigger neuronal hyperexcitability as NPY inhibits seizure activity (Baraban, 2004). Moreover, decreased KCC2 expression correlates with increased extracellular BDNF (Rivera et al. 2002; Rivera et al. 1999); although, other studies suggest BDNF provides neuroprotection (Biagini et al. 2001). Aside from synaptic activity, modified voltage gated ion channels can

promote excitability. In the epileptic lateral EC layer III, the decreased HCN mRNA expression and hyperpolarizing-activated cation current (I_h) favours action potential spiking (Shah et al. 2004); similarly, a reduction of HCN1 mRNA is reported within the epileptic DG (Bender et al. 2003). However, despite the reported enhanced excitability of the epileptic DG recent studies highlight the inability of the DG to activate CA3 networks (Ang et al. 2006; Biagini et al. 2005).

The reduction, or lack, of CA3 network responsiveness to inputs arising from the DG is puzzling, as the hippocampal trisynaptic loop has been hypothesized to amplify limbic seizures (Pare et al. 1992). Investigations in pilocarpine-treated tissue utilizing voltage sensitive dyes or intrinsic optical signals reveal minimal CA3 responses following DG stimulation (Ang et al. 2006). In addition, while direct activation of epileptic CA3 elicits a response (Biagini et al. 2005), antidromic activation of the Schaffer collaterals fails to activate CA3 networks (Ang et al. 2006). These results are contradictory but both studies report minimal CA3 damage. The contribution of network hippocampal hyperexcitability is thought to be a result of CA1 and subicular activation through EC layer III inputs, a pathway defined as the temporoammonic pathway (TA) (Deadwyler et al. 1975; Ang et al. 2006; Biagini et al. 2005; D'Antuono et al. 2002; Wozny et al. 2005). To this end, the TA can serve as alternative route to amplify limbic seizures without the aid of CA3 outputs.

The above studies indicate that the hippocampal formation can still contribute to epileptiform events. Under these conditions, epileptic CA1 networks would substitute for the hypoactivate CA3 neurons. In pilocarpine-treated CA1, studies reveal spontaneous bursting combined with an up regulation of T-Type calcium mediated intrinsically bursting neurons (Sanabria et al. 2001). In addition, augmented excitation may be affected by axonal sprouting (Esclapez et al. 1999) and the loss of

the parvalbumin positive inhibitory interneuronal synapses on the axonal initial segment of CA1 pyramidal cells (Dinocourt et al. 2003). These events may account for the reports of reduced quantal release of GABA (Hirsch et al. 1999) and decreased inhibitory post-synaptic potentials (Stief et al. 2007).

Collectively, these investigations demonstrate a focus on the hippocampal formation in pilocarpine-treated tissue. Although, there are additional structures external to the hippocampus implicated in TLE. Recent investigations reveal a more positive $GABA_A$ receptor mediated reversal point in the pilocarpine treated amygdala (Benini and Avoli 2006) and the perirhinal cortex (Benini and Avoli, unpublished data). In the following sections of the introduction, I will discuss the role of the subiculum, and the entorhinal and insular cortices in TLE.

0.7 The Role of the Subiculum in TLE

0.7.1 Anatomy

The subicular complex is comprised of 3 subdivisions, the subiculum, presubiculum and the parasubiculum (Lopes da Silva et al. 1990; Witter et al. 1989). At the cytoarchitectural level, the subiculum is similar to the three layered allocortex, of the hippocampal formation, as it consists of a molecular layer, an enlarged pyramidal cell layer and a polymorphic layer (O'Mara et al. 2001). In contrast, the presubiculum and the parasubiculum are multilaminar and exhibit structural similarities to the EC (O'Mara 2005).

The subiculum functions as the primary structural output of the hippocampal formation with inputs that terminate in layer V of the EC (Kohler 1985; Tamamaki and Nojyo 1995). More specifically, the proximal and distal subicular subdivisions direct

their projections towards the medial EC and lateral EC, respectively (Tamamaki and Nojyo 1995; Witter et al. 1990). In addition, the subiculum is the recipient of converging inputs from CA1 and EC layer III; the latter input constitutes the temporoammonic pathway (Baks-Te Bulte et al. 2005; Witter et al. 2000). Subicular network interactions also occur with additional structures implicated in TLE such as the perirhinal cortex (Swanson et al. 1978) and amygdala (Canteras and Swanson 1992).

0.7.2 The epileptic subiculum

The majority of electrophysiological studies of the subiculum have involved *in vitro* slice preparations and the intrinsic firing properties of subicular pyramidal cells. In control tissue, regular firing and intrinsic bursting neurons have been identified within the subiculum (Mattia et al. 1993). Similar as to what has been described in layer V of neocortical structures (Connors and Gutnick 1990), the intrinsic bursting properties of subicular pyramidal cells are mediated through T-type calcium currents (Wellmer et al. 2002). Studies indicate a variable proportion of regular firing versus intrinsically bursting neurons in control tissue, yet most reports agree upon a larger population of intrinsically bursting cells (Knopp et al. 2005; Mattia et al. 1993; O'Mara et al. 2001; Wellmer et al. 2002). These observations are intriguing as the presence of intrinsic bursters has been hypothesized to predispose a structure to epileptiform activity (Connors and Gutnick 1990).

Interestingly, this large population of subicular intrinsically bursting activity may determine the magnitude of synaptic intensity towards the EC. The physiological regulation of subicular activity, however, is governed through an inhibitory network that becomes apparent following synaptic activation of CA1 (Behr et al. 1998), EC

layer III (Behr et al. 1998), or focal subicular stimulation (Menendez de la Prida et al. 2002) . These inhibitory processes may serve as an excitatory brake within the subiculum thereby precluding excessive excitatory hippocampal output from activating the EC (Dickson and Alonso 1997; Lopantsev and Avoli 1998a; Tolner et al. 2005). To this end, the subiculum can be viewed as a network filter that regulates the output of the hippocampal formation towards the parahippocampus. Although, when this structural gate becomes compromised a condition of network hyperexcitation can result.

Recently, *in vitro* studies performed in subicular tissue, obtained from epileptic patients, indicated the paradoxical depolarizing effects of the inhibitory neurotransmitter GABA (Cohen et al. 2002) as well as an augmented sodium persistent current (Vreugdenhil et al. 2004). In line with this view, kindling paradigms have demonstrated a reduction of subicular inhibitory interneurons (van Vliet et al. 2004), while pilocarpine treated tissue had an increased quantity of intrinsic subicular bursting cells (Wellmer et al. 2002). The combination of these results demonstrates the inherent ability of the subiculum to contribute to epileptiform events.

In contrast to this evidence, a recent study indicates that the pathophysiology of the subiculum is non conducive to epileptiform activity due to the observations of a reduced number of intrinsic bursters, and decreased dendritic arborisation (Knopp et al. 2005). However, additional factors such as functional alterations to the voltage gated ion channels (Vreugdenhil et al. 2004), a reduced affinity for GABA (Ragozzino et al. 2005), and a more positive Cl^- reversal point can contribute to epileptiform activity (Palma et al. 2006). These data demonstrate that subtle structural and inhibitory network modifications can enhance subicular hyperexcitability.

0.8 The Role of the Entorhinal Cortex in TLE

0.8.1 Anatomy

The EC is a five layered limbic structure that is the recipient of hippocampal and neocortical output (Deacon et al. 1983; Kohler 1985; Tamamaki and Nojyo 1995). Due to the parallel processing of the EC, this structure is anatomically and functionally subdivided into the medial EC and lateral EC (Hamam et al. 2002; Hamam et al. 2000); the respective and reciprocal connections of the EC are speculated to integrate and segregate information (Dolorfo and Amaral 1998a). Activation of the EC can originate from the subiculum where efferent fibres terminate in layer V (Kohler 1985; Tamamaki and Nojyo 1995); alternatively, neocortical efferents enter the EC through layers II/III (Deacon et al. 1983; Dolorfo and Amaral 1998a). To this end, the parallel information flow from EC layer V can enter the neocortex (Insausti et al. 1997; Swanson and Kohler 1986), or extend to EC layers II/III; the latter route can provide hippocampal re-entry to the DG or hippocampal CA1/ subiculum via the perforant and temporoammonic pathways, respectively (Baks-Te Bulte et al. 2005; Dolorfo and Amaral 1998b; Ruth et al. 1988). In addition, the EC exhibits network connectivity with the perirhinal cortex, piriform cortex and insular cortices (Burwell and Amaral 1998).

0.8.2 The epileptic entorhinal cortex

The majority of human epileptic studies have focused upon the hippocampal formation; however, it is only as of recent the epileptogenicity of the EC has been addressed. *In vivo* recordings in TLE patients indicate that the EC interacts with hippocampal networks (Rutecki et al. 1989) and demonstrates seizure origin (Spencer and Spencer 1994). This network synchronization also generates fast

oscillatory ripple waveforms (> 200 Hz), which may serve as an electrographic signature exclusive to pathological activity (Bragin et al. 2004). Further insights, via molecular techniques, suggest the decreased expression of NPY1R and 5HTA receptors facilitate reduced network inhibition (Jamali et al. 2006). Moreover, anatomical studies reveal that the epileptic EC is structurally altered as evidenced by volumetric reduction (Bernasconi et al. 1999) and pyramidal cell loss in medial EC layers II/III (Du et al. 1995; Du et al. 1993).

Additional investigations of the EC have utilized control animal tissue in the combined hippocampal entorhinal cortical slice and the *in vitro* whole brain. In these preparations, network synchronization and robust ictal discharges displayed deep layer entorhinal cortical origin by enhancing network function through potassium A channel blockade (Lopantsev and Avoli 1998a; b), nominal extracellular Mg^{2+} (Jones and Heinemann 1988), $GABA_A$ receptor antagonism (Jones and Lambert 1990a; b; Uva et al. 2005), elevated $[K^+]_o$ (Bear and Lothman 1993) and cholinergic agonists (Dickson and Alonso 1997; Nagao et al. 1996). The activity of the EC also activates adjacent structures as *in vitro* ictal discharges demonstrated bidirectional routes of propagation and invaded the subiculum, the hippocampal formation, amygdala, and the parahippocampus (Barbarosie and Avoli 1997; Benini et al. 2003; de Guzman et al. 2004; Klueva et al. 2003; Uva et al. 2005). While alternative forms of *in vitro* epileptiform events are AMPA/kainate receptor sensitive, ictal waveforms can be blocked through NMDA receptor antagonism (Avoli et al. 1996; Jones and Heinemann 1988), spontaneous interictal activity (Barbarosie and Avoli 1997; Librizzi and de Curtis 2003) and high frequency electrical stimulation (Barbarosie and Avoli 1997; Benini et al. 2003). The use of convulsive agents has provided valuable insight in understanding the network machinery of the EC; although, the investigated tissue

lacks the neuronal damage observed in clinical conditions of TLE. To this end, the chronic seizure models of TLE have addressed this limitation.

Investigations of the EC, in chronic seizures paradigms, have often focused upon the medial superficial layers (Kobayashi et al. 2003; Kumar and Buckmaster 2006; Shah et al. 2004; Wozny et al. 2005). Inhibitory neuronal loss during the latent and chronic seizure periods lead to enhanced excitation in MEC layer II and reduced $GABA_A$ receptor mediated inhibition; these modifications ensure an increased synaptic drive on the DG (Kobayashi and Buckmaster 2003; Kobayashi et al. 2003). The amplified excitation of EC layer II may also be a result of decreased GABAergic input from functional layer III inhibitory interneurons (Kumar and Buckmaster 2006); however, this lack of network interaction seems counterintuitive as layer III networks become hyperexcitable following pyramidal cell death (Scharfman et al. 1998). If a lack of communication exists between layers II/III, evidence suggests the function of EC layer II may be governed by the network properties of EC layer V (Dickson and Alonso 1997).

In contrast to the EC superficial mantle, the deep layers of the EC may be more conducive to epileptiform activity. Investigations in MEC layer V, in control tissue, exhibits recurrent excitatory connections combined with minimal inhibitory input (Woodhall et al. 2005). In epileptic tissue, acquired from electrically kindled and pilocarpine treated animals, medial EC layer V displays enhanced excitation and functionally altered NMDA receptors (Fountain et al. 1998; Yang et al. 2006). Additional perturbations also occur in the often overlooked lateral EC. This trend may be a result of diminished neuronal death in the lateral EC; however, additional factors other than cellular death can contribute to a hyperexcitable network. Unlike additional structures implicated in TLE, the EC portrays subtle structural defects (Dawodu and

Thom 2005). Investigations of lateral EC layer III, during the latent phase in kainic acid treated rodents, report attenuated I_h activity which favours intrinsic and network excitation (Shah et al. 2004). The importance of the lateral EC is further reinforced as ablation of the lateral subdivision provides seizure relief in epileptic rats (Kopniczky et al. 2005). The combination of these studies indicates the EC is a hyperexcitable structure that plays a pivotal role in the epileptogenesis of TLE.

0.9 The Role of the Insular Cortex in TLE

0.9.1 Anatomy

The human insula lies buried in the lateral sulcus (Reil 1809), and can only be visualized by retraction of the frontal and temporal lobes, which is an opening referred to as the limen insula (Carpenter 1985). The IC is comprised of 3 distinct regions referred to as the agranular, dysgranular and granular cortices (Mesulam and Mufson 1982a). At the cytoarchitectural level, 3 strata in the agranular cortex consist primarily of pyramidal cells (Flynn et al. 1999). This structural organization differs considerably from layers II and IV of the granule and dysgranular cortices due to the presence of granule cells (Flynn et al. 1999).

The network connectivity of the IC extends to neuronal territories implicated in TLE. Within limbic structures, the agranular cortex exhibits reciprocal connectivity within the perirhinal and piriform cortices and the EC (Burwell and Amaral 1998; McIntyre et al. 1996; Mesulam and Mufson 1982b; Reep and Winans 1982). In contrast, the dysgranular and granular cortices have unidirectional efferents to the amygdala (Shi and Cassell 1998).

0.9.2 The epileptic insular cortex

In the 1950s, Penfield provided the first report implicating the IC in the epileptogenesis of TLE (Penfield and Jasper 1954). There was no direct evidence and this speculation was based upon the occurrence of persistent seizures following temporal lobectomy. Interestingly, the difficulties in identifying insular seizures were a combination of the anatomical location of the IC and the technological limitations of the EEG (Isnard et al. 2004). Through the utilization of depth electrodes, Isnard et al (2000) demonstrated focal onset of insular seizures. In this particular study, temporal lobectomy provided complete seizure relief when ictal events where not of insular origin (Isnard et al. 2000).

Anatomically, the IC would be expected to undergo network hyperexcitation as it is the recipient of structural inputs from three epileptogenic structures: the EC, the perirhinal cortex, and the piriform cortex. (Burwell and Amaral 1998; McIntyre et al. 1996; Mesulam and Mufson 1982b; Reep and Winans 1982). However, anatomical connections do not always correlate with functional connectivity. In the *in vitro* whole brain, the IC can be activated through entorhinal and piriform networks; unexpectedly, perirhinal cortical stimulation produced far field effects in the IC (Biella et al. 2003). Similar physiological events have been identified with perirhinal – entorhinal cortical interactions, which were attributed to inhibitory networks (Biella et al. 2002). These results suggest GABAergic inhibition may exist between the perirhinal cortex and IC. Under epileptic conditions the break down of these inhibitory networks may promote the propagation of seizure activity. In line with this viewpoint, $GABA_A$ receptor antagonism generates *in vitro* whole brain epileptiform events that traverse the entorhinal and perirhinal cortices (Federico and MacVicar 1996; Uva et al. 2005). This removal of network inhibition is further illustrated in the *in vitro* brain slice, where bicuculline induced ($GABA_A$ receptor antagonist) epileptiform discharges originate

and propagate within the agranular IC and perirhinal cortex (Demir et al. 1998). The utilization of these *in vitro* models demonstrates the hyperexcitability of the IC and its network synchronization with adjacent parahippocampal structures.

The paucity of electrophysiological studies in the IC makes it difficult to understand how this structure would behave in epileptic tissue. Investigations in nociception have revealed the colocalization of GABA and enkephalins within the agranular IC layer II (Evans et al. 2007) and $GABA_B$ receptor mediated output in layer V (Ohara et al. 2003). When this information is extrapolated to the conditions of network hyperexcitability, the data suggest that the IC contains the neurochemical resources to generate network synchronization. The combination of endogenous opioids and GABA, prove interesting, as μ–opioids can hyperperpolarize inhibitory neurons and desynchronize the network. Modulation of network activity through μ–opioid receptors is reported in the *in vitro* hippocampal-entorhinal slice (Avoli et al. 1996) and the basolateral amygdala (Finnegan et al. 2006). As such, the relationship of opioid circuitry to GABA systems in the IC and how they function within an epileptic network remains to be determined.

0.10.0 References:

Acharya MM, and Katyare SS. Structural and functional alterations in mitochondrial membrane in picrotoxin-induced epileptic rat brain. *Exp Neurol* 192: 79-88, 2005.

Andre VM, Flores-Hernandez J, Cepeda C, Starling AJ, Nguyen S, Lobo MK, Vinters HV, Levine MS, and Mathern GW. NMDA receptor alterations in neurons from pediatric cortical dysplasia tissue. *Cereb Cortex* 14: 634-646, 2004.

Ang CW, Carlson GC, and Coulter DA. Massive and specific dysregulation of direct cortical input to the hippocampus in temporal lobe epilepsy. *J Neurosci* 26: 11850-11856, 2006.

Arriza JL, Eliasof S, Kavanaugh MP, and Amara SG. Excitatory amino acid transporter 5, a retinal glutamate transporter coupled to a chloride conductance. *Proceedings of the National Academy of Sciences of the United States of America* 94: 4155-4160, 1997.

Arriza JL, Fairman WA, Wadiche JI, Murdoch GH, Kavanaugh MP, and Amara SG. Functional comparisons of three glutamate transporter subtypes cloned from human motor cortex. *J Neurosci* 14: 5559-5569, 1994.

Avoli M, Barbarosie M, Lucke A, Nagao T, Lopantsev V, and Kohling R. Synchronous GABA-mediated potentials and epileptiform discharges in the rat limbic system in vitro. *J Neurosci* 16: 3912-3924, 1996.

Avoli M, D'Antuono M, Louvel J, Kohling R, Biagini G, Pumain R, D'Arcangelo G, and Tancredi V. Network and pharmacological mechanisms leading to epileptiform synchronization in the limbic system in vitro. *Prog Neurobiol* 68: 167-207, 2002.

Avoli M, and Olivier A. Electrophysiological properties and synaptic responses in the deep layers of the human epileptogenic neocortex in vitro. *J Neurophysiol* 61: 589-606, 1989.

Baks-Te Bulte L, Wouterlood FG, Vinkenoog M, and Witter MP. Entorhinal projections terminate onto principal neurons and interneurons in the subiculum: a quantitative electron microscopical analysis in the rat. *Neuroscience* 136: 729-739, 2005.

Bandyopadhyay S, and Hablitz JJ. NR2B antagonists restrict spatiotemporal spread of activity in a rat model of cortical dysplasia. *Epilepsy Res* 72: 127-139, 2006.

Barbarosie M, and Avoli M. CA3-driven hippocampal-entorhinal loop controls rather than sustains in vitro limbic seizures. *J Neurosci* 17: 9308-9314, 1997.

Bear J, and Lothman EW. An in vitro study of focal epileptogenesis in combined hippocampal-parahippocampal slices. *Epilepsy Res* 14: 183-193, 1993.

Beck H, Blumcke I, Kral T, Clusmann H, Schramm J, Wiestler OD, Heinemann U, and Elger CE. Properties of a delayed rectifier potassium current in dentate granule cells isolated from the hippocampus of patients with chronic temporal lobe epilepsy. *Epilepsia* 37: 892-901, 1996.

Beck H, Clusmann H, Kral T, Schramm J, Heinemann U, and Elger CE. Potassium currents in acutely isolated human hippocampal dentate granule cells. *J Physiol* 498 (Pt 1): 73-85, 1997.

Behr J, Gloveli T, and Heinemann U. The perforant path projection from the medial entorhinal cortex layer III to the subiculum in the rat combined hippocampal-entorhinal cortex slice. *Eur J Neurosci* 10: 1011-1018, 1998.

Ben-Ari Y, Cherubini E, Corradetti R, and Gaiarsa JL. Giant synaptic potentials in immature rat CA3 hippocampal neurones. *J Physiol* 416: 303-325, 1989.

Bender RA, Soleymani SV, Brewster AL, Nguyen ST, Beck H, Mathern GW, and Baram TZ. Enhanced expression of a specific hyperpolarization-activated cyclic nucleotide-gated cation channel (HCN) in surviving dentate gyrus granule cells of human and experimental epileptic hippocampus. *J Neurosci* 23: 6826-6836, 2003.

Benini R, and Avoli M. Altered inhibition in lateral amygdala networks in a rat model of temporal lobe epilepsy. *J Neurophysiol* 95: 2143-2154, 2006.

Benini R, and Avoli M. Rat subicular networks gate hippocampal output activity in an in vitro model of limbic seizures. *J Physiol* 566: 885-900, 2005.

Benini R, D'Antuono M, Pralong E, and Avoli M. Involvement of amygdala networks in epileptiform synchronization in vitro. *Neuroscience* 120: 75-84, 2003.

Bernasconi N, Bernasconi A, Andermann F, Dubeau F, Feindel W, and Reutens DC. Entorhinal cortex in temporal lobe epilepsy: a quantitative MRI study. *Neurology* 52: 1870-1876, 1999.

Biagini G, Avoli M, Marcinkiewicz J, and Marcinkiewicz M. Brain-derived neurotrophic factor superinduction parallels anti-epileptic--neuroprotective treatment in the pilocarpine epilepsy model. *J Neurochem* 76: 1814-1822, 2001.

Biagini G, D'Arcangelo G, Baldelli E, D'Antuono M, Tancredi V, and Avoli M. Impaired activation of CA3 pyramidal neurons in the epileptic hippocampus. *Neuromolecular Med* 7: 325-342, 2005.

Biella G, Uva L, and de Curtis M. Propagation of neuronal activity along the neocortical-perirhinal-entorhinal pathway in the guinea pig. *J Neurosci* 22: 9972-9979, 2002.

Biella GR, Gnatkovsky V, Takashima I, Kajiwara R, Iijima T, and de Curtis M. Olfactory input to the parahippocampal region of the isolated guinea pig brain reveals weak entorhinal-to-perirhinal interactions. *Eur J Neurosci* 18: 95-101, 2003.

Bordey A, and Spencer DD. Distinct electrophysiological alterations in dentate gyrus versus CA1 glial cells from epileptic humans with temporal lobe sclerosis. *Epilepsy Res* 59: 107-122, 2004.

Bragin A, Wilson CL, Almajano J, Mody I, and Engel J, Jr. High-frequency oscillations after status epilepticus: epileptogenesis and seizure genesis. *Epilepsia* 45: 1017-1023, 2004.

Brown DA, and Adams PR. Muscarinic suppression of a novel voltage-sensitive K+ current in a vertebrate neurone. *Nature* 283: 673-676, 1980.

Buckle PJ, and Haas HL. Enhancement of synaptic transmission by 4-aminopyridine in hippocampal slices of the rat. *J Physiol* 326: 109-122, 1982.

Buckmaster PS, Zhang GF, and Yamawaki R. Axon sprouting in a model of temporal lobe epilepsy creates a predominantly excitatory feedback circuit. *J Neurosci* 22: 6650-6658, 2002.

Burwell RD, and Amaral DG. Perirhinal and postrhinal cortices of the rat: interconnectivity and connections with the entorhinal cortex. *J Comp Neurol* 391: 293-321, 1998.

Canteras NS, and Swanson LW. Projections of the ventral subiculum to the amygdala, septum, and hypothalamus: a PHAL anterograde tract-tracing study in the rat. *J Comp Neurol* 324: 180-194, 1992.

Caraiscos VB, Elliott EM, You-Ten KE, Cheng VY, Belelli D, Newell JG, Jackson MF, Lambert JJ, Rosahl TW, Wafford KA, MacDonald JF, and Orser BA. Tonic inhibition in mouse hippocampal CA1 pyramidal neurons is mediated by alpha5 subunit-containing gamma-aminobutyric acid type A receptors. *Proceedings of the National Academy of Sciences of the United States of America* 101: 3662-3667, 2004.

Carpenter M. *Core Text of Neuroanatomy*. Baltimore: 1985.

Cavalheiro EA, Leite JP, Bortolotto ZA, Turski WA, Ikonomidou C, and Turski L. Long-term effects of pilocarpine in rats: structural damage of the brain triggers kindling and spontaneous recurrent seizures. *Epilepsia* 32: 778-782, 1991.

Cereghetti GM, and Scorrano L. The many shapes of mitochondrial death. *Oncogene* 25: 4717-4724, 2006.

Charriaut-Marlangue C, Aggoun-Zouaoui D, Represa A, and Ben-Ari Y. Apoptotic features of selective neuronal death in ischemia, epilepsy and gp 120 toxicity. *Trends in neurosciences* 19: 109-114, 1996.

Chatrian GE, Bergamini L, Dondey M, Klass DW, Lennox-Buchthal M, and Petersen I. A glossary of terms most commonly used by clinical electroencephalographers. *Electroencephalogray and Clininical Neurophysiology* 37: 538-548, 1974.

Chen G, Trombley PQ, and van den Pol AN. Excitatory actions of GABA in developing rat hypothalamic neurones. *J Physiol* 494 (Pt 2): 451-464, 1996.

Chen Q, He S, Hu XL, Yu J, Zhou Y, Zheng J, Zhang S, Zhang C, Duan WH, and Xiong ZQ. Differential roles of NR2A- and NR2B-containing NMDA receptors in

activity-dependent brain-derived neurotrophic factor gene regulation and limbic epileptogenesis. *J Neurosci* 27: 542-552, 2007.

Clarke VR, and Collingridge GL. Characterisation of the effects of ATPA, a GLU(K5) receptor selective agonist, on excitatory synaptic transmission in area CA1 of rat hippocampal slices. *Neuropharmacology* 42: 889-902, 2002.

Cohen I, Navarro V, Clemenceau S, Baulac M, and Miles R. On the origin of interictal activity in human temporal lobe epilepsy in vitro. *Science* 298: 1418-1421, 2002.

Connors BW, and Gutnick MJ. Intrinsic firing patterns of diverse neocortical neurons. *Trends in neurosciences* 13: 99-104, 1990.

Covolan L, and Mello LE. Temporal profile of neuronal injury following pilocarpine or kainic acid-induced status epilepticus. *Epilepsy Res* 39: 133-152, 2000.

D'Antuono M, Benini R, Biagini G, D'Arcangelo G, Barbarosie M, Tancredi V, and Avoli M. Limbic network interactions leading to hyperexcitability in a model of temporal lobe epilepsy. *J Neurophysiol* 87: 634-639, 2002.

D'Antuono M, de Guzman P, Kano T, and Avoli M. Ripple activity in the dentate gyrus of dishinibited hippocampus-entorhinal cortex slices. *Journal of neuroscience research* 80: 92-103, 2005.

Dawodu S, and Thom M. Quantitative neuropathology of the entorhinal cortex region in patients with hippocampal sclerosis and temporal lobe epilepsy. *Epilepsia* 46: 23-30, 2005.

de Guzman P, D'Antuono M, and Avoli M. Initiation of electrographic seizures by neuronal networks in entorhinal and perirhinal cortices in vitro. *Neuroscience* 123: 875-886, 2004.

Deadwyler SA, West JR, Cotman CW, and Lynch G. Physiological studies of the reciprocal connections between the hippocampus and entorhinal cortex. *Experimental neurology* 49: 35-57, 1975.

Deacon TW, Eichenbaum H, Rosenberg P, and Eckmann KW. Afferent connections of the perirhinal cortex in the rat. *J Comp Neurol* 220: 168-190, 1983.

Delgado-Escueta AV, Wilson WA, Olsen RW, and Porter RJ. Jasper's basic mechanisms of the epilepsies. *In: Advances in Neurology* Vol 79, 3rd edition: 1999.

Demir R, Haberly LB, and Jackson MB. Voltage imaging of epileptiform activity in slices from rat piriform cortex: onset and propagation. *J Neurophysiol* 80: 2727-2742, 1998.

Dickson CT, and Alonso A. Muscarinic induction of synchronous population activity in the entorhinal cortex. *J Neurosci* 17: 6729-6744, 1997.

Dinocourt C, Petanjek Z, Freund TF, Ben-Ari Y, and Esclapez M. Loss of interneurons innervating pyramidal cell dendrites and axon initial segments in the CA1 region of the hippocampus following pilocarpine-induced seizures. *J Comp Neurol* 459: 407-425, 2003.

Dolorfo CL, and Amaral DG. Entorhinal cortex of the rat: organization of intrinsic connections. *The Journal of comparative neurology* 398: 49-82, 1998a.

Dolorfo CL, and Amaral DG. Entorhinal cortex of the rat: topographic organization of the cells of origin of the perforant path projection to the dentate gyrus. *J Comp Neurol* 398: 25-48, 1998b.

Dreier JP, and Heinemann U. Regional and time dependent variations of low Mg2+ induced epileptiform activity in rat temporal cortex slices. *Exp Brain Res* 87: 581-596, 1991.

Du F, Eid T, Lothman EW, Kohler C, and Schwarcz R. Preferential neuronal loss in layer III of the medial entorhinal cortex in rat models of temporal lobe epilepsy. *J Neurosci* 15: 6301-6313, 1995.

Du F, Whetsell WO, Jr., Abou-Khalil B, Blumenkopf B, Lothman EW, and Schwarcz R. Preferential neuronal loss in layer III of the entorhinal cortex in patients with temporal lobe epilepsy. *Epilepsy Res* 16: 223-233, 1993.

During MJ, and Spencer DD. Extracellular hippocampal glutamate and spontaneous seizure in the conscious human brain. *Lancet* 341: 1607-1610, 1993.

Dzhala VI, and Staley KJ. Mechanisms of fast ripples in the hippocampus. *J Neurosci* 24: 8896-8906, 2004.

Dzhala VI, Talos DM, Sdrulla DA, Brumback AC, Mathews GC, Benke TA, Delpire E, Jensen FE, and Staley KJ. NKCC1 transporter facilitates seizures in the developing brain. *Nature medicine* 11: 1205-1213, 2005.

Engel J, Jr. Mesial temporal lobe epilepsy: what have we learned? *Neuroscientist* 7: 340-352, 2001.

Engel JJ, P W, and H.G. W. Mesial temporal lobe epilepsy. *Epilepsy: a comprehensive textbook Lippincott-Raven, Philadelphia* 2417-2726, 1997.

Esclapez M, Hirsch JC, Ben-Ari Y, and Bernard C. Newly formed excitatory pathways provide a substrate for hyperexcitability in experimental temporal lobe epilepsy. *J Comp Neurol* 408: 449-460, 1999.

Evans JM, Bey V, Burkey AR, and Commons KG. Organization of endogenous opioids in the rostral agranular insular cortex of the rat. *J Comp Neurol* 500: 530-541, 2007.

Fairman WA, Vandenberg RJ, Arriza JL, Kavanaugh MP, and Amara SG. An excitatory amino-acid transporter with properties of a ligand-gated chloride channel. *Nature* 375: 599-603, 1995.

Falconer MA. Genetic and related aetiological factors in temporal lobe epilepsy. A review. *Epilepsia* 12: 13-31, 1971.

Federico P, and MacVicar BA. Imaging the induction and spread of seizure activity in the isolated brain of the guinea pig: the roles of GABA and glutamate receptors. *J Neurophysiol* 76: 3471-3492, 1996.

Feng L, Molnar P, and Nadler JV. Short-term frequency-dependent plasticity at recurrent mossy fiber synapses of the epileptic brain. *J Neurosci* 23: 5381-5390, 2003.

Finnegan TF, Chen SR, and Pan HL. Mu opioid receptor activation inhibits GABAergic inputs to basolateral amygdala neurons through Kv1.1/1.2 channels. *J Neurophysiol* 95: 2032-2041, 2006.

Flynn F, Bensonoe F, and Ardila A. Anatomy of the insula - functional and clinical correlates. *Aphasiology* 13: 55-78, 1999.

Fountain NB, Bear J, Bertram EH, 3rd, and Lothman EW. Responses of deep entorhinal cortex are epileptiform in an electrogenic rat model of chronic temporal lobe epilepsy. *J Neurophysiol* 80: 230-240, 1998.

French JA, Williamson PD, Thadani VM, Darcey TM, Mattson RH, Spencer SS, and Spencer DD. Characteristics of medial temporal lobe epilepsy: I. Results of history and physical examination. *Ann Neurol* 34: 774-780, 1993.

Gabriel S, Njunting M, Pomper JK, Merschhemke M, Sanabria ER, Eilers A, Kivi A, Zeller M, Meencke HJ, Cavalheiro EA, Heinemann U, and Lehmann TN. Stimulus and potassium-induced epileptiform activity in the human dentate gyrus from patients with and without hippocampal sclerosis. *J Neurosci* 24: 10416-10430, 2004.

Gibbs JW, 3rd, Shumate MD, and Coulter DA. Differential epilepsy-associated alterations in postsynaptic GABA(A) receptor function in dentate granule and CA1 neurons. *J Neurophysiol* 77: 1924-1938, 1997.

Gloor P. Mesial temporal sclerosis: historical background and an overview from a modern perspective. *In: Lüders, H (Ed), Epilepsy Surgery Raven, New York* 689-703, 1991.

Gloor P. *The temporal lobe and limbic system*. New York: Oxford University Press, 1997, p. xii, 865.

Glykys J, and Mody I. Hippocampal network hyperactivity after selective reduction of tonic inhibition in GABA A receptor alpha5 subunit-deficient mice. *J Neurophysiol* 95: 2796-2807, 2006.

Goncalves Pereira PM, Insausti R, Artacho-Perula E, Salmenpera T, Kalviainen R, and Pitkanen A. MR volumetric analysis of the piriform cortex and cortical amygdala in drug-refractory temporal lobe epilepsy. *Ajnr* 26: 319-332, 2005.

Gulledge AT, and Stuart GJ. Excitatory actions of GABA in the cortex. *Neuron* 37: 299-309, 2003.

Gulyas AI, Sik A, Payne JA, Kaila K, and Freund TF. The KCl cotransporter, KCC2, is highly expressed in the vicinity of excitatory synapses in the rat hippocampus. *Eur J Neurosci* 13: 2205-2217, 2001.

Hamam BN, Amaral DG, and Alonso AA. Morphological and electrophysiological characteristics of layer V neurons of the rat lateral entorhinal cortex. *J Comp Neurol* 451: 45-61, 2002.

Hamam BN, Kennedy TE, Alonso A, and Amaral DG. Morphological and electrophysiological characteristics of layer V neurons of the rat medial entorhinal cortex. *J Comp Neurol* 418: 457-472, 2000.

Harvey A. The role of febrile convulsions in mesial temporal sclerosis. *In: The epilepsies: etiologies and prevention* 125-131, 1999.

Hirsch JC, Agassandian C, Merchan-Perez A, Ben-Ari Y, DeFelipe J, Esclapez M, and Bernard C. Deficit of quantal release of GABA in experimental models of temporal lobe epilepsy. *Nature neuroscience* 2: 499-500, 1999.

Holmes KH, Bilkey DK, and Laverty R. The infusion of an NMDA antagonist into perirhinal cortex suppresses amygdala-kindled seizures. *Brain research* 587: 285-290, 1992.

Houser CR, and Esclapez M. Downregulation of the alpha5 subunit of the GABA(A) receptor in the pilocarpine model of temporal lobe epilepsy. *Hippocampus* 13: 633-645, 2003.

Insausti R, Herrero MT, and Witter MP. Entorhinal cortex of the rat: cytoarchitectonic subdivisions and the origin and distribution of cortical efferents. *Hippocampus* 7: 146-183, 1997.

Isnard J, Guenot M, Ostrowsky K, Sindou M, and Mauguiere F. The role of the insular cortex in temporal lobe epilepsy. *Ann Neurol* 48: 614-623, 2000.

Isnard J, Guenot M, Sindou M, and Mauguiere F. Clinical manifestations of insular lobe seizures: a stereo-electroencephalographic study. *Epilepsia* 45: 1079-1090, 2004.

Isokawa M, Avanzini G, Finch DM, Babb TL, and Levesque MF. Physiologic properties of human dentate granule cells in slices prepared from epileptic patients. *Epilepsy Res* 9: 242-250, 1991.

Jackson GD, McIntosh AM, Briellmann RS, and Berkovic SF. Hippocampal sclerosis studied in identical twins. *Neurology* 51: 78-84, 1998.

Jamali S, Bartolomei F, Robaglia-Schlupp A, Massacrier A, Peragut JC, Regis J, Dufour H, Ravid R, Roll P, Pereira S, Royer B, Roeckel-Trevisiol N, Fontaine M, Guye M, Boucraut J, Chauvel P, Cau P, and Szepetowski P. Large-scale expression study of human mesial temporal lobe epilepsy: evidence for dysregulation of the neurotransmission and complement systems in the entorhinal cortex. *Brain* 129: 625-641, 2006.

Jandova K, Pasler D, Antonio LL, Raue C, Ji S, Njunting M, Kann O, Kovacs R, Meencke HJ, Cavalheiro EA, Heinemann U, Gabriel S, and Lehmann TN. Carbamazepine-resistance in the epileptic dentate gyrus of human hippocampal slices. *Brain* 129: 3290-3306, 2006.

Jones RS, and Heinemann U. Synaptic and intrinsic responses of medical entorhinal cortical cells in normal and magnesium-free medium in vitro. *J Neurophysiol* 59: 1476-1496, 1988.

Jones RS, and Lambert JD. The role of excitatory amino acid receptors in the propagation of epileptiform discharges from the entorhinal cortex to the dentate gyrus in vitro. *Exp Brain Res* 80: 310-322, 1990a.

Jones RS, and Lambert JD. Synchronous discharges in the rat entorhinal cortex in vitro: site of initiation and the role of excitatory amino acid receptors. *Neuroscience* 34: 657-670, 1990b.

Jutila L, Ylinen A, Partanen K, Alafuzoff I, Mervaala E, Partanen J, Vapalahti M, Vainio P, and Pitkanen A. MR volumetry of the entorhinal, perirhinal, and temporopolar cortices in drug-refractory temporal lobe epilepsy. *Ajnr* 22: 1490-1501, 2001.

Kano T, Inaba Y, and Avoli M. Periodic oscillatory activity in parahippocampal slices maintained in vitro. *Neuroscience* 130: 1041-1053, 2005.

Khazipov R, Esclapez M, Caillard O, Bernard C, Khalilov I, Tyzio R, Hirsch J, Dzhala V, Berger B, and Ben-Ari Y. Early development of neuronal activity in the primate hippocampus in utero. *J Neurosci* 21: 9770-9781, 2001.

Kivi A, Lehmann TN, Kovacs R, Eilers A, Jauch R, Meencke HJ, von Deimling A, Heinemann U, and Gabriel S. Effects of barium on stimulus-induced rises of [K+]o in human epileptic non-sclerotic and sclerotic hippocampal area CA1. *The European journal of neuroscience* 12: 2039-2048, 2000.

Klueva J, Munsch T, Albrecht D, and Pape HC. Synaptic and non-synaptic mechanisms of amygdala recruitment into temporolimbic epileptiform activities. *Eur J Neurosci* 18: 2779-2791, 2003.

Knopp A, Kivi A, Wozny C, Heinemann U, and Behr J. Cellular and network properties of the subiculum in the pilocarpine model of temporal lobe epilepsy. *J Comp Neurol* 483: 476-488, 2005.

Kobayashi M, and Buckmaster PS. Reduced inhibition of dentate granule cells in a model of temporal lobe epilepsy. *J Neurosci* 23: 2440-2452, 2003.

Kobayashi M, Wen X, and Buckmaster PS. Reduced inhibition and increased output of layer II neurons in the medial entorhinal cortex in a model of temporal lobe epilepsy. *J Neurosci* 23: 8471-8479, 2003.

Kohler C. Intrinsic projections of the retrohippocampal region in the rat brain. I. The subicular complex. *J Comp Neurol* 236: 504-522, 1985.

Kopniczky Z, Dobo E, Borbely S, Vilagi I, Detari L, Krisztin-Peva B, Bagosi A, Molnar E, and Mihaly A. Lateral entorhinal cortex lesions rearrange afferents, glutamate receptors, increase seizure latency and suppress seizure-induced c-fos expression in the hippocampus of adult rat. *J Neurochem* 95: 111-124, 2005.

Kumar SS, and Buckmaster PS. Hyperexcitability, interneurons, and loss of GABAergic synapses in entorhinal cortex in a model of temporal lobe epilepsy. *J Neurosci* 26: 4613-4623, 2006.

Kwan P, and Brodie MJ. Early identification of refractory epilepsy. *N Engl J Med* 342: 314-319, 2000.

Lewis DV. Febrile convulsions and mesial temporal sclerosis. *Current opinion in neurology* 12: 197-201, 1999.

Librizzi L, and de Curtis M. Epileptiform ictal discharges are prevented by periodic interictal spiking in the olfactory cortex. *Ann Neurol* 53: 382-389, 2003.

Lindekens H, Smolders I, Khan GM, Bialer M, Ebinger G, and Michotte Y. In vivo study of the effect of valpromide and valnoctamide in the pilocarpine rat model of focal epilepsy. *Pharmaceutical research* 17: 1408-1413, 2000.

Liou AK, Clark RS, Henshall DC, Yin XM, and Chen J. To die or not to die for neurons in ischemia, traumatic brain injury and epilepsy: a review on the stress-activated signaling pathways and apoptotic pathways. *Prog Neurobiol* 69: 103-142, 2003.

Lopantsev V, and Avoli M. Laminar organization of epileptiform discharges in the rat entorhinal cortex in vitro. *J Physiol* 509 (Pt 3): 785-796, 1998a.

Lopantsev V, and Avoli M. Participation of GABAA-mediated inhibition in ictallike discharges in the rat entorhinal cortex. *J Neurophysiol* 79: 352-360, 1998b.

Lopes da Silva FH, Witter MP, Boeijinga PH, and Lohman AH. Anatomic organization and physiology of the limbic cortex. *Physiological reviews* 70: 453-511, 1990.

Martire M, Castaldo P, D'Amico M, Preziosi P, Annunziato L, and Taglialatela M. M channels containing KCNQ2 subunits modulate norepinephrine, aspartate, and GABA release from hippocampal nerve terminals. *J Neurosci* 24: 592-597, 2004.

Masukawa LM, Higashima M, Hart GJ, Spencer DD, and O'Connor MJ. NMDA receptor activation during epileptiform responses in the dentate gyrus of epileptic patients. *Brain research* 562: 176-180, 1991.

Masukawa LM, Higashima M, Kim JH, and Spencer DD. Epileptiform discharges evoked in hippocampal brain slices from epileptic patients. *Brain research* 493: 168-174, 1989.

Mathern GW, Babb TL, Vickrey BG, Melendez M, and Pretorius JK. The clinical-pathogenic mechanisms of hippocampal neuron loss and surgical outcomes in temporal lobe epilepsy. *Brain* 118 (Pt 1): 105-118, 1995.

Mathern GW, Mendoza D, Lozada A, Pretorius JK, Dehnes Y, Danbolt NC, Nelson N, Leite JP, Chimelli L, Born DE, Sakamoto AC, Assirati JA, Fried I, Peacock WJ, Ojemann GA, and Adelson PD. Hippocampal GABA and glutamate transporter immunoreactivity in patients with temporal lobe epilepsy. *Neurology* 52: 453-472, 1999.

Mattia D, Hwa GG, and Avoli M. Membrane properties of rat subicular neurons in vitro. *J Neurophysiol* 70: 1244-1248, 1993.

McIntyre DC, Kelly ME, and Staines WA. Efferent projections of the anterior perirhinal cortex in the rat. *J Comp Neurol* 369: 302-318, 1996.

Meldrum BS. Excitotoxicity and selective neuronal loss in epilepsy. *Brain pathology (Zurich, Switzerland)* 3: 405-412, 1993.

Menendez de la Prida L, Suarez F, and Pozo MA. The effect of different morphological sampling criteria on the fraction of bursting cells recorded in the rat subiculum in vitro. *Neurosci Lett* 322: 49-52, 2002.

Mesulam MM, and Mufson EJ. Insula of the old world monkey. I. Architectonics in the insulo-orbito-temporal component of the paralimbic brain. *J Comp Neurol* 212: 1-22, 1982a.

Mesulam MM, and Mufson EJ. Insula of the old world monkey. III: Efferent cortical output and comments on function. *J Comp Neurol* 212: 38-52, 1982b.

Monyer H, Burnashev N, Laurie DJ, Sakmann B, and Seeburg PH. Developmental and regional expression in the rat brain and functional properties of four NMDA receptors. *Neuron* 12: 529-540, 1994.

Mothet JP, Parent AT, Wolosker H, Brady RO, Jr., Linden DJ, Ferris CD, Rogawski MA, and Snyder SH. D-serine is an endogenous ligand for the glycine site of the N-methyl-D-aspartate receptor. *Proceedings of the National Academy of Sciences of the United States of America* 97: 4926-4931, 2000.

Nagao T, Alonso A, and Avoli M. Epileptiform activity induced by pilocarpine in the rat hippocampal-entorhinal slice preparation. *Neuroscience* 72: 399-408, 1996.

Niessen HG, Angenstein F, Vielhaber S, Frisch C, Kudin A, Elger CE, Heinze HJ, Scheich H, and Kunz WS. Volumetric magnetic resonance imaging of functionally relevant structural alterations in chronic epilepsy after pilocarpine-induced status epilepticus in rats. *Epilepsia* 46: 1021-1026, 2005.

Nowak L, Bregestovski P, Ascher P, Herbet A, and Prochiantz A. Magnesium gates glutamate-activated channels in mouse central neurones. *Nature* 307: 462-465, 1984.

Nusser Z, and Mody I. Selective modulation of tonic and phasic inhibitions in dentate gyrus granule cells. *J Neurophysiol* 87: 2624-2628, 2002.

O'Mara S. The subiculum: what it does, what it might do, and what neuroanatomy has yet to tell us. *Journal of anatomy* 207: 271-282, 2005.

O'Mara SM, Commins S, Anderson M, and Gigg J. The subiculum: a review of form, physiology and function. *Prog Neurobiol* 64: 129-155, 2001.

Ohara PT, Granato A, Moallem TM, Wang BR, Tillet Y, and Jasmin L. Dopaminergic input to GABAergic neurons in the rostral agranular insular cortex of the rat. *Journal of neurocytology* 32: 131-141, 2003.

Palma E, Amici M, Sobrero F, Spinelli G, Di Angelantonio S, Ragozzino D, Mascia A, Scoppetta C, Esposito V, Miledi R, and Eusebi F. Anomalous levels of Cl- transporters in the hippocampal subiculum from temporal lobe epilepsy patients make GABA excitatory. *Proceedings of the National Academy of Sciences of the United States of America* 103: 8465-8468, 2006.

Pare D, deCurtis M, and Llinas R. Role of the hippocampal-entorhinal loop in temporal lobe epilepsy: extra- and intracellular study in the isolated guinea pig brain in vitro. *J Neurosci* 12: 1867-1881, 1992.

Parent JM, Elliott RC, Pleasure SJ, Barbaro NM, and Lowenstein DH. Aberrant seizure-induced neurogenesis in experimental temporal lobe epilepsy. *Ann Neurol* 59: 81-91, 2006.

Parent JM, Janumpalli S, McNamara JO, and Lowenstein DH. Increased dentate granule cell neurogenesis following amygdala kindling in the adult rat. *Neurosci Lett* 247: 9-12, 1998.

Penfield W, and Jasper W. *Epilepsy and the functional anatomy of the human brain*. Boston: Little, Brown, 1954.

Peng Z, Huang CS, Stell BM, Mody I, and Houser CR. Altered expression of the delta subunit of the GABAA receptor in a mouse model of temporal lobe epilepsy. *J Neurosci* 24: 8629-8639, 2004.

Perreault P, and Avoli M. 4-aminopyridine-induced epileptiform activity and a GABA-mediated long-lasting depolarization in the rat hippocampus. *J Neurosci* 12: 104-115, 1992.

Priel MR, dos Santos NF, and Cavalheiro EA. Developmental aspects of the pilocarpine model of epilepsy. *Epilepsy Res* 26: 115-121, 1996.

Proper EA, Hoogland G, Kappen SM, Jansen GH, Rensen MG, Schrama LH, van Veelen CW, van Rijen PC, van Nieuwenhuizen O, Gispen WH, and de Graan PN. Distribution of glutamate transporters in the hippocampus of patients with pharmaco-resistant temporal lobe epilepsy. *Brain* 125: 32-43, 2002.

Racine RJ. Modification of seizure activity by electrical stimulation. II. Motor seizure. *Electroencephalography and clinical neurophysiology* 32: 281-294, 1972.

Ragozzino D, Palma E, Di Angelantonio S, Amici M, Mascia A, Arcella A, Giangaspero F, Cantore G, Di Gennaro G, Manfredi M, Esposito V, Quarato PP, Miledi R, and Eusebi F. Rundown of GABA type A receptors is a dysfunction associated with human drug-resistant mesial temporal lobe epilepsy. *Proceedings of the National Academy of Sciences of the United States of America* 102: 15219-15223, 2005.

Reckziegel G, Beck H, Schramm J, Elger CE, and Urban BW. Electrophysiological characterization of Na+ currents in acutely isolated human hippocampal dentate granule cells. *J Physiol* 509 (Pt 1): 139-150, 1998.

Reep RL, and Winans SS. Afferent connections of dorsal and ventral agranular insular cortex in the hamster Mesocricetus auratus. *Neuroscience* 7: 1265-1288, 1982.

Regesta G, and Tanganelli P. Clinical aspects and biological bases of drug-resistant epilepsies. *Epilepsy Res* 34: 109-122, 1999.

Reil J. Untersuchungen uber den Bau des grossen Gehirns im menschenÐVierte Forsetzung Viii. *Archives of Physiology,* 9: 136-146, 1809.

Remy S, and Beck H. Molecular and cellular mechanisms of pharmacoresistance in epilepsy. *Brain* 129: 18-35, 2006.

Represa A, and Ben-Ari Y. Trophic actions of GABA on neuronal development. *Trends in neurosciences* 28: 278-283, 2005.

Rivera C, Li H, Thomas-Crusells J, Lahtinen H, Viitanen T, Nanobashvili A, Kokaia Z, Airaksinen MS, Voipio J, Kaila K, and Saarma M. BDNF-induced TrkB activation down-regulates the K+-Cl- cotransporter KCC2 and impairs neuronal Cl- extrusion. *The Journal of cell biology* 159: 747-752, 2002.

Rivera C, Voipio J, Payne JA, Ruusuvuori E, Lahtinen H, Lamsa K, Pirvola U, Saarma M, and Kaila K. The K+/Cl- co-transporter KCC2 renders GABA hyperpolarizing during neuronal maturation. *Nature* 397: 251-255, 1999.

Rivera C, Voipio J, Thomas-Crusells J, Li H, Emri Z, Sipila S, Payne JA, Minichiello L, Saarma M, and Kaila K. Mechanism of activity-dependent downregulation of the neuron-specific K-Cl cotransporter KCC2. *J Neurosci* 24: 4683-4691, 2004.

Roch C, Leroy C, Nehlig A, and Namer IJ. Magnetic resonance imaging in the study of the lithium-pilocarpine model of temporal lobe epilepsy in adult rats. *Epilepsia* 43: 325-335, 2002.

Rossi DJ, Oshima T, and Attwell D. Glutamate release in severe brain ischaemia is mainly by reversed uptake. *Nature* 403: 316-321, 2000.

Rutecki PA, Grossman RG, Armstrong D, and Irish-Loewen S. Electrophysiological connections between the hippocampus and entorhinal cortex in patients with complex partial seizures. *J Neurosurg* 70: 667-675, 1989.

Rutecki PA, and Yang Y. Ictal epileptiform activity in the CA3 region of hippocampal slices produced by pilocarpine. *J Neurophysiol* 79: 3019-3029, 1998.

Ruth RE, Collier TJ, and Routtenberg A. Topographical relationship between the entorhinal cortex and the septotemporal axis of the dentate gyrus in rats: II. Cells projecting from lateral entorhinal subdivisions. *J Comp Neurol* 270: 506-516, 1988.

Salmenpera T, Kalviainen R, Partanen K, Mervaala E, and Pitkanen A. MRI volumetry of the hippocampus, amygdala, entorhinal cortex, and perirhinal cortex after status epilepticus. *Epilepsy Res* 40: 155-170, 2000.

Sanabria ER, Su H, and Yaari Y. Initiation of network bursts by Ca2+-dependent intrinsic bursting in the rat pilocarpine model of temporal lobe epilepsy. *J Physiol* 532: 205-216, 2001.

Scharfman HE, Goodman JH, Du F, and Schwarcz R. Chronic changes in synaptic responses of entorhinal and hippocampal neurons after amino-oxyacetic acid (AOAA)-induced entorhinal cortical neuron loss. *Journal of neurophysiology* 80: 3031-3046, 1998.

Scharfman HE, Goodman JH, and Sollas AL. Actions of brain-derived neurotrophic factor in slices from rats with spontaneous seizures and mossy fiber sprouting in the dentate gyrus. *J Neurosci* 19: 5619-5631, 1999.

Scharfman HE, Goodman JH, and Sollas AL. Granule-like neurons at the hilar/CA3 border after status epilepticus and their synchrony with area CA3 pyramidal cells: functional implications of seizure-induced neurogenesis. *J Neurosci* 20: 6144-6158, 2000.

Scharfman HE, Sollas AL, Smith KL, Jackson MB, and Goodman JH. Structural and functional asymmetry in the normal and epileptic rat dentate gyrus. *J Comp Neurol* 454: 424-439, 2002.

Schuchmann S, Buchheim K, Meierkord H, and Heinemann U. A relative energy failure is associated with low-Mg2+ but not with 4-aminopyridine induced seizure-like events in entorhinal cortex. *J Neurophysiol* 81: 399-403, 1999.

Schumacher TB, Beck H, Steinhauser C, Schramm J, and Elger CE. Effects of phenytoin, carbamazepine, and gabapentin on calcium channels in hippocampal granule cells from patients with temporal lobe epilepsy. *Epilepsia* 39: 355-363, 1998.

Schwartzkroin PA, and Knowles WD. Intracellular study of human epileptic cortex: in vitro maintenance of epileptiform activity? *Science* 223: 709-712, 1984.

Shah MM, Anderson AE, Leung V, Lin X, and Johnston D. Seizure-induced plasticity of h channels in entorhinal cortical layer III pyramidal neurons. *Neuron* 44: 495-508, 2004.

Shashidharan P, Huntley GW, Meyer T, Morrison JH, and Plaitakis A. Neuron-specific human glutamate transporter: molecular cloning, characterization and expression in human brain. *Brain research* 662: 245-250, 1994.

Sheng M, Cummings J, Roldan LA, Jan YN, and Jan LY. Changing subunit composition of heteromeric NMDA receptors during development of rat cortex. *Nature* 368: 144-147, 1994.

Shi CJ, and Cassell MD. Cascade projections from somatosensory cortex to the rat basolateral amygdala via the parietal insular cortex. *J Comp Neurol* 399: 469-491, 1998.

Sierra-Paredes G, Galan-Valiente J, Vazquez-Illanes MD, Aguilar-Veiga E, Soto-Otero R, Mendez-Alvarez E, and Sierra-Marcuno G. Extracellular amino acids in the rat hippocampus during picrotoxin threshold seizures in chronic microdialysis experiments. *Neurosci Lett* 248: 53-56, 1998.

Smolders I, Khan GM, Lindekens H, Prikken S, Marvin CA, Manil J, Ebinger G, and Michotte Y. Effectiveness of vigabatrin against focally evoked pilocarpine-induced seizures and concomitant changes in extracellular hippocampal and cerebellar glutamate, gamma-aminobutyric acid and dopamine levels, a microdialysis-electrocorticography study in freely moving rats. *The Journal of pharmacology and experimental therapeutics* 283: 1239-1248, 1997.

Spencer SS, and Spencer DD. Entorhinal-hippocampal interactions in medial temporal lobe epilepsy. *Epilepsia* 35: 721-727, 1994.

Staba RJ, Wilson CL, Bragin A, Fried I, and Engel J, Jr. Sleep states differentiate single neuron activity recorded from human epileptic hippocampus, entorhinal cortex, and subiculum. *J Neurosci* 22: 5694-5704, 2002.

Stief F, Zuschratter W, Hartmann K, Schmitz D, and Draguhn A. Enhanced synaptic excitation-inhibition ratio in hippocampal interneurons of rats with temporal lobe epilepsy. *Eur J Neurosci* 25: 519-528, 2007.

Strowbridge BW, Masukawa LM, Spencer DD, and Shepherd GM. Hyperexcitability associated with localizable lesions in epileptic patients. *Brain research* 587: 158-163, 1992.

Swanson LW, and Kohler C. Anatomical evidence for direct projections from the entorhinal area to the entire cortical mantle in the rat. *J Neurosci* 6: 3010-3023, 1986.

Swanson LW, Wyss JM, and Cowan WM. An autoradiographic study of the organization of intrahippocampal association pathways in the rat. *J Comp Neurol* 181: 681-715, 1978.

Tamamaki N, and Nojyo Y. Preservation of topography in the connections between the subiculum, field CA1, and the entorhinal cortex in rats. *J Comp Neurol* 353: 379-390, 1995.

Tessler S, Danbolt NC, Faull RL, Storm-Mathisen J, and Emson PC. Expression of the glutamate transporters in human temporal lobe epilepsy. *Neuroscience* 88: 1083-1091, 1999.

Theodore WH, Spencer SS, Wiebe S, Langfitt JT, Ali A, Shafer PO, Berg AT, and Vickrey BG. Epilepsy in North America: a report prepared under the auspices of the global campaign against epilepsy, the International Bureau for Epilepsy, the International League Against Epilepsy, and the World Health Organization. *Epilepsia* 47: 1700-1722, 2006.

Thompson SE, Ayman G, Woodhall GL, and Jones RS. Depression of Glutamate and GABA Release by Presynaptic GABA(B) Receptors in the Entorhinal Cortex in Normal and Chronically Epileptic Rats. *Neurosignals* 15: 202-215, 2007.

Tolner EA, Kloosterman F, van Vliet EA, Witter MP, Silva FH, and Gorter JA. Presubiculum stimulation in vivo evokes distinct oscillations in superficial and deep entorhinal cortex layers in chronic epileptic rats. *J Neurosci* 25: 8755-8765, 2005.

Tortorella A, Halonen T, Sahibzada N, and Gale K. A crucial role of the alpha-amino-3-hydroxy-5-methylisoxazole-4-propionic acid subtype of glutamate receptors in piriform and perirhinal cortex for the initiation and propagation of limbic motor seizures. *The Journal of pharmacology and experimental therapeutics* 280: 1401-1405, 1997.

Tu B, Timofeeva O, Jiao Y, and Nadler JV. Spontaneous release of neuropeptide Y tonically inhibits recurrent mossy fiber synaptic transmission in epileptic brain. *J Neurosci* 25: 1718-1729, 2005.

Tyzio R, Cossart R, Khalilov I, Minlebaev M, Hubner CA, Represa A, Ben-Ari Y, and Khazipov R. Maternal oxytocin triggers a transient inhibitory switch in GABA signaling in the fetal brain during delivery. *Science* 314: 1788-1792, 2006.

Urban L, Aitken PG, Friedman A, and Somjen GG. An NMDA-mediated component of excitatory synaptic input to dentate granule cells in 'epileptic' human hippocampus studied in vitro. *Brain research* 515: 319-322, 1990.

Uruno K, O'Connor MJ, and Masukawa LM. Alterations of inhibitory synaptic responses in the dentate gyrus of temporal lobe epileptic patients. *Hippocampus* 4: 583-593, 1994.

Uva L, Librizzi L, Wendling F, and de Curtis M. Propagation dynamics of epileptiform activity acutely induced by bicuculline in the hippocampal-parahippocampal region of the isolated Guinea pig brain. *Epilepsia* 46: 1914-1925, 2005.

van Vliet EA, Aronica E, Tolner EA, Lopes da Silva FH, and Gorter JA. Progression of temporal lobe epilepsy in the rat is associated with immunocytochemical changes in inhibitory interneurons in specific regions of the hippocampal formation. *Exp Neurol* 187: 367-379, 2004.

van Vliet EA, da Costa Araujo S, Redeker S, van Schaik R, Aronica E, and Gorter JA. Blood-brain barrier leakage may lead to progression of temporal lobe epilepsy. *Brain* 130: 521-534, 2007.

VanLandingham KE, Heinz ER, Cavazos JE, and Lewis DV. Magnetic resonance imaging evidence of hippocampal injury after prolonged focal febrile convulsions. *Ann Neurol* 43: 413-426, 1998.

Vreugdenhil M, Hoogland G, van Veelen CW, and Wadman WJ. Persistent sodium current in subicular neurons isolated from patients with temporal lobe epilepsy. *Eur J Neurosci* 19: 2769-2778, 2004.

Walther H, Lambert JD, Jones RS, Heinemann U, and Hamon B. Epileptiform activity in combined slices of the hippocampus, subiculum and entorhinal cortex during perfusion with low magnesium medium. *Neurosci Lett* 69: 156-161, 1986.

Wellmer J, Su H, Beck H, and Yaari Y. Long-lasting modification of intrinsic discharge properties in subicular neurons following status epilepticus. *Eur J Neurosci* 16: 259-266, 2002.

Wiebe S, Blume WT, Girvin JP, and Eliasziw M. A randomized, controlled trial of surgery for temporal-lobe epilepsy. *N Engl J Med* 345: 311-318, 2001.

Williams PA, Wuarin JP, Dou P, Ferraro DJ, and Dudek FE. Reassessment of the effects of cycloheximide on mossy fiber sprouting and epileptogenesis in the pilocarpine model of temporal lobe epilepsy. *J Neurophysiol* 88: 2075-2087, 2002.

Wilson WA, Swartzwelder HS, Anderson WW, and Lewis DV. Seizure activity in vitro: a dual focus model. *Epilepsy Res* 2: 289-293, 1988.

Witter MP, Groenewegen HJ, Lopes da Silva FH, and Lohman AH. Functional organization of the extrinsic and intrinsic circuitry of the parahippocampal region. *Progress in neurobiology* 33: 161-253, 1989.

Witter MP, Ostendorf RH, and Groenewegen HJ. Heterogeneity in the Dorsal Subiculum of the Rat. Distinct Neuronal Zones Project to Different Cortical and Subcortical Targets. *Eur J Neurosci* 2: 718-725, 1990.

Witter MP, Wouterlood FG, Naber PA, and Van Haeften T. Anatomical organization of the parahippocampal-hippocampal network. *Annals of the New York Academy of Sciences* 911: 1-24, 2000.

Woodhall GL, Bailey SJ, Thompson SE, Evans DI, and Jones RS. Fundamental differences in spontaneous synaptic inhibition between deep and superficial layers of the rat entorhinal cortex. *Hippocampus* 15: 232-245, 2005.

Woodin MA, Ganguly K, and Poo MM. Coincident pre- and postsynaptic activity modifies GABAergic synapses by postsynaptic changes in Cl- transporter activity. *Neuron* 39: 807-820, 2003.

Wozny C, Gabriel S, Jandova K, Schulze K, Heinemann U, and Behr J. Entorhinal cortex entrains epileptiform activity in CA1 in pilocarpine-treated rats. *Neurobiol Dis* 19: 451-460, 2005.

Wozny C, Kivi A, Lehmann TN, Dehnicke C, Heinemann U, and Behr J. Comment on "On the origin of interictal activity in human temporal lobe epilepsy in vitro". *Science* 301: 463; author reply 463, 2003.

Yang J, Woodhall GL, and Jones RS. Tonic facilitation of glutamate release by presynaptic NR2B-containing NMDA receptors is increased in the entorhinal cortex of chronically epileptic rats. *J Neurosci* 26: 406-410, 2006.

Ziburkus J, Cressman JR, Barreto E, and Schiff SJ. Interneuron and pyramidal cell interplay during in vitro seizure-like events. *J Neurophysiol* 95: 3948-3954, 2006.

Chapter 1: Subiculum Network Excitability is Increased in a Rodent Model of Temporal Lobe Epilepsy

1.0 Linking Text & Information About Publication

The subiculum occupies a pivotal location, within the limbic system, as the primary structural output of the hippocampal trisynaptic loop. *In vitro* investigations indicate the inhibitory network properties of the subiculum attenuate CA1 inputs and thus subsequent hippocampal output activity. However, this inhibitory gating function is altered in pilocarpine treated tissue and may serve to amplify limbic seizures via entorhinal cortical interactions (D'Antuono et. al,2002; Wozny et al., 2005). Complimentary to this viewpoint, *in vitro* studies in the human epileptic subiculum indicate modified $GABA_A$ receptor mediated mechanisms promote spontaneous epileptiform discharges (Cohen et al., 2002).

In our studies of the pilocarpine treated subiculum we addressed the network interactions of the epileptic subiculum with CA1 and the entorhinal cortex. We further investigated whether perturbations in $GABA_A$ receptor mediated inhibition occur in the pilocapine treated subiculum and whether alterations occur at the level of the KCC2.

1.1 Abstract

In this study we used *in vitro* electrophysiology along with immunohistochemistry and molecular techniques to study the subiculum - a limbic structure that gates the information flow from and to the hippocampus - in pilocarpine-treated epileptic rats. Comparative data were obtained from age-matched non-epileptic controls (NEC). Subicular neurons in hippocampal-entorhinal cortex slices of epileptic rats: (i) were hyperexcitable when activated by CA1 or EC inputs; and (ii) generated spontaneous postsynaptic potentials at higher frequencies than NEC cells. Analysis of

pharmacologically isolated, $GABA_A$ receptor-mediated inhibitory post-synaptic potentials revealed more positive reversal potentials in epileptic tissue (-67.8±6.3 mV, n=16 *vs.* -74.8±3.6 mV in NEC, n=13; $p<0.001$) combined with a reduction in peak conductance (17.6±11.3 nS *vs.* 41.1±26.7 nS in NEC; $p<0.003$). These electrophysiological data correlated in the epileptic subiculum with (i) reduced levels of mRNA expression and immunoreactivity of the neuron-specific potassium-chloride cotransporter 2; (ii) decreased number of parvalbumin-positive cells; and (iii) increased synaptophysin (a putative marker of sprouting) immunoreactivity. These findings identify an increase in network excitability within the subiculum of pilocarpine-treated, epileptic rats and point at a reduction in inhibition as an underlying mechanism.

1.2 Introduction

Temporal lobe epilepsy (TLE) patients present with limbic seizures that involve the temporal neocortex and deep limbic structures such as the hippocampus, amygdala and entorhinal cortex (EC) (Bragin et al., 2005; Spencer and Spencer 1994). A common finding in this epileptic disorder is a pattern of neuronal damage (termed mesial temporal sclerosis or Ammon's horn sclerosis) characterized by neuronal loss in the CA1/CA3 subfields and dentate hilus, EC layer III and amygdala (Mathern et al., 1995; Houser, 1999). Similar histopathological patterns are observed in laboratory animals following treatment with convulsants such as pilocarpine (Turski et al., 1983) or kainic acid (Tuunanene et al., 1999), as well as subsequent to repetitive electrical stimulation (Sloviter, 1987; Gorter et al., 2001; Nissinen et al., 2000). These procedures induce an initial convulsive response that is followed within approximately 2 weeks by recurrent limbic seizures.

Limbic network hyperexcitability in TLE and animal models mimicking this disorder is associated with dysfunction of voltage-gated currents (Su et al., 2002; Shah et al., 2005), synaptic reorganization (Sutula et al., 1988, 1989; Houser et al., 1990; Perez et al., 1996), and alterations in GABA receptor-mediated inhibition (Buhl et al., 1996; Doherty and Dingledine, 2001; Williams et al 1993, Khalilov et al., 2003, Kobayashi et al., 2003). These investigations have been centered upon the hippocampal subdivisions CA1 and CA3, and the dentate gyrus. However, the subiculum has recently been demonstrated to play a fundamental role in experimental models of TLE (D'Antuono et al., 2002; Wellmer et al., 2002; Knopp et al., 2005; Biagini et al., 2005). In line with this view, spontaneous interictal activity has been shown to occur in the human epileptic subiculum in an *in vitro* slice preparation (Cohen et al., 2002; Wozny et al., 2003), while Vreugdenhil et al. (2004) reported augmented voltage-gated, Na^+ persistent current in human subicular cells. Overall, this evidence indicates that the subiculum may play a fundamental role in epileptiform synchronization and thus in the generation of limbic seizures in TLE patients. Hence, in this study, electrophysiological recordings in conjunction with molecular and histochemical analysis were used to determine whether GABAergic mechanisms are altered in the epileptic rat subiculum. Data obtained from epileptic animals treated with pilocarpine were compared with those from age-matched, non epileptic controls (NECs).

1.3 Methods

1.3.1 Preparation of pilocarpine treated rats

Procedures approved by the Canadian Council of Animal Care were used to induce *status epilepticus* (SE) in adult male Sprague-Dawley rats weighing 150-200g at the time of injection. All efforts were made to minimize the number of animals used and

their suffering. Briefly, rats were injected with a single dose of pilocarpine hydrochloride (380-400mg/Kg, i.p). To reduce the discomforts caused by peripheral activation of muscarinic receptors, methyl scopolamine (1mg/Kg i.p) was administered 30 min prior to the pilocarpine injection. The animals' behavior was monitored for approx. 4 h following pilocarpine and scored according to Racine's classification (Racine et al., 1972). Only rats that experienced SE (stage 3-5) for 30 minutes or more (48.6±8.3 min, mean±SEM) were included in the pilocarpine group and used for *in vitro* electrophysiological studies approximately 4 months (17±1week; n=27 rats) following the pilocarpine injection. Since it has been previously established (Cavalheiro et al., 1991; Priel et al., 1996) that all adult rats that experience pilocarpine-induced SE later exhibit spontaneous recurrent seizures, only a subset of animals from the pilocarpine group were video-monitored and the presence of spontaneous behavioral seizures was confirmed in virtually all of them (n=11 out of 12 rats). In this study, rats receiving a saline injection instead of pilocarpine were used as NECs.

1.3.2 Electrophysiology procedures

Brain slices from NEC and pilocarpine-treated epileptic rats were obtained according to the procedures established by the Canadian Council of Animal Care. Rats were decapitated under halothane anesthesia, the brain was extracted and placed in cold (1-3°C) oxygenated artificial cerebrospinal fluid (ACSF). Horizontal brain slices (450 μm-thick) that included the EC, the subiculum and the hippocampus proper, were cut with a vibratome along the horizontal plane of the brain that was tilted by approx. 10° along a posterosuperior-anteroinferior plane passing between the lateral olfactory tract and the brain stem base. Combined hippocampal-EC slices were transferred to

an interface tissue chamber and superfused with oxygenated (95%O_2, 5%CO_2) ACSF at 32-34°C. ACSF composition was (in mM): NaCl 124, KCl 2, KH_2PO_4 1.25, $MgSO_4$ 2, $CaCl_2$ 2, $NaHCO_3$ 26, and glucose 10. 3,3-(2-carboxypiperazin-4-yl)-propyl-1-phosphonate (CPP, 10 μM) and 6-Cyano-7-nitroquinoxaline-2,3-dione (CNQX, 10 μM) were bath applied. Chemicals were acquired from Sigma-Aldrich Canada Ltd. (Oakville, Ontario, Canada) and Tocris Cookson Inc. (Ellisville, MO, USA).

Field potential recordings were performed with ACSF-filled glass electrodes (tip diameter: <8 μm; resistance: 2–10 MΩ) that were connected to a Cyberamp 380 amplifier (Axon Instruments, Union City, CA, USA). Intracellular sharp-electrodes were filled with 3M potassium acetate (tip resistance: 90-120 MΩ) and coupled to an Axoclamp 2A amplifier (Axon Instruments) with an internal bridge circuit for intracellular current injection. The resistance compensation was monitored throughout the experiment and adjusted as required. The fundamental electrophysiological parameters of the subicular and the EC neurons included in this study were measured as follows: (i) resting membrane potential (RMP) after cell withdrawal (ii) apparent input resistance (Ri) from the maximum voltage change in response to a hyperpolarizing current pulse (< -0.5 nA) (iii) action potential amplitude (APA) and (iv) action potential duration (APD). Activation of neuronal networks was performed via a concentric bipolar electrode (Frederick Haer and Co., Bowdoinham, ME, USA) that was positioned in CA1 stratum radiatum (Fig. 3 and Fig. 4), layer III of the lateral EC (Fig. 5) or subiculum. In all experiments, the minimum stimulus intensity (duration= 100 μs) that produced a reliable response was selected.

Field potential and intracellular signals were fed to a computer interface (Digidata 1322A, Axon Instruments) and were acquired and stored using the pClamp 8.0 software (Axon Instruments). Subsequent analysis of these data was performed

with the Clampfit 9 software (Axon Instruments). The reversal potential of spontaneous post-synaptic potentials (PSPs) and stimulus-induced, pharmacologically isolated inhibitory post synaptic potentials (IPSPs) was determined by linear regression from the plot of their amplitude versus membrane potential. The peak conductance of the latter responses was calculated by linear regression analysis from the plot of the relation between injected current and membrane potential deflections before and after the extracellular stimulus at latencies of approx. 10 ms (*cf.*, Williams et al., 1993).

1.3.3 Real-Time PCR

Total RNA was prepared from EC and subiculum of NEC and pilocarpine-treated epileptic rats using Trizol (Invitrogen, Milano, Italy). The total RNA was run on a 2% agarose gel and quantified by densitometric analysis using the Gel Doc, Biorad (Milano, Italy). Total RNA (1 µg) was reverse transcribed using the first-strand synthesis system for RT-PCR (Superscript, Invitrogen). Relative Real-Time PCR was performed in a Real-Time Thermocycler (MX 3000, Stratagene, Milano, Italy) using the Brilliant SYBR Green QPCR Master Mix according to manufacturer instructions. All PCR reactions were coupled to melting-curve analysis to confirm the specificity of amplification. Quantitative data were normalized to expression of housekeeping gene beta-actin. Specific primers for rat potassium-chloride cotransporter 2 (KCC2) and beta-actin were designed to amplify short DNA fragments (beta-actin forward 5'-aggcatcctgaccctgaagtac-3'; beta-actin reverse 5'- gaggcatacagggacaacacag-3'; KCC2 forward 5'-ttcatcaacagcacggacac-3'; KCC2 reverse 5'-cttcttctttccgccctcat-3'). The relative quantitation was analyzed with the software that accompanied the thermal cycler.

1.3.3 Histopathology procedures

For morphological studies, pilocarpine-treated and NEC animals were anesthetized (chloral-hydrate 450 mg/kg i.p.) and perfused via the ascending aorta with 100 ml saline followed by 300 ml 4% paraformaldehyde dissolved in 0.1 M phosphate buffer (pH 7.4). After dissection, the brains were postfixed for an additional 4 h in the same fixative at 4°C. After cryoprotection by immersion in 15% and 30% sucrose-phosphate buffer solutions, the brains were frozen and cut horizontally from the ventral side by a freezing microtome.

Differences in KCC2 immunoreactivity were assessed with a polyclonal antibody (Upstate, NY, USA) that has been shown to be specific (Vale et al., 2003; Grob and Mouginot, 2005; Lohrke et al., 2005). In addition, changes in the parvalbumin-positive interneuron subpopulation - which is critically involved in TLE (de Felipe et al., 1993) - were investigated by using a mouse monoclonal antibody (Swant, Bellinzona, CH). We also analyzed the changes in synaptophysin, a putative marker of functionally active sprouted nerve terminals (Proper et al., 2000) by employing a previously characterized rabbit polyclonal antibody for synaptophysin (Bahler et al., 1991; kindly provided by Dr. F. Benfenati, Genua, Italy). Antibodies for KCC2 (1:1000), parvalbumin (diluted 1:2000), and synaptophysin (1:5000) were used on 50 μm-thick horizontal sections obtained, respectively, at levels 7.3-7.6 from bregma. Some sections (one section out of four, four series for each animal) were stained with toluidine blue to clearly identify the various anatomical regions of the hippocampal formation and to assess the presence of neuronal damage (see Fig. 1A). Immunohistochemistry was performed using the avidin-biotin complex technique and diaminobenzidine as chromogen (*cf.*, Biagini et al., 2005). Endogenous

peroxidase was blocked by 0.1% phenylhydrazine in phosphate buffered saline (PBS) for 20 min, followed by several washes in PBS preceding the incubation with primary antibodies. Secondary antibodies and the avidin-peroxidase complex were purchased from Amersham Italia (Milan, Italy) and diluted 1:200 and 1:300 respectively. The stained sections were analyzed by densitometry using image analysis software (KS 300, Zeiss Kontron, Munich, Germany) (*cf.*, Biagini et al., 2001; 2005). Four sections for each animal were investigated and averaged for statistical analysis. Briefly, the value of non-specific mean gray tone was measured in an area of the slide immediately outside the section close, respectively, to subiculum or EC (Fig. 1A,B). An area of the angular bundle was taken as index of background labelling (Fig. 1B), since KCC2 and synaptophysin are not detectable in axons and glial cells (Bahler et al., 1991; Williams et al., 1999). Mean gray values of specific immunostaining were measured in subicular and EC areas identified as follows. The subiculum was defined by its enlarged and loosely packed pyramidal layer, clearly distinguishable from the narrow pyramidal cell layer of CA1 in toluidine blue-stained sections (Fig. 1A), and by differences in neuronal cell size when compared with the presubiculum; in addition, we divided the subiculum into two halves: the one close to CA1 was defined as proximal subiculum, while that close to presubiculum was defined as distal subiculum (Fig. 1B) (*cf.* Naber et al., 2001). The EC was identified by its classical lamination in six layers and, particularly, by the presence of the more intensely stained layer II that, when continuous, marked the medial EC or, when discontinuous because of the "islandic" neuronal organization (Witter 1993), marked the lateral EC (delimited by arrowheads in Fig. 1A). To measure mean grey tone values using the KS 300 software, these areas were manually selected (Fig. 1B) by an expert neuroanatomist (G.B.) that was blinded to animal codes. Transmittance percentage values (T%) of

total and non-specific staining were then obtained by dividing the mean grey tone value of every area analyzed by the mean grey tone value of the background. Optical density (OD) values were then calculated according to the formula OD = -log T%, for both non-specific grey tone values and specifically labeled areas. The specific OD was obtained by deducting non-specific OD from total OD for each studied region (Biagini et al., 2001). Neuronal counts of parvalbumin-positive interneurons was as described by Biagini et al. (2005). Sections were used for parvalbumin immunostaining were then rehydrated through various passages in decreasing ethanol solutions, counterstained with toluidine blue, and analysed by the KS 300 software to measure the subicular area.

1.3.4 Statistical method

Measurements in the text are expressed as mean±S.E.M. and *n* indicates the number of samples studied under each specific protocol. The results obtained were compared with the Student's t-test or Mann-Whitney test and were considered statistically significant if $p<0.05$.

1.4 Results

1.4.1 Unaltered intrinsic cellular properties in NEC and pilocarpine-treated subiculum

As previously shown (Mattia et al., 1997; Su et al., 2002; Knopp et al., 2005), intracellular injection of depolarizing current pulses (duration= 1s) induced two patterns of firing in subicular neurons recorded in NEC and pilocarpine-treated slices. The first consisted of an initial burst of action potentials followed by regular firing (Fig.

2Aa and Ba), while the second was characterized by regular, repetitive firing only (Fig. 2 Ab and Bb). Quantification of the incidence of these two firing patterns demonstrated similar proportions in pilocarpine-treated (intrinsic bursting, n= 16; regular firing, n= 13) and in NEC (intrinsic bursting, n= 14; regular firing n= 14) tissue. In addition, subicular neurons recorded in the two types of tissue displayed similar fundamental intrinsic properties (Table 1). As depicted in Fig. 2 (Ac and Bc), steady depolarization of regular firing neurons from RMP to membrane potentials above -54 mV produced the appearance of rhythmic subthreshold oscillations in the theta range (regular firing: NEC= 6.5±0.8 Hz, n=5, pilocarpine= 6.6±1.1 Hz, n=5; intrinsic bursting: NEC= 5.6±0.8 Hz n=5, pilocarpine= 5.9±0.6 Hz, n=5) that were combined with action potential discharge. The membrane potentials at which 'subthreshold' membrane oscillations appeared and the threshold for action potential generation were also similar in NEC and pilocarpine-treated, epileptic subicular neurons (Table 1).

1.4.2 Activation of CA1 inputs demonstrates hyperexcitability within the epileptic subiculum

Single-shock electrical stimuli delivered in the CA1 stratum radiatum of NEC and pilocarpine-treated slices produced similar low amplitude, negative deflecting, field potential responses in subiculum (Fig. 3A and B, Field traces in the top samples). In contrast, remarkable differences could be identified in the recorded intracellular signals. As shown in Fig. 3A (-71 mV trace), CA1 stimulation invariably produced a sequence of depolarizing-hyperpolarizing post-synaptic responses in NEC subicular cells recorded at RMP (n=14); in addition, these stimulus-induced responses became purely depolarizing when the membrane potential was brought to values more negative than -80 mV with injection of steady negative current (Fig. 3A, -81 mV and -

88 mV traces), while at depolarized membrane levels they were characterized by a single action potential followed by a robust hyperpolarization (Fig. 3A, -66 mV). At variance, two types of stimulus-induced intracellular responses were recorded in the pilocarpine-treated subiculum (Fig. 3B). In the first group of neurons (n= 18) single-shock stimuli produced depolarizing post-synaptic activity at both RMP and at hyperpolarized membrane potentials (Fig. 3Ba, -71, -77 and -88 mV traces) while at depolarized membrane values these responses comprised of action potential bursts or doublets (Fig. 3Ba, -65 mV trace). In the second group of pilocarpine-treated subicular cells (n=11), CA1 stimulation elicited bursting responses at RMP or at depolarized membrane values (Fig. 3Bb; -70 and -83 mV traces). Moreover, when action potential bursting was prevented by injecting steady negative current, we identified an underlying slow depolarization that followed the initial excitatory post-synaptic potential (EPSP) (Fig. 3Bb, -92 mV trace). These characteristics were found to be independent of the intrinsic firing properties of subicular cells.

1.4.3 Subicular cells in pilocarpine-treated slices have a lower threshold to synaptic stimuli than in NEC tissue

The findings reported in the previous section suggest that increased network excitability characterizes the pilocarpine-treated, epileptic subiculum. To this end, we compared the input-output curves of the intracellular responses generated by subicular neurons following CA1 single-shock stimuli in NEC and pilocarpine-treated slices. As shown in Fig. 4A, focal stimuli with strength ranging between 100 and 200 μA produced either no or minimal post-synaptic responses in NEC subicular neurons (n= 5). These cells generated overt post-synaptic depolarizations only when the

current intensity was increased to 450 μA, while a single action potential occurred in response to stimuli delivered at ≥500 μA.

In contrast, when this stimulation protocol was applied to pilocarpine-treated slices we could identify a lower activation threshold. Thus, a depolarizing response was elicited by CA1 stimuli with current intensity of 100 μA and then it increased in amplitude following stimuli at 150 μA (Fig. 4B). Moreover, in all pilocarpine-treated subicular neurons (n= 6), single shock stimulation at approx. 200 μA was sufficient to elicit action potential firing characterized by either doublets or bursts of action potentials. To assess network excitability we defined 100% as the current threshold required to elicit depolarizing PSPs prior to action potential spiking. Analysis of the relation between current intensity and depolarizing response amplitude (prior to action potential generation) revealed that pilocarpine-treated subicular cells required significantly less current to generate responses comparable to those in NEC tissue (Fig. 4C).

1.4.4 Activation of EC layer III produces multiphasic activity in the pilocarpine-treated subiculum

We further assessed subicular network excitability in NEC and pilocarpine-treated tissue by analyzing the responses induced by electrical stimuli delivered in EC layer III (Fig. 5). At resting membrane potentials, in NEC slices, extracellular stimulation elicited a low amplitude field response that was paralleled by a monophasic depolarizing PSP with a duration of 101.9±7.3 ms (Fig. 5A; n=13). As illustrated in Figure 5A, sequential injection of steady positive current from -93 mV progressively reduced the amplitude of the depolarizing PSP and unmasked a hyperpolarization at -61 mV. In contrast, focal stimuli in pilocarpine-treated tissue (n=13 cells) consistently

produced multiphasic post-synaptic responses lasting up to 491.9±38.5 ms (Fig. 5B). This activity persisted at hyperpolarized membrane potentials while injection of steady depolarizing current made single action potentials, which were not followed by any hyperpolarizing component, appear (Fig. 5B, -56 mV). The duration of the subicular responses to EC stimuli recorded in NEC and pilocarpine-treated slices is quantified in Fig. 5C ($p<0.0001$).

1.4.5 Spontaneous synaptic activity in NEC and pilocarpine-treated subiculum

As illustrated in Fig. 6A (-73 mV trace), low amplitude spontaneous PSPs comprising depolarizing and hyperpolarizing components, occurred at RMP with intervals of 8.0±0.7 s in NEC subicular neurons (n=12). Hyperpolarizing the membrane of these cells through negative current injection, produced an inversion of the hyperpolarizing component (Fig. 6A, -94 mV trace). In contrast, injection of steady depolarizing current made the depolarizing and hyperpolarizing components of the PSP decrease and increase, respectively, along with the appearance of subthreshold voltage-dependent oscillatory activity (arrows) at membrane potentials less negative than -60 mV (Fig. 6A, -60 mV trace).

Intracellular recordings from pilocarpine-treated subicular cells (n=10) also demonstrated the presence of spontaneous PSPs that, however, had an increased rate of occurrence (intervals= 2.7±0.4 s; $p<0.0001$ independent t-test) when compared with NEC tissue (Fig. 6 B and C). In addition, pilocarpine-treated subicular neurons generated spontaneous depolarizing PSPs both at membrane values of -70 mV (RMP) and of -83 mV (Fig. 5B). Thus, at RMP pilocarpine-treated subicular cells did not exhibit the biphasic EPSP/IPSP sequence observed in NEC tissue. As

illustrated in Fig. 6B (-62 mV), injection of positive current in pilocarpine-treated cells transformed depolarizing PSPs into hyperpolarizing events coinciding with oscillatory activity (arrow) and single action potential spiking. Analysis of the reversal potential of the spontaneous PSPs revealed a more positive value in pilocarpine-treated tissue (-62.4±0.9, n=17) than in NEC (-65.8±0.9 mV, n= 16) ($p<0.02$) (Fig. 6D).

1.4.6 Reversal potential of 'monosynaptic' IPSPs in NEC and pilocarpine-treated subicular neurons

To isolate GABAergic activity we performed intracellular recordings in subicular neurons of NEC and pilocarpine-treated slices in the presence of an NMDA receptor antagonist (CPP= 10 μM) and of an AMPA/kainate receptor blocker (CNQX= 10 μM). Under these pharmacological conditions, focal subicular stimulation elicited a presumptive IPSP that was often characterized by a fast and a slow component (Fig. 7A). Serial application of $GABA_A$ (picrotoxin, 50 μM, n=5) and $GABA_B$ (CGP 35348, 10 μM; n= 4) receptor antagonists demonstrated that the fast component of the stimulus-induced IPSP was $GABA_A$ receptor-mediated (not illustrated). In these experiments we analyzed the stimulus-induced responses recorded at different membrane potentials by injecting pulses of hyperpolarizing and depolarizing current. By doing so we could identify the reversal potential of the stimulus-induced fast IPSP along with the associated peak conductance. Single-shock stimulation in NEC and pilocarpine-treated cells produced $GABA_A$ receptor-mediated IPSP reversal points of -75 mV (Fig. 7C, black dots) and -66 mV (Fig. 7C, open dots), respectively. Analysis of additional samples for the $GABA_A$ receptor-mediated IPSP, revealed a more positive reversal point (-67.8±6.3 mV; n=16, 8 regular fire and 8 intrinsic bursting; $p<0.001$, independent t-test) within the pilocarpine treated subiculum as compared to NEC

tissue (-74.8 ±3.6 mV; n=13, 9 regular firing and 4 intrinsic bursting) (Fig. 7D). Alteration of the IPSP reversal point was mirrored by a significant reduction ($p<0.003$; independent t-test) in the $GABA_A$ receptor mediated IPSP peak conductance in pilocarpine-treated epileptic cells (i.e., 17.6±11.3 nS *vs* 41.5±26.7 nS in NEC) (Fig. 7D).

1.4.7 Reversal potential of 'monosynaptic' IPSPs generated by EC layer V neurons from NEC and pilocarpine-treated rats

Using a similar protocol, we assessed whether $GABA_A$ receptor activity was altered in neurons recorded in EC layer V of epileptic tissue. As shown in Fig. 8, NEC and pilocarpine-treated neurons in this limbic area had similar reversal potentials (i.e., -72.3±3.8 mV, n=7, for NEC and -69.8±5.2 mV, n=13, for pilocarpine-treated EC cells; $p<0.27$, independent t-test). Moreover, the peak conductance of the $GABA_A$ receptor-mediated IPSP was not different ($p<0.89$; independent t-test) in NEC (10.3±4.1 nS, n= 7) and pilocarpine-treated (12.8±8.6 nS, n= 13) EC neurons (Fig. 8D).

1.4.8 Reduced KCC2 expression in the pilocarpine treated subiculum

The more depolarized reversal potential of the $GABA_A$ receptor-mediated IPSP identified in pilocarpine treated subicular cells led us to assess whether the expression of KCC2 was changed. As illustrated in Fig. 9A, RT-PCR analysis revealed a 44.0±6.1% reduction in KCC2 mRNA expression level within the subiculum, but not in the EC of pilocarpine-treated, epileptic rats (n= 5) as compared with NECs (n= 5). We also used a commercially-available antibody reported to be specific for KCC2 (Vale et al., 2003; Grob and Mouginot, 2005; Lohrke et al., 2005). By doing so we could localize in NEC subiculum the presence of KCC2 immunopositivity both in nerve fibers and on the surface of neuronal cell bodies (Fig.

9C); in contrast, the cytoplasm appeared completely devoid of any signal (note that the arrowheads in the inset of Fig. 9C point at neuronal somas that appear white). This localization was consistent with previous reports on KCC2 expression in the mature brain (Lorke et al., 2005; Vale et al., 2005).

Immunohistochemical analysis of the epileptic rat subiculum demonstrated a decrease in KCC2 positivity (Fig. 9D). These findings were also quantified by using optical density analysis. As illustrated in Fig. 9B, we found a significant ($p<0.05$) decrease (-25%) in KCC2 immunoreactivity in the subiculum of epileptic rats (n=9) as compared to NEC (n= 8). Therefore, these findings demonstrate a reduced expression of both mRNA and KCC2 protein in the pilocarpine-treated, epileptic subiculum supporting a malfunction in the extrusion of intracellular Cl^- and thus the different IPSP reversal potential values.

1.4.9 Histopathological evaluation of neuronal damage

Next, we studied whether interneuronal loss or neuronal sprouting were present in the subiculum and EC of pilocarpine-treated, epileptic rats. Parvalbumin-positive cells were found to be homogeneously distributed both in the subiculum (Fig. 10A and B) and in the EC (Fig. 10C and D). However, a reduced area of immunostaining could always be identified in the subiculum of pilocarpine-treated animals.

By counting parvalbumin-positive cells in the ventral subiculum (level 7.6 mm from bregma), we found a significant ($p<0.01$) decrease (-65%) in parvalbumin-stained neurons in pilocarpine-treated rats (n=9) as compared with NECs (n=8) (Fig. 10E). However, the area covered by subicular neurons, measured in toluidine blue-stained sections was only slightly decreased in pilocarpine-treated animals ($0.38\pm0.06 mm^2$) compared with NEC (0.40 ± 0.03 mm^2; not statistically different).

Following the surprising results obtained by counting parvalbumin-positive cells at this level, we decided to further analyze the subiculum considering a dorsal level (3.6 mm from bregma), since the lesion extent was described to vary along the hippocampal longitudinal axis by other authors (Turski et al., 1983). Interestingly, a significant ($p<0.01$) decrease (-40%) was also observed in the dorsal subiculum. However, the area covered by subicular neurons, measured in toluidine blue-stained sections was only slightly decreased in pilocarpine-treated animals ($0.38\pm0.06 mm^2$) compared with NEC (0.40 ± 0.03 mm^2; not statistically different). Parvalbumin-positive cells were also counted in the superficial layers of medial EC and lateral EC in the same ventral sections, but no differences were found between the two groups of animals (Fig. 10, compare NEC in C with pilocarpine-treated in D, as well as quantified data in panel E), thus confirming the results reported by Du et al. (1995).

Finally, we investigated the distribution of immunoreactivity for synaptophysin (Fig. 11), which is considered to be a marker of functionally sprouted nerve fibers (Proper et al., 2000). Here, we found the presence of well-delimited patches of increased immunoreactivity in dentate gyrus, subiculum and EC of pilocarpine-treated rats (arrows in Fig. 11B and corresponding insets). In the dentate gyrus, patches of increased immunoreactivity were localized in the inner molecular layer and were thus reminiscent of the mossy fiber sprouting reported in TLE patients (Sutula et al., 1989) and animal models (Sutula et al., 1988). When the subiculum was separated in proximal and distal areas according to Witter (1993) (see also Fig. 1B), patches of increased immunoreactivity were more evident in the distal areas that are known to be innervated by the medial EC (Naber et al., 2001); this was also the EC region in which we could identify patches of increased synaptophysin immunoreactivity localized in the superficial layers (Fig. 11B).

Semiquantitative evaluation of optical density values in NEC and pilocarpine-treated rats is shown in Fig. 11C for both subiculum and EC. Significantly ($p<0.01$) higher staining intensity was found in proximal and distal subiculum as well as in medial and lateral EC ($p<0.05$) of pilocarpine-treated rats when compared to NECs (Fig. 11C). Therefore, these findings demonstrate a general increase of synaptophysin immunostaining in the subiculum and EC of pilocarpine-treated, epileptic rats.

1.5 Discussion

Our study demonstrates that the subiculum of pilocarpine-treated, epileptic rats is hyperexcitable at the network level as indicated by its increased responsiveness to CA1 and lateral EC layer III stimulation along with an increased frequency of spontaneous PSPs. We have also found that a mechanism contributing to subicular hyperexcitability corresponds to a dysfunction of $GABA_A$ receptor-mediated inhibition characterized by positive shift in IPSP reversal potentials coupled with a decreased IPSP peak conductance. Moreover, these functional perturbations in GABAergic activity were presumably caused by a reduction in KCC2 expression along with a decreased number of parvalbumin-positive interneurons. Finally, we have found enhanced synaptophysin immunoreactivity in both subiculum and EC of epileptic animals.

1.5.1 Network hyperexcitability in the epileptic subiculum

Subicular neurons recorded intracellularly from epileptic tissue generate bursts or doublets of action potentials in response to stimuli delivered in the CA1 stratum radiatum; in contrast, such procedure consistently disclosed a single action potential followed by a hyperpolarization in NEC subicular cells. Moreover, input-output curves

of the stimulus-induced responses identified a lower activation threshold in the epileptic subicular network. This evidence is in line with recent studies that have documented subicular hyperexcitability in epileptic tissue during electrical stimulation or $GABA_A$ receptor antagonism (Knopp et al., 2005). However, in contrast to the results by Knopp et al (2005), we did not observe any synaptic bursting in NEC subiculum; this difference may have been dependent upon their adopted stimulus intensity.

We further demonstrated that the altered subicular responsiveness was not limited to activation from CA1, but also involved inputs arising from the lateral EC layer III. Our study as well as previous investigations have shown that synaptic inhibition is prevalent within the NEC subiculum following EC stimulation (Behr et al.,1998; Maccaferri and McBain, 1995). In contrast, subicular activation by EC inputs in pilocarpine tissue revealed increased network excitation as indicated by the enhanced duration of the response that was characterized by multiphasic PSPs. In addition, hyperpolarizing synaptic potentials could not be recorded in pilocarpine tissue, as opposed to the NEC, thus further suggesting a perturbation in inhibitory and excitatory properties of the epileptic subiculum. Interestingly, this EC-subiculum network interaction correlates with the data obtained by studying epileptiform synchronization induced by 4-aminopyridine in pilocarpine-treated, epileptic mice (D'Antuono et al., 2002). While we observed increased network hyperexcitability in the epileptic subiculum, we did not detect a correlation with the intrinsic properties of subicular neurons.

A characteristic that was also indicative of network hyperexcitability within the epileptic subiculum was the higher frequency of spontaneous PSPs when compared to NEC subicular cells. Previous *in vitro* studies in tissue obtained from epileptic

patients (Cohen et al., 2002; Wozny et al., 2003) as well as kainic acid (Shah et al., 2005) or pilocarpine-treated rats (Kobayashi et al., 2003, Sanabria et al., 2001; Knopp et al., 2005) have shown the presence of network-driven phenomena.

1.5.2 Reduced GABAergic inhibition within the pilocarpine-treated subiculum

We also discovered that the reversal potential of the spontaneous PSPs recorded in epileptic tissue was characterized by a positive shift suggesting decreased network inhibition. This aspect was further investigated by establishing the reversal potential of the stimulus-induced IPSPs generated by NEC and pilocarpine-treated epileptic subicular cells in the presence of glutamatergic antagonists. We found that the reversal potential of the $GABA_A$ receptor component of this IPSP was more positive in pilocarpine-treated neurons than in NEC cells. Such a decrease in reversal potential may account for attenuated inhibition and thus for the synaptic hyperexcitability documented following CA1 or EC stimulation. These data are also in keeping with the presence of depolarizing GABAergic events in the subiculum of human epileptic tissue (Cohen et al., 2002, Wonzy et al., 2003).

Our results of a more positive fast IPSP reversal point can be attributed to an accumulation of intracellular Cl^- resulting from a reduced expression of the KCC2. Under normal physiological conditions, the classical hyperpolarzing GABAergic response relies upon a low intracellular Cl^- concentration due to Cl^- extrusion by KCC2. This mechanism, however, can become altered in conditions of network hyperexcitability. Accordingly, recent investigations have shown that KCC2 in the hippocampus is downregulated after kindling-induced seizures *in vivo* or by exogenous applications of BDNF or neurotrophin 4 *in vitro* (Rivera et al., 2002). In

addition, Rivera et al. (2004) have reported that interictal epileptiform activity in hippocampal slices down-regulates KCC2 mRNA and protein expression in CA1 pyramidal neurons. Indeed, by utilizing RT-PCR and immunohistochemical analysis we found a significant reduction in KCC2 mRNA and protein expression in the pilocarpine-treated subiculum *vs.* NEC. As such, the more depolarized $GABA_A$ receptor induced IPSP reversal potential identified in pilocarpine-treated neurons is most likely caused by a reduction in KCC2 expression and the functional consequence of increased intracellular Cl^-. Hence, our data reinforce the evidence that a reduction in KCC2 expression may contribute to epileptic hyperexcitability.

Pharmacologically isolated IPSPs generated by pilocarpine-treated epileptic subicular cells are also characterized by a decreased peak conductance when compared with similar events in NEC tissue. This change, which is expected to decrease the IPSP shunting action, may relate to decreased number of interneurons (see below), as well as to alterations in $GABA_A$ receptor subunits (Houser and Escalpez, 2003; Olsen et al., 2004; Friedman et al., 1994). These factors may also contribute towards reduced subicular network inhibition coupled with an augmented excitatory drive.

1.5.3 Structural changes in subicular and EC networks

The perturbations of network inhibition observed in the subiculum of pilocarpine-treated rats also appear to be contributed by a decrease of interneurons along with synaptic re-organization. First, we have found that parvalbumin-positive cells, which represent about 50% of interneurons in the rodent cortex (Kawaguchi and Kubota, 1993; Kubota et al., 1994) are markedly decreased in ventral and dorsal subiculum but not in EC. Similar findings have been reported in different TLE animal models (Du

et al., 1995; van Vliet et al., 2004). A reduction in the number of parvalbumin-positive interneurons has been also found in the CA1 subfield (André et al., 2001) and in the dentate hilus (Gorter et al., 2001) of epileptic animals, which correlated with the development of spontaneous seizures following SE. Interestingly, parvalbumin-positive cells are also decreased in the neocortex (de Felipe et al., 1993) and hippocampus (Arellano et al., 2004) of epileptic patients presenting with intractable seizures. It should be however mentioned that these studies failed in disclosing significant differences in parvalbumin-positive cells in the human epileptic subiculum, suggesting a possible inconsistency with the animal model. Alternatively, the decrease of parvalbumin-labeled interneurons may result from reduced expression of this calcium binding protein following repeated seizures (Sloviter et al., 1991; Vizi et al., 2004), thus depending on the frequency by which a certain neuronal area is recruited by seizures.

Subiculum hyperexcitability may also be contributed by neuronal sprouting, as recently evidenced by tracing studies in rats made epileptic with different procedures (Cavazos et al., 2004). Mossy fiber sprouting has been described in the dentate gyrus and CA3 subfield of TLE patients (Sutula et al., 1989; Houser et al., 1990; Houser, 1999; Proper et al., 2000) and epileptic rats (Ben-Ari, 1985; Sutula et al., 1988; Gorter et al., 2001). We have investigated the possibility that neuronal sprouting took place in our rats by means of synaptophysin immunostaining. Synaptophysin is a synaptic vesicle-associated protein (Bahler et al., 1991) known to be upregulated by neuronal activity (Li et al., 2002; Valtorta et al., 2004) and lesion (Kadish and van Groen, 2003). Although it is not a classical marker of sprouting, changes in synaptophysin immunoreactivity have been taken as indirect index of increased nerve terminal density or activity in epileptic patients (Proper et al., 2000) as well as in animals

(Chen et al., 1996; Li et al., 2002). Here, we have identified an increase in synaptophysin immunostaining in several limbic areas, possibly suggesting neuronal sprouting in pilocarpine-treated rats as reported in the kainic acid model (Chen et al., 1996), or indicating increased synaptic vesicle density. These changes appeared to be more evident in distal subiculum and medial EC, that are reciprocally interconnected (Naber et al., 2001). Increased synaptophysin immunoreactivity was also found in the hippocampus of pharmacoresistant TLE patients (Proper et al., 2000). Sprouting in the EC superficial layers has been reported to occur in human TLE tissue by analyzing the immunoreactivity of the highly polysialylated neural cell adhesion molecule (Mikkonen et al., 1998).

In conclusion, our findings highlight a change in subicular neuron excitability in epileptic rats that depends on multiple mechanisms. At the molecular level, KCC2 expression is downregulated thus varying the neuronal response to GABAergic inputs. At the cellular level, parvalbumin interneurons are highly decreased, possibly hampering the control of neuronal excitability, while the upregulation of synaptophysin immunostaining, as also found in the dentate gyrus and EC, favours the hypothesis of increased network coupling in the epileptic subiculum. This evidence along with findings from other laboratories (Cohen et al., 2002; Cavazos et al., 2004; Knopp et al., 2005) indicate in the subiculum a key region in the control of epileptic activity.

1.6 Acknowledgements

This study was supported by grants from the Canadian Institutes of Health Research (CIHR; grant 8109), the Savoy Foundation, the Citizens United for Research in Epilepsy (CURE), the Italian Ministry of Education, University and Research (PRIN 2003), and the Pierfranco and Luisa Mariani Foundation (R-06-50). We thank Dr. M.

D'Antuono for participating in the KCC2 experiments and Ms. T. Papadopoulos for secretarial assistance.

1.7 References

Arellano JI, Munoz A, Ballesteros-Yanez I, Sola RG, DeFelipe J. 2004. Histopathology and reorganization of chandelier cells in the human epileptic sclerotic hippocampus. Brain 127: 45-64.

Bahler M, Klein RL, Wang JK, Benfenati F, Greengard P. 1991. A novel synaptic vesicle-associated phosphoprotein: SVAPP-120. J Neurochem 57:423-430.

Behr J, Gloveli T, Heinemann U. 1998. The perforant path projection from the medial entorhinal cortex layer III to the subiculum in the rat combined hippocampal-entorhinal cortex slice. Eur J Neurosci 10:1011-1018.

Ben-Ari Y. 1985. Limbic seizure and brain damage produced by kainic acid: mechanisms and relevance to human temporal lobe epilepsy. Neuroscience 14: 375-403.

Biagini G, Babinski K, Avoli M, Marcinkiewicz M, Seguela P. 2001. Regional and subunit-specific downregulation of acid-sensing ion channels in the pilocarpine model of epilepsy. Neurobiol Dis 8: 45-58.

Biagini G, D'Arcangelo G, Baldelli E, D'Antuono M, Tancredi V, Avoli M. 2005. Impaired activation of CA3 pyramidal neurons in the epileptic hippocampus. Neuromol Med 7: 325-342.

Bragin A, Wilson CL, Staba RJ, Reddick M, Fried I, and Engel J Jr. 2002. Interictal high-frequency oscillations (80-500 Hz) in the human epileptic brain: entorhinal cortex. Ann Neurol 52: 407-415.

Buhl EH, Otis TS, Mody I. 1996. Zinc-induced collapse of augmented inhibition by GABA in a temporal lobe epilepsy model. Science 271: 369-373.

Cavalheiro EA, Leite JP, Bortolotto ZA, Turski WA, Ikonomidou C, Turski L. 1991. Long-term effects of pilocarpine in rats: structural damage of the brain triggers kindling and spontaneous recurrent seizures. Epilepsia 32: 778-782.

Cavazos JE, Jones SM, Cross DJ. 2004. Sprouting and synaptic reorganization in the subiculum and CA1 region of the hippocampus in acute and chronic models of partial-onset epilepsy. Neuroscience 126: 677-688.

Chen LS, Wong JG, Banerjee PK, Snead OC. 1996. Kainic acid-induced focal cortical seizure is associated with an increase of synaptophysin immunoreactivity in the cortex. Exp Neurol 141: 25-31.

Cohen I, Navarro V, Clemenceau S, Baulac M, Miles R. 2002. On the origin of interictal activity in human temporal lobe epilepsy in vitro. Science 298:1418-1421.

D'Antuono M, Benini R, Biagini G, D'Arcangelo G, Barbarosie M, Tancredi V, Avoli M. 2002 .Limbic network interactions leading to hyperexcitability in a model of temporal lobe epilepsy. J Neurophysiol 87: 634-639.

de Curtis M, Pare D. 2004. The rhinal cortices: a wall of inhibition between the neocortex and the hippocampus. Prog Neurobiol 74: 101-110.

de Felipe J, Garcia Sola R, Marco P, del Rio MR, Pulido P, Ramon y Cajal S. 1993. Selective changes in the microorganization of the human epileptogenic neocortex revealed by parvalbumin immunoreactivity. Cereb Cortex 3:39-48.

Doherty J, Dingledine R. 2001. Reduced excitatory drive onto interneurons in the dentate gyrus after status epilepticus. J Neurosci 21:2048-2057.

Du F, Eid T, Lothman EW, Kohler C, Schwarcz R. 1995. Preferential neuronal loss in layer III of the medial entorhinal cortex in rat models of temporal lobe epilepsy. J Neurosci 15: 6301–6313.

Friedman LK, Pellegrini-Giampietro DE, Sperber EF, Bennett MV, Moshe SL, Zukin RS. 1994. Kainate-induced status epilepticus alters glutamate and GABAA receptor gene expression in adult rat hippocampus: an in situ hybridization study. J Neurosci 14:2697-2707.

Gorter JA, van Vliet EA, Aronica E, Lopes da Silva FH. 2001. Progression of spontaneous seizures after status epilepticus is associated with mossy fibre sprouting and extensive bilateral loss of hilar parvalbumin and somatostatin-immunoreactive neurons. Eur J Neurosci 13:657-669.

Grob M, Mouginot D. 2005. Heterogeneous chloride homeostasis and GABA responses in the median preoptic nucleus of the rat. J Physiol 569: 885-901.

Houser CR, Esclapez M. 2003. Downregulation of the alpha5 subunit of the GABA(A) receptor in the pilocarpine model of temporal lobe epilepsy. Hippocampus 13:633-645.

Houser CR, Miyashiro JE, Swartz BE, Walsh GO, Rich JR, Delgado-Escueta AV. 1990. Altered patterns of dynorphin immunoreactivity suggest mossy fiber reorganization in human hippocampal epilepsy. J Neurosci 10: 267-282.

Houser CR. 1999. Neuronal loss and synaptic reorganization in temporal lobe epilepsy. In: Delgado-Escuetta AV, Wilson WA, Olsen RW, Porter RJ, editors. Jasper's Basic Mechanisms of the Epilepsies. Third Edition: Advances in Neurology, vol. 79, 3rd edition. Lippincott Williams & Wilkins Philadelphia.

Kadish I, Van Groen T. 2003. Differences in lesion-induced hippocampal plasticity between mice and rats. Neuroscience 116: 499-509.

Kawaguchi Y, Kubota Y. 1993. Correlation of physiological subgroupings of nonpyramidal cells with parvalbumin- and calbindinD28kimmunoreactive neurons in layer V of rat frontal cortex. J Neurophysiol 70: 387–396.

Khalilov I, Holmes GL, Ben-Ari Y. 2003. In vitro formation of a secondary epileptogenic mirror focus by interhippocampal propagation of seizures. Nat Neurosci 6: 1079-1085.

Knopp A, Kivi A, Wozny C, Heinemann U, Behr J. 2005. Cellular and network properties of the subiculum in the pilocarpine model of temporal lobe epilepsy. J Comp Neurol 483: 476-488.

Kobayashi M, Wen X, Buckmaster PS. 2003. Reduced inhibition and increased output of layer II neurons in the medial entorhinal cortex in a model of temporal lobe epilepsy J Neurosci 23: 8471-8479.

Kubota Y, Hattori R, Yui Y. 1994. Three distinct subpopulations of GABAergic neurons in rat frontal agranular cortex. Brain Res 649: 159–173.

Li S, Reinprecht I, Fahnestock M, Racine RJ. 2002. Activity-dependent changes in synaptophysin immunoreactivity in hippocampus, piriform cortex, and entorhinal cortex of the rat. Neuroscience 115: 1221-1229.

Lohrke S, Srinivasan G, Oberhofer M, Doncheva E, Friauf E. 2005. Shift from depolarizing to hyperpolarizing glycine action occurs at different perinatal ages in superior olivary complex nuclei. Eur J Neurosci 22: 2708-2722.

Maccaferri G, McBain CJ. 1995. Passive propagation of LTD to stratum oriens-alveus inhibitory neurons modulates the temporoammonic input to the hippocampal CA1 region. *Neuron* 15: 137-145.

Mathern GW, Pretorius JK, Babb TL. 1995. Quantified patterns of mossy fiber sprouting and neuron densities in hippocampal and lesional seizures. J Neurosurg 82: 211–219.

Mattia D, Kawasaki H, Avoli M. 1997. In vitro electrophysiology of rat subicular bursting neurons Hippocampus 7: 48-57.

Mikkonen M, Soininen H, Kalvianen R, Tapiola T, Ylinen A, Vapalahti M, Paljarvi L, Pitkanen A. 1998. Remodeling of neuronal circuitries in human temporal lobe epilepsy: increased expression of highly polysialylated neural cell adhesion molecule in the hippocampus and the entorhinal cortex. Ann Neurol 44: 923–934.

Naber PA, Lopes da Silva FH, Witter MP. 2001. Reciprocal connections between the entorhinal cortex and hippocampal fields CA1 and the subiculum are in register with the projections from CA1 to the subiculum. Hippocampus 11: 99-104.

Nissinen J, Halonen T, Koivisto E, Pitkanen A. 2000. A new model of chronic temporal lobe epilepsy induced by electrical stimulation of the amygdala in rat. Epilepsy Res 38: 177-205.

Olsen RW, Chang CS, Li G, Hanchar HJ, Wallner M. 2004. Fishing for allosteric sites on GABA(A) receptors. Biochem Pharmacol 68: 1675-1684.

Perez Y, Morin F, Beaulieu C, Lacaille JC. 1996. Axonal sprouting of CA1 pyramidal cells in hyperexcitable hippocampal slices of kainate-treated rats. Eur J Neurosci 8: 736–748.

Priel MR, dos Santos NF, Cavalheiro EA. 1996. Developmental aspects of the pilocarpine model of epilepsy. Epilepsy Res 26: 115-121.

Proper EA, Oestreicher AB, Jansen GH, Veelen CW, van Rijen PC, Gispen WH, de Graan PN. 2000. Immunohistochemical characterization of mossy fibre sprouting in the hippocampus of patients with pharmacoresistant temporal lobe epilepsy. Brain 123: 19-30.

Racine RJ. 1972. Modification of seizure activity by electrical stimulation. II. Motor seizure. Electroencephalogr Clin Neurophysiol 32: 281-94.

Rivera C, Li H, Thomas-Crusells J, Lahtinen H, Viitanen T, Nanobashvili A, Kokaia Z, Airaksinen MS, Voipio J, Kaila K, Saarma M. 2002. BDNF-induced TrkB activation down-regulates the K^+-Cl^- cotransporter KCC2 and impairs neuronal Cl- extrusion J Cell Biol 159: 747-752.

Rivera C, Voipio J, Thomas-Crusells J, Li H, Emri Z, Sipila S, Payne JA, Minichiello L, Saarma M, Kaila K. 2004. Mechanism of activity-dependent downregulation of the neuron-specific K-Cl cotransporter KCC2. J Neurosci 24: 4683-4691.

Sanabria ER, Su H, Yaari Y. 2001. Initiation of network bursts by Ca2+-dependent intrinsic bursting in the rat pilocarpine model of temporal lobe epilepsy J Physiol 532: 205-216.

Shah MM, Anderson AE, Leung V, Lin X, Johnston D. 2004. Seizure-induced plasticity of h channels in entorhinal cortical layer III pyramidal neurons. Neuron 44: 495-508.

Tuunanen J, Lukasiuk K, Halonen T, Pitkanen A. 1999. Status epilepticus-induced neuronal damage in the rat amygdaloid complex: distribution, time-course and mechanisms. Neuroscience 94: 473-495.

Sloviter RS. 1987. Decreased hippocampal inhibition and a selective loss of interneurons in experimental epilepsy. Science 235: 73–76.

Sloviter RS, Sollas AL, Barbaro NM, Laxer KD. 1991. Calcium binding protein (calbindin-D28K) and parvalbumin immunocytochemistry in the normal and epileptic human hippocampus. J Comp Neurol 308: 381-396.

Spencer SS, Spencer DD. 1994. Entorhinal-hippocampal interactions in medial temporal lobe epilepsy. Epilepsia 35: 721-727.

Su H, Sochivko D, Becker A, Chen J, Jiang Y, Yaari Y, Beck H. 2002. Upregulation of a T-type Ca^{2+} channel causes a long-lasting modification of neuronal firing mode after status epilepticus. J Neurosci 22: 3645–3655.

Sutula T, Cascino G, Cavazos J, Parada I, Ramirez L. 1989. Mossy fiber synaptic reorganization in the epileptic human temporal lobe. Ann Neurol 26: 321-330.

Sutula T, He XX, Cavazos J, Scott G. 1998. Synaptic reorganization in the hippocampus induced by abnormal functional activity. Science 239: 11147-11150.

Turski WA, Cavalheiro EA, Schwarz M, Czuczwar SJ, Kleinrok Z, Turski L. 1983. Limbic seizures produced by pilocarpine in rats: behavioral, electroencephalographic and neuropathological study. Behav. Brain Res 9: 315–335.

Vale C, Schoorlemmer J, Sanes DH. 2003. Deafness disrupts chloride transporter function and inhibitory synaptic transmission. J Neurosci 23: 7516 –7524.

Vale C, Caminos E, Martinez-Galan JR, Juiz JM. 2005. Expression and developmental regulation of the K^+-Cl^- cotransporter KCC2 in the cochlear nucleus. Hear Res 206: 107-115.

Valtorta F, Pennuto M, Bonanomi D, Benfenati F. 2004. Synaptophysin: leading actor or walk-on role in synaptic vesicle exocytosis? Bioessays 26: 445-453.

Wozny C, Kivi A, Lehmann TN, Dehnicke C, Heinemann U, Behr J. 2003. Comment on "On the origin of interictal activity in human temporal lobe epilepsy in vitro". Science 301: 463.

van Vliet EA, Aronica E, Tolner EA, Lopes da Silva FH, Gorter JA. 2004. Progression of temporal lobe epilepsy in the rat is associated with immunocytochemical changes in inhibitory interneurons in specific regions of the hippocampal formation. Exp Neurol 187: 367-379.

Vizi S, Bagosi A, Krisztin-Peva B, Gulya K, Mihaly A. 2004. Repeated 4-aminopyridine seizures reduce parvalbumin content in the medial mammillary nucleus of the rat brain. Brain Res Mol Brain Res 131:110-118.

Vreugdenhil M, Hoogland G, van Veelen CW, Wadman WJ. 2004. Persistent sodium current in subicular neurons isolated from patients with temporal lobe epilepsy. Eur J Neurosci 19: 2769-2778.

Wellmer J, Su H, Beck H, Yaari Y. 2002. Long-lasting modification of intrinsic discharge properties in subicular neurons following status epilepticus. Eur J Neurosci 16: 259-266.

Williams JR, Sharp JW, Kumari VG, Wilson M, Payne JA. 1999. The neuron-specific K-Cl cotransporter, KCC2. Antibody development and initial characterization of the protein. J Biol Chem 274: 12656-12664.

Williams S, Vachon P, Lacaille JC. 1993. Monosynaptic GABA mediated inhibitory postsynaptic potentials in CA1 pyramidal of hyperexcitable hippocampal slices from kainic acid-treated rats. Neuroscience 52: 541–554.

Witter MP. 1993. Organization of the entorhinal-hippocampal system: a review of current anatomical data. Hippocampus 3: 33–44.

1.8 Figures

Figure 1-1:

Localization of anatomical areas of the hippocampal formation. In A, microphotograph of a toluidine blue-stained horizontal section from a pilocarpine-treated rat. Note that layer II in the entorhinal cortex (EC) is clearly identified as composed by a broader and continuous lamina in the medial EC while in the lateral EC (delimited by arrowheads) it appears to be composed by dispersed "islands" of neuronal elements. The other layers and the lamina dissecans (ld) are also indicated. Note that the dashed area in the subiculum shows the location where intracellular recordings were obtained. In B, areas of interest used to investigate the changes in subicular and EC neuronal network activities are shown. Areas marked in blue and red identify the different regions of the subiculum and EC sampled to measure grey tone values after immunohistochemistry in the proximal (proxSub) and distal (distSub) subiculum and in the lateral (LEC) and medial EC (MEC). The white ellipse in the angular bundle (ab) indicates the area used for the background (bg) staining, while the yellow ellipse close to the section indicates the procedure to measure nonspecific (ns) grey tone values. Other abbreviations: CA, cornu Ammonis; DG, dentate gyrus; H, hilus of dentate gyrus; paraSub, parasubiculum; preSub, presubiculum; Prh, perirhinal cortex. Scale bar, 500 μm.

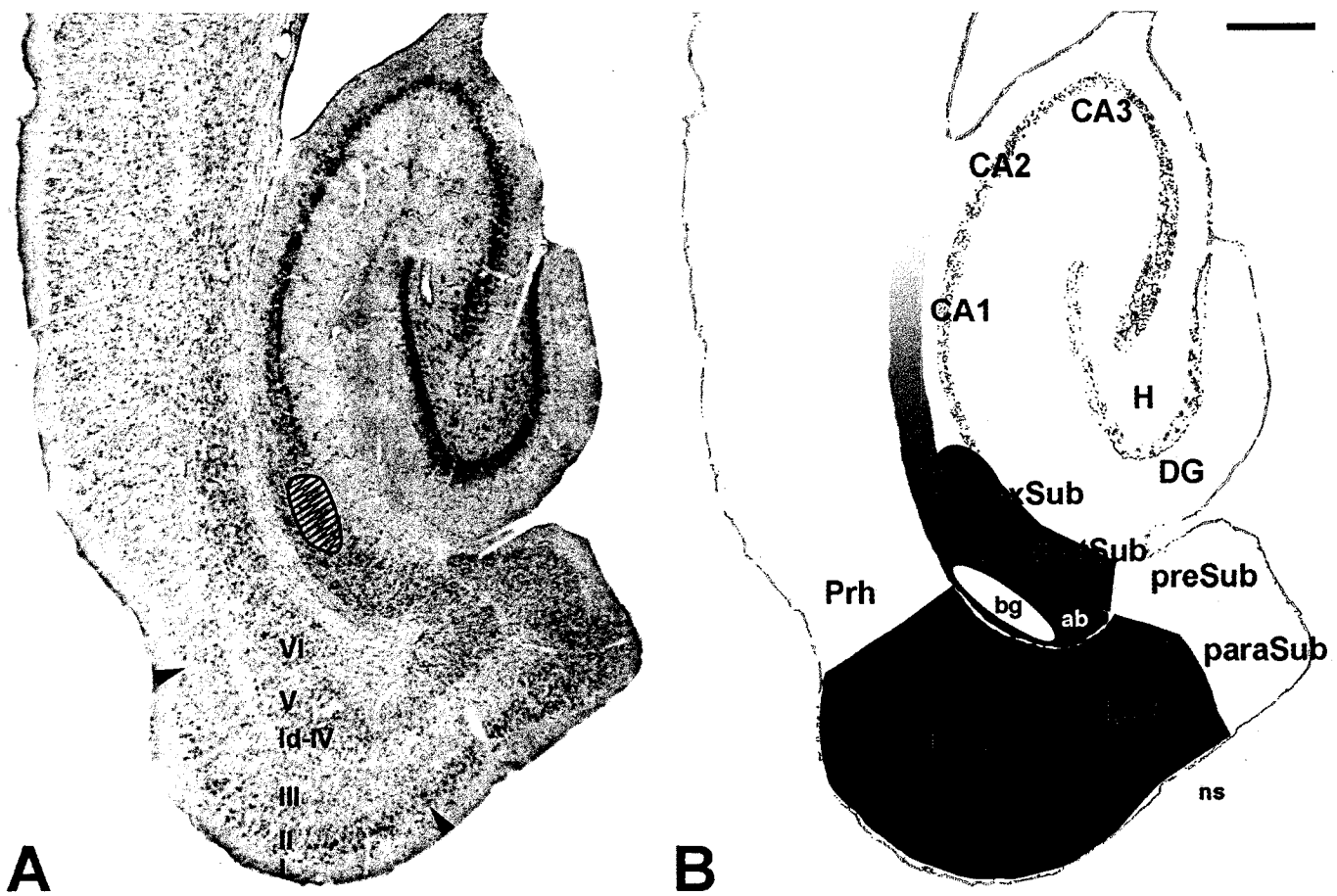
A
VI
V
Id-IV
III
II
B
CA3
CA2
CA1
H
DG
Sub
Sub
preSub
Prh
bg
ab
paraSub
ns

Figure 1

Figure 1-2:

Intrinsic firing and subthreshold oscillations generated by subicular neurons in NEC and pilocarpine-treated tissue. Two types of firing patterns are generated by subicular neurons in NEC (**A**) and pilocarpine (**B**) treated slices during injection of depolarizing current: (i) action potential bursting coupled with regular action potential firing (**Aa** and **Ba**) or regular firing (**Ab** and **Bb**). Comparison of NEC and pilocarpine (**Ac** and **Bc**) treated regular firing subicular neurons produced subthreshold oscillatory activity when depolarized from RMP. Quantification of subthreshold oscillations through power spectral analysis demonstrates that subthreshold activity oscillates within a theta band of 6-9 Hz.

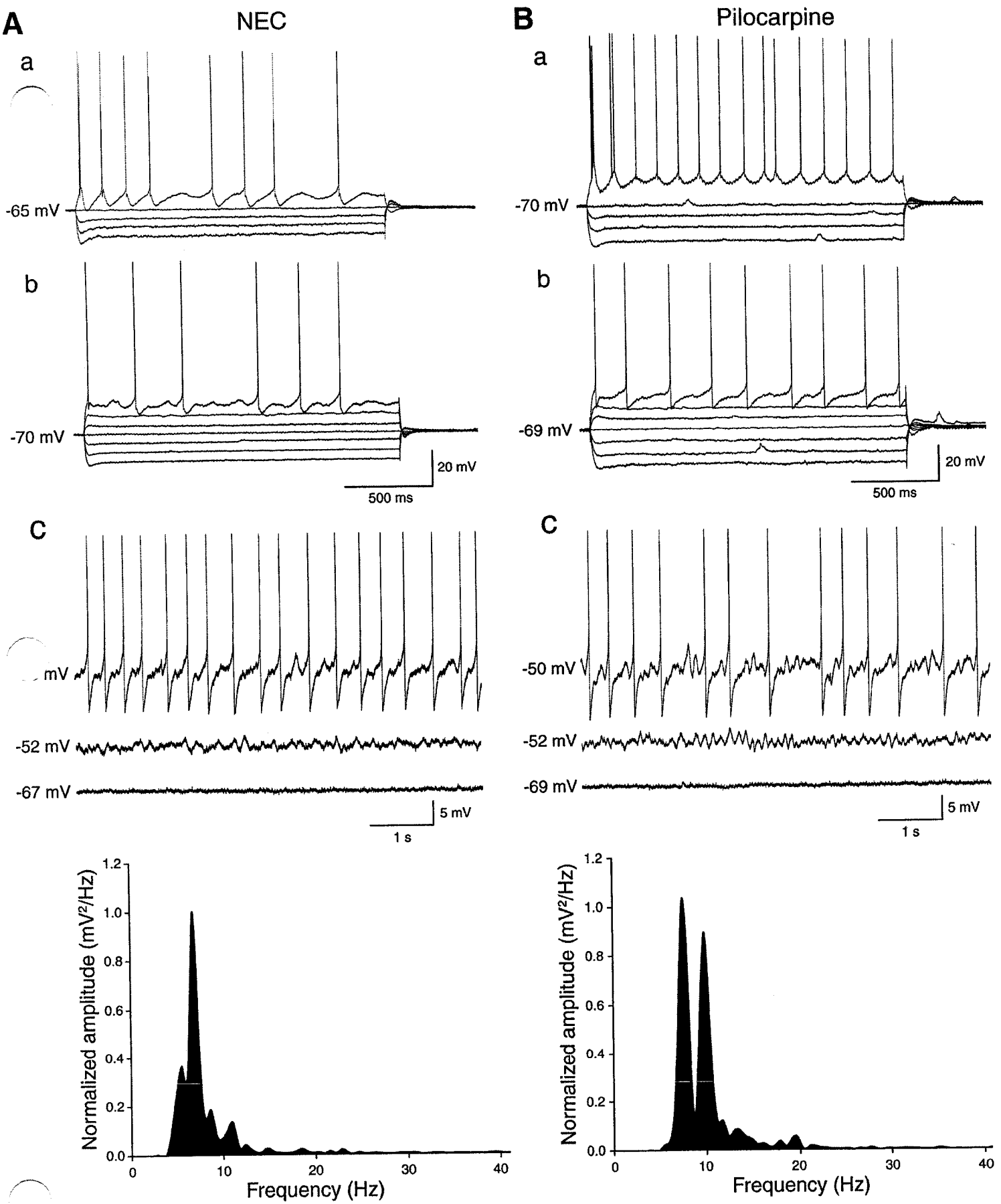
A
NEC
a
-65 mV
b
-70 mV
20 mV
500 ms
B
Pilocarpine
a
-70 mV
b
-69 mV
20 mV
500 ms
C
mV
-52 mV
-67 mV
5 mV
1 s
C
-50 mV
-52 mV
-69 mV
5 mV
1 s
Normalized amplitude (mV²/Hz)
1.2
1.0
0.8
0.6
0.4
0.2
0.0
0
10
20
30
40
Frequency (Hz)
Normalized amplitude (mV²/Hz)
1.2
1.0
0.8
0.6
0.4
0.2
0.0
0
10
20
30
40
Frequency (Hz)

Figure 2

Figure 1-3:

Activation of CA1 networks demonstrates hyperexcitability within the epileptic subiculum. A: In NEC tissue, CA1 single-shock stimulation elicits a sequence of depolarizing-hyperpolarizing post-synaptic responses at -71 mV (RMP). Hyper-polarization to -77 mV, -81 mV and -88 mV produces stimulus-induced depolarizing post-synaptic events, whereas electrical stimulation at -66 mV elicits a single action potential. **Ba**: In pilocarpine-treated subicular neurons, single-shock stimulation of the CA1 area elicits action potential bursting at -65 mV while a depolarizing post – synaptic response is seen at RMP and at further hyperpolarized potentials. **Bb:** In other experiments, pilocarpine-treated subicular neurons generate all-or-none stimulus-induced bursting activity. Action potential bursts were halted upon further hyperpolarization of the membrane to -92 mV.

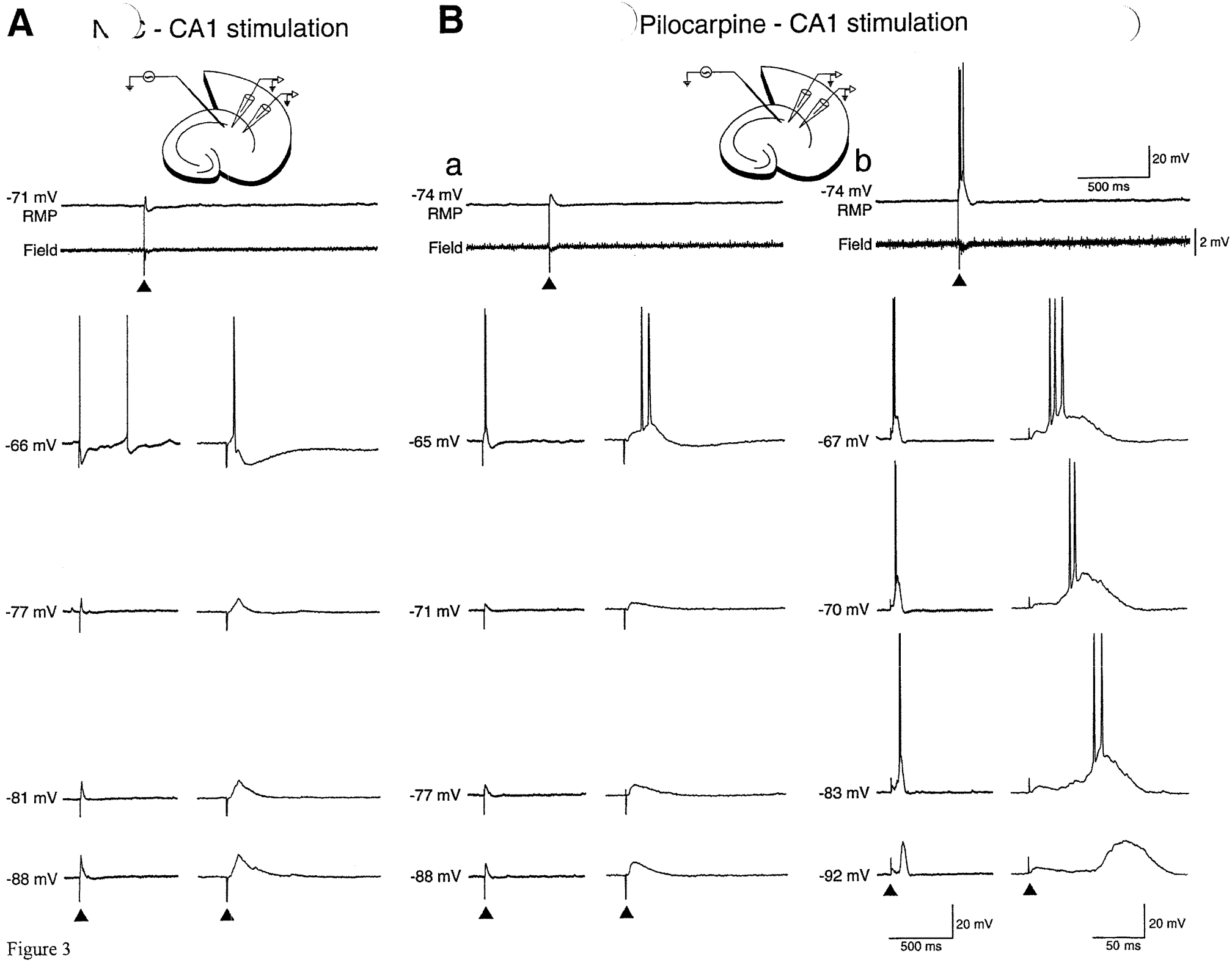
A
- CA1 stimulation
-71 mV
RMP
Field
-66 mV
-77 mV
-81 mV
-88 mV
B
Pilocarpine - CA1 stimulation
a
-74 mV
RMP
Field
-65 mV
-71 mV
-77 mV
-88 mV
b
20 mV
500 ms
-74 mV
RMP
Field
2 mV
-67 mV
-70 mV
-83 mV
-92 mV
20 mV
500 ms
20 mV
50 ms

Figure 3

Figure 1-4:

Pilocarpine-treated subicular neurons exhibit a lower threshold of activation. A: CA1 stimulation (duration of the stimulus= 100 μs) at increasing intensities in NEC tissue produces hyperpolarizing responses (200 μA) and depolarizing events (450 μA), whereas a strength of 500 uA is sufficient to elicit a single action potential. **B:** In contrast, a stimulus of lower intensity in CA1 is required to elicit depolarizing responses (100 μA and 150 μA) and action potential bursting (200 μA) in pilocarpine-treated subicular neurons. **C:** Graphical display of the average input-output curves of the post-synaptic responses generated prior to the appearance of action potential(s), in pilocarpine treated tissue (black dots; n=6) compared to NEC (open dots; n=5). Boltzman sigmoidal parameters were used to fit the current–response relationship. Stimulus to evoke the half amplitude of response (NEC: 315.6 ± 3.3 μA and Pilocarpine: 147.1 ± 3.8 μA) and slope (NEC: 56.6 ± 2.9 and pilocarpine: 4.6 ± 4.3) were statistically significant (half amplitude of response: $p<0.00001$; slope: $p<0.0003$).

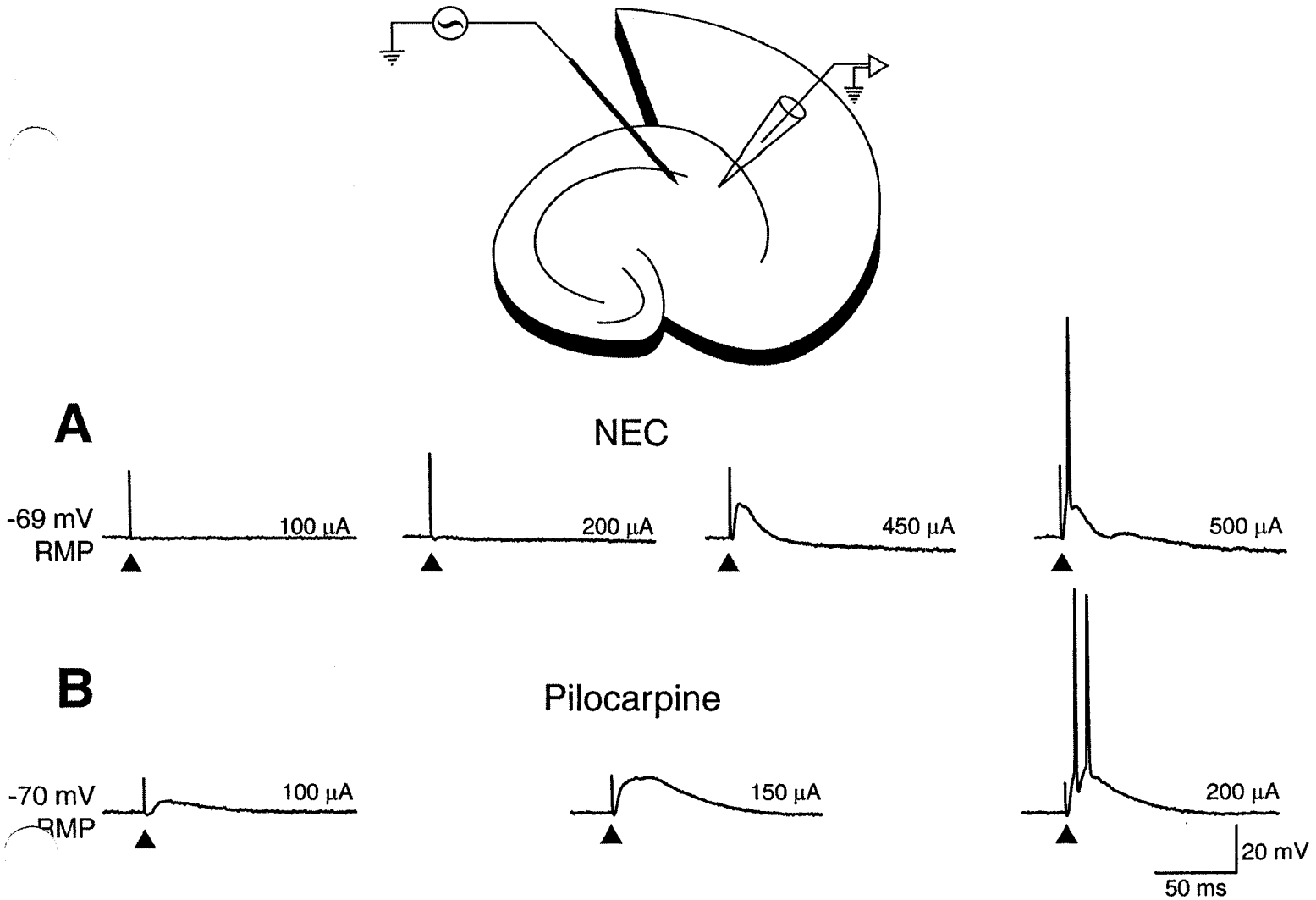
A
NEC
-69 mV
RMP
100 µA
200 µA
450 µA
500 µA
B
Pilocarpine
-70 mV
RMP
100 µA
150 µA
200 µA
20 mV
50 ms

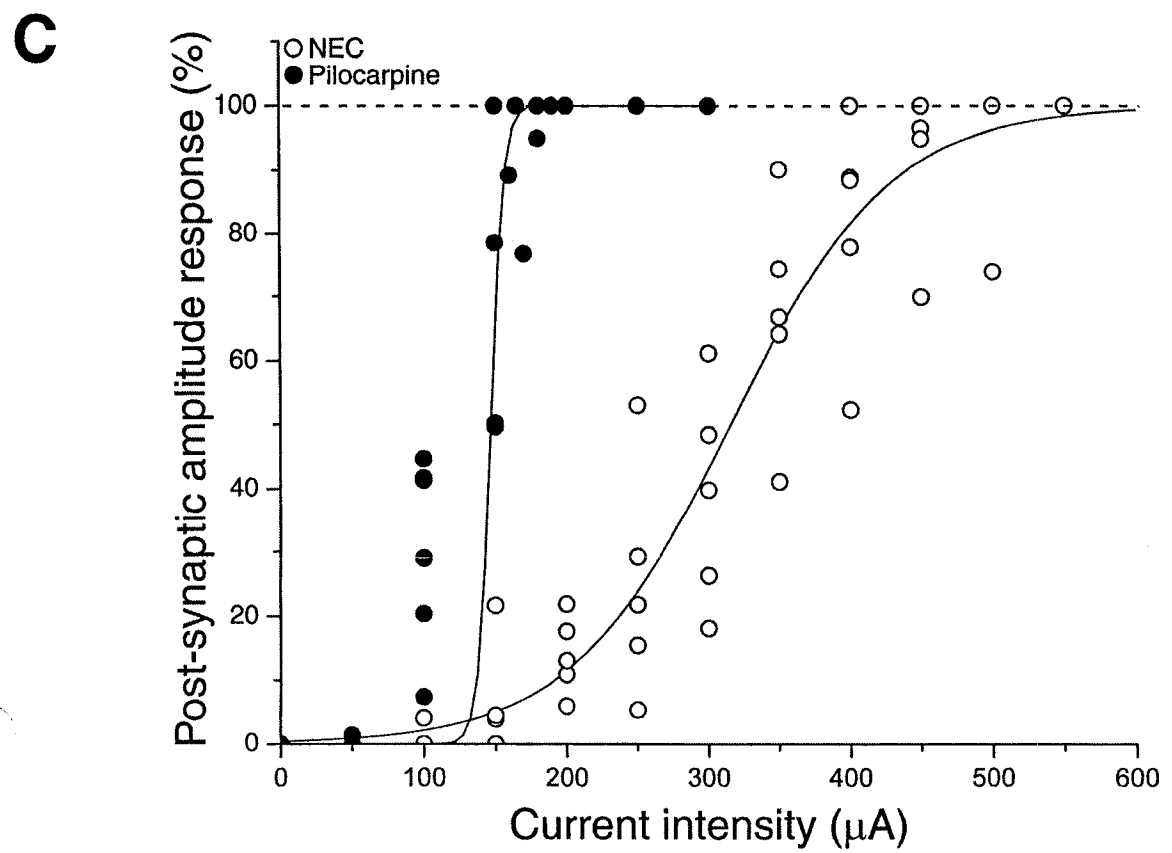
C
NEC
Pilocarpine
Post-synaptic amplitude response (%)
0
20
40
60
80
100
0
100
200
300
400
500
600
Current intensity (µA)

Figure 4

Figure 1-5:

Activation of EC layer III generates hyperexcitable responses in the pilocarpine-treated subiculum. A: Single shock stimulation of EC layer III elicits a monophasic post-synaptic response in the NEC subiculum. **B:** In contrast, EC layer III activation within pilocarpine treated tissue produced multiphasic post-synaptic activity within the subiculum. **C:** The pilocarpine treated subiculum produced a response of enhanced duration that was significantly different from the subicular response in the NEC (NEC: 101.93 ± 7.33ms *vs.* Pilocarpine: 491.89 ± 38.54 ms; $p<0.0001$)

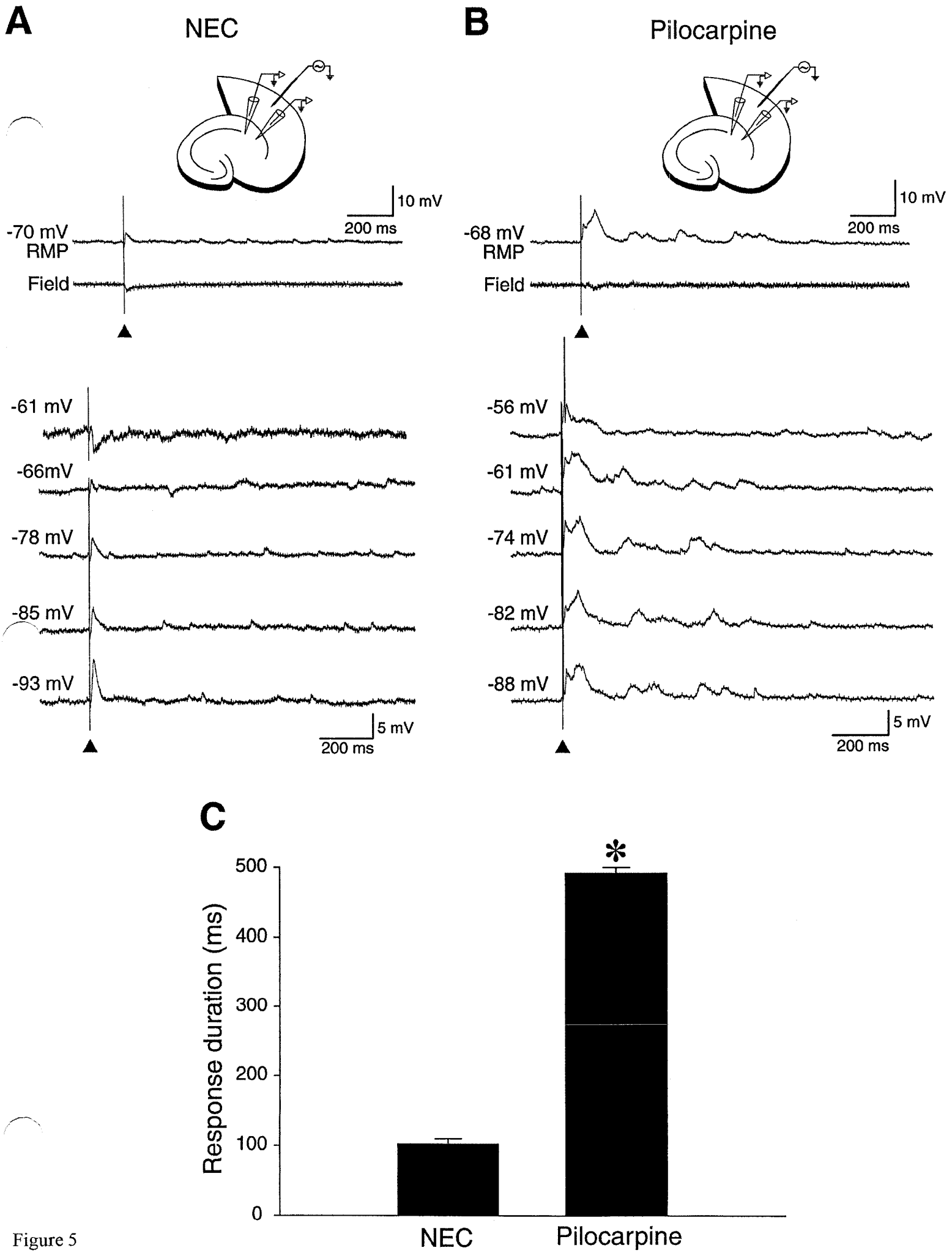
A
NEC
10 mV
200 ms
-70 mV
RMP
Field
-61 mV
-66mV
-78 mV
-85 mV
-93 mV
5 mV
200 ms
B
Pilocarpine
10 mV
200 ms
-68 mV
RMP
Field
-56 mV
-61 mV
-74 mV
-82 mV
-88 mV
5 mV
200 ms
C
Response duration (ms)
500
400
300
200
100
0
*
NEC
Pilocarpine

Figure 5

Figure 1-6:

Higher frequency of post-synaptic potentials (PSPs) within the pilocarpine-treated subiculum. A: Intracellular recordings in the subiculum of NEC slices demonstrate spontaneous PSPs exhibiting excitatory and inhibitory components at -73 mV. Depolarizing PSPs occur at -94 mV whereas at -60 mV these events were mainly hyperpolarizing. **B**: Subicular neurons in pilocarpine treated tissue exhibited depolarizing PSPs at -70 mV and -83 mV while hyperpolarizing PSPs occur during steady depolarization to -62 mV. **C:** Pilocarpine-treated subicular neurons exhibit a higher frequency of spontaneous PSPs as compared to those recorded in NEC slices ($p<0.0001$, independent t-test). **D:** The reversal potential of spontaneous PSPs in NEC *vs* pilocarpine-treated tissue was significantly different ($p<0.02$).

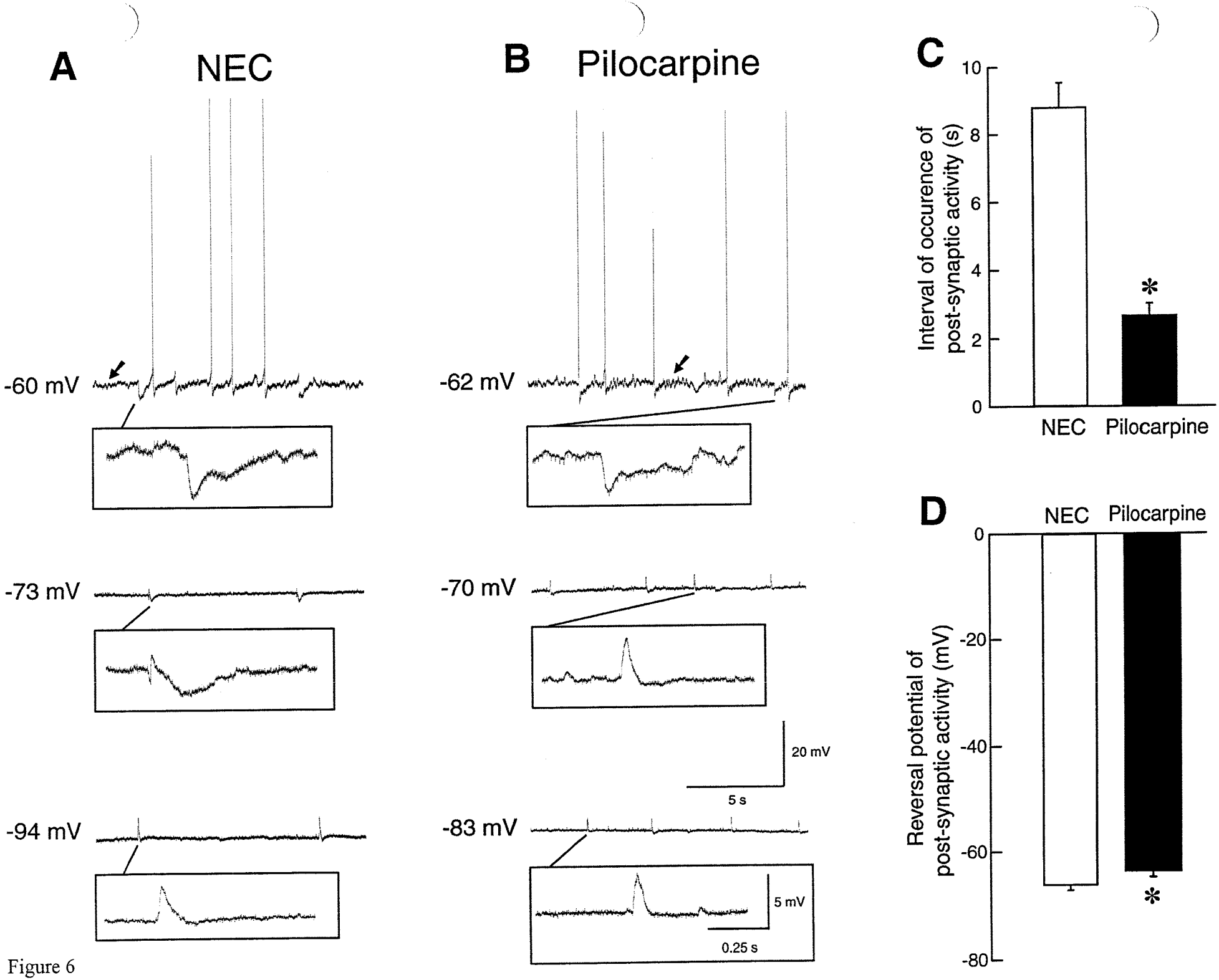
A
NEC
-60 mV
-73 mV
-94 mV
B
Pilocarpine
-62 mV
-70 mV
20 mV
5 s
-83 mV
5 mV
0.25 s
C
Interval of occurence of post-synaptic activity (s)
10
8
6
4
2
0
NEC
Pilocarpine
*
D
NEC
Pilocarpine
Reversal potential of post-synaptic activity (mV)
0
-20
-40
-60
-80
*

Figure 6

Figure 1-7:

The pilocarpine-treated subiculum exhibits a more positive $GABA_A$ receptor mediated IPSP. A and B:Single shock stimulation (100 μs) at different membrane potentials elicit "isolated" IPSPs in the presence of glutamatergic antagonists (CPP+CNQX, 10 μM for both drugs). Sharp-electrode intracellular recordings were performed in NEC **(A)** and pilocarpine-treated tissue **(B)**. Insets: expansion of the intracellular recordings of the IPSPs recorded in NEC and pilocarpine-treated tissue. Note that at -66mV hyperpolarizing synaptic potentials occur in NEC, whereas depolarizing potentials occur in the pilocarpine-treated cell. **C:** The IPSP reversal point in the NEC subiculum is -75 mV (black dots) whereas the pilocarpine-treated subiculum exhibits a value of -66 mV. **D:** Mean values of the "isolated" IPSPs are significantly more positive ($p<0.001$; independent t-test) in pilocarpine-treated tissue compared to NEC. Note also that a significant reduction in the IPSP peak conductance occurs in the pilocarpine-treated subiculum ($p<0.003$; independent t-test).

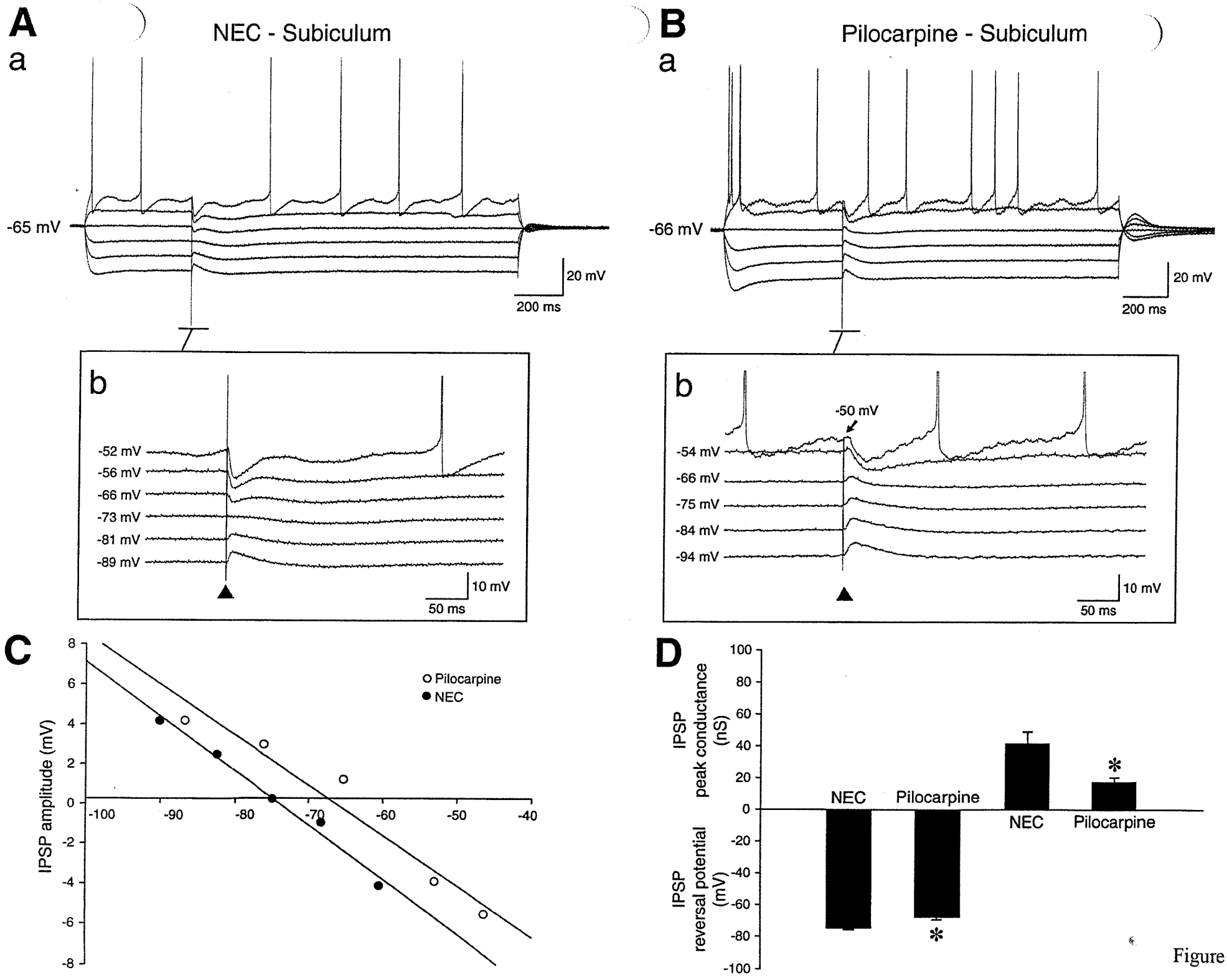
A
NEC - Subiculum
a
-65 mV
20 mV
200 ms
b
-52 mV
-56 mV
-66 mV
-73 mV
-81 mV
-89 mV
10 mV
50 ms
B
Pilocarpine - Subiculum
a
-66 mV
20 mV
200 ms
b
-50 mV
-54 mV
-66 mV
-75 mV
-84 mV
-94 mV
10 mV
50 ms
C
Pilocarpine
NEC
IPSP amplitude (mV)
8
6
4
2
0
-2
-4
-6
-8
-100
-90
-80
-70
-60
-50
-40
D
IPSP peak conductance (nS)
100
80
60
40
20
0
NEC
Pilocarpine
NEC
Pilocarpine
*
*
IPSP reversal potential (mV)
-20
-40
-60
-80
-100

Figure 7

Figure 1-8:

Assessment of the Cl reversal potential of the GABAA receptor mediated IPSP in layer V of the entorhinal cortex A and B. Inhibitory post-synaptic activity isolated via application of the glutamatergic antagonists CPP and CNQX (10 μM in both cases). In NEC (**A**) and pilocarpine treated tissue (**B**), single shock stimulation in layer V of the entorhinal cortex produced depolarizing and hyperpolarizing inhibitory post-synaptic responses at negative and positive membrane potentials, respectively. **C:** Regression analysis demonstrated the Cl^- reversal point in NEC to be -76 mV and -75 mV in the pilocarpine-treated EC. **D:** Comparison of the averages of the Cl^-; reversal point (NEC: -72.3±3.8 mV, n=7; Pilocarpine: -69.8±5.2 mV, n=13; $p<0.27$; independent t-test) and Cl^- conductance (NEC: 10.3±4.1 nS; pilocarpine; 12.8±8.6 nS; $p<0.89$; independent t-test)

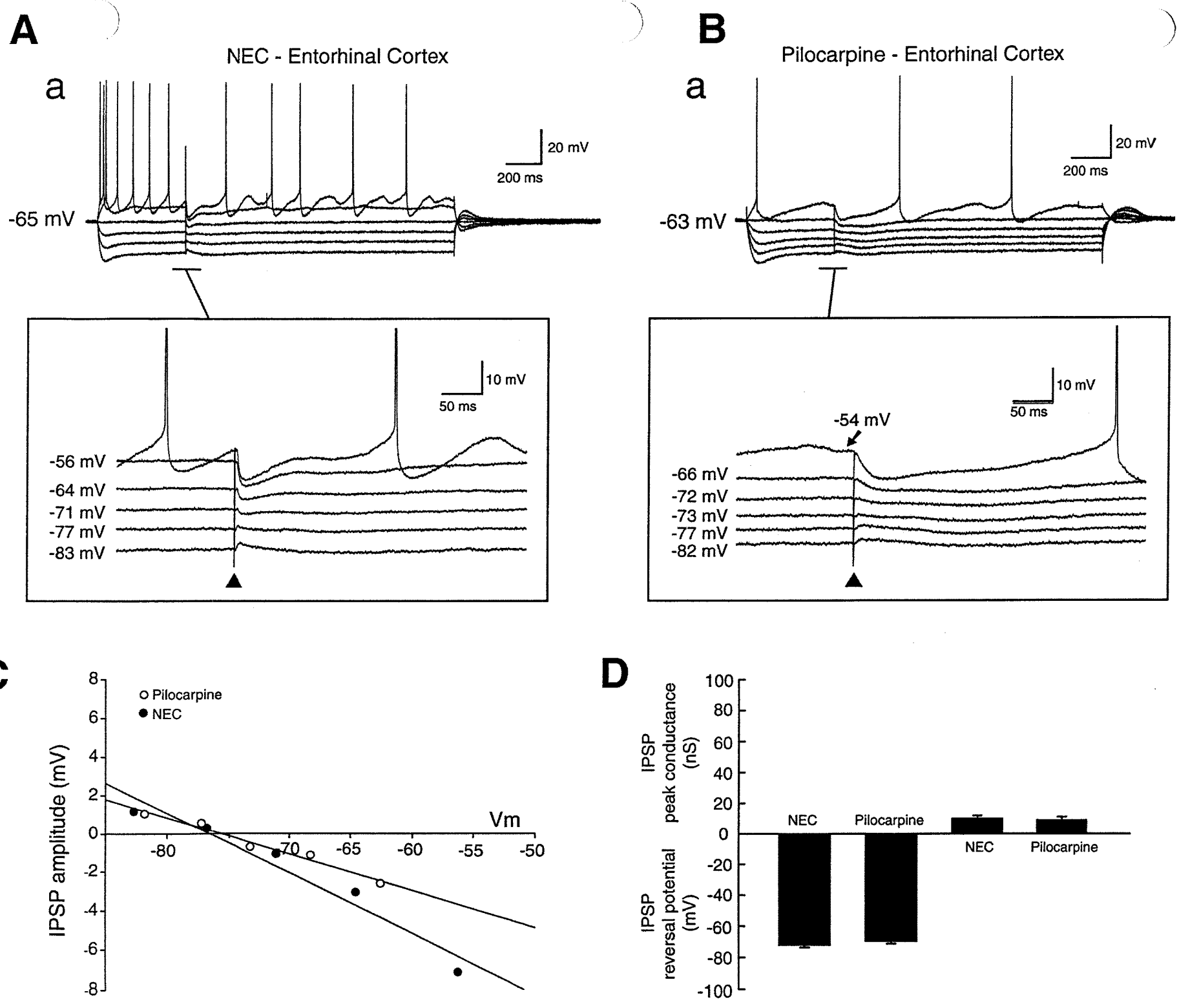
A
NEC - Entorhinal Cortex
a
20 mV
200 ms
-65 mV
10 mV
50 ms
-56 mV
-64 mV
-71 mV
-77 mV
-83 mV
B
Pilocarpine - Entorhinal Cortex
a
20 mV
200 ms
-63 mV
10 mV
50 ms
-54 mV
-66 mV
-72 mV
-73 mV
-77 mV
-82 mV
C
Pilocarpine
NEC
IPSP amplitude (mV)
Vm
8
6
4
2
0
-2
-4
-6
-8
-80
-70
-65
-60
-55
-50
D
IPSP peak conductance (nS)
IPSP reversal potential (mV)
100
80
60
40
20
0
-20
-40
-60
-80
-100
NEC
Pilocarpine
NEC
Pilocarpine

Figure 8

Figure 1-9:

KCC2 expression in pilocarpine-treated and NEC rats. In **A**: KCC2 mRNA levels in pilocarpine-treated EC and subiculum (n=5), expressed as percentage of NEC (n=5) values. In **B**: KCC2 immunoreactivity in the subiculum of NEC (n=8) and epileptic rats (n=9). * $p < 0.05$ *vs.* control values, Mann-Whitney test. In **C** and **D**: Distribution of KCC2 immunoreactivity in the subiculum of NEC and pilocarpine-treated rats, respectively. Note the wide distribution of KCC2 in the grey matter, while the angular bundle (ab) is scarcely stained. As shown in the inset (**C**), immunoreactivity is visible in nerve fibers and on the surface of neuronal somas, while the cytoplasm is unstained (arrow-heads). Abbreviations: alv, alveus; ml, molecular layer; sp, pyramidal layer; sr, stratum radiatum. The asterisk indicates the presubiculum. Scale bar, 150 μm for **C** and **D**, 50μm for the inset.

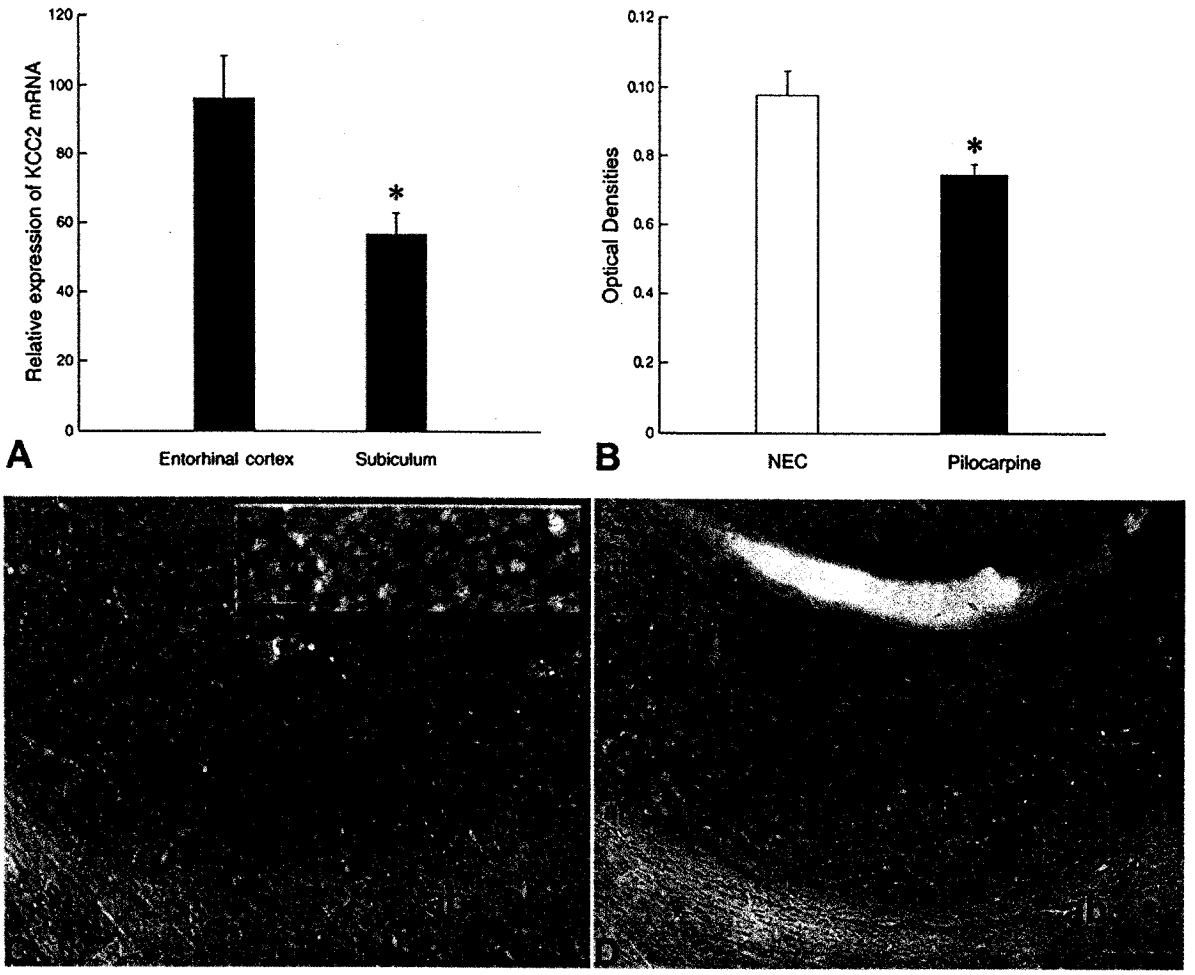
120
100
80
60
40
20
0
Relative expression of KCC2 mRNA
*
A
Entorhinal cortex
Subiculum
0.12
0.10
0.8
0.6
0.4
0.2
0
Optical Densities
*
B
NEC
Pilocarpine

Figure 9

Figure 1-10:

Parvalbumin immunoreactivity in the subiculum and EC of age matched NEC and pilocarpine-treated rats. A & B. Immunohistochemical staining in the ventral subiculum (7.6 mm from bregma) reveals a reduced number of parvalbumin positive inhibitory interneurons in pilocarpine-treated rats (**B**). The inset in B magnifies a parvalbumin-positive interneuron. **C & D:** distribution of parvalbumin-positive cells in the EC of NEC (**C**) and epileptic rats (**D**). **E**: quantitative analysis reveals a significant reduction ($p<0.01$, Mann-Whitney test) of inhibitory interneurons in the epileptic subiculum *vs.* NEC (saline treated) both at ventral and dorsal (3.6 mm from bregma) levels. In contrast, parvalbumin cell number was unaltered in the superficial layers of the lateral and medial EC. Scale bar: 250 µm.

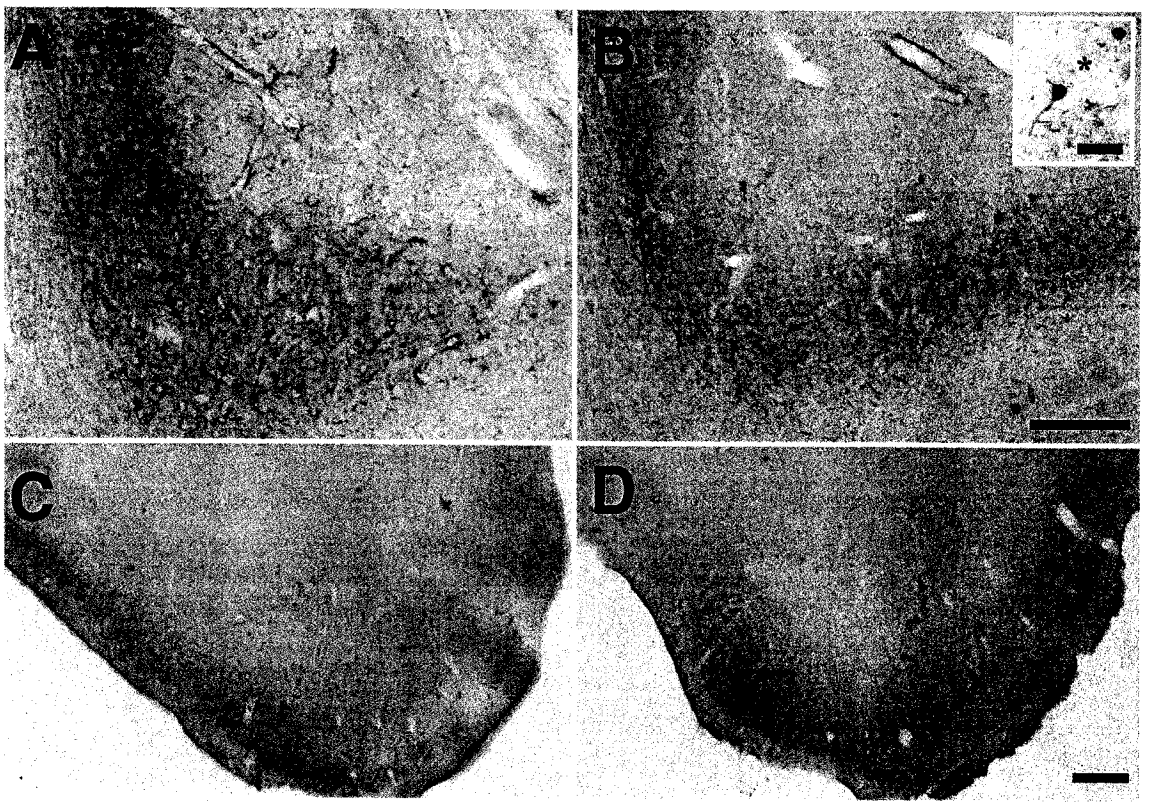
A
B
C
D

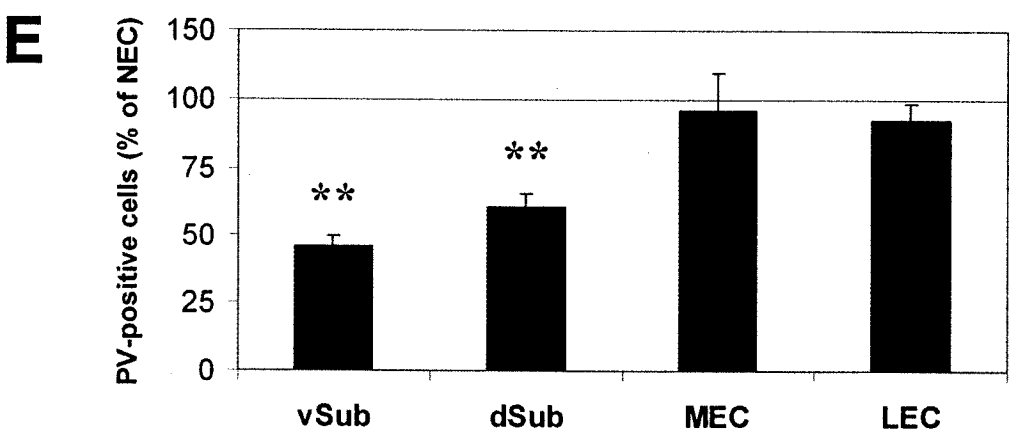
E
PV-positive cells (% of NEC)
150
100
75
50
25
0
**
**
vSub
dSub
MEC
LEC

Figure 10

Figure 1-11:

Changes in synaptophysin immunoreactive levels in NEC (A) and pilocarpine-treated epileptic rats (B). The arrows point to patches of highly dense synaptophysin immunoreactivity, respectively magnified in the insets on the right side (arrowheads), in the molecular layer of dentate gyrus (DG), the distal subiculum (distSub), and in the superficial layers of the medial EC (MEC). In panel **C**, densitometric analysis of synaptophysin immunoreactivity demonstrates higher levels in the subiculum and EC of pilocarpine-treated epileptic rats (see Fig. 1 for indications on the sampling procedure). Other abbreviations: CA1, cornu Ammonis 1; gl, granule layer; proxSub, proximal subiculum. *=$p<0.05$, **=$p<0.01$, Mann-Whitney test. Scale bars, 500 µm for A and B, 100 µm for the insets.

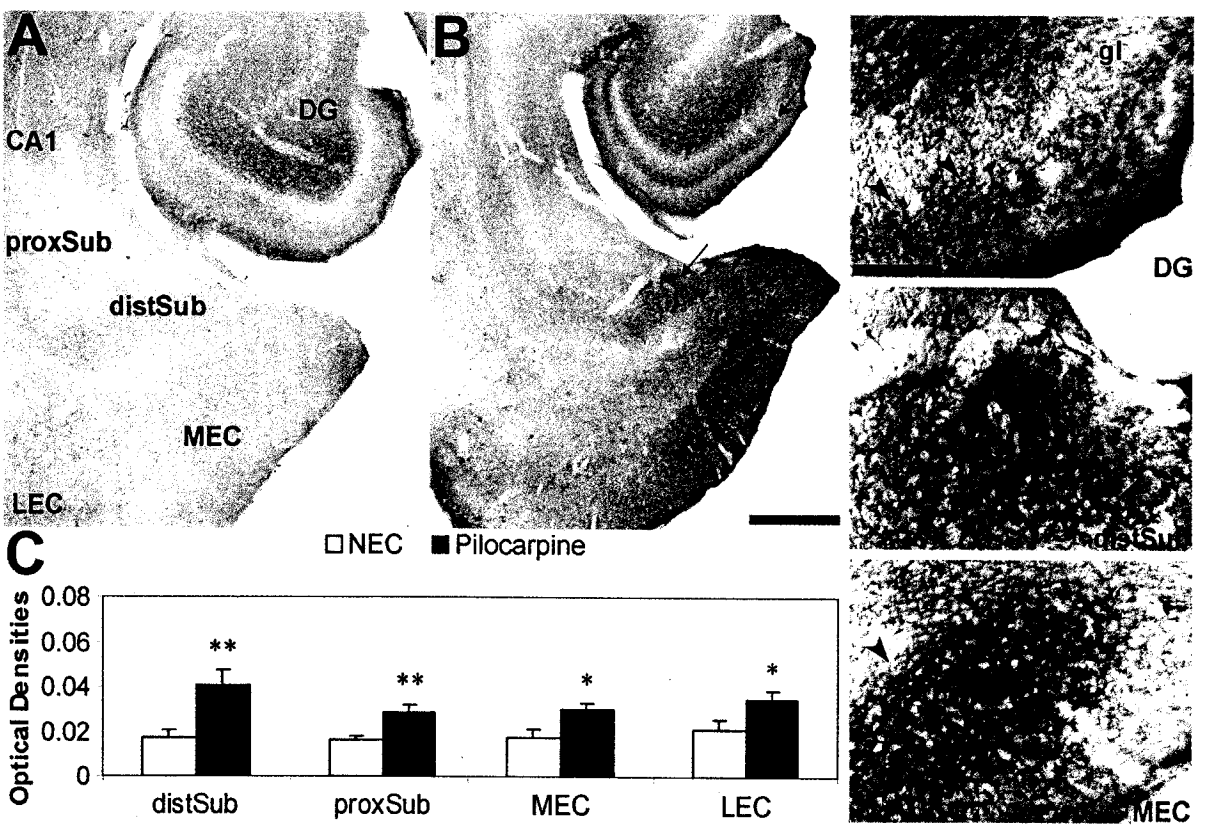
A
CA1
DG
proxSub
distSub
MEC
LEC
B
gl
DG
distSub
MEC
C
NEC
Pilocarpine
Optical Densities
0.08
0.06
0.04
0.02
0
**
**
*
*
distSub
proxSub
MEC
LEC

Figure 11

Table 1-1:

Intrinsic neuronal properties of NEC and pilocarpine-treated subicular neurons.

A comparison of the resting membrane potential (RMP), the input resistance (IR) and the action potential amplitude (APA) and action potential duration (APD) in the NEC and pilocarpine treated subiculum. Additional properties include membrane potential for subthreshold oscillatory activity as well as action potential generation.

Intrinsic properties of NEC subicular neurons

Firing Pattern	RMP (mV)	IR (MΩ)	APA (mV)	APD (ms)	Oscillatory threshold (mV)	AP threshold (mV)
Regular Firing (n = 14)	-69.7 ± 0.8	42.3 ± 2.9	89.2 ± 2.5	1.3 ± 0.1	-54.5 ± 0.5	-50.5 ± 0.9
Intrinsic Bursting (n = 14)	-66.7 ± 1.1	35.2 ± 3.1	88.8 ± 1.9	1.3 ± 0.1	-56.7 ± 1.8	-54.7 ± 1.0

Intrinsic properties of pilocarpine treated subicular neurons

Firing Pattern	RMP (mV)	IR (MΩ)	APA (mV)	APD (ms)	Oscillatory threshold (mV)	AP threshold (mV)
Regular Firing (n = 13)	-66.7 ± 0.8	43.7 ± 3.7	91.4 ± 2.8	1.4 ± 0.1	-53.2 ± 2.3	-49.9 ± 1.1
Intrinsic Bursting (n = 16)	-69.0 ± 1.1	39.4 ± 3.7	88.9 ± 2.1	1.3 ± 0.1	-58.7 ± 0.9	-54.8 ± 0.9

Table 1

Chapter 2: Network Hyperexcitability in the Deep Layers of the Pilocarpine-Treated Entorhinal Cortex

2.0 Linking Text & Information About Publication

In the presence of convulsive agents, robust ictal discharges originate from the deep layers of the entorhinal cortex and propagate towards and throughout adjacent limbic structures. As discussed in chapter 1, multiphasic activity appeared in the pilocarpine treated subiculum following electrical activation of the epileptic entorhinal cortex. This evidence implicates the epileptogenic nature of the entorhinal cortex.

Most investigations of the entorhinal cortex in chronic seizure models have often focused upon the superficial layers and medial subdivision. In my next series of experiments, I investigated the properties of layer V of the pilocarpine treated entorhinal cortex and its network interactions in the lateral and medial subdivisions. I further assessed the role of NMDA receptor function in the entorhinal cortex and its importance in maintaining *in vitro* epileptiform activity. This study was submitted to the Journal of Neurophysiology in a manuscript titled "Network hyperexcitability in the deep layers of the pilocarpine-treated entorhinal cortex" (de Guzman P, Inaba Y, de Curtis M and Avoli M)

2.1 Abstract

We report in this study that epileptiform discharges can occur spontaneously (duration= 2.60±0.49 s) or be induced by electrical stimuli (duration= 2.50±0.62 s) in entorhinal cortex (EC) slices from pilocarpine-treated rats, but not in slices from age-matched, non-epileptic control (NEC). These network-driven epileptiform events consist of field oscillatory sequences at frequencies greater than 200 Hz that most often initiate in the lateral EC and propagate to the medial EC with 25-63 ms delays. The

NMDA receptor antagonist CPP depresses the rate of occurrence ($p<0.01$) of spontaneous epileptiform discharges but fails in blocking them. Paradoxically, stimulus-induced epileptiform responses are enhanced in duration during CPP application. Concomitant application of NMDA and non-NMDA glutamatergic antagonists abolishes spontaneous and stimulus-induced epileptiform events. Intracellular recordings from lateral EC layer V cells indicate a lower frequency spontaneous hyperpolarizing postsynaptic potentials ($p<0.002$) in pilocarpine-treated tissue than in NEC both under control conditions and with glutamatergic receptor blockade. Finally, the reversal potential of pharmacologically isolated $GABA_A$ receptor-mediated inhibitory postsynaptic potentials has similar values in the two types of tissue. Collectively, these results indicate that reduced inhibition within the pilocarpine-treated EC layer V may promote network epileptic hyperexcitability.

2.2 Introduction

The entorhinal cortex (EC) is a limbic structure that receives anatomical inputs from the amygdala, the perirhinal cortex and the hippocampal formation (Burwell and Amaral 1998). One of the physiological functions of the EC is to participate in spatial memory and learning (Hafting et al. 2005). Moreover, in pathophysiological conditions, such as human temporal lobe epilepsy (TLE), the EC exhibits dysfunctional neurotransmission (Jamali et al. 2006), neuronal death (Du et al. 1993) and volumetric reduction (Bernasconi et al. 1999).

In vitro electrophysiological studies of the EC have demonstrated that bath application of convulsants promote robust epileptiform activity. This experimental approach has allowed us to further understand the EC network machinery, as it may exploit synaptic or intrinsic properties unique to this structure (Avoli et al. 1996; de

Guzman et al. 2004; Dickson et al. 2000; Uva et al. 2005). However, these acute experiments focused on seizure-like events involving tissue that does not exhibit the network changes that are associated with a chronic condition such as TLE. Furthermore, pharmacological manipulations (e.g., the application of convulsant drugs) alter EC excitability, making it difficult to identify subtle functional alterations that may be present in the epileptic tissue.

Investigating chronic models of TLE can address these limitations. Thus, studies in kainic acid- or pilocarpine-treated animals have shown patterns of neuronal death similar to those observed in human TLE along with alterations in network function (Ben-Ari 1985; Biagini et al. 2005; Covolan and Mello 2000; Du et al. 1995; Tolner et al. 2005; van Vliet et al. 2004). Most of these investigations have addressed the superficial layers of the medial EC and have identified both enhanced network interactions and altered intrinsic neuronal properties (Kobayashi et al. 2003; Kumar and Buckmaster 2006; Shah et al. 2004; Tolner et al. 2005; Wozny et al. 2005). In addition, layer V of the medial EC of pilocarpine-treated tissue has been reported to exhibit changes in excitatory presynaptic activity (Yang et al. 2006). These studies indicate that network changes within the medial EC can lead to hyperexcitability, thus contributing to epileptiform synchronization and limbic seizures. However, the contribution of the lateral EC to TLE development remains under-investigated. Therefore, by employing field potential and intracellular recordings, we assessed here the network interactions of layer V networks of the lateral EC in slices obtained from non-epileptic control (NEC) and pilocarpine-treated rats.

2.3 Methods

2.3.1 Preparation of pilocarpine-treated rats

Adult, male Sprague Dawley rats (150-200g) were subjected to intraperitoneal injections with the cholinergic agonist pilocarpine (380 mg/kg, i.p.) (*cf.* de Guzman et al., 2006) according to procedures approved by the Canadian Council of Animal Care. All efforts were made to minimize the number of animals used and their suffering. To prevent discomfort induced through peripheral muscarinic receptor stimulation, rats were treated with i.p. injection of scopolamine methylnitrate (1 mg/kg) 30 min prior to pilocarpine injection. Animal behavior was monitored for 6 h after pilocarpine injection and scored according to the classification of Racine (1972). Pilocarpine treated rats that experienced *status epilepticus* (Racine stages 3-5) for 30 min or more (duration= 46±5 min, n= 52) were defined as the experimental group and studied within 4 months (17±1 week; n= 52) subsequent to pilocarpine injection. Previous investigations have established that adult rats that experience pilocarpine-induced *status epilepticus* will develop chronic seizure activity (Cavalheiro et al. 1991; Priel et al. 1996). As such, pilocarpine-treated animals that were video-monitored showed spontaneous behavioral seizures (n= 26). Age-matched NEC rats - injected i.p. with saline - did not develop *status epilepticus* or any other form of epileptic behavior.

2.3.2 Electrophysiology procedures

Brain slices from NEC and pilocarpine-treated epileptic rats were obtained according to the procedures established by the Canadian Council of Animal Care. Animals were decapitated under halothane anesthesia, the brain was extracted and placed in cold (1-3°C) oxygenated artificial cerebrospinal fluid (ACSF). Horizontal brain slices (450 μm-thick) that included the EC, the subiculum and the hippocampus proper, were cut with a vibratome along a horizontal plane of the brain that was tilted by approx. 10°

along a posterosuperior-anteroinferior plane passing between the lateral olfactory tract and the brain stem base (Avoli et al. 1996). Combined hippocampal-EC slices were transferred to an interface tissue chamber and superfused with oxygenated (95%O_2, 5%CO_2) ACSF at 32-34°C. ACSF composition was (in mM): NaCl 124, KCl 2, KH_2PO_4 1.25, $MgSO_4$ 2, $CaCl_2$ 2, $NaHCO_3$ 26, and glucose 10. Ifenprodil (10 μM), 3,3-(2-carboxypiperazin-4-yl)-propyl-1-phosphonate (CPP, 10 μM), 6-cyano-7-nitroquinoxaline-2,3-dione (CNQX, 10 μM) and picrotoxin (50 μM) were bath applied. Chemicals were acquired from Sigma-Aldrich Canada Ltd. (Oakville, Ontario, Canada) and Tocris Cookson Inc. (Ellisville, MO, USA).

Field potential recordings were performed with ACSF-filled glass electrodes (tip diameter: <8 μm; resistance: 2–10 MΩ) that were connected to a Cyberamp 380 amplifier (Axon Instruments, Union City, CA, USA). Lateral EC neurons were recorded intracellularly with sharp-electrodes that were filled with 3M potassium acetate (tip resistance= 90-120 MΩ) and coupled to an Axoclamp 2A amplifier (Axon Instruments) with an internal bridge circuit for intracellular current injection. Resistance compensation was monitored throughout the experiment and adjusted as required. The fundamental electrophysiological parameters of lateral EC neurons were measured as follows: (i) resting membrane potential (RMP) after cell withdrawal (ii) apparent input resistance (Ri) from the maximum voltage change in response to hyperpolarizing current pulses (< -0.5 nA) (iii) action potential amplitude (APA) and (iv) action potential duration (APD). Neuronal network activation was made via a concentric bipolar electrode (Frederick Haer and Co., Bowdoinham, ME, USA) positioned in lateral EC layer V. In all experiments, the minimum stimulus intensity (duration= 100 μs) eliciting a reliable response was selected.

Field potential and intracellular signals were fed to a computer interface (Digidata 1322A, Axon Instruments) and were acquired and stored using the pClamp 8.0 software (Axon Instruments). Subsequent analysis of these data was performed with the Clampfit 9 software (Axon Instruments). For each field potential trace, the onset of epileptiform activity was determined relative to the earliest deflection from the baseline recording. The reversal potential of stimulus-induced, pharmacologically isolated inhibitory post-synaptic potentials (IPSPs) was determined by linear regression from the plot of their amplitude versus membrane potential.

2.3.3 Statistical methods

Measurements in the text are expressed as mean±S.E.M. and *n* indicates the number of samples studied under each specific protocol. The results obtained were compared with the Student's t-test or Mann-Whitney test and were considered statistically significant if $p<0.05$.

2.4 Results

2.4.1 Epileptiform activity is a hallmark of the pilocarpine-treated EC

As illustrated in Fig. 1A, spontaneous hypersynchronous activity was not recorded from the EC in brain slices obtained from NEC animals (n= 35 slices from 24 rats). In these experiments extracellular focal stimuli delivered in the EC deep layers elicited transient monophasic or biphasic field potentials (duration= 0.14±0.05 s, n=16; Fig. 1Aa). In contrast, spontaneous field discharges occurred in 36 of 49 pilocarpine-treated EC slices that were obtained from 31 animals (Fig. 1B). These epileptiform discharges (duration= 2.60±0.49 s; interval of occurrence= 35.2±4.3 s; n= 36) consisted in the lateral EC layer V of a series of negative deflections arising from a

slow negative shift coinciding with an initial positive waveform in layers II and III (Fig. 1Ba). Similar field events (duration= 2.50±0.62 s, n= 49) were elicited in all pilocarpine-treated slices by electrical stimuli (Fig. 1Bb).

As illustrated in Fig. 2, the onset of both spontaneous and stimulus-induced epileptiform events recorded from the lateral EC of pilocarpine-treated slices consisted of transient repetitive runs of fast oscillatory activity (duration= 52.8±5.7 ms, n=22). Power spectral analysis (following a band pass filtering from 100 Hz to 1000 Hz) of the initial component of the field discharges recorded from the lateral EC layer V demonstrated fast oscillatory ripple activity exceeding 200Hz (Fig. 2Ab,c and Bb,c). In contrast, quantification of the frequency of the late component of the epileptiform events, via power spectra, indicated oscillations at 20 Hz (not shown).

2.4.2 Network interactions within the pilocarpine-treated EC

Next, we assessed the initiation and propagation of epileptiform discharges in the deep layers of both lateral and medial EC subdivisions. The slice schematic on the top part of Fig. 3 illustrates the position of the field potential recording electrodes and of the stimulating electrode that was located in the lateral EC. Electrical stimuli delivered in NEC slices - which did not generate any spontaneous field activity - elicited a monophasic negative deflection in the lateral EC that was followed by a biphasic positive-negative waveform in the medial EC (n=6; Fig. 3A). In contrast, slices from pilocarpine-treated rats generated spontaneous epileptiform events that originated from the lateral (n= 6, Fig 3Ba) or medial EC (n= 3, Fig. 3Bb) and subsequently propagated to the medial and lateral EC, respectively. Propagation delays between the two structures produced a variable travel time between 25 and 63 ms (n=9). In the distribution histogram shown in Fig. 3C, we arbitrarily defined

territorial lag times from the lateral EC towards the medial EC as negative whereas the reverse direction (medial EC→lateral EC) was classified as positive. This variability in bidirectional propagation could be restricted to a unidirectional movement from lateral to medial EC following stimulation of lateral EC layer V along with a more confined time lag distribution (4 to 24 ms; n=9) (Fig. 3D).

2.4.3 Firing properties of layer V lateral EC neurons in both NEC and pilocarpine-treated tissue

We further investigated whether the firing patterns and the intrinsic properties of lateral EC layer V neurons were altered in the epileptic tissue compared to NEC. Intracellular injection of depolarizing current pulses (duration= 1s) induced two patterns of firing in lateral EC neurons analyzed in both types of tissue. The first consisted of regular, repetitive firing only (Fig 4Aa and Ba), while the second was characterized by an initial burst of action potentials followed by regular firing (Fig 4Ab and Bb). Quantification of these two firing patterns in NEC (regular firing, n= 25; intrinsic bursting, n= 6) and pilocarpine-treated slices (regular firing, n= 47; intrinsic bursting, n= 8) demonstrated in both cases a higher incidence of regular firing neurons compared to intrinsic bursters. In addition, lateral EC neurons recorded in the two types of tissue displayed similar fundamental intrinsic properties (Table 1).

2.4.4 Intracellular characteristics of spontaneous and stimulus-induced events in NEC and pilocarpine-treated lateral EC neurons

Single-shock stimulation produced an initial depolarizing response that was followed by biphasic hyperpolarizing components in lateral EC layer V neurons recorded at RMP in NEC slices (Fig. 5A, -67 mV). Cell membrane hyperpolarization to values more negative than -80 mV with injection of steady negative current increased the

amplitude of the stimulus-induced depolarizing component and markedly reduced the subsequent hyperpolarizations (Fig. 5A, -80 mV trace). In contrast, active depolarization of these cells disclosed a robust hyperpolarizing response (Fig. 5A, -51 mV trace), that was at times preceded by a single action potential (not shown). Hence, all layer V neurons (26/26) recorded from the NEC lateral EC generated sequences of excitatory post-synaptic potential (EPSP)-IPSP in response to single-shock electrical stimuli.

In contrast, stimulus-induced (n= 56/75 neurons from 72 slices) and spontaneous (n=50/75 neurons from 72 slices) action potential bursting was recorded intracellularly from layer V neurons of the lateral EC in pilocarpine-treated slices. At RMP both stimulus-induced and spontaneous discharges were characterized by a depolarizing envelope that was overridden by action potential bursting (Fig. 5B, -69 mV and -71 mV). Membrane hyperpolarization to values more negative than RMP increased the amplitude of the stimulus-induced and spontaneous depolarizing envelopes (Fig. 5B, -82 mV and -82 mV, respectively). Conversely, steady depolarization of these neurons to membrane values around -50 mV reduced the amplitude of these depolarizations (Fig. 5B, -50 mV and -52 mV, respectively). Within the range of membrane potentials tested in these experiments (i.e., from -85 to -50 mV) stimulus-induced and spontaneous depolarizations triggered similar amounts of action potential discharge. In addition, as expected from a network-driven synaptic event, changing the neuron membrane potential did not modify the rate of occurrence of the spontaneous epileptiform depolarizations.

2.4.5 Epileptiform activity in pilocarpine-treated EC persists during NMDA receptor antagonism but is abolished by a non-NMDA glutamatergic antagonist

We further characterized the dependence of spontaneous network-driven epileptiform activity (duration= 1.75±0.32 s, interval= 32.7±9.6s, n= 5) on ionotropic glutamatergic mechanisms (Fig. 6A). Bath application of the NR2B receptor antagonist ifenprodil (10 μM, n= 5) did not modify the duration or the rate of occurrence of these spontaneous events. Synchronous discharges also persisted following application of CPP (10 μM, n= 5) although this NMDA receptor antagonist increased significantly ($p<0.01$) their interval of occurrence (Fig. 6A). Subsequent application of CNQX blocked spontaneous network bursting (Fig. 6A; n= 5). The effects of these ionotropic glutamatergic antagonists on the duration and rate of occurrence of spontaneous epileptiform events are summarized in Fig. 6B and C.

In these experiments we also tested the effects of NMDA and non-NMDA glutamatergic antagonism on the paroxysmal depolarizations elicited by single-shock stimuli delivered in lateral EC layer V of pilocarpine-treated slices. Bath application of ifenprodil did not influence these stimulus-induced epileptiform discharges (n= 5), while subsequent application of CPP (n=6) caused an enhanced network response characterized by a single action potential followed by sustained discharges (Fig. 7A). This apparent augmented response was associated with a significant increase in latency following the stimulus. Finally, subsequent addition of CNQX (10 μM, n= 6) abolished the stimulus-induced epileptiform discharges and revealed a monosynaptic post-synaptic potential (PSP). The effects induced by these ionotropic glutamatergic antagonists on the duration and latency of the stimulus-induced epileptiform responses are quantified in the plots shown in Fig. 7B and C.

2.4.6 Reduced GABAergic inhibition in the pilocarpine-treated EC

Spontaneous hyperpolarizing post-synaptic potentials (PSPs) were recorded from NEC EC layer V neurons analyzed at RMP under control conditions (Fig. 8A, -73 mV). These events occurred at intervals ranging from 7.4 to 34.9 s (12.5±1.1 s, n= 7 neurons); this value differed from what observed in pilocarpine-treated layer V lateral EC (Fig 8A, -68 mV) as similar PSPs occurred at significantly longer intervals in these neurons (Fig 8B, 28.5±4.9 s, n= 12, $p<0.002$ independent t-test).

Spontaneous hyperpolarizing PSPs, recorded at RMP during concomitant application of CPP (10 μM) and CNQX (10 μM) were also more frequent in NEC (interval of occurrence= 14.4±1.6 s, n=6) as compared to pilocarpine-treated cells (interval of occurrence= 73.3±18.9 s, n=7; $p<0.00001$) (Fig. 8C and D). As shown in Fig. 8C and E, the amplitude of these PSPs was smaller in pilocarpine-treated cells (2.15±0.17 mV, n= 6) than in NEC (5.14±1.14 mV, n= 6; $p<0.0002$). Finally, during blockade of glutamatergic receptors, NEC and pilocarpine-treated EC neurons responded to local electrical stimuli with intracellular potentials that were characterized by similar reversal values (Fig. 8F and G; -75.4±1.1 mV, n=6 for NEC and -73.2±1.6 mV, n=6, for pilocarpine-treated EC cells; $p>0.05$, independent t-test). Subsequent bath application of the $GABA_A$ receptor antagonist picrotoxin (50 μM, n= 6) blocked both spontaneous and stimulus-induced IPSP activity in both types of tissue (not illustrated).

2.5 Discussion

We have found that the lateral EC in slices obtained from pilocarpine-treated animals can generate spontaneous epileptiform events that do not occur in NEC tissue. These discharges initiated most often within the lateral EC, and entrained the medial EC.

We have also demonstrated that this type of epileptiform activity is not NMDA receptor-dependent, as spontaneous and stimulus-induced synchronous bursting persisted following NMDA receptor antagonism. Finally, we have established that spontaneous, presumably $GABA_A$ receptor-mediated, PSPs in epileptic lateral EC neurons were reduced in amplitude and in frequency, thus suggesting that network hyperexcitability in the pilocarpine-treated lateral EC may result from impaired inhibition.

2.5.1 Network hyperexcitability within the pilocarpine-treated EC

Experiments performed in kindled rats have provided evidence for EC hyperexcitability, although no spontaneous network activity was reported (Fountain et al. 1998). Utilizing simultaneous field potential recordings, we have found that spontaneous network discharges in the absence of acute application of epileptogenic agents occur within the lateral EC. In line with this observation, convulsant treatments in control slices have demonstrated that synchronous epileptiform discharges are generated in the medial EC as well as that this epileptiform activity originates in the deep layers (Dickson and Alonso 1997; Jones and Heinemann 1988; Lopantsev and Avoli 1998a, b).

The spontaneous network discharges recorded from EC slices of pilocarpine-treated animals exhibit bidirectional routes of propagation between the medial and lateral component of this limbic structure. Accordingly, similar characteristics have been reported for the epileptiform activities recorded in the EC of control tissue slices in the presence of convulsants (de Guzman et al. 2004; Klueva et al. 2003; Uva et al. 2005). These studies collectively demonstrate that enhanced excitation can promote network reverberation within the EC as reported in *in vitro* whole brain studies (Biella et al. 2002a; Biella et al. 2002b; Gnatkovsky and de Curtis 2006). It should also be

emphasized that the paroxysmal network synchronization identified in pilocarpine-treated lateral EC is supported by the occurrence of brief bursts of transient, high frequency oscillations in layer V at the onset of spontaneous and stimulus-induced epileptiform events. High frequency oscillations exceeding 200 Hz, deemed pathological, may serve as a surrogate marker of epileptogenicity (Bragin et al. 2004) as suggested by intracranial recordings performed in the EC of TLE patients (Bragin et al. 2002b; Jirsch et al. 2006) and by *in vivo* recordings in the temporal cortex of kainic acid-treated rodents (Bragin et al. 2002a; Tolner et al. 2005).

The hyperexcitabilty of pilocarpine-treated layer V lateral EC cells also emerged following electrical stimulation. Single-shock stimuli in NEC slices elicited PSPs consisting of an initial depolarizing response (presumably an EPSP that could eventually trigger a single action potential) followed by biphasic hyperpolarizing components (Behr et al. 1998; Williams et al. 1993)). In contrast, EC neurons recorded in slices from pilocarpine-treated animals responded to similar electrical stimuli by generating paroxsysmal epileptiform activity. A decreased threshold of network responses to stimuli has been reported to occur in EC superficial layers (Kobayashi et al. 2003; Kumar and Buckmaster 2006) and subiculum (Cohen et al. 2002; de Guzman et al. 2006) of epileptic tissue.

We also addressed whether network hyperexcitability within the pilocarpine-treated EC could be attributed to changes in intrinsic neuronal properties. However, RMP, Ri, and APA were not different in layer V neurons recorded in NEC and pilocarpine-treated animals. In both conditions, an overwhelming number of regular firing neurons was observed compared to intrinsic bursters, which is line with studies performed in layer V of the lateral (Hamam et al. 2002; Rosenkranz and Johnston 2006) and medial (Hamam et al. 2000) EC in control tissue. As such, we conclude that

factors involving recurrent excitatory connectivity and attenuated inhibition may contribute to the hyperexcitablity of the deep layer EC (Dhillon and Jones 2000; Woodhall et al. 2005).

2.5.2 Reduced network inhibition in the pilocarpine-treated EC

Previous studies in control tissue have shown a significantly reduced network inhibition in EC layer V compared to layer II (Woodhall et al. 2005). In our pilocarpine-treated tissue, lateral EC layer V neurons revealed a lower frequency of spontaneous post-synaptic events. These results, which suggest decreased network inhibition within the pilocarpine-treated lateral EC layer V, were further reinforced by data obtained in the presence of glutamatergic antagonists. We have found that lateral EC layer V neurons in pilocarpine-treated slices produced a lower frequency of IPSP activity along with significantly reduced amplitudes than NEC cells. Thus, these findings indicate a diminished GABAergic inhibition of layer V pyramidal cells when compared to the NEC. In parallel with these results, EC layer II is subject to reduced network inhibition in the pilocarpine-treated EC (Kobayashi et al. 2003). However, the attenuated inhibition identified in EC layer V neurons was not associated with a change in $GABA_A$ receptor-mediated IPSP reversal potential, unlike previous studies performed in the subiculum of human epileptic patients (Cohen et al. 2002) and pilocarpine-treated animals (de Guzman et al. 2006). Overall, our data suggest that disinhibition within the EC could result from reduced inhibitory input rather than alterations in Cl^- extrusion mechanisms. Attenuated network inhibition resulting from a reduced excitatory drive on inhibitory interneurons, has been reported in the hippocampus and EC layers II/III (Bekenstein and Lothman 1993; Kumar and Buckmaster 2006; Sloviter et al. 2003; Williams et al. 1993). Additional alterations

regarding a reduction of NPY and 5-HT activity may contribute to network hyperexcitability within the EC (Jamali et al. 2006).

2.5.3 Glutamatergic mechanisms in the pilocarpine-treated EC

The presence of spontaneous epileptiform activity in pilocarpine-treated EC involves reduced network inhibition leading to a presumed over-expression of glutamatergic mechanisms. We have, however, found that EC network hyperexcitability is not dependent upon NMDA receptors. Previous investigations in control tissue have revealed that NMDA receptor blockade abolishes ictal-like activity (Avoli et al. 1996; de Guzman et al. 2004). In contrast, both spontaneous and stimulus-induced epileptiform discharges in pilocarpine-treated EC appeared to be resistant to NMDA receptor antagonism.

A recent investigation of EC layer V neurons in pilocarpine-treated slices has revealed an alteration in NR2B receptor function thus suggesting a developmental regression of this NMDA receptor subtype (Yang et al. 2006). In contrast, we have found in our experiments that spontaneous or stimulus-induced epileptiform discharges were not influenced by NR2B receptor antagonism. Since the presence of the NR2B receptor is reported to be age-dependent, these different results may reflect the younger age of the animals used in the study of Yang et al (2006). However, we have also found that spontaneous epileptiform discharges in pilocarpine-treated EC persisted in the presence of full NMDA receptor blockade even though it occurred at longer intervals. Interestingly, single-shock stimulation during CPP application produced a delayed response consisting of a prolonged bursting sequence, thereby suggesting an apparent augmentation of network discharge. The delayed occurrence, combined with the gradual rising and sustained

action potential firing, following single-shock stimuli during NMDA receptor blockade may be caused by reduced NMDA-dependent depolarization and synchronization. Thus, under these experimental conditions, blockade of NMDA receptors could delay the development of a bursting sequence that is sustained by AMPA/kainite receptors coupled with the subsequent recruitment of cholinergic synapses to promote network reverberation (Cobb and Davies 2005).

Kindling studies in the dentate gyrus indicate that NMDA receptor blockade does not preclude seizure development (Brandt et al. 2003) nor contributes to the maintenance of seizure activity (Sayin et al. 1999). Therefore, factors such as reduced inhibitory inputs (Kumar and Buckmaster 2006) as well as increased synaptic sprouting (de Guzman et al. 2006) leading to over-function of AMPA/kainate receptor-mediated mechanisms, should be taken into account for the hyperexcitability demonstrated in the pilocarpine-treated rats. In keeping with this view, spontaneous and stimulus-induced epileptiform discharges were abolished upon AMPA/kainate receptor antagonism.

2.6 Conclusions

Our study indicates that the pilocarpine-treated EC is hyperexcitable. The epileptic EC has been demonstrated to interact with the subiculum and CA1; this limbic circuit has been suggested to enhance network reverberation and to increase excitation under epileptic conditions (Biagini et al. 2005; D'Antuono et al. 2002; Wozny et al. 2005). As such, the pilocarpine-treated EC exhibits hyperexcitable network properties that contribute to the generation and propagation of seizure activity across limbic structures. As of recent, most investigations have focused on the medial EC while the lateral EC received scarce attention. Nonetheless, in chronic models of

seizure activity, the lateral EC layer III has been shown to enhance subicular activity (de Guzman et al. 2006) and to display altered intrinsic neuronal properties (Shah et al. 2004). Furthermore, lateral EC ablation has been reported to attenuate limbic seizures thus underscoring the epileptic role of this area (Kopniczky et al. 2005). Further investigation of the lateral EC is required as it may represent an important therapeutic target for controlling limbic seizures in TLE patients

2.7 Acknowledgements

This study was supported by grants from the Canadian Institutes of Health Research (CIHR; grant 8109), the Savoy Foundation and the Mariani Foundation.

2.8 References

Avoli M, Barbarosie M, Lucke A, Nagao T, Lopantsev V, and Kohling R. Synchronous GABA-mediated potentials and epileptiform discharges in the rat limbic system in vitro. *J Neurosci* 16: 3912-3924, 1996.

Behr J, Gloveli T, and Heinemann U. The perforant path projection from the medial entorhinal cortex layer III to the subiculum in the rat combined hippocampal-entorhinal cortex slice. *Eur J Neurosci* 10: 1011-1018, 1998.

Bekenstein JW and Lothman EW. Dormancy of inhibitory interneurons in a model of temporal lobe epilepsy. *Science* 259: 97-100, 1993.

Ben-Ari Y. Limbic seizure and brain damage produced by kainic acid: mechanisms and relevance to human temporal lobe epilepsy. *Neuroscience* 14: 375-403, 1985.

Bernasconi N, Bernasconi A, Andermann F, Dubeau F, Feindel W, and Reutens DC. Entorhinal cortex in temporal lobe epilepsy: a quantitative MRI study. *Neurology* 52: 1870-1876, 1999.

Biagini G, D'Arcangelo G, Baldelli E, D'Antuono M, Tancredi V, and Avoli M. Impaired activation of CA3 pyramidal neurons in the epileptic hippocampus. *Neuromolecular Med* 7: 325-342, 2005.

Biella G, Uva L, and de Curtis M. Propagation of neuronal activity along the neocortical-perirhinal-entorhinal pathway in the guinea pig. *J Neurosci* 22: 9972-9979, 2002a.

Biella G, Uva L, Hofmann UG, and de Curtis M. Associative interactions within the superficial layers of the entorhinal cortex of the guinea pig. *J Neurophysiol* 88: 1159-1165, 2002b.

Bragin A, Mody I, Wilson CL, and Engel J, Jr. Local generation of fast ripples in epileptic brain. *J Neurosci* 22: 2012-2021, 2002a.

Bragin A, Wilson CL, Almajano J, Mody I, and Engel J, Jr. High-frequency oscillations after status epilepticus: epileptogenesis and seizure genesis. *Epilepsia* 45: 1017-1023, 2004.

Bragin A, Wilson CL, Staba RJ, Reddick M, Fried I, and Engel J, Jr. Interictal high-frequency oscillations (80-500 Hz) in the human epileptic brain: entorhinal cortex. *Ann Neurol* 52: 407-415, 2002b.

Brandt C, Potschka H, Loscher W, and Ebert U. N-methyl-D-aspartate receptor blockade after status epilepticus protects against limbic brain damage but not against epilepsy in the kainate model of temporal lobe epilepsy. *Neuroscience* 118: 727-740, 2003.

Burwell RD and Amaral DG. Cortical afferents of the perirhinal, postrhinal, and entorhinal cortices of the rat. *J Comp Neurol* 398: 179-205, 1998.

Cavalheiro EA, Leite JP, Bortolotto ZA, Turski WA, Ikonomidou C, and Turski L. Long-term effects of pilocarpine in rats: structural damage of the brain triggers kindling and spontaneous recurrent seizures. *Epilepsia* 32: 778-782, 1991.

Cobb SR and Davies CH. Cholinergic modulation of hippocampal cells and circuits. *J Physiol* 562: 81-88, 2005.

Cohen I, Navarro V, Clemenceau S, Baulac M, and Miles R. On the origin of interictal activity in human temporal lobe epilepsy in vitro. *Science* 298: 1418-1421, 2002.

Covolan L and Mello LE. Temporal profile of neuronal injury following pilocarpine or kainic acid-induced status epilepticus. *Epilepsy Res* 39: 133-152, 2000.

D'Antuono M, Benini R, Biagini G, D'Arcangelo G, Barbarosie M, Tancredi V, and Avoli M. Limbic network interactions leading to hyperexcitability in a model of temporal lobe epilepsy. *J Neurophysiol* 87: 634-639, 2002.

de Guzman P, D'Antuono M, and Avoli M. Initiation of electrographic seizures by neuronal networks in entorhinal and perirhinal cortices in vitro. *Neuroscience* 123: 875-886, 2004.

de Guzman P, Inaba Y, Biagini G, Baldelli E, Mollinari C, Merlo D, and Avoli M. Subiculum network excitability is increased in a rodent model of temporal lobe epilepsy. *Hippocampus* 16: 843-860, 2006.

Dhillon A and Jones RS. Laminar differences in recurrent excitatory transmission in the rat entorhinal cortex in vitro. *Neuroscience* 99: 413-422, 2000.

Dickson CT and Alonso A. Muscarinic induction of synchronous population activity in the entorhinal cortex. *J Neurosci* 17: 6729-6744, 1997.

Dickson CT, Magistretti J, Shalinsky MH, Fransen E, Hasselmo ME, and Alonso A. Properties and role of I(h) in the pacing of subthreshold oscillations in entorhinal cortex layer II neurons. *J Neurophysiol* 83: 2562-2579, 2000.

Du F, Eid T, Lothman EW, Kohler C, and Schwarcz R. Preferential neuronal loss in layer III of the medial entorhinal cortex in rat models of temporal lobe epilepsy. *J Neurosci* 15: 6301-6313, 1995.

Du F, Whetsell WO, Jr., Abou-Khalil B, Blumenkopf B, Lothman EW, and Schwarcz R. Preferential neuronal loss in layer III of the entorhinal cortex in patients with temporal lobe epilepsy. *Epilepsy Res* 16: 223-233, 1993.

Fountain NB, Bear J, Bertram EH, 3rd, and Lothman EW. Responses of deep entorhinal cortex are epileptiform in an electrogenic rat model of chronic temporal lobe epilepsy. *J Neurophysiol* 80: 230-240, 1998.

Gnatkovsky V and de Curtis M. Hippocampus-mediated activation of superficial and deep layer neurons in the medial entorhinal cortex of the isolated guinea pig brain. *J Neurosci* 26: 873-881, 2006.

Hafting T, Fyhn M, Molden S, Moser MB, and Moser EI. Microstructure of a spatial map in the entorhinal cortex. *Nature* 436: 801-806, 2005.

Hamam BN, Amaral DG, and Alonso AA. Morphological and electrophysiological characteristics of layer V neurons of the rat lateral entorhinal cortex. *J Comp Neurol* 451: 45-61, 2002.

Hamam BN, Kennedy TE, Alonso A, and Amaral DG. Morphological and electrophysiological characteristics of layer V neurons of the rat medial entorhinal cortex. *J Comp Neurol* 418: 457-472, 2000.

Jamali S, Bartolomei F, Robaglia-Schlupp A, Massacrier A, Peragut JC, Regis J, Dufour H, Ravid R, Roll P, Pereira S, Royer B, Roeckel-Trevisiol N, Fontaine M, Guye M, Boucraut J, Chauvel P, Cau P, and Szepetowski P. Large-scale expression study of human mesial temporal lobe epilepsy: evidence for dysregulation of the neurotransmission and complement systems in the entorhinal cortex. *Brain* 129: 625-641, 2006.

Jirsch JD, Urrestarazu E, LeVan P, Olivier A, Dubeau F, and Gotman J. High-frequency oscillations during human focal seizures. *Brain* 129: 1593-1608, 2006.

Jones RS and Heinemann U. Synaptic and intrinsic responses of medical entorhinal cortical cells in normal and magnesium-free medium in vitro. *J Neurophysiol* 59: 1476-1496, 1988.

Klueva J, Munsch T, Albrecht D, and Pape HC. Synaptic and non-synaptic mechanisms of amygdala recruitment into temporolimbic epileptiform activities. *Eur J Neurosci* 18: 2779-2791, 2003.

Kobayashi M, Wen X, and Buckmaster PS. Reduced inhibition and increased output of layer II neurons in the medial entorhinal cortex in a model of temporal lobe epilepsy. *J Neurosci* 23: 8471-8479, 2003.

Kopniczky Z, Dobo E, Borbely S, Vilagi I, Detari L, Krisztin-Peva B, Bagosi A, Molnar E, and Mihaly A. Lateral entorhinal cortex lesions rearrange afferents, glutamate receptors, increase seizure latency and suppress seizure-induced c-fos expression in the hippocampus of adult rat. *J Neurochem* 95: 111-124, 2005.

Kumar SS and Buckmaster PS. Hyperexcitability, interneurons, and loss of GABAergic synapses in entorhinal cortex in a model of temporal lobe epilepsy. *J Neurosci* 26: 4613-4623, 2006.

Lopantsev V and Avoli M. Laminar organization of epileptiform discharges in the rat entorhinal cortex in vitro. *J Physiol* 509 (Pt 3): 785-796, 1998a.

Lopantsev V and Avoli M. Participation of GABAA-mediated inhibition in ictallike discharges in the rat entorhinal cortex. *J Neurophysiol* 79: 352-360, 1998b.

Priel MR, dos Santos NF, and Cavalheiro EA. Developmental aspects of the pilocarpine model of epilepsy. *Epilepsy Res* 26: 115-121, 1996.

Rosenkranz JA and Johnston D. Dopaminergic regulation of neuronal excitability through modulation of Ih in layer V entorhinal cortex. *J Neurosci* 26: 3229-3244, 2006.

Sayin, Rutecki P, and Sutula T. NMDA-dependent currents in granule cells of the dentate gyrus contribute to induction but not permanence of kindling. *J Neurophysiol* 81: 564-574, 1999.

Shah MM, Anderson AE, Leung V, Lin X, and Johnston D. Seizure-induced plasticity of h channels in entorhinal cortical layer III pyramidal neurons. *Neuron* 44: 495-508, 2004.

Sloviter RS, Zappone CA, Harvey BD, Bumanglag AV, Bender RA, and Frotscher M. "Dormant basket cell" hypothesis revisited: relative vulnerabilities of dentate gyrus mossy cells and inhibitory interneurons after hippocampal status epilepticus in the rat. *J Comp Neurol* 459: 44-76, 2003.

Tolner EA, Kloosterman F, van Vliet EA, Witter MP, Silva FH, and Gorter JA. Presubiculum stimulation in vivo evokes distinct oscillations in superficial and deep entorhinal cortex layers in chronic epileptic rats. *J Neurosci* 25: 8755-8765, 2005.

Uva L, Librizzi L, Wendling F, and de Curtis M. Propagation dynamics of epileptiform activity acutely induced by bicuculline in the hippocampal-parahippocampal region of the isolated Guinea pig brain. *Epilepsia* 46: 1914-1925, 2005.

van Vliet EA, Aronica E, Tolner EA, Lopes da Silva FH, and Gorter JA. Progression of temporal lobe epilepsy in the rat is associated with immunocytochemical changes in inhibitory interneurons in specific regions of the hippocampal formation. *Exp Neurol* 187: 367-379, 2004.

Williams S, Vachon P, and Lacaille JC. Monosynaptic GABA-mediated inhibitory postsynaptic potentials in CA1 pyramidal cells of hyperexcitable hippocampal slices from kainic acid-treated rats. *Neuroscience* 52: 541-554, 1993.

Woodhall GL, Bailey SJ, Thompson SE, Evans DI, and Jones RS. Fundamental differences in spontaneous synaptic inhibition between deep and superficial layers of the rat entorhinal cortex. *Hippocampus* 15: 232-245, 2005.

Wozny C, Gabriel S, Jandova K, Schulze K, Heinemann U, and Behr J. Entorhinal cortex entrains epileptiform activity in CA1 in pilocarpine-treated rats. *Neurobiol Dis* 19: 451-460, 2005.

Yang J, Woodhall GL, and Jones RS. Tonic facilitation of glutamate release by presynaptic NR2B-containing NMDA receptors is increased in the entorhinal cortex of chronically epileptic rats. *J Neurosci* 26: 406-410, 2006.

2.9 Figures

Figure 2-1:

Spontaneous network discharges can be recorded in the pilocarpine-treated lateral EC - In the NEC and pilocarpine-treated tissues, three simultaneous field potential electrodes were positioned in lateral EC layers II, III and V combined with a bipolar stimulator in lateral EC layer V (see slice schematic) **A:** No spontaneous field potential activity occurs in the NEC tissue while single-shock stimulation produces a negative-positive deflecting transient waveform (expanded inset in **Aa**). **B:** In contrast the pilocarpine-treated lateral EC demonstrates spontaneous and stimulus-induced (triangle, **Bb**) network discharges that consist of multiple population spikes (expanded insets: **Ba and Bb**) and appear to propagate throughout layers II, III and V.

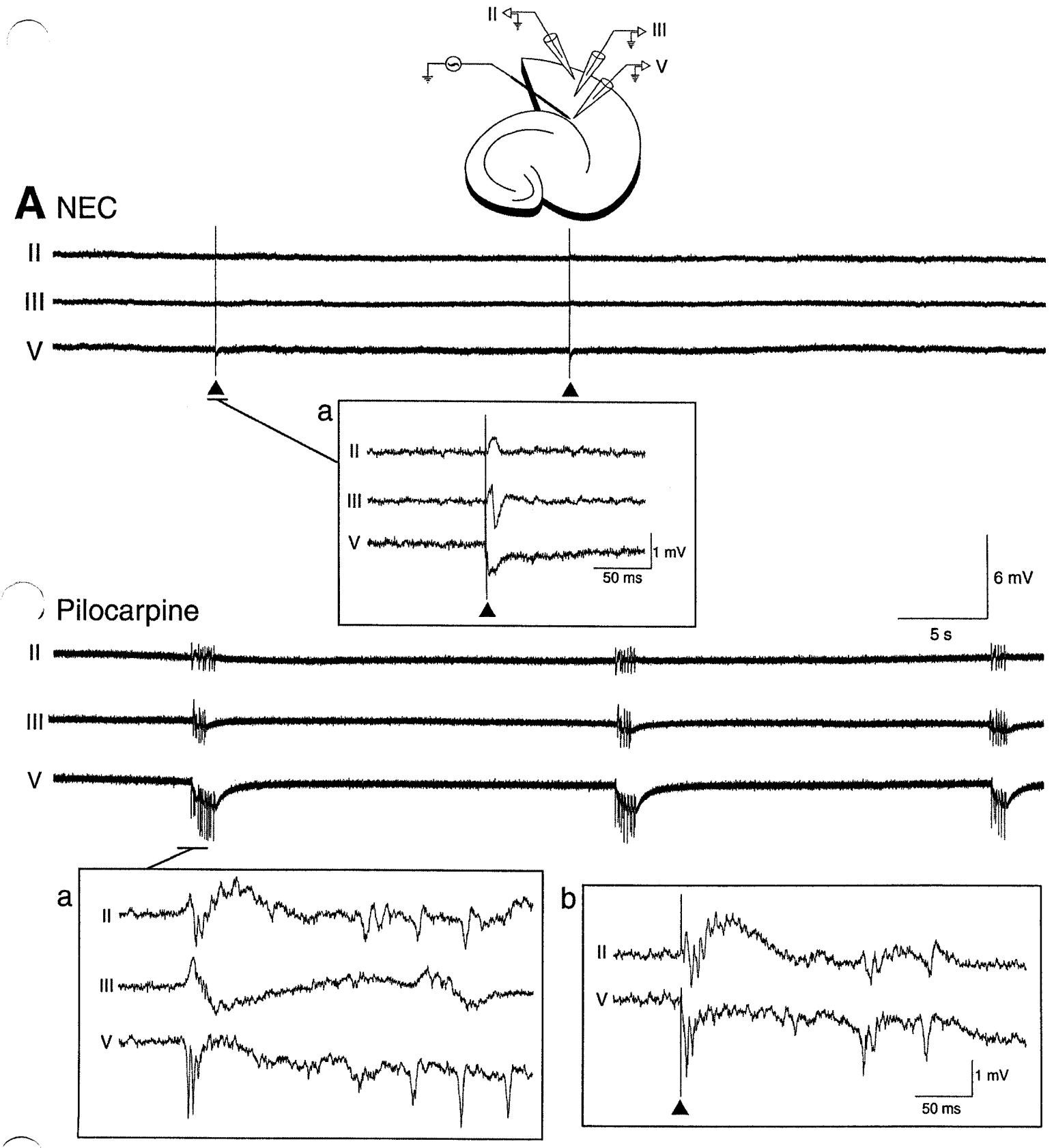
II
III
V
A NEC
II
III
V
a
II
III
V
1 mV
50 ms
6 mV
5 s
Pilocarpine
II
III
V
a
II
III
V
b
II
V
1 mV
50 ms

Fig. 1

Figure 2-2:

Fast oscillatory ripple activity occurs in the pilocarpine-treated lateral EC layer V. A and B: Spontaneous and stimulus-induced (triangle) network bursting consist of a negative deflecting waveform on which multiple population spikes occurr. Band pass filtering (100 – 1000Hz: **Ab and Bb**) reveals a transient discharge of fast oscillatory activity (expanded insets). Power spectral analyses of spontaneous (**Ac**) and stimulus induced (**Bc**) transient discharges demonstrates network oscillations greater than 200 Hz.

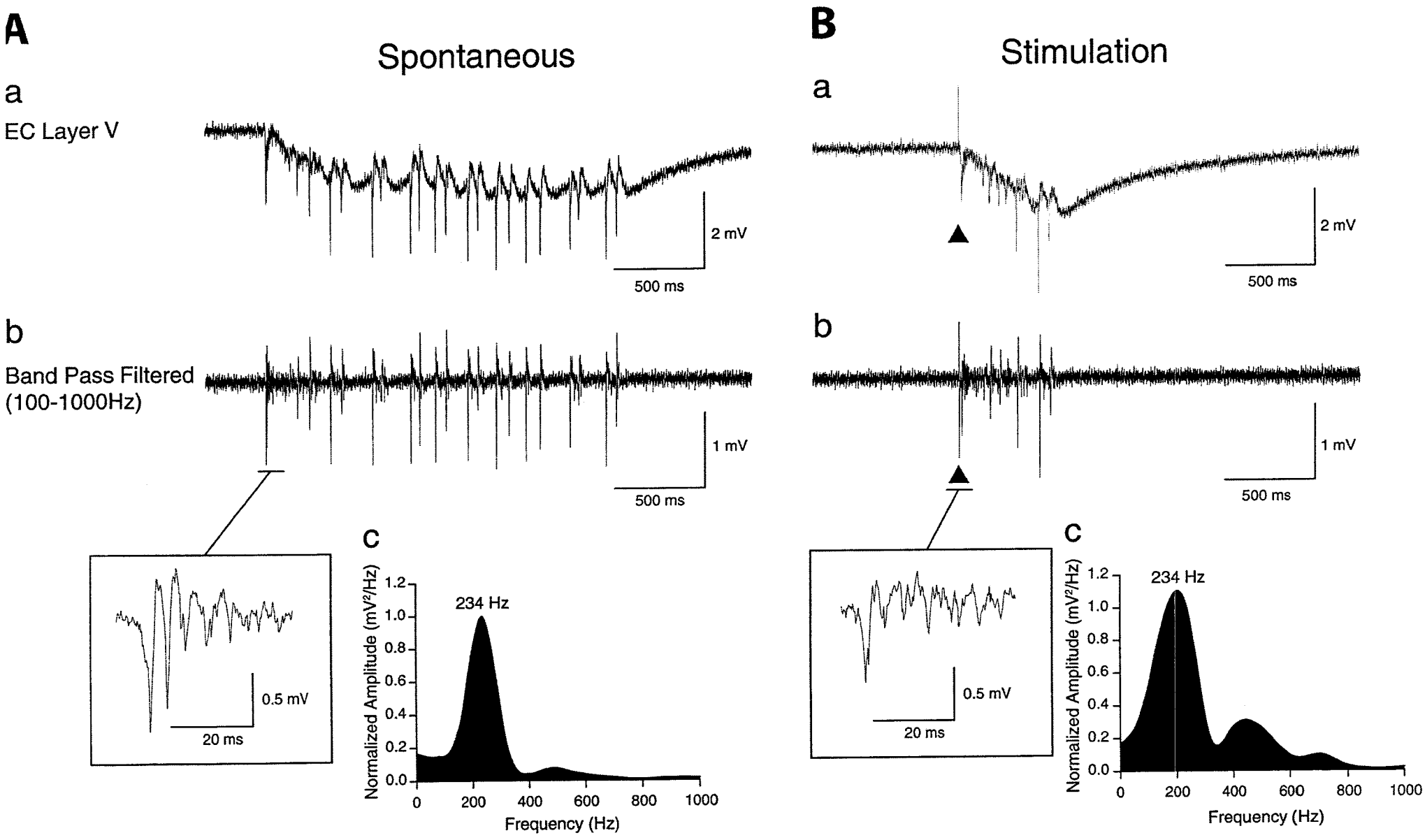
A
Spontaneous
a
EC Layer V
2 mV
500 ms
b
Band Pass Filtered
(100-1000Hz)
1 mV
500 ms
0.5 mV
20 ms
c
234 Hz
Normalized Amplitude (mV²/Hz)
Frequency (Hz)
B
Stimulation
a
2 mV
500 ms
b
1 mV
500 ms
0.5 mV
20 ms
c
234 Hz
Normalized Amplitude (mV²/Hz)
Frequency (Hz)

Fig. 2

Figure 2-3:

Spontaneous network activity propagates between both structures within the pilocarpine-treated EC. Dual field potential electrodes where positioned within layer V of the lateral EC (LEC) and medial EC (MEC) combined with a bipolar stationed in LEC layer V (slice schematic). **A:** Single shock stimulation (triangle) in NEC tissue, elicits a negative deflection followed by a biphasic waveform in the LEC and MEC, respectively. Expanded inset: network activity from the LEC propagates towards the MEC following stimulation. **B:** In two different slices, spontaneous epileptiform activity originates from the LEC (**Ba**: expanded inset) or MEC (**Bb**: expanded inset) and subsequently propagates to the MEC or LEC, respectively. Electrical stimulation in LEC (triangle) elicits network discharge that spreads to the MEC (expanded inset: **Ba** and **Bb**). **C:** Graphical distribution of the delay times (ms) of spontaneous activity from the LEC→MEC and MEC→LEC in two pilocarpine-treated slices. **D**: A more confined time lag distribution (i.e., LEC→MEC) emerges when electrical stimuli are delivered in LEC.

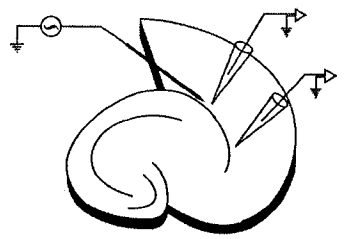

A

NEC

LEC layer V

MEC layer V

1 mV

5s

1 mV

20 ms

B a

Pilocarpine

LEC layer V

MEC layer V

1 mV

5s

1 mV

20 ms

1 mV

20 ms

b

4 s

LEC layer V

MEC layer V

1 mV

5s

1 mV

20 ms

1 mV

20 ms

C

Number of Events

0 2 4 6 8

-80 -60 -40 -20 0 20 40

D

Number of Events

0 2 4 6 8 10

-30 -20 -10 0 10 20 30

Figure 2-4:

Intrinsic firing patterns of lateral EC layer V neurons in NEC and pilocarpine-treated tissue. Two types of firing patterns are recorded from layer V lateral EC neurons in NEC (**A**) and pilocarpine-treated (**B**) slices during injection of depolarizing current: (i) regular repetitive action potential firing (**Aa** and **Ba**) or (ii) initial bursts (expanded insets) followed by regular action potential spiking (**Ab** and **Bb).**

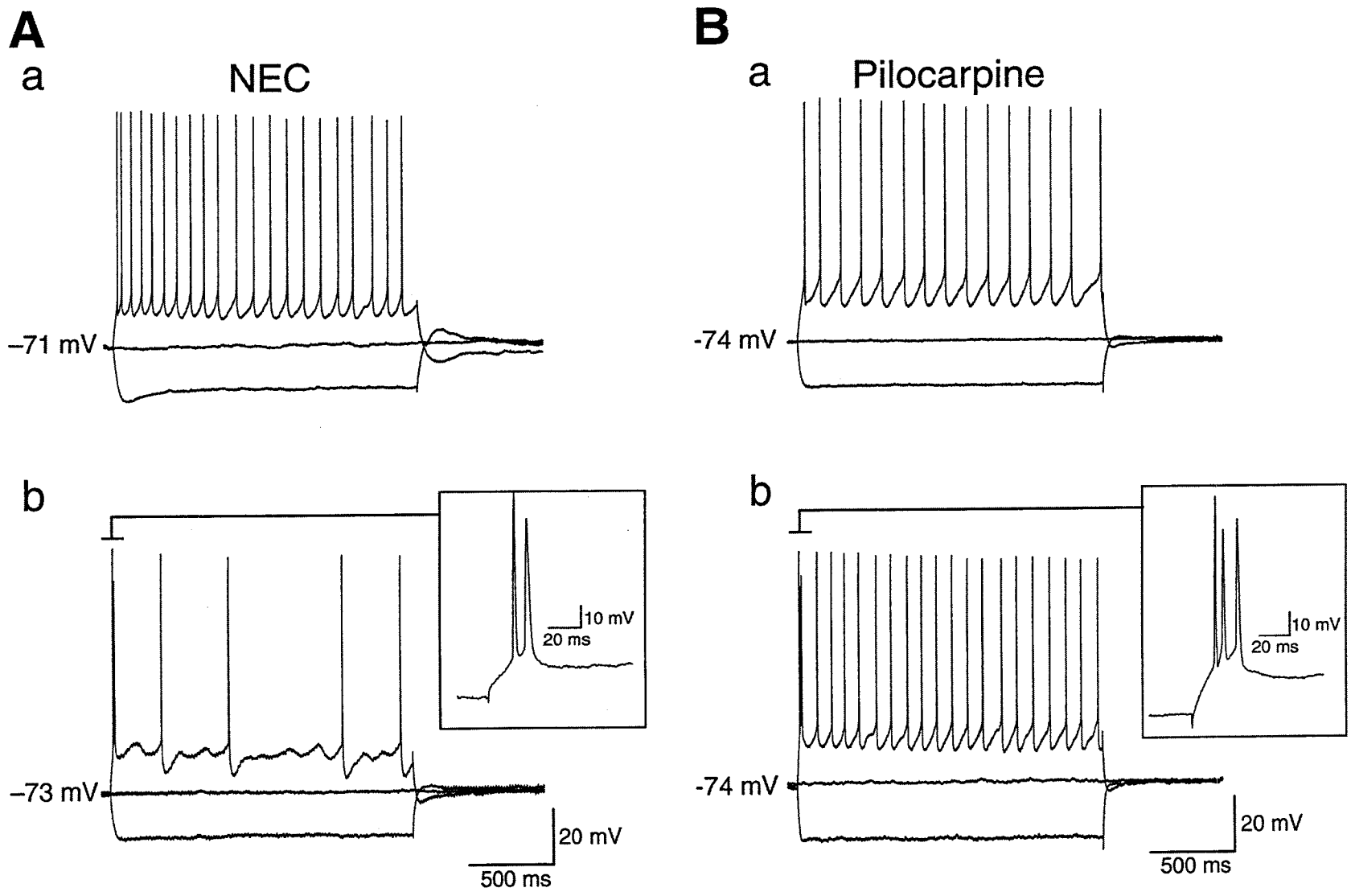
A
a
NEC
–71 mV
b
10 mV
20 ms
–73 mV
20 mV
500 ms
B
a
Pilocarpine
-74 mV
b
10 mV
20 ms
-74 mV
20 mV
500 ms

Fig. 4

Figure 2-5:

Single-shock stimulation and spontaneous network activity are synaptically driven in pilocarpine-treated lateral EC layer V neurons. A: Single-shock stimulation (triangle) elicits a depolarizing hyperpolarizing post-synaptic response at -67 mV (RMP) in a NEC lateral EC layer V neuron. Electrical stimuli at hyperpolarized (-80 mV) and depolarized (-51 mV) membrane potentials elicit depolarizing and hyperpolarizing PSPs, respectively. **B:** Stimulus-induced (triangle) and spontaneous epileptiform activity recorded at RMP (-69 mV and -71 mV) in pilocarpine-treated tissue is characterized by action potential bursting. The amplitude of the depolarizing envelope increases at -82 mV, whereas a reduction occurs at -50 mV and -52 mV.

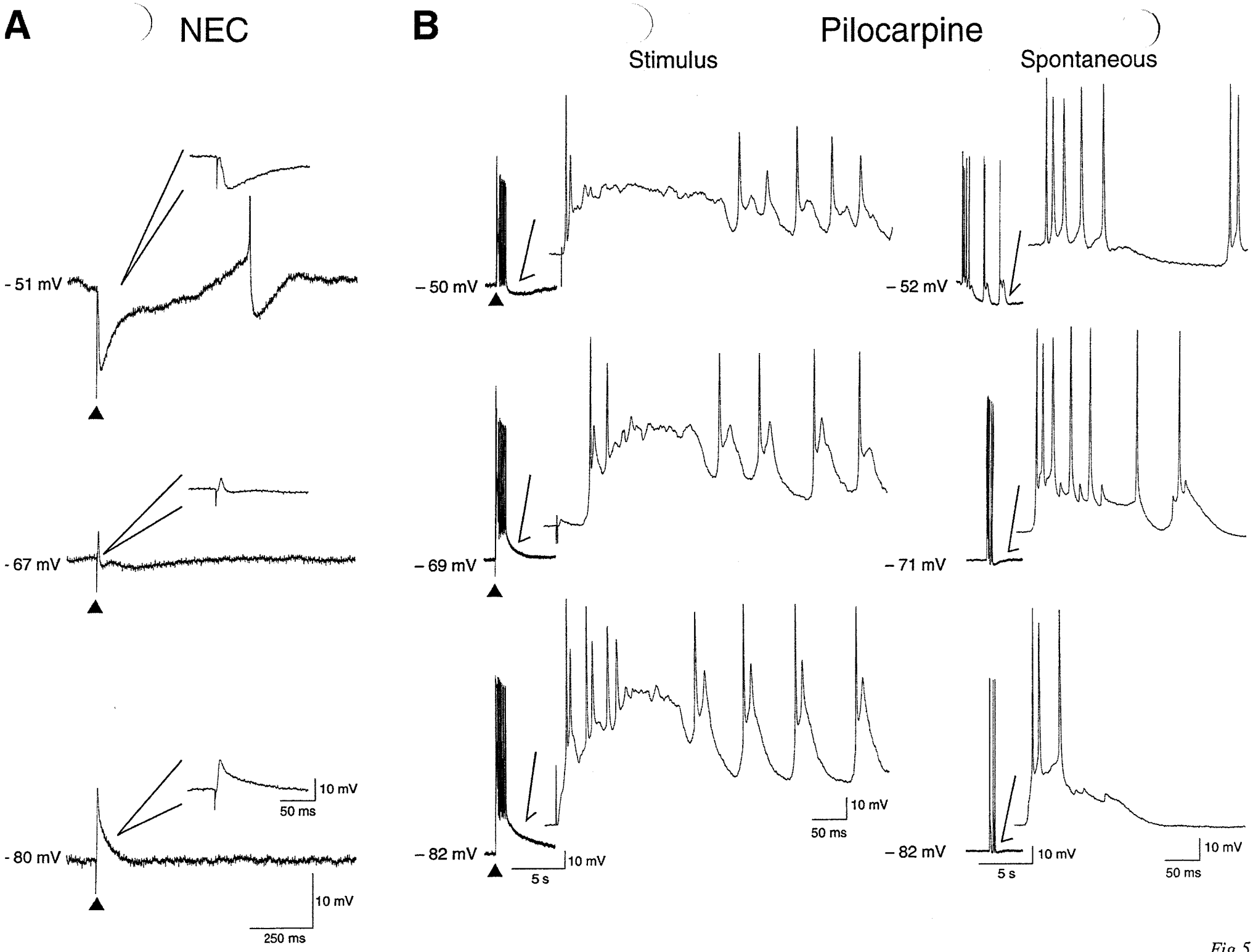
A
NEC
- 51 mV
- 67 mV
- 80 mV
10 mV
50 ms
10 mV
250 ms
B
Pilocarpine
Stimulus
Spontaneous
– 50 mV
– 52 mV
– 69 mV
– 71 mV
– 82 mV
– 82 mV
10 mV
50 ms
10 mV
5 s
10 mV
5 s
10 mV
50 ms

Fig.5

Figure 2-6:

Spontaneous epileptiform activity and NMDA receptor blockade in pilocarpine-treated slices. A: Simultaneous intracellular and field potential recordings demonstrate spontaneous network bursting within the pilocarpine-treated lateral EC layer V. Note that spontaneous bursting persist in the presence of ifenprodil (10 μM) and CPP (10 μM), but is blocked subsequent to CNQX (10 μM) application; under this pharmacological procedure, single-shock stimulation induces a depolarizing post-synaptic response. **B** and **C:** Quantitative summary of the effects induced by the glutamatergic receptor antagonists on the duration and interval of occurrence of the spontaneous network discharges; note that these parameters are not significantly altered by ifenprodil while CPP significantly increases the interval of occurrence ($p<0.01$).

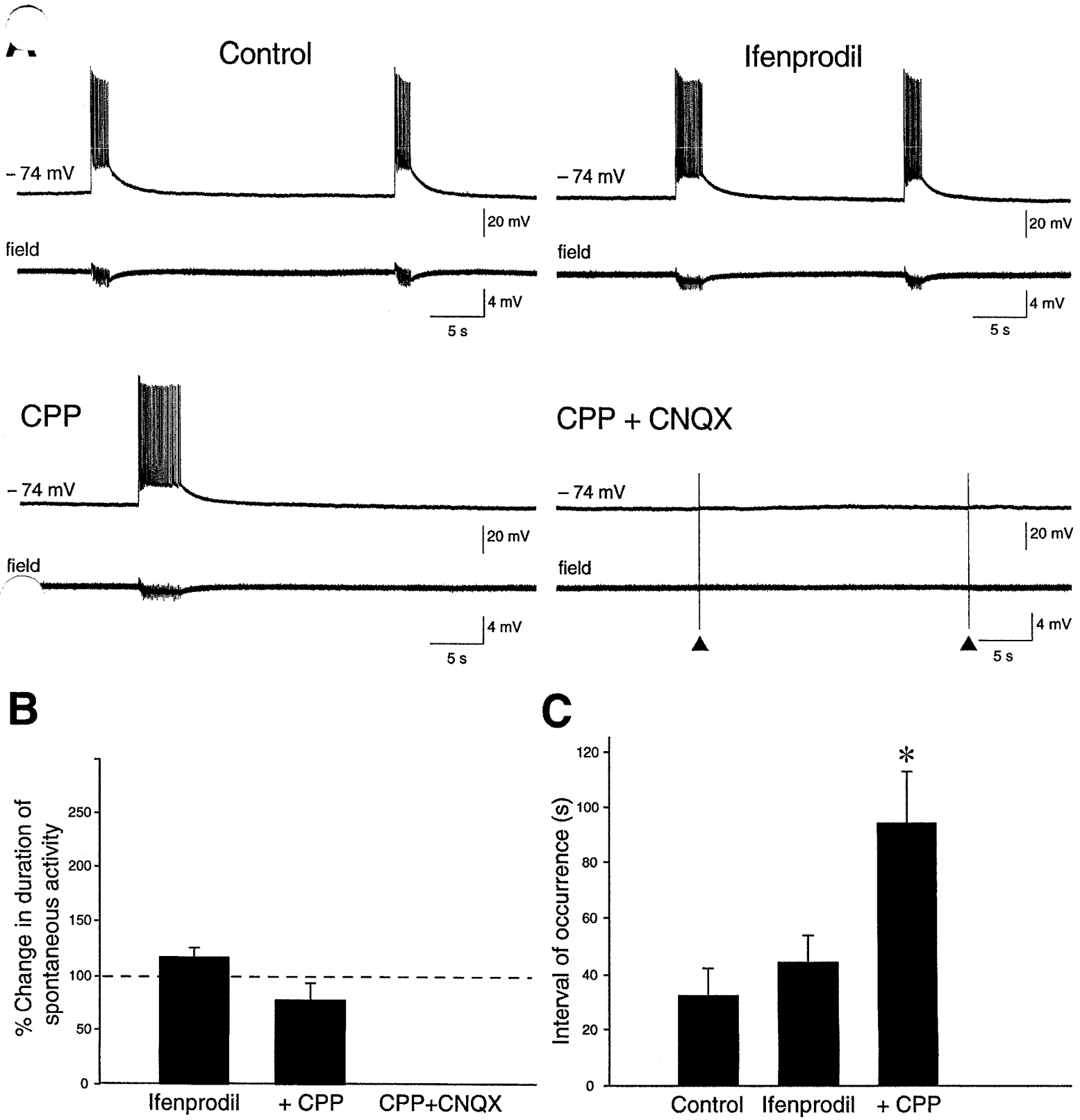
Control
Ifenprodil
CPP
CPP + CNQX
– 74 mV
20 mV
field
4 mV
5 s
B
% Change in duration of spontaneous activity
250
200
150
100
50
0
Ifenprodil
+ CPP
CPP+CNQX
C
Interval of occurrence (s)
120
100
80
60
40
20
0
*
Control
Ifenprodil
+ CPP

Fig. 6

Figure 2-7:

NMDA receptor blockade paradoxically enhances the duration of single-shock-induced epileptiform discharges. A: Single-shock stimulation (triangle, duration= 100 μs) in lateral EC layer V in the pilocarpine elicits a network epileptiform response as indicated by simultaneous intracellular and field potential recordings. Bath application of ifenprodil does not change this epileptiform response while CPP (10 μM) enhances its duration and increases its latency. Note also that the stimulus-induced epileptiform response is blocked following application of CNQX (10 μM). **B** and **C:** Quantitative summary of the duration and latency of the stimulus-induced network bursting. Note that a prolongation and an increased latency of the epileptiform response ($p<0.00001$ in both cases) occurs following NMDA receptor blockade with CPP.

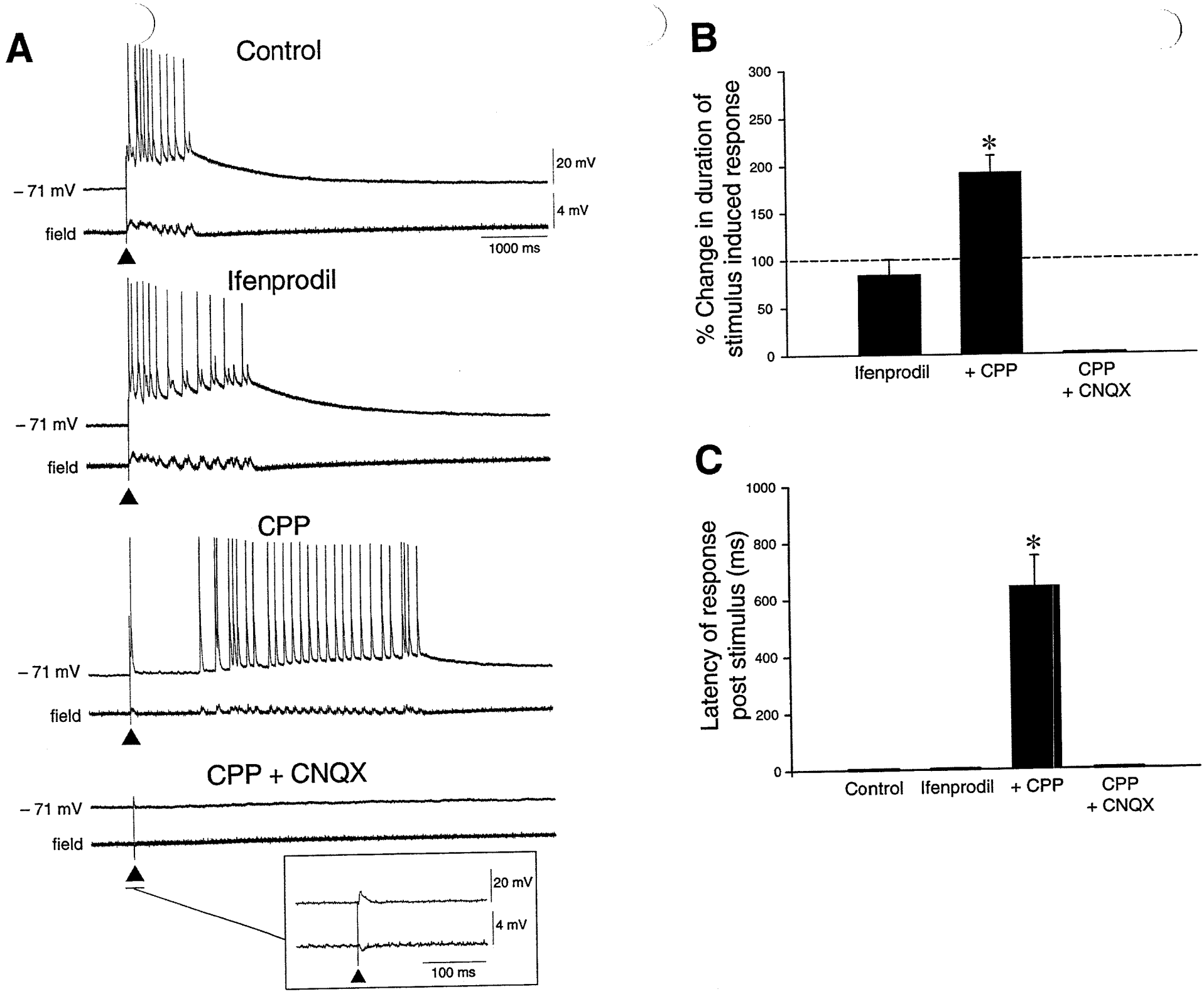
A
Control
20 mV
4 mV
– 71 mV
field
1000 ms
Ifenprodil
– 71 mV
field
CPP
– 71 mV
field
CPP + CNQX
– 71 mV
field
20 mV
4 mV
100 ms
B
% Change in duration of stimulus induced response
300
250
200
150
100
50
0
*
Ifenprodil
+ CPP
CPP + CNQX
C
Latency of response post stimulus (ms)
1000
800
600
400
200
0
*
Control
Ifenprodil
+ CPP
CPP + CNQX

Fig. 7

Figure 2-8:

Reduced frequency of IPSP activity in layer V of the pilocarpine treated lateral EC. **A**: Intracellular recordings at RMP from lateral EC layer V neurons in NEC and pilocarpine-treated tissue demonstrate spontaneous hyperpolarizing PSPs under control conditions. **B**: Graphic representation of the intervals of occurrence of hyperpolarizing PSPs recorded under control conditions from lateral EC layer V neurons in NEC and pilocarpine-treated tissue; note that the interval of occurrence is significantly longer in pilocarpine-treated neurons than in NEC ($p<0.002$). **C:** Intracellular recordings at RMP from layer V lateral EC neurons in NEC and pilocarpine-treated tissue reveal spontaneous hyperpolarizing PSPs during NMDA (CPP 10 μM) and AMPA/Kainate receptor (CNQX 10 μM) blockade. **D** and **E**: Quantitative summary of the interval of occurrence and amplitude of spontaneous hyperpolarizing PSPs recorded from NEC and pilocarpine-treated neurons under glutmatergic receptor blockade; note that significant differences ($p<0.00001$ and $p<0.0002$, respectively) occur for both parameters. **F:** Stimulus-induced PSP recorded in the presence of CPP (10 μM)+CNQX (10 μM) at different membrane potentials from NEC and pilocarpine-treated EC neurons. **G**: Graphical display of the stimulus-induced PSP reversal points in NEC and pilocarpine-treated EC cells; note that these values are not significantly different ($p>0.05$).

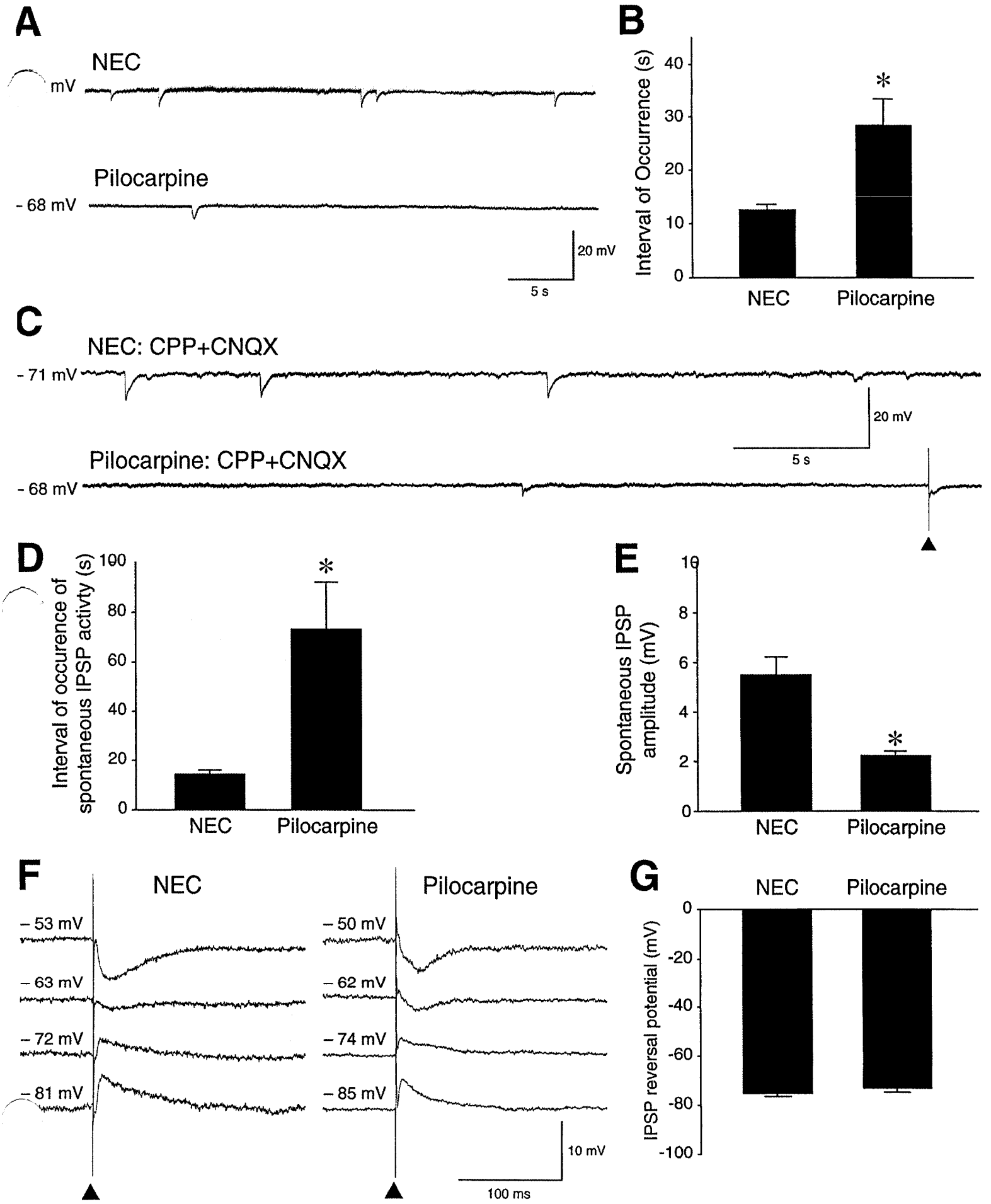
A
NEC
mV
Pilocarpine
- 68 mV
20 mV
5 s
B
Interval of Occurrence (s)
40
30
20
10
0
*
NEC
Pilocarpine
C
NEC: CPP+CNQX
- 71 mV
20 mV
5 s
Pilocarpine: CPP+CNQX
- 68 mV
D
Interval of occurence of spontaneous IPSP activty (s)
100
80
60
40
20
0
*
NEC
Pilocarpine
E
Spontaneous IPSP amplitude (mV)
10
8
6
4
2
0
*
NEC
Pilocarpine
F
NEC
Pilocarpine
– 53 mV
– 63 mV
– 72 mV
– 81 mV
– 50 mV
– 62 mV
– 74 mV
– 85 mV
10 mV
100 ms
G
NEC
Pilocarpine
IPSP reversal potential (mV)
0
-20
-40
-60
-80
-100

Figure 08

Table 2-1:

Table 1 - Intrinsic neuronal properties of NEC and pilocarpine-treated lateral EC layer V neurons. These properties included resting membrane potential (RMP), input resistance (R_i), action potential amplitude (APA) and action potential duration (APD).

NEC Lateral Entorhinal Cortex

Firing Pattern	RMP (mV)	Ri (MΩ)	APA (mV)	APD (ms)
Regular Firing (n = 25)	-70.1 ± 1.0	46.1 ± 2.5	90.2 ± 1.1	1.3 ± 0.1
Intrinsic Bursting (n = 6)	-66.7 ± 2.9	46.7 ± 7.5	82.6 ± 2.7	1.3 ± 0.1

Pilocarpine - Treated Lateral Entorhinal Cortex

Firing Pattern	RMP (mV)	Ri (MΩ)	APA (mV)	APD (ms)
Regular Firing (n = 47)	-69.2 ± 0.8	49.3 ± 2.2	87.1 ± 1.1	1.2 ± 0.1
Intrinsic Bursting (n = 8)	-69.8 ± 1.9	49.9 ± 4.4	96.6 ± 1.9	1.1 ± 0.1

Table 1

Chapter 3: NMDA Receptor-Mediated Transmission Contributes to Network 'Hyperexcitability' in the Rat Insular Cortex

3.0 Linking Text & Information About Publication

The previous chapters of my Ph.D. thesis have addressed the function and underlying mechanisms of the epileptic subiculum and entorhinal cortex in the pilocarpine treated animal model of TLE. However, a structure that has recently been implicated in drug resistant TLE is the insular cortex. Through the serendipitous use of depth electrode recordings, Isnard et al. (2004) identified seizure activity originating from this structure. In this particular study, seizures originated from either the entorhinal cortex or insular cortex; when seizures demonstrated insular origin, surgical removal of the entorhinal cortex failed to control seizure activity. To date, the majority of studies of the insular cortex has only been investigated through molecular and anatomical methods; however, there are no investigations that have electrophysiologically characterized the *in vitro* insular cortex. The study presented in this chapter summarizes the results published in the European Journal of Neuroscience in 2006 in a manuscript entitled "NMDA receptor-mediated transmission contributes to network 'hyperexcitability' in the rat insular cortex" (Authors: Inaba Y, de Guzman P, Avoli M).

3.1 Abstract

The insular cortex (IC) plays distinct roles under physiological and pathological conditions. However, the mechanisms regulating excitability in this area remain unknown. By employing field potential and sharp-electrode intracellular recordings in horizontal rat brain slices comprising the IC and the perirhinal cortex (PC) we studied

here the intrinsic and network characteristics of neurons in the agranular IC. These cells generated regular action potential firing with weak adaptation during intracellular injection of depolarizing current pulses, and were pyramidal in shape when neurobiotin filled. Spontaneous, field events (duration= 2.3±0.25 s; intervals of occurrence= 44.9±6.3 s) were identified in 22/52 slices and corresponded in IC neurons to intracellular depolarizations with action potential firing. Similar field and intracellular discharges were elicited in all slices by electrical stimuli. Antagonizing NMDA receptors blocked the spontaneous activity and reduced or abolished the stimulus-induced discharges. In the latter cases, stimuli elicited depolarizing events that became hyperpolarizing at approx. -64 mV suggesting the contribution of $GABA_A$ receptor-mediated conductances. Our findings identify for the first time some functional properties of agranular IC neurons and point at a powerful NMDA receptor-mediated mechanism implementing network hyperexcitability. This feature may contribute to the role of IC in neurological disorders.

3.2 Introduction

Although the insular cortex (IC) is not part of the temporal lobe, it is closely related to it anatomically and participates to the integration of autonomic response with ongoing behaviour and emotion (Allen et al., 1991; Augustine, 1996). The IC is also involved in processing somaesthetic stimuli and plays a role in pain (Frot & Mauguière, 2003; Jasmin et al., 2003, 2004). Moreover, seizures in temporal lobe epileptic patients invade the IC and can originate in this area (Silfvenius et al., 1964; Isnard et al., 2000, 2004; Bouilleret et al., 2002). Indeed, Isnard et al. (2000, 2004) have reported that while drug-refractory epileptic patients with seizures propagating to IC are fully controlled by temporal lobectomy, those with ictal events originating in IC respond

poorly to this surgical procedure. In line with these findings, experimental evidence highlights a role for the IC in the rat amygdaloid kindling model (Kodama et al., 2001; Ferland et al., 1998).

In spite of a remarkable amount of findings on IC connectivity and of evidence supporting its role in epileptic disorders and pain, no data are available on the electro-physiological characteristics of this area. Therefore, we used here field potential and intracellular recordings in an *in vitro* brain slice preparation to identify some intrinsic and synaptic properties of cells in the rat agranular IC. Our data report the presence of powerful excitatory events that can occur spontaneously, are supported by NMDA receptors, and are presumably accompanied by the activation of inhibitory mechanisms.

3.3 Methods

Male, Sprague-Dawley rats (350-400 g) were decapitated under halothane anesthesia according to the procedures established by the Canadian Council of Animal Care. All efforts were made to minimize the number of animals used and their suffering. The brain was quickly removed and placed in cold (1-3 °C), oxygenated artificial cerebrospinal fluid (ACSF). Horizontal slices (450 µm) were then cut using a vibratome (*cf.*, Kano et al., 2005). In this study, we used slices matching the plates identified by Paxinos and Watson (1998) at around -6.6 mm from the bregma; these slices contained the IC and the perirhinal cortex (PC). Slices were then transferred into a tissue chamber where they lay at the interface between ACSF and humidified gas (95% O_2, 5% CO_2) at 34 °C. ACSF composition (pH= 7.4) was (in mM): NaCl 124, KCl 2, KH_2PO_4 1.25, $MgSO_4$ 2, $CaCl_2$ 2, $NaHCO_3$ 26, and glucose 10. 6-cyano-7-nitroquinoxaline-2,3-dione (CNQX, 10 µM), 3,3-(2-carboxypiperazin-4-yl)-propyl-1-

phosphonate (CPP, 10 μM), phenobarbital (PHB, 500 μM) and 3-Aminopropyl (diethoxymethyl) phosphonoic acid (CGP 55845, 4 μM). were bath applied. Chemicals were acquired from Sigma (St. Louis, MO, USA) with the exception of CNQX and CPP (obtained from Tocris Cookson, Langford, UK).

Field potential and sharp-electrode intracellular recordings were made with glass pipettes that were filled with ACSF (resistance= 2-5 MΩ) and 3M K-acetate (resistance= 70-120 MΩ), respectively. Extra- and intracellular signals were fed to high-impedance amplifiers with internal bridge circuit for intracellular current injection. Resistance compensation was monitored throughout the experiment and adjusted as required. Electrophysiological recordings in IC were obtained from the agranular portion that was identified by using the perirhinal fissure at the level of the IC as a point of reference (Fig. 1A).

The IC cell passive membrane properties were measured as follows: (i) resting membrane potential (RMP) after cell withdrawal; (ii) apparent input resistance from the maximum voltage change in response to hyperpolarizing current pulses (<-0.5 nA); (iii) action potential amplitude from the baseline; and (iv) action potential duration at half-amplitude. The firing patterns of IC cells were established by injecting depolarizing current pulses. Extra- and intracellular signals were fed to a computer interface, acquired and stored using the pClamp 9 software and analyzed with the Clampfit 9 software (both from Axon Instruments, Union City, CA, USA). Electrical stimuli (50-100 μs; <200 μA) were delivered through bipolar, stainless steel electrodes. The recording and stimulating electrode location in the slice is shown in Fig. 1A. In some experiments the IC and PC were surgically isolated at the start of the experiment by a cut made under visual control with a razor blade (dotted line in Fig. 1A).

For intracellular labeling, electrodes were filled with 2% neurobiotin dissolved in 2M K-acetate. Neurobiotin was applied by injecting depolarizing current pulses (0.5-1 nA, 3.3 Hz, 150ms) for >10 min. Only one cell was filled in each slice. At the end of the experiment, slices were processed as described by D'Antuono et al. (2001). Measurements are expressed as mean±SEM and *n* indicates the number of slices or neurons. Data were compared with the Student's t-test and were considered significant if $p<0.05$.

3.4 Results

Neurons (n= 27) recorded in the IC at 400-1200 µm from the pia responded to intracellular depolarizing pulses by generating trains of action potentials with weak adaptation (Fig. 1Ba), although a burst of 2-3 action potentials with intervals <6 ms could occur at pulse onset (asterisk); these cells were therefore classified as regularly spiking (McCormick *et al.*, 1985). Neurobiotin-filled IC cells (n= 14/27) displayed pyramidal-like shape with a distinct apical dendrite directed towards the pia and extensive basal dendritic tree (Fig.1Bb). The fundamental electrophysiological properties of neurobiotin-filled and non-labeled cells were similar ($p> 0.21$) thus suggesting that the sampled neuronal populations exhibited comparable intrinsic physiological properties. By pooling the values obtained from labeled and unlabeled IC cells (n= 27) we found: (i) RMP = -74.2±1.2 mV; (ii) apparent input resistance= 45.7±2.5 MΩ; (iii) action potential amplitude= 94.6±2.7 mV; and (iv) action potential duration= 1.7±0.4 ms.

A striking characteristic of the brain slices analyzed in this study was the presence of synchronous field discharges that occurred spontaneously in 22 of 52 slices (duration= 2.3±0.25 s; intervals of occurrence= 44.9±6.3 s) or following electrical

stimuli delivered in PC (response duration= 1.3±0.2 s, n=10) or IC (duration= 1.4±0.1 s, n=15) in all experiments (Fig. 1C). Spontaneous events (duration= 1.7±0.2 s; intervals of occurrence= 84.1±10.9 s; n=6) were still present in IC after surgical cut from PC (not shown). Spontaneous and stimulus-induced events corresponded in IC cells to sustained intracellular depolarizations leading to repetitive action potential discharges (Fig. 1C). Hyperpolarizing or depolarizing the neuron with steady current injection increased or decreased, respectively, the amplitude of these depolarizations (Figs. 1C and 2A), thus suggesting that they were contributed by synaptic conductances. Moreover, bringing the membrane to depolarized levels disclosed hyperpolarizing potentials during the initial part of the response (Fig. 2A, arrows in -60 mV panel) while long-lasting (up to 4 s) hyperpolarizations terminated the intracellular events (Figs. 1C and 2A, asterisks). The rate of occurrence of the spontaneous events was not influenced by changing the RMP (not shown), further indicating that this activity was network-driven.

To determine the mechanisms underlying the occurrence of network discharges in the IC we assessed the effects of the NMDA receptor antagonist CPP. As shown in Fig. 2B, CPP abolished the spontaneous activity in 5 experiments while reducing the duration of the stimulus-induced events. This latter aspect was analyzed in 6 additional slices that did not generate any spontaneous activity. Overall, the duration of the stimulus-induced responses was reduced by CPP to 18.3± 3.7 % of what seen in control (n= 7), while only a depolarizing-hyperpolarizing potential sequence was observed in the remaining experiments (n=6; Fig. 3A, +CPP). In addition, by changing the RMP we found that the polarity of the stimulus-induced intracellular response measured at a latency of approx. 50 ms inverted in polarity at -64.3±2.9 mV

(n=8; Fig. 3Bc) suggesting the participation of $GABA_A$ receptor-mediated conductances (CPP+CGP 55845; Fig. 3Ba).

To test this hypothesis we bath applied PHB, a drug that is known to enhance $GABA_A$ receptor-mediated mechanisms (Barker & McBurney, 1979; Twyman et al., 1989). As illustrated in Fig. 3B, PHB produced a more negative reversal potential (from -64.5±6.4 mV to -69.4±4.2 mV, n= 3) of the response induced by PC stimuli but also decreased synaptic responsiveness, presumably via an interaction with excitatory glutamatergic processes. Therefore, to firmly establish the presence of $GABA_A$ receptor-mediated activity within the IC network we used focal stimuli during bath application of glutamatergic (CPP+CNQX) and $GABA_B$ (CGP 55845) receptor antagonists. Under these conditions, stimuli delivered close (<150 μm) to the recorded cell induced at RMP a short-lasting depolarization inverting in polarity at -71.6±1.3 mV (n= 8; Fig. 3C). Moreover, further application of PHB caused a significant negative shift in its reversal potential (from -69.3±0.6 to -78.9±2.2; n=3, $p<0.05$) along with a prolongation of the response (Fig. 3C). Finally, we found that bath application of the $GABA_A$ receptor antagonist picrotoxin (50 μM; n=3) abolished the synaptic response induced by close electrical stimuli during application of glutamatergic and $GABA_B$ receptor antagonists (not shown).

3.5 Discussion

We have found here that the rat agranular IC analyzed with field potential and intracellular recordings in an *in vitro* slice preparation generates spontaneous or stimulus-induced synchronous events that are: (i) associated with synaptic depolarizations leading to sustained action potential firing, (ii) supported by NMDA receptor-mediated mechanisms, and (iii) accompanied by the activation of $GABA_A$ receptor-mediated,

inhibitory conductances. These characteristics suggest that the agranular IC is "hyperexcitable" as compared to limbic or neocortical networks maintained *in vitro* in normal ACSF, since cells in these structures rarely generate spontaneous activity and respond to stimuli with EPSP-single action potentials (Schwartzkroin, 1975; Connors et al., 1982; Jones & Lambert, 1990; Martina et al., 2001). We have also established that the IC cells recorded intracellularly were regularly firing and pyramidal in shape when labeled with neurobiotin.

NMDA receptors play a unique role in the occurrence of spontaneous and stimulus-induced discharges in the IC. Indeed, at the best of our knowledge, these data are the first to identify an essential role for NMDA receptors in the generation of spontaneous network activity in brain slices bathed in normal ACSF. This evidence may imply that Mg^{2+} exerts a reduced control on NMDA receptor channels in the agranular IC. NMDA receptors are indeed known to contribute to epileptogenesis and represent a target for antiepileptic drug therapy (Rogawski, 1998). In addition, the trigger for the NMDA receptor-mediated events identified in IC may result from mixed non-NMDA and $GABA_A$ receptor-mediated conductances. The latter view is further reinforced by the sensitivity of the stimulus-induced response to application of the barbiturate PHB (Nicoll et al., 1975; Barker & McBurney, 1979; Twyman et al., 1989). The presence of inhibitory conductances during the activity recorded in IC slices is in line with evidence obtained from epileptic human brain tissue indicating that spontaneous inhibitory potentials can be sufficiently synchronous to support field potential discharges (Cohen et al., 2002; Köhling et al., 1998).

In conclusion, our data point at a powerful NMDA receptor-mediated mechanism implementing network hyperexcitability in rat agranular IC. These findings may be relevant for understanding the role of the IC in epileptic disorders (Isnard et al.,

2000, 2004; Bouilleret et al., 2002; Kodama et al., 2001; Ferland et al., 1998) and in central pain (Frot & Mauguière, 2003; Jasmin et al., 2003, 2004).

3.6 Acknowledgements

This study was supported by grants from the Canadian Institutes of Health Research (CIHR; grant 8109) and the Savoy Foundation.

3.7 References

Allen, G.V., Saper, C.B., Hurley, K.M., & Cechetto, D.F. (1999) Organization of visceral and limbic connections in the insular cortex of the rat. *J. Comp. Neurol.*, **311**, 1-16.

Augustine, J.R. (1996) Circuitry and functional aspects of the insular lobe in primates including humans. *Brain Res. Rev.*, **22**, 229-244.

Barker, J.L., & McBurney, R.N. (1979) Phenobarbitone modulation of postsynaptic GABA receptor function on cultured mammalian neurons. Proc. R. Soc. Lond. B. Biol Sci., 206, 319-327.

Bouilleret, V., Dupont, S., Spelle, L., Baulac, M., Samson, Y., & Semah F. (2002) Insular cortex involvement in mesiotemporal lobe epilepsy: a positron emission tomography study. *Ann. Neurol.*, **51**, 202-208.

Cohen, I., Navarro, V., Clemenceau, S., Baulac, M., & Miles, R. (2002) On the origin of interictal activity in human temporal lobe epilepsy in vitro. *Science*, **298**, 1418-1421.

Connors, B.W., Gutnick, M.J., & Prince D.A. (1982) Electrophysiological properties of neocortical neurons in vitro. *J. Neurophysiol.*, **48**, 1302-1320.

D'Antuono, M., Biagini, G., Tancredi, V., & Avoli, M. (2001) Electrophysiology of regular firing cells in the rat perirhinal cortex. *Hippocampus*, **11**, 662-672.

Ferland, R.J., Nierenberg, J., & Applegate, C.D. (1998) A role for the bilateral involvement of perirhinal cortex in generalized kindled seizure expression. *Exp. Neurol.*, **151**, 124-137.

Frot, M., & Mauguiere, F. (2003) Dual representation of pain in the operculo-insular cortex in humans. *Brain*, **126**, 438-450.

Isnard, J., Guenot, M., Ostrowsky, K., Sindou, M., & Mauguiere, F. (2000) The role of the insular cortex in temporal lobe epilepsy. *Ann. Neurol.*, **48**, 614-623.

Isnard, J., Guenot, M., Sindou, M., & Mauguiere, F. (2004) Clinical manifestations of insular lobe seizures: a stereo-electroencephalographic study. *Epilepsia*, 45, 1079-1090.

Jasmin, L., Rabkin, S.D., Granato, A., Boudah, A., & Ohara, P.T. (2003) Analgesia and hyperalgesia from GABA-mediated modulation of the cerebral cortex. *Nature*, **424**, 316-320.

Jasmin, L., Burkey, A.R., Granato, A., & Ohara, P.T. (2004) Rostral agranular insular cortex and pain areas of the central nervous system: a tract-tracing study in the rat. *J. Comp. Neurol.*, **468**, 425-440.

Jones, R.S., & Lambert, J.D. (1970) Synchronous discharges in the rat entorhinal cortex in vitro: site of initiation and the role of excitatory amino acid receptors. *Neuroscience*, **34**, 657-670.

Kano, T., Inaba, Y., & Avoli, M. (2005) Periodic oscillatory activity in parahippocampal slices maintained in vitro. *Neuroscience*, **130**, 1041-1053.

Kodama, M., Yamada, N., Sato, K., Sato, T., Morimoto, K., & Kuroda, S. (2001) The insular but not the perirhinal cortex is involved in the expression of fully-kindled amygdaloid seizures in rats. *Epilepsy Res.*, **46**, 169-178.

Köhling, R., Lucke, A., Straub, H., Speckmann, E.J., Tuxhorn, I., Wolf, P., Pannek, H., & Oppel, F. (1998) Spontaneous sharp waves in human neocortical slices excised from epileptic patients. *Brain*, **121**, 1073-1087.

Martina, M., Royer, S., & Pare, D. (2001) Propagation of neocortical inputs in the perirhinal cortex. *J. Neurosci.*, **21**, 2878-2888.

McCormick, D.A., Connors, B.W., Lighthall, J.W., & Prince, D.A. (1985) Comparative electrophysiology of pyramidal and sparsely spiny stellate neurons of the neocortex. *J. Neurophysiol.*, **54**, 782-806.

Nicoll, R.A., Eccles, J.C., Oshima, T., & Rubia F. (1975) Prolongation of hippocampal inhibitory postsynaptic potentials by barbiturates. *Nature*, **258**, 625-627.

Paxinos, G., & Watson, C. (1998). The rat brain in stereotaxic coordinates. Fourth edition. Academic Press.

Rogawski, M.A. (1998) Mechanism-specific pathways for new antiepileptic drug discovery. *Adv. Neurol.*, **76**, 11-27.

Twyman, R.E., Rogers, C.J., & Macdonald, R.L. (1999) Differential regulation of gamma aminobutyric acid receptor channels by diazepam and phenobarbital. *Ann. Neurol.*, **25**, 213-220.

Schwartzkroin, P.A. (1975) Characteristics of CA1 neurons recorded intracellularly in the hippocampal in vitro slice preparation. *Brain Res.*, **85**, 423-436.

Silfvenius, H., Gloor, P., & Rasmussen, T. (1964) Evaluation of insular ablation in surgical treatment of temporal lobe epilepsy. *Epilepsia*, **5**, 307–320.

3.8 Figures

Figure 3-1:

Drawing of the brain slice preparation used in this study, showing the position of recording and stimulating electrodes. Note that the agranular IC (arrow) was identified by taking the perirhinal fissure (asterisk) as point of reference. The dotted line highlights the location of the cut used to isolate the IC from PC. B: Responses to the injection of pulses of hyperpolarizing (-0.6 and -0.2 nA) and depolarizing (0.2 nA) intracellular current (a) generated by an IC cell that was filled with neurobiotin (b); note that this cell generates rhythmic action potential firing while the asterisk identifies the first 2 action potentials that occurred at intervals <6 ms. C: Spontaneous and stimulus-induced activity recorded in the IC with intracellular and field potential recordings. The RMP of this neuron was -72 mV while stimulation was delivered in PC. Note that hyperpolarization of the neuronal membrane, through negative current injection, increases the amplitude of the depolarizing envelope as well as that a hyperpolarization terminates the intracellular discharge (asterisk) in the -72 mV sample. In this and following figures focal electrical stimuli are identified with triangles.

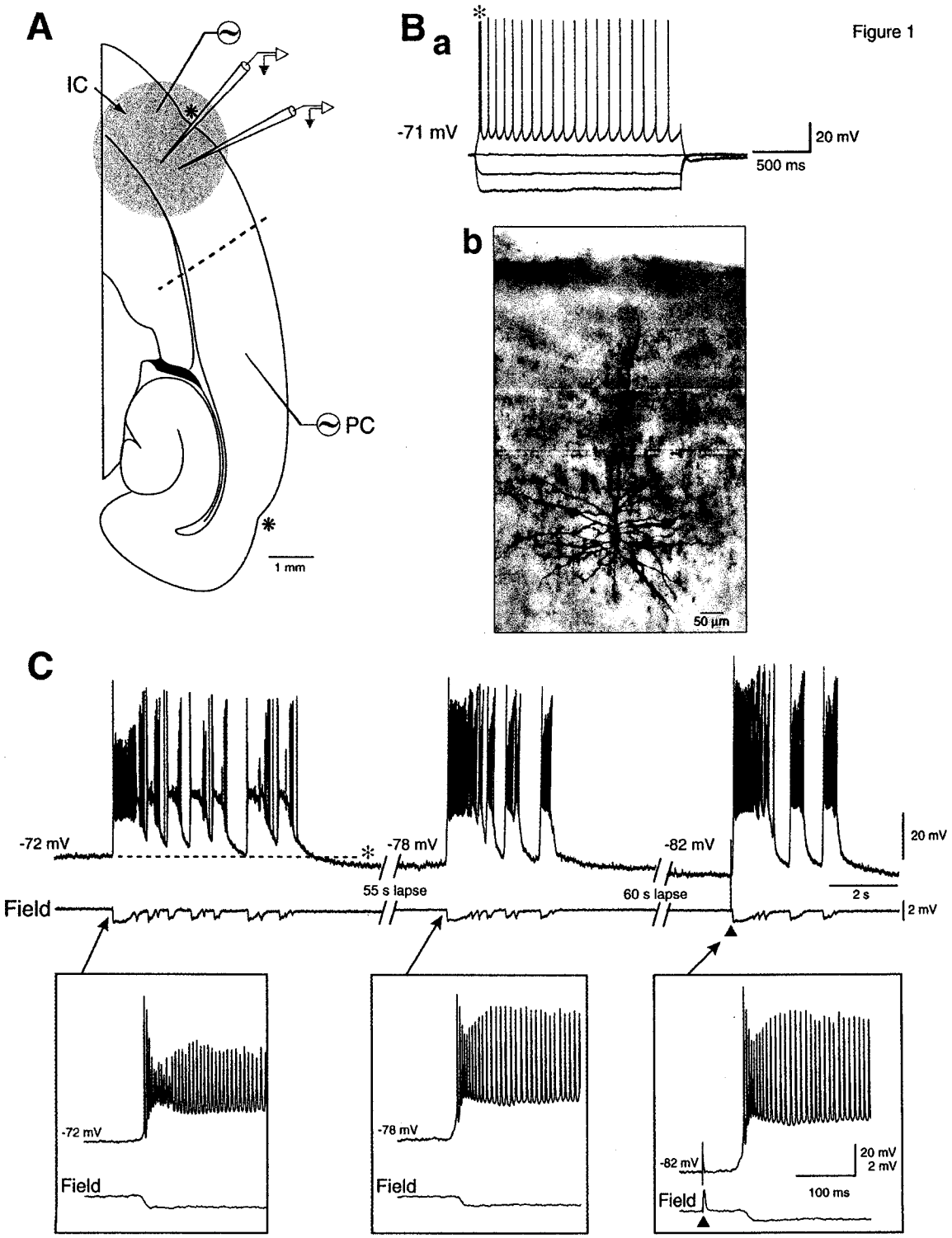
A
IC
PC
1 mm
B a
-71 mV
20 mV
500 ms
b
50 µm
C
-72 mV
-78 mV
-82 mV
20 mV
55 s lapse
60 s lapse
2 s
Field
2 mV
-72 mV
Field
-78 mV
Field
-82 mV
20 mV
2 mV
100 ms
Field

Figure 1

Figure 3-2:

A: Field and intracellular characteristics of the responses recorded in the IC following single-shock stimuli delivered in the PC at RMP (-78 mV) and during injection of depolarizing (-60 mV) and hyperpolarizing (-90 mV) steady current. Note that hyperpolarizing or depolarizing the neuron with steady current injection increases or decreases, respectively, the amplitude of the stimulus-induced depolarizations. Note also in the -60 mV panel that depolarizing the neuron discloses hyperpolarizing potentials during the initial part of the intracellular response (arrows) as well as a slow post-discharge hyperpolarization (asterisk). **B**: Effects induced by the NMDA receptor antagonist CPP on the spontaneous and stimulus-induced discharges recorded in the IC. Stimuli were delivered in the IC. Note that CPP reversibly abolishes the spontaneous activity and reduces the duration of the stimulus-induced discharge.

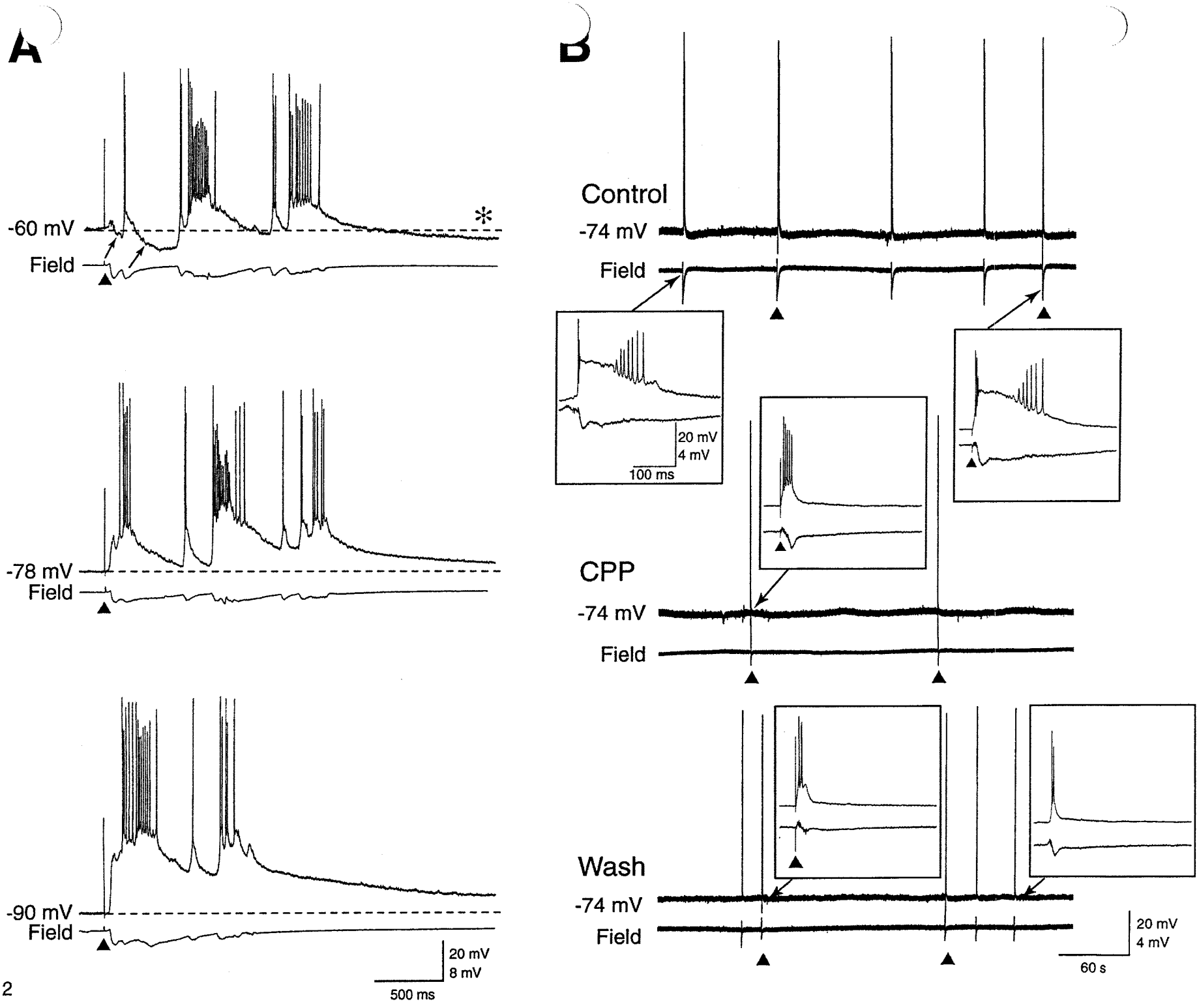
A
-60 mV
Field
*
-78 mV
Field
-90 mV
Field
20 mV
8 mV
500 ms
B
Control
-74 mV
Field
20 mV
4 mV
100 ms
CPP
-74 mV
Field
Wash
-74 mV
Field
20 mV
4 mV
60 s

Figure 2

Figure 3-3:

Stimulus-induced responses recorded in control ACSF and following bath application of NMDA and non-NMDA glutamatergic receptor antagonists. A: CPP blocks the stimulus-induced discharge thus revealing a depolarizing postsynaptic response with latency similar to what seen under control. **B**: Effects induced by changing the membrane potential (Vm) with current injection on the polarity of the synaptic responses induced by PC stimulation during CPP+CGP 55845 (Control) and CPP+CGP 55845+PHB. Raw data are shown in **a**; note in **b** that the reversal points obtained by measuring the response amplitude (calculated at ~55 ms after the stimulus) were -64 mV (CPP+CGP 55845) and -70 mV (CPP+CGP 35348+PHB). **C**: Responses induced by focal IC stimulation during application of medium containing CPP+CNQX+CGP 55845 (Control) and CPP+CNQX+CGP 55845+PHB. Raw data are illustrated in **a** while in **b** normalized intracellular traces obtained under both conditions are superimposed; note that PHB (red traces) causes an increase in response duration. Plot of the amplitude of the stimulus-induced responses recorded at different membrane potentials (Vm) is shown in **c**. Note that reversal points of -68 mV and -78 mV occur during control and PHB conditions, respectively. Amplitude of response was assessed at 17 ms after stimulus artifact.

Figure 3

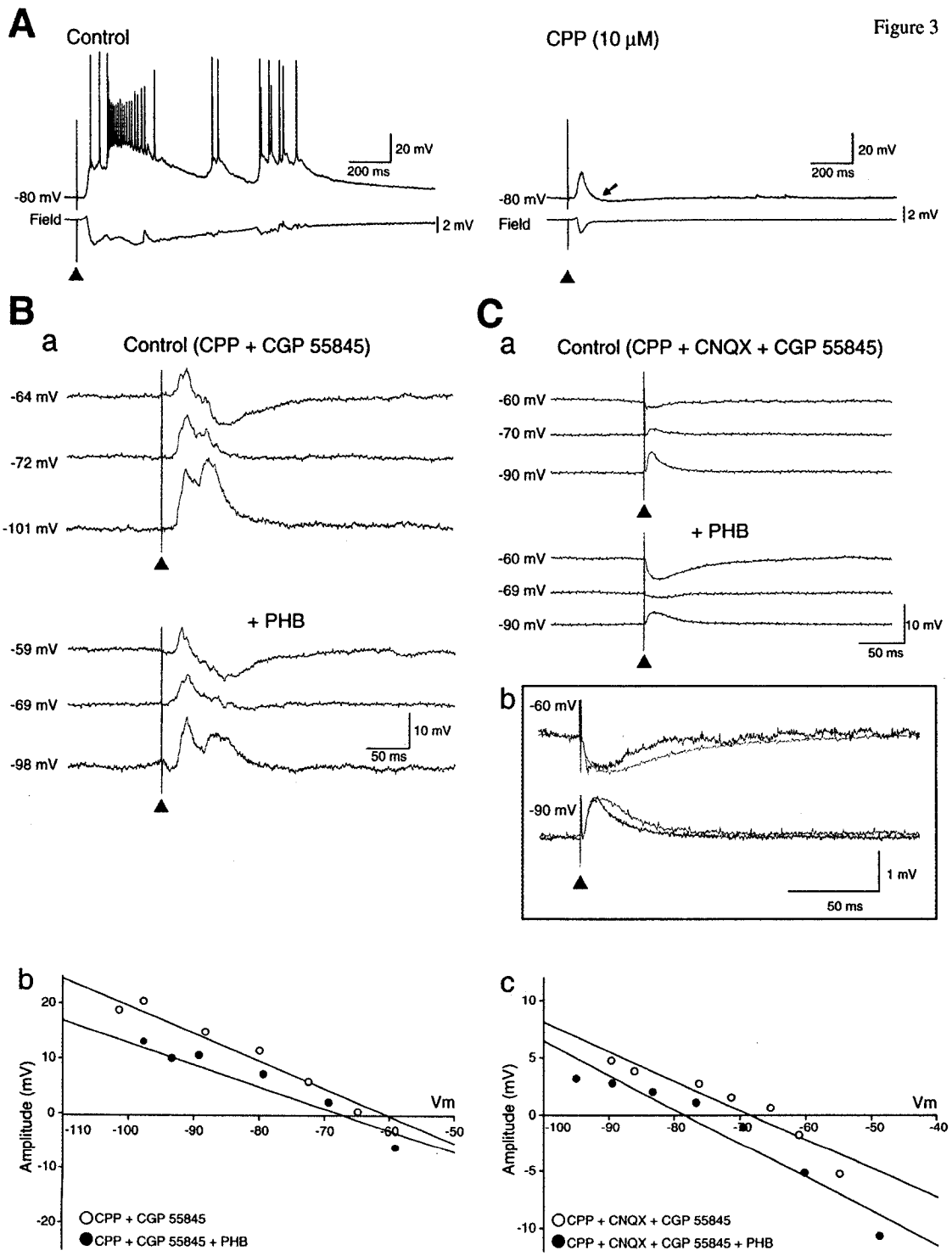
A
Control
CPP (10 µM)
20 mV
200 ms
-80 mV
Field
2 mV
B
a
Control (CPP + CGP 55845)
-64 mV
-72 mV
-101 mV
+ PHB
-59 mV
-69 mV
-98 mV
10 mV
50 ms
C
a
Control (CPP + CNQX + CGP 55845)
-60 mV
-70 mV
-90 mV
+ PHB
-69 mV
b
1 mV
b
Amplitude (mV)
Vm
CPP + CGP 55845
CPP + CGP 55845 + PHB
c
CPP + CNQX + CGP 55845
CPP + CNQX + CGP 55845 + PHB

Conclusion

0.1 Summary of Research Findings

The main findings of my Ph.D. investigations are indicated below:

1. The pilocarpine-treated subiculum demonstrated an enhanced network response from CA1 and LEC layer III inputs. This network excitability within the pilocarpine-treated subiculum is attributed to a more positive $GABA_A$ receptor mediated reversal point combined with reduced KCC2 expression. Additional factors include decreased levels of parvalbumin positive inhibitory neurons and increased synaptic sprouting within the subiculum (Chapter 1).

2. The spontaneous and stimulus induced bursting within the deep layers of the pilocarpine-treated entorhinal cortex may be a consequence of the reduced frequency and amplitude of spontaneous $GABA_A$ receptor mediated IPSPs. While we did not observe an alteration in the fast IPSP reversal point, the synaptic sprouting within EC Layer V may have contributed to network hyperexcitability (Chapter 2).

3. In our investigations of the control tissue of the IC, we report that spontaneous bursting was NMDA receptor dependent and occurs concomitantly with $GABA_A$ receptor mediated conductances (Chapter 3)

0.2 Can the epileptic subiculum contribute to the amplification of limbic seizures?

Chapter 1 of my thesis indicates that subtle network alterations occur within the pilocarpine-treated subiculum. Previous investigations, in the presence of convulsive agents, have demonstrated that the isolated subicular network is capable of generating epileptiform activity (Benini and Avoli 2005). If epileptiform events can occur within an isolated structure, an increase of hyperexcitability would be expected from external inputs. In the clinical condition, this would be problematic for epileptic patients as the subiculum receives network input from epileptogenic structures (entorhinal cortex and CA1) via the TA pathway.

The network modifications of epileptic CA1 demonstrate increased synaptic sprouting in chronic seizure models (Esclapez et al. 1999); these experiments also indicated enhanced network excitability due to the upregulation of intrinsically bursting neurons and reduced GABAergic input (Hirsch et al. 1999; Wellmer et al. 2002). In addition, epileptic lateral EC layer III neurons suggest enhanced synaptic activity may occur through reduced I_h function (Shah et al. 2004). The convergence of these epileptogenic structures within a modified subicular network may contribute to amplified limbic seizures. In line with this viewpoint, investigations in pilocarpine treated tissue utilizing intrinsic optical signals, voltage sensitive dyes, or convulsive agents suggest the augmentation of limbic seizures via the temporoammonic pathway (Ang et al. 2006; Biagini et al. 2005; D'Antuono et al. 2002; Wozny et al. 2005).

Moreover, in our studies we attribute the epileptic properties of the subiculum to synaptic excitation. We indicate that an equal proportion of regular firing neurons and intrinsic bursters occur within the subiculum; while others report either an

increase or reduction of intrinsically bursting epileptic subicular neurons (Knopp et al. 2005; Wellmer et al. 2002). However, strict categorization of intrinsic cell firing properties into intrinsic bursters or regular firing is an oversimplification of a complex and dynamic process. Regular action potential firing can be altered into a state of intrinsic bursting while the reverse is also true (Steriade 2004). This flexibility of intrinsic firing is dependent upon the membrane potential and as such makes it difficult to carefully discern and classify neuronal firing properties. Taken together, these discrepancies in the proportions of bursting neurons indicate that they may not necessarily be a prerequisite for epileptogenesis. Indeed, additional cortical structures such as the highly epileptogenic parahippocampal territories (Avoli et al. 1996; de Guzman et al. 2004; Kelly and McIntyre 1996; Lopantsev and Avoli 1998) have not been demonstrated to exhibit an extensive population of intrinsic bursting neurons indicating that alternative factors such as synaptic mechanisms may be favoured.

0.3 What are the additional factors that contribute to network hyperexcitability within the epileptic entorhinal cortex?

My investigations in chapter 2 demonstrate, for this first time, spontaneous network bursting within layer V of the pilocarpine treated EC in the absence of convulsive agents. We further demonstrate that this *in vitro* epileptiform activity can propagate to both EC subdivisions and is resilient to NMDA receptor blockade. We attributed this level of network hyperexcitability to the reduction of $GABA_A$ receptor mediated network inhibition. Although, additional factors may contribute to these events.

Recent investigations in the human epileptic EC demonstrate reduced expression of NPY receptors. This event would trigger neuronal hyperexcitability as the overall action of NPY is to inhibit seizure activity (Baraban 2004). In line with this

viewpoint, NPY inhibits *in vitro* epileptiform discharges in the EC and hippocampal formation (Klapstein and Colmers 1997; Woldbye et al. 2002). Additional alterations would include a reduced I_h function, which favours increased action potential spiking in lateral EC layer V and layer III (Rosenkranz and Johnston 2006; Shah et al. 2004). Further modifications that may impact the presence of inhibition within EC layer V is presynaptic modulation of neurotransmission. Studies in pilocarpine treated tissue indicate that blockade of the NR2B subunit reduces the occurrence of excitatory post-synaptic current (EPSC) (Yang et al. 2006). In our investigations of EC layer V, bath application of ifenprodil (selective NR2B receptor antagonist) was unable to block spontaneous or stimulus induced bursting. Other studies report that utilization of ifenprodil can block the spread of discharges in cortical dysplatic tissue (Bandyopadhyay and Hablitz 2006). Although, a recent study in the DG indicated that NR2B antagonism did not prevent status epilepticus or mossy fibre sprouting; although, NR2A antagonism precluded behavioural seizures (Chen et al. 2007). Moreover, a recent study in epileptic EC layer V reports that functional alterations in presynaptic $GABA_B$ receptors promote increased and reduced frequencies of EPSC and inhibitory post-synaptic current (IPSC), respectively (Thompson et al. 2007). Collectively, these events demonstrate that multiple factors may contribute to the epileptogenesis of the EC.

0.4 How can the insular cortex contribute to the generation of seizure activity?

In chapter 3, we (co-authors) report the first electrophysiological characterization of the agranular IC in control tissue. Surprisingly, spontaneous bursting activity occurred in 42% of slices. This spontaneous bursting was NMDA receptor

dependent, which differed considerably from the glutamatergic mechanisms involved in my findings of the epileptic EC (Chapter 2).

The investigations of the IC, which have focused on nociception, have demonstrated the presence of endogenous opioid receptors colocalized with GABA (Evans et al. 2007; Ohara et al. 2003). When extrapolated to *in vitro* epilepsy models, these neurochemicals contribute to network synchronization (Avoli et al. 1996; Finnegan et al. 2006). In fact, preliminary evidence in control tissue demonstrates that μ-opioid receptor activation blocks spontaneous network bursting, presumably, through hyperpolarization of inhibitory interneurons (Finnegan et al. 2006).

Moreover, the IC demonstrates anatomical connectivity with structures, implicated in TLE, within the parahippocampus. If either of these structures become epileptogenic, the epileptiform activity of these regions could influence the IC. This viewpoint is illustrated in clinical TLE, as depth electrode studies demonstrate seizures of insula onset or the propagation of ictal events of limbic origin into the IC (Isnard et al. 2000; Isnard et al. 2004). To this end, further investigations are required to understand the mechanisms involved in the generation of epileptiform activity in the IC and its role in TLE.

0.5 Concluding remarks

My investigations in the epileptic subiculum and EC demonstrate that two epileptic structures may contribute to the amplification of limbic seizures. The examination of the IC, in control tissue, reveals that the IC possesses the network machinery to contribute to epileptiform activity. While clinical data demonstrate seizures of insular origin, the dearth of synaptic and intrinsic mechanisms of the IC limit the physiological

understanding of this structure. Further research is required to characterize and determine the mechanisms involved, in the IC, within epileptic tissue. To this end, the investigations of epileptic phenomena should encompass not only the hippocampal formation but also extend to neuronal structures within the paralimbic belt.

0.6 References

Ang CW, Carlson GC, and Coulter DA. Massive and specific dysregulation of direct cortical input to the hippocampus in temporal lobe epilepsy. *J Neurosci* 26: 11850-11856, 2006.

Avoli M, Barbarosie M, Lucke A, Nagao T, Lopantsev V, and Kohling R. Synchronous GABA-mediated potentials and epileptiform discharges in the rat limbic system in vitro. *J Neurosci* 16: 3912-3924, 1996.

Bandyopadhyay S, and Hablitz JJ. NR2B antagonists restrict spatiotemporal spread of activity in a rat model of cortical dysplasia. *Epilepsy Res* 72: 127-139, 2006.

Baraban SC. Neuropeptide Y and epilepsy: recent progress, prospects and controversies. *Neuropeptides* 38: 261-265, 2004.

Benini R, and Avoli M. Rat subicular networks gate hippocampal output activity in an in vitro model of limbic seizures. *J Physiol* 566: 885-900, 2005.

Biagini G, D'Arcangelo G, Baldelli E, D'Antuono M, Tancredi V, and Avoli M. Impaired activation of CA3 pyramidal neurons in the epileptic hippocampus. *Neuromolecular Med* 7: 325-342, 2005.

Chen Q, He S, Hu XL, Yu J, Zhou Y, Zheng J, Zhang S, Zhang C, Duan WH, and Xiong ZQ. Differential roles of NR2A- and NR2B-containing NMDA receptors in activity-dependent brain-derived neurotrophic factor gene regulation and limbic epileptogenesis. *J Neurosci* 27: 542-552, 2007.

D'Antuono M, Benini R, Biagini G, D'Arcangelo G, Barbarosie M, Tancredi V, and Avoli M. Limbic network interactions leading to hyperexcitability in a model of temporal lobe epilepsy. *J Neurophysiol* 87: 634-639, 2002.

de Guzman P, D'Antuono M, and Avoli M. Initiation of electrographic seizures by neuronal networks in entorhinal and perirhinal cortices in vitro. *Neuroscience* 123: 875-886, 2004.

Esclapez M, Hirsch JC, Ben-Ari Y, and Bernard C. Newly formed excitatory pathways provide a substrate for hyperexcitability in experimental temporal lobe epilepsy. *J Comp Neurol* 408: 449-460, 1999.

Evans JM, Bey V, Burkey AR, and Commons KG. Organization of endogenous opioids in the rostral agranular insular cortex of the rat. *J Comp Neurol* 500: 530-541, 2007.

Finnegan TF, Chen SR, and Pan HL. Mu opioid receptor activation inhibits GABAergic inputs to basolateral amygdala neurons through Kv1.1/1.2 channels. *J Neurophysiol* 95: 2032-2041, 2006.

Hirsch JC, Agassandian C, Merchan-Perez A, Ben-Ari Y, DeFelipe J, Esclapez M, and Bernard C. Deficit of quantal release of GABA in experimental models of temporal lobe epilepsy. *Nature neuroscience* 2: 499-500, 1999.

Isnard J, Guenot M, Ostrowsky K, Sindou M, and Mauguiere F. The role of the insular cortex in temporal lobe epilepsy. *Ann Neurol* 48: 614-623, 2000.

Isnard J, Guenot M, Sindou M, and Mauguiere F. Clinical manifestations of insular lobe seizures: a stereo-electroencephalographic study. *Epilepsia* 45: 1079-1090, 2004.

Kelly ME, and McIntyre DC. Perirhinal cortex involvement in limbic kindled seizures. *Epilepsy Res* 26: 233-243, 1996.

Klapstein GJ, and Colmers WF. Neuropeptide Y suppresses epileptiform activity in rat hippocampus in vitro. *J Neurophysiol* 78: 1651-1661, 1997.

Knopp A, Kivi A, Wozny C, Heinemann U, and Behr J. Cellular and network properties of the subiculum in the pilocarpine model of temporal lobe epilepsy. *J Comp Neurol* 483: 476-488, 2005.

Lopantsev V, and Avoli M. Laminar organization of epileptiform discharges in the rat entorhinal cortex in vitro. *J Physiol* 509 (Pt 3): 785-796, 1998.

Ohara PT, Granato A, Moallem TM, Wang BR, Tillet Y, and Jasmin L. Dopaminergic input to GABAergic neurons in the rostral agranular insular cortex of the rat. *Journal of neurocytology* 32: 131-141, 2003.

Rosenkranz JA, and Johnston D. Dopaminergic regulation of neuronal excitability through modulation of Ih in layer V entorhinal cortex. *J Neurosci* 26: 3229-3244, 2006.

Shah MM, Anderson AE, Leung V, Lin X, and Johnston D. Seizure-induced plasticity of h channels in entorhinal cortical layer III pyramidal neurons. *Neuron* 44: 495-508, 2004.

Steriade M. Neocortical cell classes are flexible entities. *Nature reviews* 5: 121-134, 2004.

Thompson SE, Ayman G, Woodhall GL, and Jones RS. Depression of Glutamate and GABA Release by Presynaptic GABA(B) Receptors in the Entorhinal Cortex in Normal and Chronically Epileptic Rats. *Neurosignals* 15: 202-215, 2007.

Wellmer J, Su H, Beck H, and Yaari Y. Long-lasting modification of intrinsic discharge properties in subicular neurons following status epilepticus. *Eur J Neurosci* 16: 259-266, 2002.

Woldbye DP, Nanobashvili A, Husum H, Bolwig TG, and Kokaia M. Neuropeptide Y inhibits in vitro epileptiform activity in the entorhinal cortex of mice. *Neurosci Lett* 333: 127-130, 2002.

Wozny C, Gabriel S, Jandova K, Schulze K, Heinemann U, and Behr J. Entorhinal cortex entrains epileptiform activity in CA1 in pilocarpine-treated rats. *Neurobiol Dis* 19: 451-460, 2005.

Yang J, Woodhall GL, and Jones RS. Tonic facilitation of glutamate release by presynaptic NR2B-containing NMDA receptors is increased in the entorhinal cortex of chronically epileptic rats. *J Neurosci* 26: 406-410, 2006.

APPENDIX A: Reprint of Chapter 1 and Waiver from Hippocampus

(SE) in adult male Sprague-Dawley rats weighing 150–200 g at the time of injection. All efforts were made to minimize the number of animals used and their suffering. Briefly, rats were injected with a single dose of pilocarpine hydrochloride (380–400 mg/kg, i.p). To reduce the discomforts caused by peripheral activation of muscarinic receptors, methyl scopolamine (1 mg/kg i.p.) was administered 30 min before the pilocarpine injection. The animals' behavior was monitored for ~4 h following pilocarpine and scored according to Racine's classification (Racine et al., 1972). Only rats that experienced SE (Stages 3–5) for 30 min or more (48.6 ± 8.3 min, mean ± standard error of mean (SEM)) were included in the pilocarpine group and used for in vitro electrophysiological studies ~4 months (17 ± 1 week; $n = 27$ rats) following the pilocarpine injection. Since it has been previously established (Cavalheiro et al., 1991; Priel et al., 1996) that all adult rats that experience pilocarpine-induced SE later exhibit spontaneous recurrent seizures, only a subset of animals from the pilocarpine group were video-monitored and the presence of spontaneous behavioral seizures was confirmed in virtually all of them ($n =$ 11 out of 12 rats). In this study, rats receiving a saline injection instead of pilocarpine were used as NECs.

Electrophysiology Procedures

Brain slices from NEC and pilocarpine-treated epileptic rats were obtained according to the procedures established by the Canadian Council of Animal Care. Rats were decapitated under halothane anesthesia, and the brain was extracted and placed in cold (1–3°C) oxygenated artificial cerebrospinal fluid (ACSF). Horizontal brain slices (450-μm thick) that included the EC, the subiculum, and the hippocampus proper were cut with a vibratome along the horizontal plane of the brain that was tilted by ~10° along a posterosuperior-anteroinferior plane passing between the lateral olfactory tract and the brain stem base. Combined hippocampal-EC slices were transferred to an interface tissue chamber and superfused with oxygenated (95% O_2, 5% CO_2) ACSF at 32–34°C. ACSF composition was : NaCl 124 mM, KCl 2 mM, KH_2PO_4 1.25 mM, $MgSO_4$ 2 mM, $CaCl_2$ 2 mM, $NaHCO_3$ 26 mM, and glucose 10 mM. 3,3-(2-Carboxypiperazin-4-yl)-propyl-1-phosphonate (CPP, 10 μM) and 6-cyano-7-nitroquinoxaline-2,3-dione (CNQX, 10 μM) were bath applied. Chemicals were acquired from Sigma-Aldrich Canada (Oakville, Ontario, Canada) and Tocris Cookson (Ellisville, MO).

Field potential recordings were performed with ACSF-filled glass electrodes (tip diameter: <8 μm; resistance: 2–10 MΩ) that were connected to a Cyberamp 380 amplifier (Axon Instruments, Union City, CA). Intracellular sharp-electrodes were filled with 3M potassium acetate (tip resistance: 90–120 MΩ) and coupled to an Axoclamp 2A amplifier (Axon Instruments) with an internal bridge circuit for intracellular current injection. The resistance compensation was monitored throughout the experiment and adjusted as required. The fundamental electrophysiological parameters of the subicular and the EC neurons included in this study were measured as follows: (i) resting membrane potential (RMP) after cell withdrawal, (ii) apparent input resistance (R_i) from the maximum voltage change in response to a hyperpolarizing current pulse (< −0.5 nA), (iii) action potential amplitude (APA), and (iv) action potential duration (APD). Activation of neuronal networks was performed via a concentric bipolar electrode (Frederick Haer and Co., Bowdoinham, ME) that was positioned in CA1 stratum radiatum (Figs. 3 and 4), layer III of the lateral EC (Fig. 5) or subiculum. In all experiments, the minimum stimulus intensity (duration = 100 μs) that produced a reliable response was selected.

Field potential and intracellular signals were fed to a computer interface (Digidata 1322A, Axon Instruments) and were acquired and stored using the pClamp 8.0 software (Axon Instruments). Subsequent analysis of these data was performed with the Clampfit 9 software (Axon Instruments). The reversal potential of spontaneous postsynaptic potentials (PSPs) and stimulus-induced, pharmacologically isolated inhibitory postsynaptic potentials (IPSPs) was determined by linear regression from the plot of their amplitude vs. membrane potential. The peak conductance of the latter responses was calculated by linear regression analysis from the plot of the relation between injected current and membrane potential deflections before and after the extracellular stimulus at latencies of ~10 ms (cf. Williams et al., 1993).

Real-Time PCR

Total RNA was prepared from EC and subiculum of NEC and pilocarpine-treated epileptic rats using Trizol (Invitrogen, Milano, Italy). The total RNA was run on a 2% agarose gel and quantified by densitometric analysis using the Gel Doc, Biorad (Milano, Italy). Total RNA (1 μg) was reverse transcribed using the first-strand synthesis system for RT-PCR (Superscript, Invitrogen). Relative RT-PCR was performed in a Real-Time Thermocycler (MX 3,000, Stratagene, Milano, Italy) using the Brilliant SYBR Green QPCR Master Mix, according to the manufacturers instructions. All PCR reactions were coupled to melting-curve analysis to confirm the specificity of amplification. Quantitative data were normalized to expression of housekeeping gene β-actin. Specific primers for rat potassium-chloride cotransporter 2 (KCC2) and β-actin were designed to amplify short DNA fragments (β-actin forward 5′-aggcatcctgaccctgaagtac-3′; β-actin reverse 5′-gaggcatacagggacaacacag-3′; KCC2 forward 5′-ttcatcaacagcacggacac-3′; KCC2 reverse 5′-cttcttctttccgccctcat-3′). The relative quantitation was analyzed with the software that accompanied the thermal cycler.

Histopathology Procedures

For morphological studies, pilocarpine-treated and NEC animals were anesthetized (chloral-hydrate 450 mg/kg i.p.) and perfused via the ascending aorta with 100 ml saline followed by 300 ml 4% paraformaldehyde dissolved in 0.1 M phosphate buffer (pH 7.4). After dissection, the brains were postfixed for an additional 4 h in the same fixative at 4°C. After cryoprotection by immersion in 15 and 30% sucrose-phosphate buffer solutions, the brains were frozen and cut horizontally from the ventral side by a freezing microtome.

Differences in KCC2 immunoreactivity were assessed with a polyclonal antibody (Upstate, NY) that has been shown to be

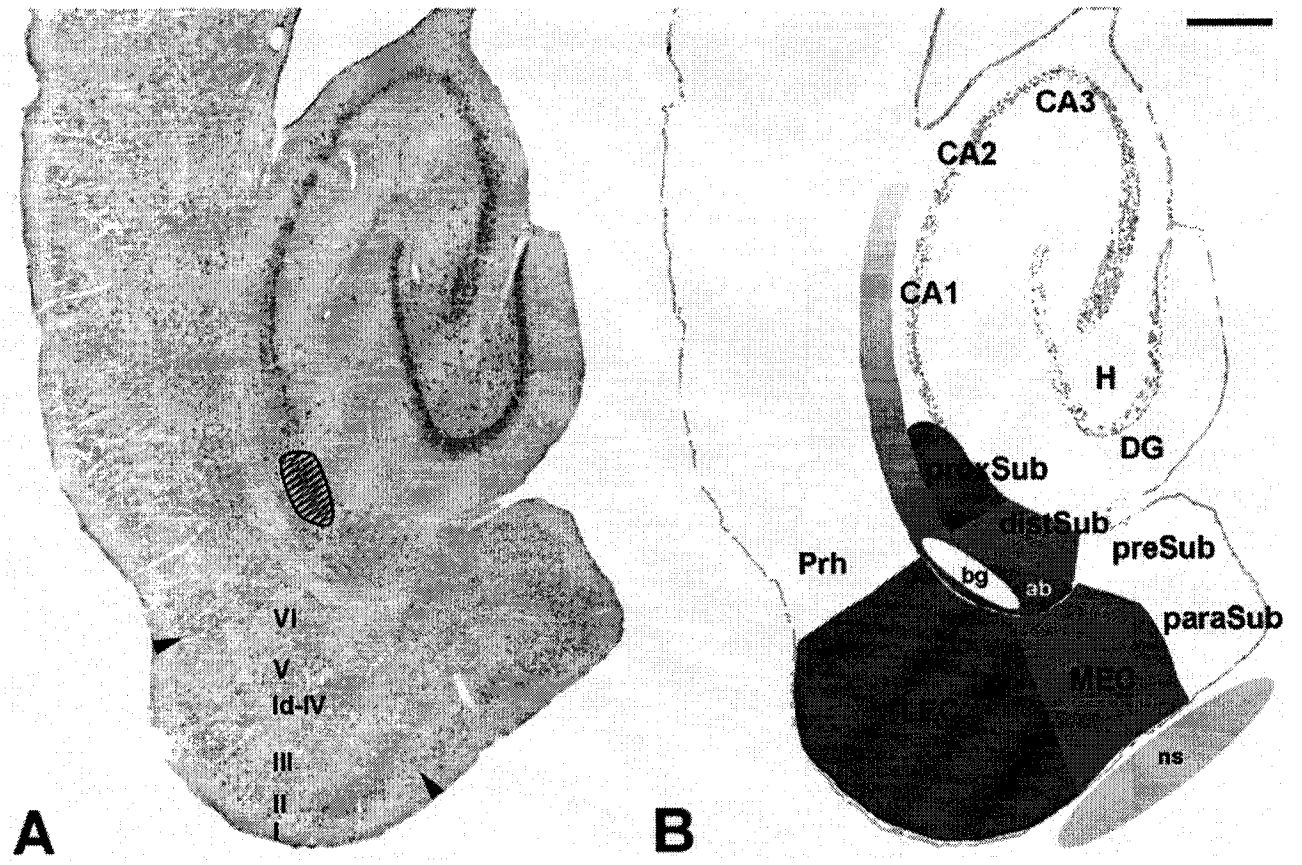

FIGURE 1. Localization of anatomical areas of the hippocampal formation. A: Microphotograph of a toluidine blue-stained horizontal section from a pilocarpine-treated rat. Note that layer II in the EC is clearly identified as composed by a broader and continuous lamina in the medial EC while in the lateral EC (delimited by arrowheads) it appears to be composed by dispersed "islands" of neuronal elements. The other layers and the lamina dissecans (ld) are also indicated. Note that the dashed area in the subiculum shows the location where intracellular recordings were obtained. B: Areas of interest used to investigate the changes in subicular and EC neuronal network activities are shown. Areas marked in blue and red identify the different regions of the subiculum and EC sampled to measure gray tone values after immunohistochemistry in the proximal (proxSub) and distal (distSub) subiculum and in the lateral (LEC) and medial EC (MEC). The white ellipse in the angular bundle (ab) indicates the area used for the background (bg) staining, while the yellow ellipse close to the section indicates the procedure to measure nonspecific (ns) gray tone values. Abbreviations used: CA, cornu ammonis; DG, DG; H, hilus of DG; paraSub, parasubiculum; preSub, presubiculum; Prh, perirhinal cortex. Scale bar, 500 μm. [Color figure can be viewed in the online issue, which is available at http://www.interscience.wiley.com.]

specific (Vale et al., 2003; Grob and Mouginot, 2005; Lohrke et al., 2005). In addition, changes in the parvalbumin-positive interneuron subpopulation—which is critically involved in TLE (de Felipe et al., 1993)—were investigated by using a mouse monoclonal antibody (Swant, Bellinzona, CH). We also analyzed the changes in synaptophysin, a putative marker of functionally active sprouted nerve terminals (Proper et al., 2000) by employing a previously characterized rabbit polyclonal antibody for synaptophysin (Bahler et al., 1991; kindly provided by Dr. F. Benfenati, Genua, Italy). Antibodies for KCC2 (1:1,000), parvalbumin (diluted 1:2,000), and synaptophysin (1:5,000) were used on 50-μm-thick horizontal sections obtained, respectively, at levels 7.3–7.6 from bregma. Some sections (one section out of four, four series for each animal) were stained with toluidine blue to clearly identify the various anatomical regions of the hippocampal formation and to assess the presence of neuronal damage (Fig. 1A). Immunohistochemistry was performed using the avidin-biotin complex technique and diaminobenzidine as chromogen (cf. Biagini et al., 2005). Endogenous peroxidase was blocked by 0.1% phenylhydrazine in phosphate-buffered saline (PBS) for 20 min, followed by several washes in PBS preceding the incubation with primary antibodies. Secondary antibodies and the avidin-peroxidase complex were purchased from Amersham Italia (Milan, Italy) and diluted 1:200 and 1:300, respectively. The stained sections were analyzed by densitometry using image analysis software (KS 300, Zeiss Kontron, Munich, Germany) (cf. Biagini et al., 2001, 2005). Four sections for each animal were investigated and averaged for statistical analysis. Briefly, the value of nonspecific mean gray tone was measured in an area of the slide immediately outside the section close, respectively, to subiculum or EC (Fig. 1A,B). An area of the angular bundle was

taken as index of background labeling (Fig. 1B), since KCC2 and synaptophysin are not detectable in axons and glial cells (Bahler et al., 1991; Williams et al., 1999). Mean gray values of specific immunostaining were measured in subicular and EC areas identified as follows. The subiculum was defined by its enlarged and loosely packed pyramidal layer, clearly distinguishable from the narrow pyramidal cell layer of CA1 in toluidine blue-stained sections (Fig. 1A), and by differences in neuronal cell size when compared with the presubiculum; in addition, we divided the subiculum into two halves: the one close to CA1 was defined as proximal subiculum, while that close to presubiculum was defined as distal subiculum (Fig. 1B) (cf. Naber et al., 2001). The EC was identified by its classical lamination in six layers and, particularly, by the presence of the more intensely stained layer II that, when continuous, marked the medial EC or, when discontinuous because of the "islandic" neuronal organization (Witter, 1993), marked the lateral EC (delimited by arrowheads in Fig. 1A). To measure mean gray tone values using the KS 300 software, these areas were manually selected (Fig. 1B) by an expert neuroanatomist (G.B.) who was blinded to animal codes. Transmittance percentage values ($T\%$) of total and nonspecific staining were then obtained by dividing the mean gray tone value of every area analyzed by the mean gray tone value of the background. Optical density (OD) values were then calculated according to the formula $OD = -\log T\%$, for both nonspecific gray tone values and specifically labeled areas. The specific OD was obtained by deducting nonspecific OD from total OD for each studied region (Biagini et al., 2001). Neuronal counts of parvalbumin-positive interneurons were as described by Biagini et al. (2005). Sections were used for parvalbumin immunostaining were then rehydrated through various passages in decreasing ethanol solutions, counterstained with toluidine blue, and analyzed by the KS 300 software to measure the subicular area.

Statistical Methods

Measurements in the text are expressed as mean ± SEM and n indicates the number of samples studied under each specific protocol. The results obtained were compared with the Student's t-test or Mann–Whitney test and were considered statistically significant if $P < 0.05$.

RESULTS

Unaltered Intrinsic Cellular Properties in NEC and Pilocarpine-Treated Subiculum

As previously shown (Mattia et al., 1997; Su et al., 2002; Knopp et al., 2005), intracellular injection of depolarizing current pulses (duration = 1 s) induced two patterns of firing in subicular neurons recorded in NEC and pilocarpine-treated slices. The first consisted of an initial burst of action potentials followed by regular firing (Fig. 2Aa and Ba), while the second was characterized by regular, repetitive firing only (Fig. 2 Ab and Bb). Quantification of the incidence of these two firing patterns demonstrated similar proportions in pilocarpine-treated (intrinsic bursting, $n = 16$; regular firing, $n = 13$) and in NEC (intrinsic bursting, $n = 14$; regular firing $n = 14$) tissue. In addition, subicular neurons recorded in the two types of tissue displayed similar fundamental intrinsic properties (Table 1). As depicted in Figure 2 (Ac and Bc), steady depolarization of regular firing neurons from RMP to membrane potentials above −54 mV produced the appearance of rhythmic subthreshold oscillations in the θ range (regular firing: NEC = 6.5 ± 0.8 Hz, $n = 5$, pilocarpine = 6.6 ± 1.1 Hz, $n = 5$; intrinsic bursting: NEC = 5.6 ± 0.8 Hz, $n = 5$, pilocarpine = 5.9 ± 0.6 Hz, $n = 5$) that were combined with action potential discharge. The membrane potentials at which "subthreshold" membrane oscillations appeared and the threshold for action potential generation were also similar in NEC and pilocarpine-treated, epileptic subicular neurons (Table 1).

Activation of CA1 Inputs Demonstrates Hyperexcitability Within the Epileptic Subiculum

Single-shock electrical stimuli delivered in the CA1 stratum radiatum of NEC and pilocarpine-treated slices produced similar low amplitude, negative deflecting, field potential responses in subiculum (Fig. 3A and B, Field traces in the top samples). In contrast, remarkable differences could be identified in the recorded intracellular signals. As shown in Figure 3A (−71 mV trace), CA1 stimulation invariably produced a sequence of depolarizing-hyperpolarizing postsynaptic responses in NEC subicular cells recorded at RMP ($n = 14$); in addition, these stimulus-induced responses became purely depolarizing when the membrane potential was brought to values more negative than −80 mV with injection of steady negative current (Fig. 3A, −81 mV and −88 mV traces), while at depolarized membrane levels they were characterized by a single action potential followed by a robust hyperpolarization (Fig. 3A, −66 mV). At variance, two types of stimulus-induced intracellular responses were recorded in the pilocarpine-treated subiculum (Fig. 3B). In the first group of neurons ($n = 18$) single-shock stimuli produced depolarizing postsynaptic activity at both RMP and at hyperpolarized membrane potentials (Fig. 3Ba, −71, −77, and −88 mV traces) while at depolarized membrane values these responses comprised of action potential bursts or doublets (Fig. 3Ba, −65 mV trace). In the second group of pilocarpine-treated subicular cells ($n = 11$), CA1 stimulation elicited bursting responses at RMP or at depolarized membrane values (Fig. 3Bb; −70 and −83 mV traces). Moreover, when action potential bursting was prevented by injecting steady negative current, we identified an underlying slow depolarization that followed the initial excitatory postsynaptic potential (EPSP) (Fig. 3Bb, −92 mV trace). These characteristics were found to be independent of the intrinsic firing properties of subicular cells.

Subicular Cells in Pilocarpine-Treated Slices Have a Lower Threshold to Synaptic Stimuli Than in NEC Tissue

The findings reported in the previous section suggest that increased network excitability characterizes the pilocarpine-

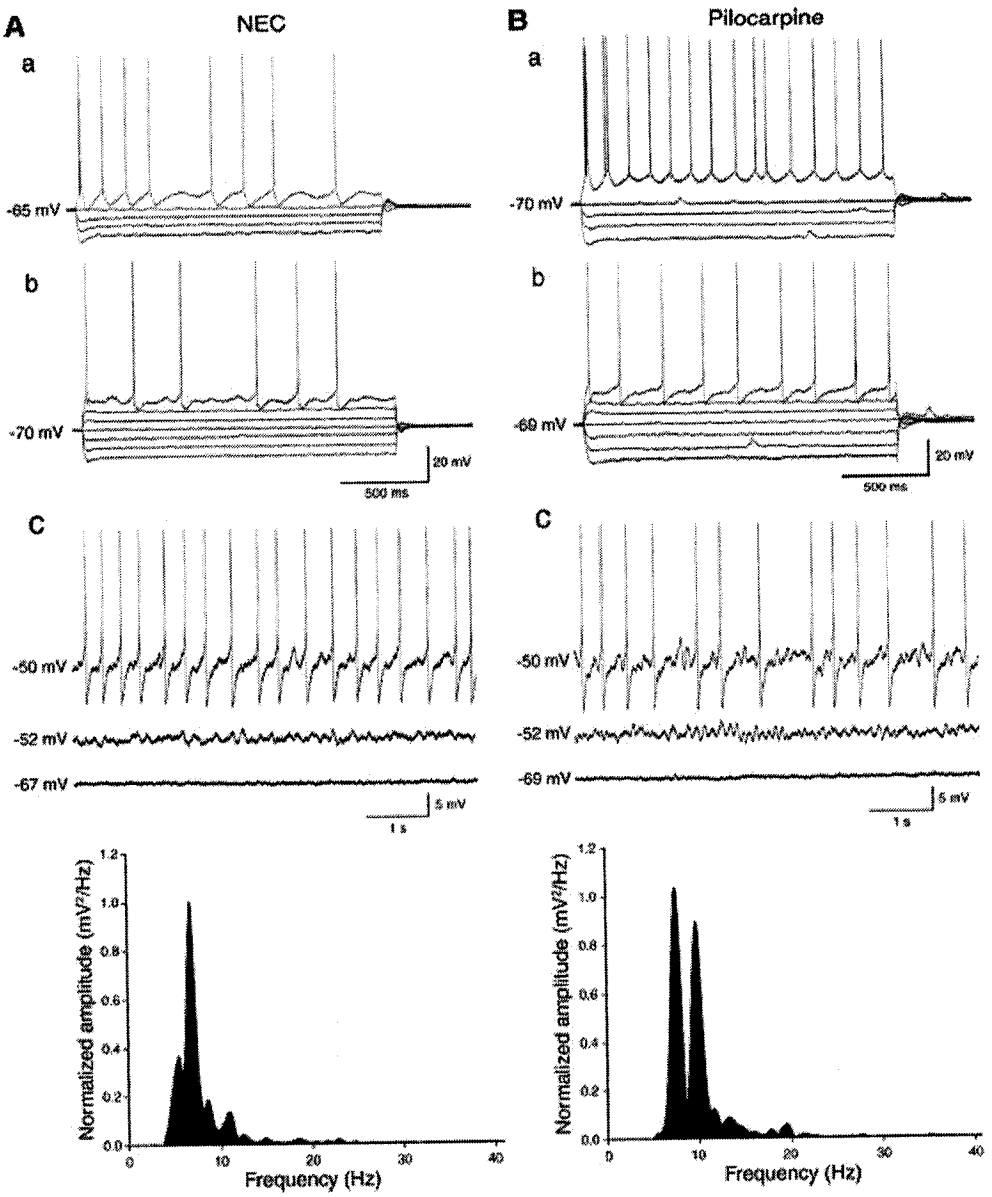

FIGURE 2. Intrinsic firing and subthreshold oscillations generated by subicular neurons in NEC and pilocarpine-treated tissue. Two types of firing patterns are generated by subicular neurons in NEC (A) and pilocarpine (B) treated slices during injection of depolarizing current: (i) action potential bursting coupled with regular action potential firing (Aa and Ba) or regular firing (Ab and Bb). Comparison of NEC and pilocarpine (Ac and Bc) treated regular firing subicular neurons produced subthreshold oscillatory activity when depolarized from RMP. Quantification of subthreshold oscillations through power spectral analysis demonstrates that subthreshold activity oscillates within a q band of 6–9 Hz.

treated, epileptic subiculum. To this end, we compared the input–output curves of the intracellular responses generated by subicular neurons following CA1 single-shock stimuli in NEC and pilocarpine-treated slices. As shown in Figure 4A, focal stimuli with strength ranging between 100 and 200 μA produced either no or minimal postsynaptic responses in NEC subicular neurons (n = 5). These cells generated overt postsynaptic depolarizations only when the current intensity was increased to 450 μA, while a single action potential occurred in response to stimuli delivered at ≥500 μA.

In contrast, when this stimulation protocol was applied to pilocarpine-treated slices, we could identify a lower activation threshold. Thus, a depolarizing response was elicited by CA1 stimuli with the current intensity of 100 μA, and then it increased in amplitude following stimuli at 150 μA (Fig. 4B). Moreover, in all pilocarpine-treated subicular neurons (n = 6),

TABLE 1.

Instrinsic Neuronal Properties of NEC and Pilocarpine-Treated Subicular Neurons

Firing pattern	RMP (mV)	IR (MΩ)	APA (mV)	APD (ms)	Oscillatory threshold (mV)	Ap threshold (mV)
			NEC subicular neurons			
Regular firing (n = 14)	−69.7 ± 0.8	42.3 ± 2.9	89.2 ± 2.3	1.3 ± 0.1	−54.5 ± 0.5	−50.5 ± 0.9
Intrinsic bursting (n = 14)	−66.7 ± 1.1	35.2 ± 3.1	88.8 ± 1.9	1.3 ± 0.1	−56.7 ± 1.8	−54.7 ± 1.0
			Pilocarpine-treated subicular neurons			
Regular firing (n = 13)	−66.7 ± 0.8	43.7 ± 3.7	91.4 ± 2.8	1.4 ± 0.1	−53.2 ± 2.3	−49.9 ± 1.1
Intrinsic bursting (n = 16)	−69.0 ± 1.1	39.4 ± 3.7	88.9 ± 2.1	1.3 ± 0.1	−58.7 ± 0.9	−54.8 ± 0.9

A comparison of the resting membrane potential (RMP), the input resistance (IR), the action potential amplitude (APA), and the action potential dutation (APD) in the NEC and pilocarpine-treated subiculum. Additional properties include membrane potential for subthreshold oscillatory activity as well as action potential generation.

single shock stimulation at ~200 μA was sufficient to elicit action potential firing characterized by either doublets or bursts of action potentials. To assess network excitability we defined 100% as the current threshold required to elicit depolarizing PSPs prior to action potential spiking. Analysis of the relation between current intensity and depolarizing response amplitude (prior to action potential generation) revealed that pilocarpine-treated subicular cells required significantly less current to generate responses comparable to those in NEC tissue (Fig. 4C).

Activation of EC Layer III Produces Multiphasic Activity in the Pilocarpine-Treated Subiculum

We further assessed subicular network excitability in NEC and pilocarpine-treated tissue by analyzing the responses induced by electrical stimuli delivered in EC layer III (Fig. 5). At resting membrane potentials, in NEC slices, extracellular stimulation elicited a low amplitude field response that was paralleled by a monophasic depolarizing PSP with a duration of 101.9 ± 7.3 ms (Fig. 5A; n = 13). As illustrated in Figure 5A, sequential injection of steady positive current from −93 mV progressively reduced the amplitude of the depolarizing PSP and unmasked a hyperpolarization at −61 mV. In contrast, focal stimuli in pilocarpine-treated tissue (n = 13 cells) consistently produced multiphasic postsynaptic responses lasting up to 491.9 ± 38.5 ms (Fig. 5B). This activity persisted at hyperpolarized membrane potentials while injection of steady depolarizing current made single action potentials, which were not followed by any hyperpolarizing component, appear (Fig. 5B, −56 mV). The duration of the subicular responses to EC stimuli recorded in NEC and pilocarpine-treated slices is quantified in Figure 5C ($P < 0.0001$).

Spontaneous Synaptic Activity in NEC and Pilocarpine-Treated Subiculum

As illustrated in Figure 6A (−73 mV trace), low amplitude spontaneous PSPs comprising depolarizing and hyperpolarizing components occurred at RMP with intervals of 8.0 ± 0.7 s in NEC subicular neurons (n = 12). Hyperpolarizing the membrane of these cells through negative current injection produced an inversion of the hyperpolarizing component (Fig. 6A, −94 mV trace). In contrast, injection of steady depolarizing current made the depolarizing and hyperpolarizing components of the PSP decrease and increase, respectively, along with the appearance of subthreshold voltage-dependent oscillatory activity (arrows) at membrane potentials less negative than −60 mV (Fig. 6A, −60 mV trace).

Intracellular recordings from pilocarpine-treated subicular cells (n = 10) also demonstrated the presence of spontaneous PSPs that, however, had an increased rate of occurrence (intervals = 2.7 ± 0.4 s; $P < 0.0001$ independent t-test) when compared with NEC tissue (Fig. 6B and C). In addition, pilocarpine-treated subicular neurons generated spontaneous depolarizing PSPs both at membrane values of −70 mV (RMP) and of −83 mV (Fig. 5B). Thus, at RMP pilocarpine-treated subicular cells did not exhibit the biphasic EPSP/IPSP sequence observed in NEC tissue. As illustrated in Figure 6B (−62 mV), injection of positive current in pilocarpine-treated cells transformed depolarizing PSPs into hyperpolarizing events coinciding with oscillatory activity (arrow) and single action potential spiking. Analysis of the reversal potential of the spontaneous PSPs revealed a more positive value in pilocarpine-treated tissue (−62.4 ± 0.9 mV, n = 17) than in NEC (−65.8 ± 0.9 mV, n = 16) ($P < 0.02$) (Fig. 6D).

Reversal Potential of "Monosynaptic" IPSPs in NEC and Pilocarpine-Treated Subicular Neurons

To isolate GABAergic activity we performed intracellular recordings in subicular neurons of NEC and pilocarpine-treated slices in the presence of an NMDA receptor antagonist (CPP = 10 μM) and of an AMPA/kainate receptor blocker (CNQX = 10 μM). Under these pharmacological conditions, focal subicular stimulation elicited a presumptive IPSP that was often characterized by a fast and a slow component (Fig. 7A). Serial application of $GABA_A$ (picrotoxin, 50 μM, n = 5) and $GABA_B$ (CGP 35348, 10 μM; n = 4) receptor antagonists demonstrated that

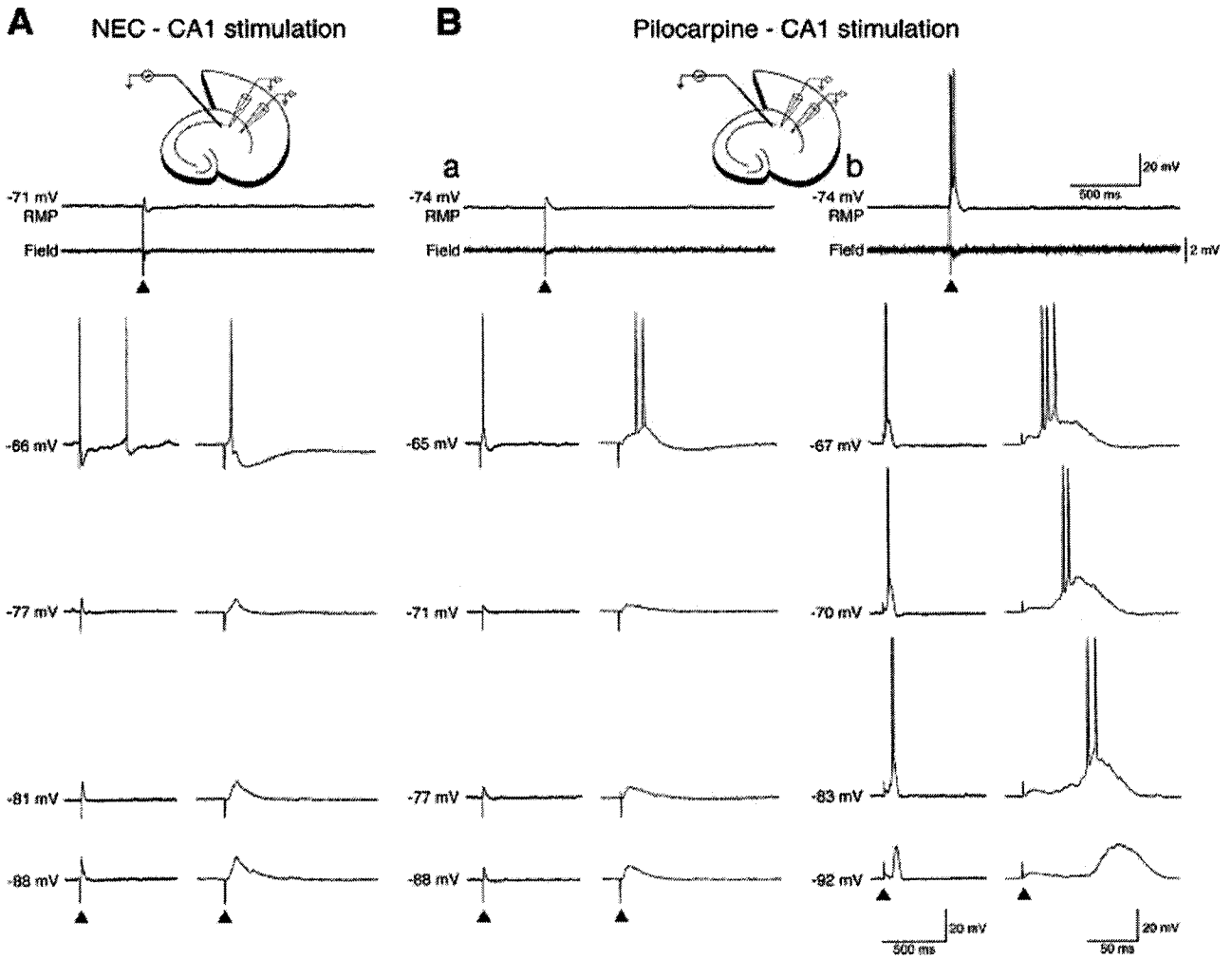

FIGURE 3. Activation of CA1 networks demonstrates hyperexcitability within the epileptic subiculum. A: In NEC tissue, CA1 single-shock stimulation elicits a sequence of depolarizing–hyperpolarizing postsynaptic responses at −71 mV (RMP). Hyperpolarization to −77, −81, and −88 mV produces stimulus-induced depolarizing postsynaptic events, whereas electrical stimulation at −66 mV elicits a single action potential. Ba: In pilocarpine-treated subicular neurons, single-shock stimulation of the CA1 area elicits action potential bursting at −65 mV while a depolarizing postsynaptic response is seen at RMP and at further hyperpolarized potentials. Bb: In other experiments, pilocarpine-treated subicular neurons generate all-or-none stimulus-induced bursting activity. Action potential bursts were halted upon further hyperpolarization of the membrane to −92 mV.

the fast component of the stimulus-induced IPSP was $GABA_A$ receptor-mediated (not illustrated). In these experiments, we analyzed the stimulus-induced responses recorded at different membrane potentials by injecting pulses of hyperpolarizing and depolarizing current. By doing so, we could identify the reversal potential of the stimulus-induced fast IPSP along with the associated peak conductance. Single-shock stimulation in NEC and pilocarpine-treated cells produced $GABA_A$ receptor-mediated IPSP reversal points of −75 mV (Fig. 7C, black dots) and −66 mV (Fig. 7C, open dots), respectively. Analysis of additional samples for the $GABA_A$ receptor-mediated IPSP, revealed a more positive reversal point (−67.8 ± 6.3 mV; $n = 16$, 8 regular fire and 8 intrinsic bursting; $P < 0.001$, independent t-test) within the pilocarpine-treated subiculum as compared to NEC tissue (−74.8 ± 3.6 mV; $n = 13$, 9 regular firing and 4 intrinsic bursting) (Fig. 7D). Alteration of the IPSP reversal point was mirrored by a significant reduction ($P < 0.003$; independent t-test) in the $GABA_A$ receptor mediated IPSP peak conductance in pilocarpine-treated epileptic cells (i.e., 17.6 ± 11.3 nS vs. 41.5 ± 26.7 nS in NEC) (Fig. 7D).

Reversal Potential of "Monosynaptic" IPSPs Generated by EC Layer V Neurons From NEC and Pilocarpine-Treated Rats

Using a similar protocol, we assessed whether $GABA_A$ receptor activity was altered in neurons recorded in EC layer V of

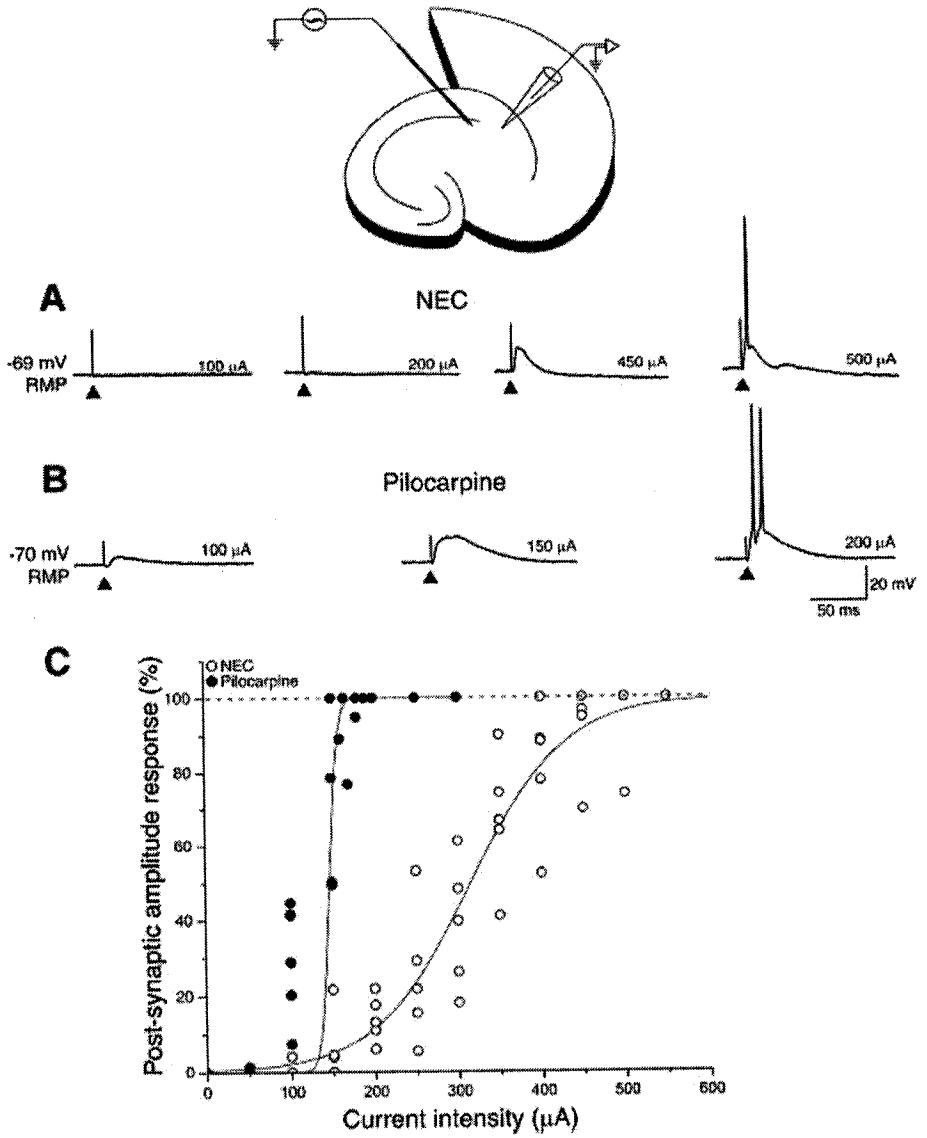

FIGURE 4. Pilocarpine-treated subicular neurons exhibit a lower threshold of activation. A: CA1 stimulation (duration of the stimulus = 100 µs) at increasing intensities in NEC tissue produces hyperpolarizing responses (200 µA) and depolarizing events (450 µA), whereas a strength of 500 µA is sufficient to elicit a single action potential. B: In contrast, a stimulus of lower intensity in CA1 is required to elicit depolarizing responses (100 and 150 µA) and action potential bursting (200 µA) in pilocarpine-treated subicular neurons. C: Graphical display of the average input–output curves of the postsynaptic responses generated prior to the appearance of action potential(s), in pilocarpine-treated tissue (black dots; n = 6) compared to NEC (open dots; n = 5). Boltzman sigmoidal parameters were used to fit the current-response relationship. Stimulus to evoke the half amplitude of response (NEC: 315.6 ± 3.3 µA and pilocarpine: 147.1 ± 3.8 µA) and slope (NEC: 56.6 ± 2.9 and pilocarpine: 4.6 ± 4.3) were statistically significant (half amplitude of response: $P < 0.00001$; slope: $P < 0.0003$).

epileptic tissue. As shown in Figure 8, NEC and pilocarpine-treated neurons in this limbic area had similar reversal potentials (i.e., −72.3 ± 3.8 mV, $n = 7$, for NEC and −69.8 ± 5.2 mV, $n = 13$, for pilocarpine-treated EC cells; $P = 0.27$, independent t-test). Moreover, the peak conductance of the $GABA_A$ receptor-mediated IPSP was not different ($P = 0.89$; independent t-test) in NEC (10.3 ± 4.1 ns, $n = 7$) and pilocarpine-treated (12.8 ± 8.6 ns, $n = 13$) EC neurons (Fig. 8D).

Reduced KCC2 Expression in the Pilocarpine-Treated Subiculum

The more depolarized reversal potential of the $GABA_A$ receptor-mediated IPSP identified in pilocarpine treated subicular cells led us to assess whether the expression of KCC2 was changed. As illustrated in Figure 9A, RT-PCR analysis revealed a 44.0 ± 6.1% reduction in KCC2 mRNA expression level within the subiculum,

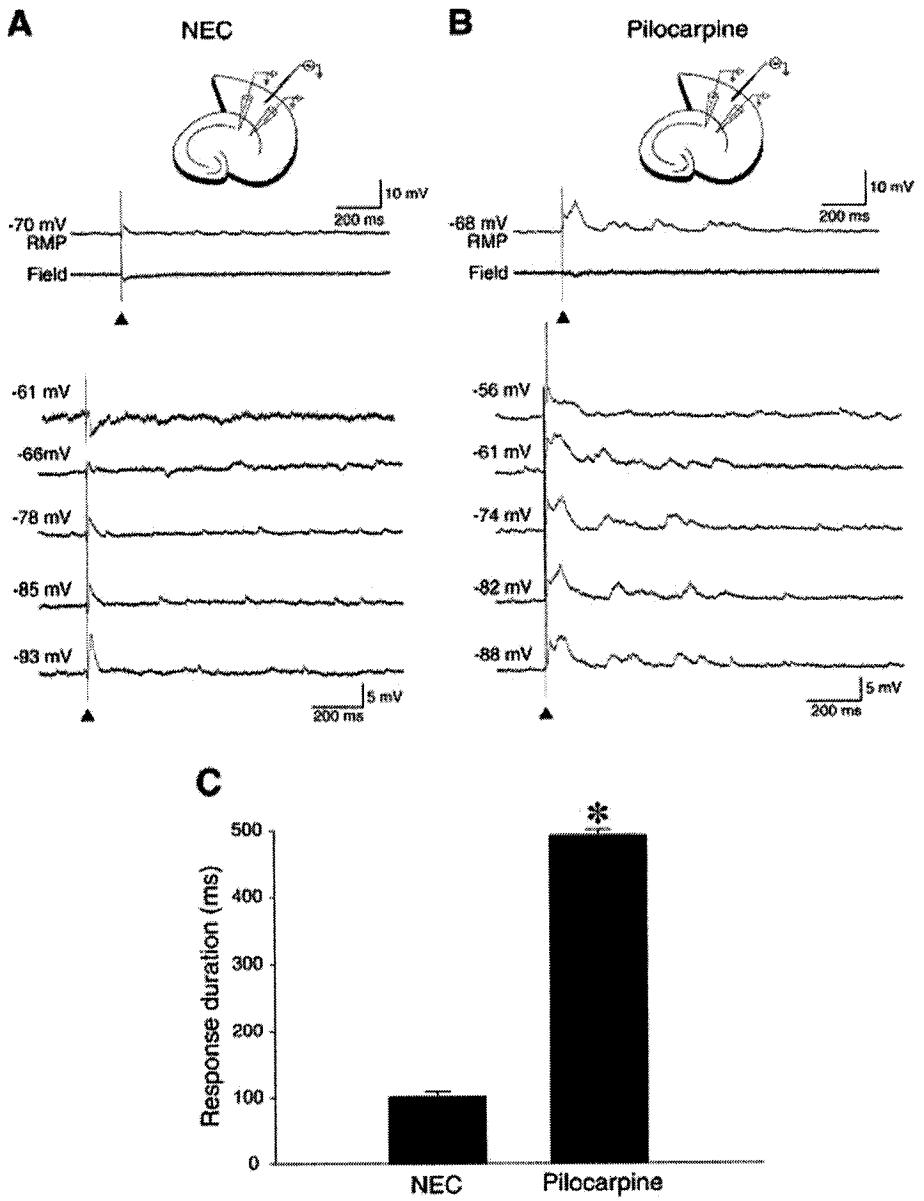

FIGURE 5. Activation of EC layer III generates hyperexcitable responses in the pilocarpine-treated subiculum. A: Single shock stimulation of EC layer III elicits a monophasic postsynaptic response in the NEC subiculum. B: In contrast, EC layer III activation within pilocarpine treated tissue produced multiphasic postsynaptic activity within the subiculum. C: The pilocarpine treated subiculum produced a response of enhanced duration that was significantly different from the subicular response in the NEC (NEC: 101.93 ± 7.33 ms vs. pilocarpine: 491.89 ± 38.54 ms; $P < 0.0001$).

but not in the EC of pilocarpine-treated, epileptic rats ($n = 5$) as compared with NECs ($n = 5$). We also used a commercially available antibody reported to be specific for KCC2 (Vale et al., 2003; Grob and Mouginot, 2005; Lohrke et al., 2005). By doing so, we could localize in NEC subiculum the presence of KCC2 immunopositivity both in nerve fibers and on the surface of neuronal cell bodies (Fig. 9C); in contrast, the cytoplasm appeared completely devoid of any signal (note that the arrowheads in the inset of Fig. 9C point at neuronal somas that appear white). This localization was consistent with previous reports on KCC2 expression in the mature brain (Lorke et al., 2005; Vale et al., 2005).

Immunohistochemical analysis of the epileptic rat subiculum demonstrated a decrease in KCC2 positivity (Fig. 9D). These findings were also quantified by using optical density analysis. As illustrated in Figure 9B, we found a significant ($P < 0.05$) decrease (−25%) in KCC2 immunoreactivity in the subiculum of epileptic rats ($n = 9$) as compared to NECs ($n = 8$). Therefore, these findings demonstrate a reduced expression of both

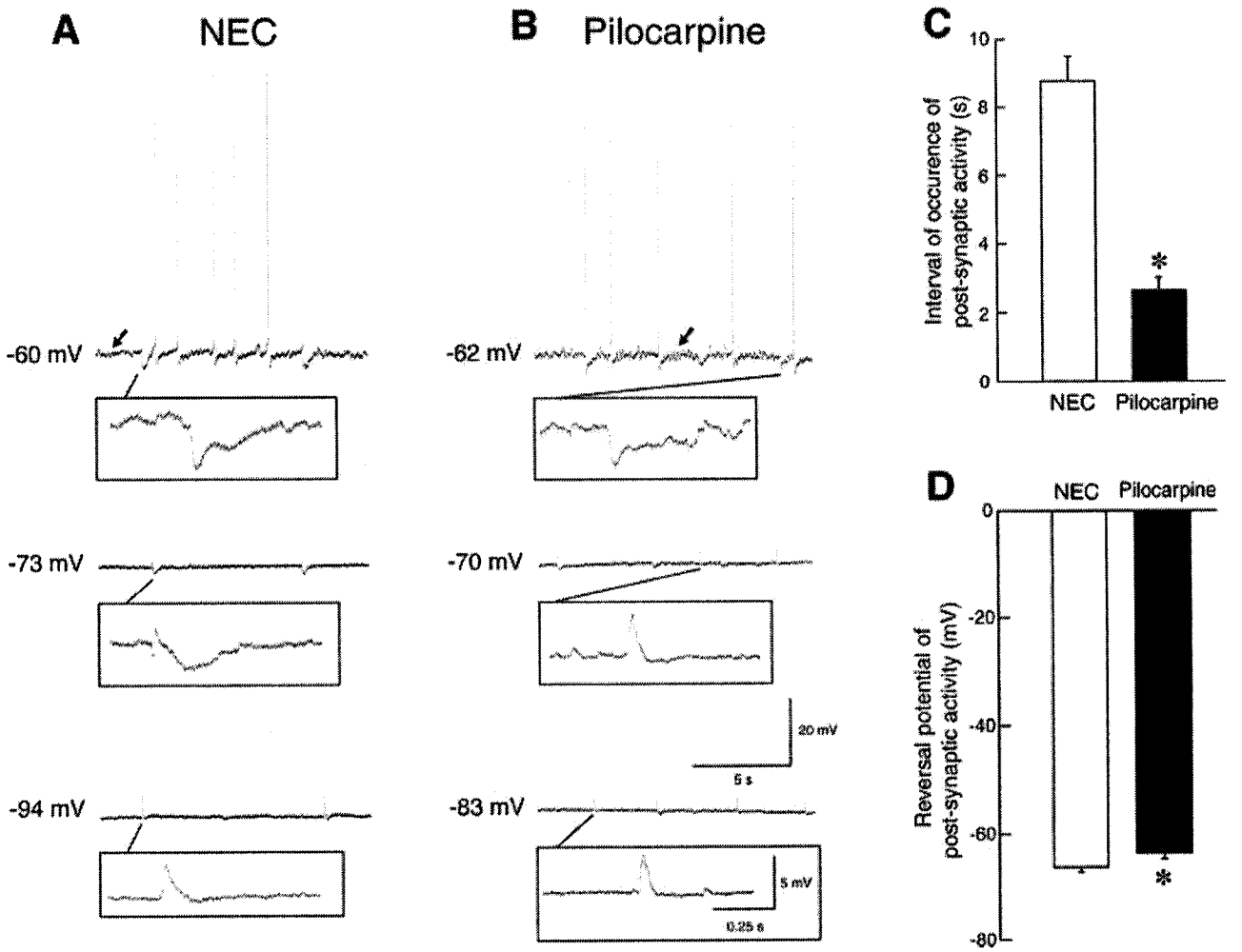

FIGURE 6. Higher frequency of postsynaptic potentials (PSPs) within the pilocarpine-treated subiculum. A: Intracellular recordings in the subiculum of NEC slices demonstrate spontaneous PSPs exhibiting excitatory and inhibitory components at −73 mV. Depolarizing PSPs occur at −94 mV whereas at −60 mV these events were mainly hyperpolarizing. B: Subicular neurons in pilocarpine treated tissue exhibited depolarizing PSPs at −70 and −83 mV while hyperpolarizing PSPs occur during steady depolarization to −62 mV. C: Pilocarpine-treated subicular neurons exhibit a higher frequency of spontaneous PSPs as compared to those recorded in NEC slices ($P < 0.0001$, independent t-test). D: The reversal potential of spontaneous PSPs in NEC vs. pilocarpine-treated tissue was significantly different ($P < 0.02$).

mRNA and KCC2 protein in the pilocarpine-treated, epileptic subiculum supporting a malfunction in the extrusion of intracellular Cl^- and thus the different IPSP reversal potential values.

Histopathological Evaluation of Neuronal Damage

Next, we studied whether interneuronal loss or neuronal sprouting were present in the subiculum and EC of pilocarpine-treated, epileptic rats. Parvalbumin-positive cells were found to be homogeneously distributed both in the subiculum (Fig. 10A,B) and in the EC (Fig. 10C and D). However, a reduced area of immunostaining could always be identified in the subiculum of pilocarpine-treated animals.

By counting parvalbumin-positive cells in the ventral subiculum (level 7.6 mm from bregma), we found a significant ($P < 0.01$) decrease (−65%) in parvalbumin-stained neurons in pilocarpine-treated rats ($n = 9$) as compared with NECs ($n = 8$) (Fig. 10E). However, the area covered by subicular neurons, measured in toluidine blue-stained sections was only slightly decreased in pilocarpine-treated animals (0.38 ± 0.06 mm^2) compared with NECs (0.40 ± 0.03 mm^2; not statistically different). Following the surprising results obtained by counting parvalbumin-positive cells at this level, we decided to further analyze the subiculum considering a dorsal level (3.6 mm from

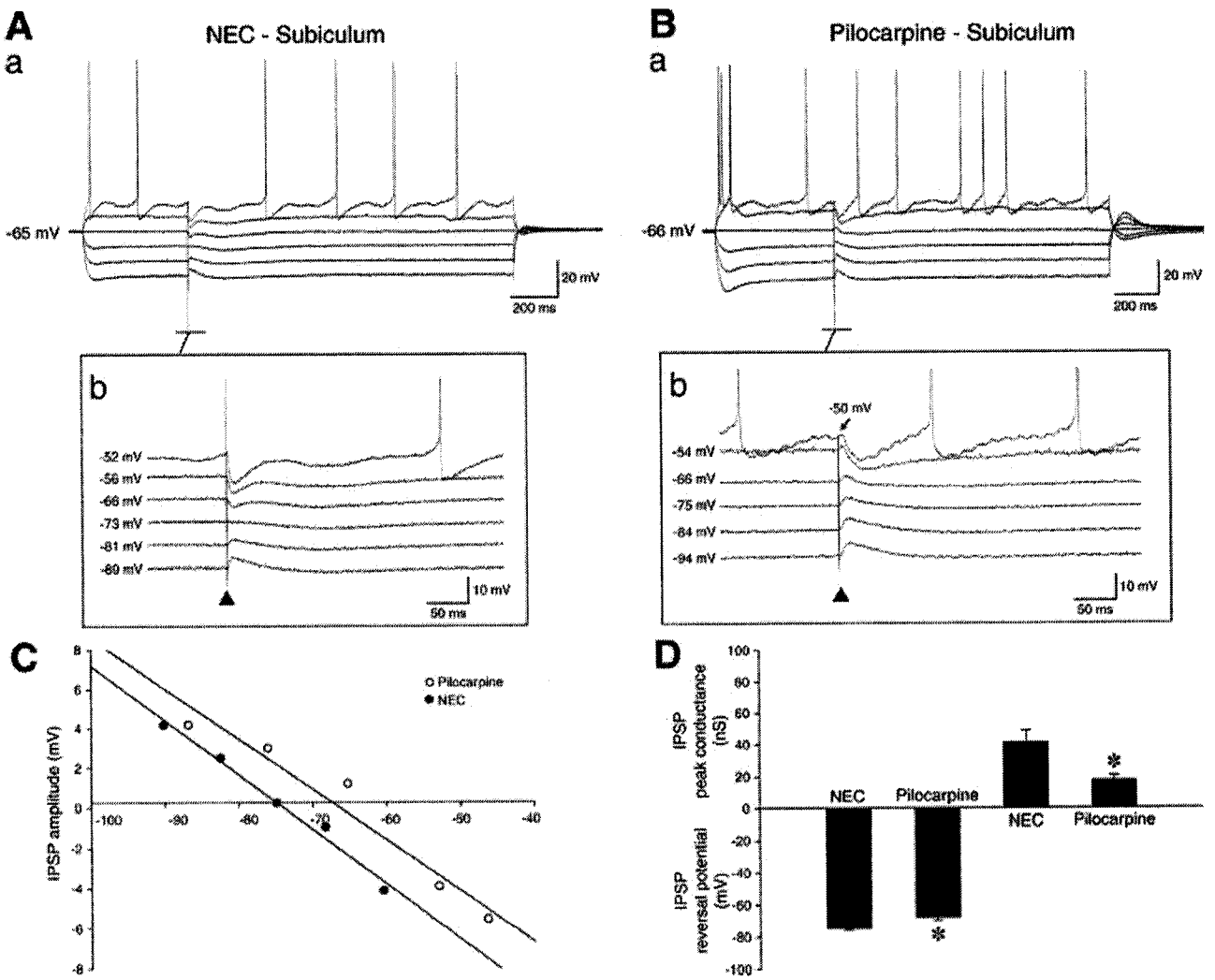

FIGURE 7. The pilocarpine treated subiculum exhibits a more positive $GABA_A$ receptor-mediated IPSP. A and B: Single shock stimulation (100 μs) at different membrane potentials elicit "isolated" IPSPs in the presence of glutamatergic antagonists (CPP + CNQX, 10 μM for both drugs). Sharp-electrode intracellular recordings were performed in NEC (A) and pilocarpine-treated tissue (B). Insets: expansion of the intracellular recordings of the IPSPs recorded in NEC and pilocarpine-treated tissue. Note that at −66mV hyperpolarizing synaptic potentials occur in NEC, whereas depolarizing potentials occur in the pilocarpine-treated cell. C: The IPSP reversal point in the NEC subiculum is −75 mV (black dots) whereas the pilocarpine-treated subiculum exhibits a value of −66 mV. D: Mean values of the "isolated" IPSPs are significantly more positive ($P < 0.001$; independent *t*-test) in pilocarpine-treated tissue compared to NEC. Note also that a significant reduction in the IPSP peak conductance occurs in the pilocarpine-treated subiculum ($P < 0.003$; independent *t*-test).

bregma), since the lesion extent was described to vary along the hippocampal longitudinal axis by other authors (Turski et al., 1983). Interestingly, a significant ($P < 0.01$) decrease (−40%) was also observed in the dorsal subiculum. However, the area covered by subicular neurons, measured in toluidine blue-stained sections was only slightly decreased in pilocarpine-treated animals (0.38 ± 0.06 mm^2) compared with NEC (0.40 ± 0.03 mm^2; not statistically different). Parvalbumin-positive cells were also counted in the superficial layers of medial EC and lateral EC in the same ventral sections, but no differences were found between the two groups of animals (Fig. 10, compare NEC in C with pilocarpine-treated in D, as well as quantified data in panel E), thus confirming the results reported by Du et al. (1995).

Finally, we investigated the distribution of immunoreactivity for synaptophysin (Fig. 11), which is considered to be a marker of functionally sprouted nerve fibers (Proper et al., 2000). Here, we found the presence of well-delimited patches of increased immunoreactivity in DG, subiculum and EC of pilocarpine-treated rats (arrows in Fig. 11B and corresponding insets). In the DG, patches of increased immunoreactivity were localized in the inner molecular layer and were thus reminiscent of the mossy fiber sprouting reported in TLE patients (Sutula et al., 1989) and animal models (Sutula et al., 1988).

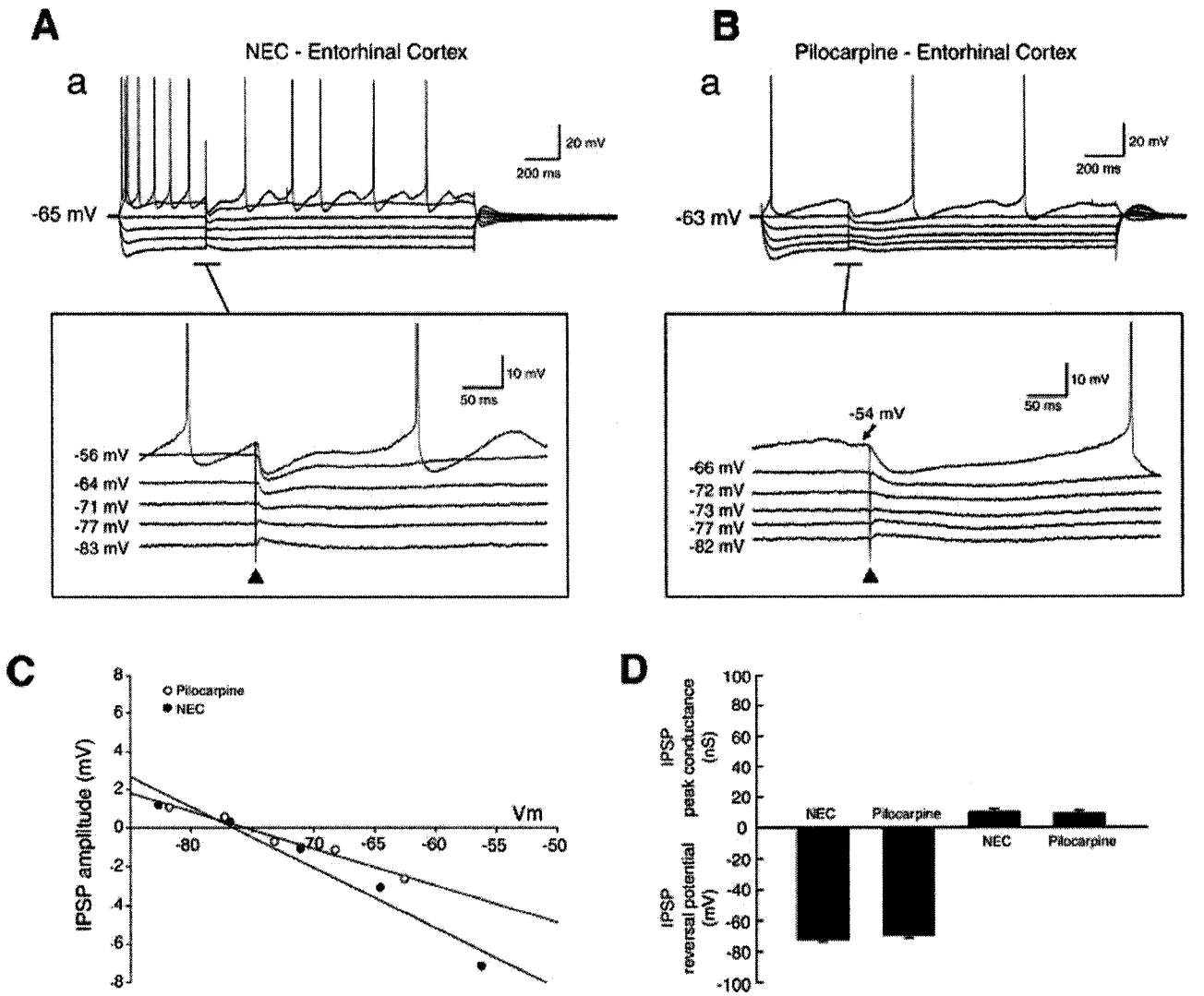

FIGURE 8. Assessment of the Cl^- reversal potential of the $GABA_A$ receptor mediated IPSP in layer V of the EC. A and B: Inhibitory postsynaptic activity isolated via application of the glutamatergic antagonists CPP and CNQX (10 μM in both cases). In NEC (A) and pilocarpine treated tissue (B), single shock stimulation in layer V of the EC produced depolarizing and hyperpolarizing inhibitory postsynaptic responses at negative and positive membrane potentials, respectively. C: Regression analysis demonstrated the Cl^- reversal point in NEC to be −76 mV and −75 mV in the pilocarpine-treated EC. D: Comparison of the averages of the Cl^-; reversal point (NEC: −72.3 ± 3.8 mV, n = 7; pilocarpine: −69.8 ± 5.2 mV, n = 13; P = 0.27; independent t-test) and Cl^- conductance (NEC: 10.3 ± 4.1 nS; pilocarpine: 12.8 ± 8.6 nS; P = 0.89; independent t-test).

When the subiculum was separated in proximal and distal areas according to Witter (1993) (see also Fig. 1B), patches of increased immunoreactivity were more evident in the distal areas that are known to be innervated by the medial EC (Naber et al., 2001); this was also the EC region in which we could identify patches of increased synaptophysin immunoreactivity localized in the superficial layers (Fig. 11B).

Semiquantitative evaluation of optical density values in NEC and pilocarpine-treated rats is shown in Figure 11C for both subiculum and EC. Significantly ($P < 0.01$) higher staining intensity was found in proximal and distal subiculum as well as in medial and lateral EC ($P < 0.05$) of pilocarpine-treated rats when compared to NECs (Fig. 11C). Therefore, these findings demonstrate a general increase of synaptophysin immunostaining in the subiculum and EC of pilocarpine-treated, epileptic rats.

DISCUSSION

Our study demonstrates that the subiculum of pilocarpine-treated, epileptic rats is hyperexcitable at the network level as indicated by its increased responsiveness to CA1 and lateral EC layer III stimulation along with an increased frequency of spontaneous PSPs. We have also found that a mechanism contributing to sub-

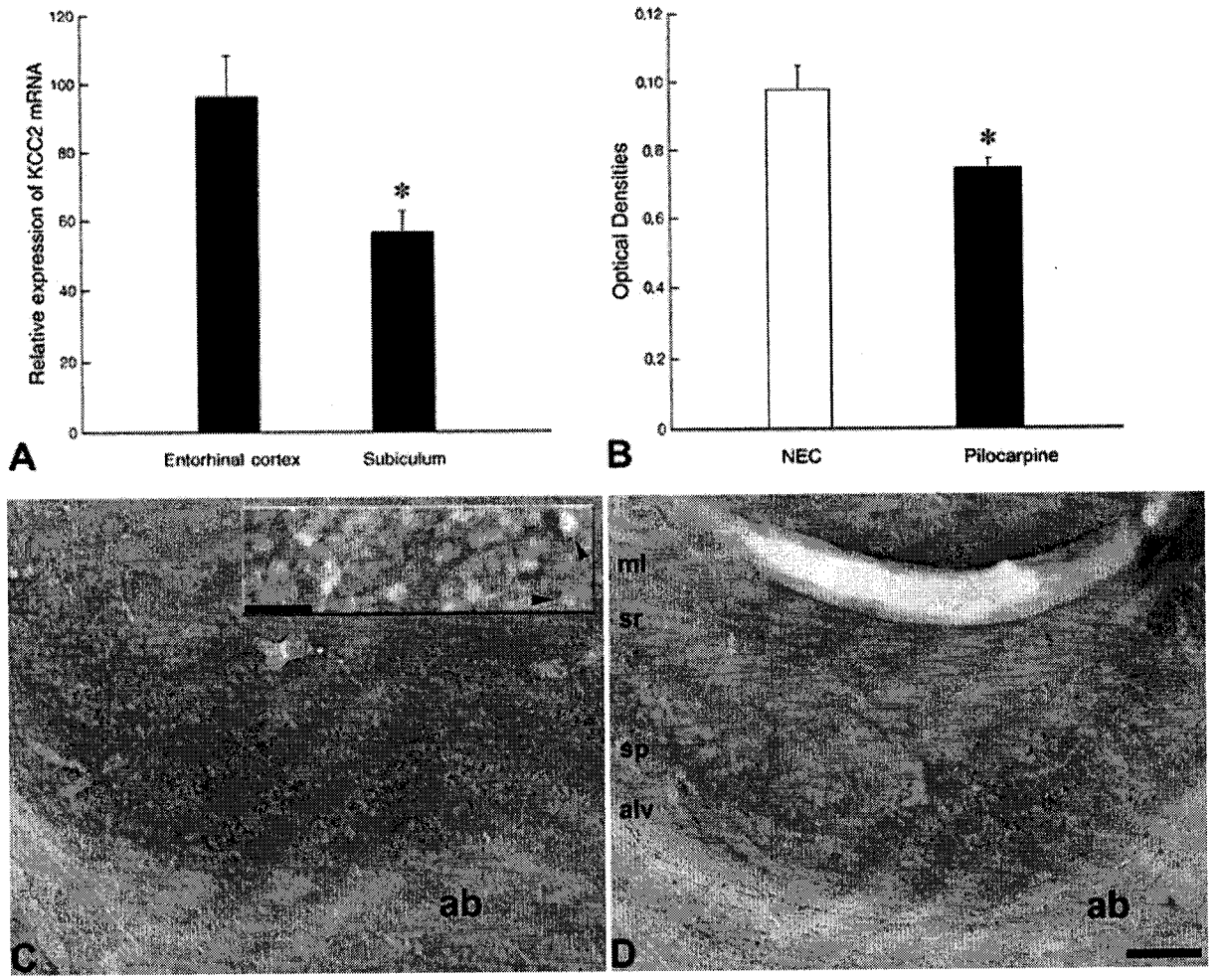

FIGURE 9. KCC2 expression in pilocarpine-treated and NEC rats. In A: KCC2 mRNA levels in pilocarpine-treated EC and subiculum (n = 5), expressed as percentage of NEC (n = 5) values. In B: KCC2 immunoreactivity in the subiculum of NEC (n = 8) and epileptic rats (n = 9). *P < 0.05 vs. control values, Mann–Whitney test. C and D: Distribution of KCC2 immunoreactivity in the subiculum of NEC and pilocarpine-treated rats, respectively. Note the wide distribution of KCC2 in the gray matter, while the angular bundle (ab) is scarcely stained. As shown in the inset (C), immunoreactivity is visible in nerve fibers and on the surface of neuronal somas, while the cytoplasm is unstained (arrowheads). Abbreviations used: alv, alveus; ml, molecular layer; sp, pyramidal layer; sr, stratum radiatum. The asterisk indicates the presubiculum. Scale bar, 150 μm for C and D, 50 μm for the inset.

icular hyperexcitability corresponds to a dysfunction of $GABA_A$ receptor-mediated inhibition characterized by positive shift in IPSP reversal potentials coupled with a decreased IPSP peak conductance. Moreover, these functional perturbations in GABAergic activity were presumably caused by a reduction in KCC2 expression along with a decreased number of parvalbumin-positive interneurons. Finally, we have found enhanced synaptophysin immunoreactivity in both subiculum and EC of epileptic animals.

Network Hyperexcitability in the Epileptic Subiculum

Subicular neurons recorded intracellularly from epileptic tissue generate bursts or doublets of action potentials in response to stimuli delivered in the CA1 stratum radiatum; in contrast, such procedure consistently disclosed a single action potential, followed by a hyperpolarization in NEC subicular cells. Moreover, input–output curves of the stimulus-induced responses identified a lower activation threshold in the epileptic subicular network. This evidence is in line with recent studies that have documented subicular hyperexcitability in epileptic tissue during electrical stimulation or $GABA_A$ receptor antagonism (Knopp et al., 2005). However, in contrast to the results by Knopp et al. (2005), we did not observe any synaptic bursting in NEC subiculum; this difference may have been dependent upon their adopted stimulus intensity.

We further demonstrated that the altered subicular responsiveness was not limited to activation from CA1, but also involved inputs arising from the lateral EC layer III. Our study as well as previous investigations have shown that synaptic inhibition is prevalent

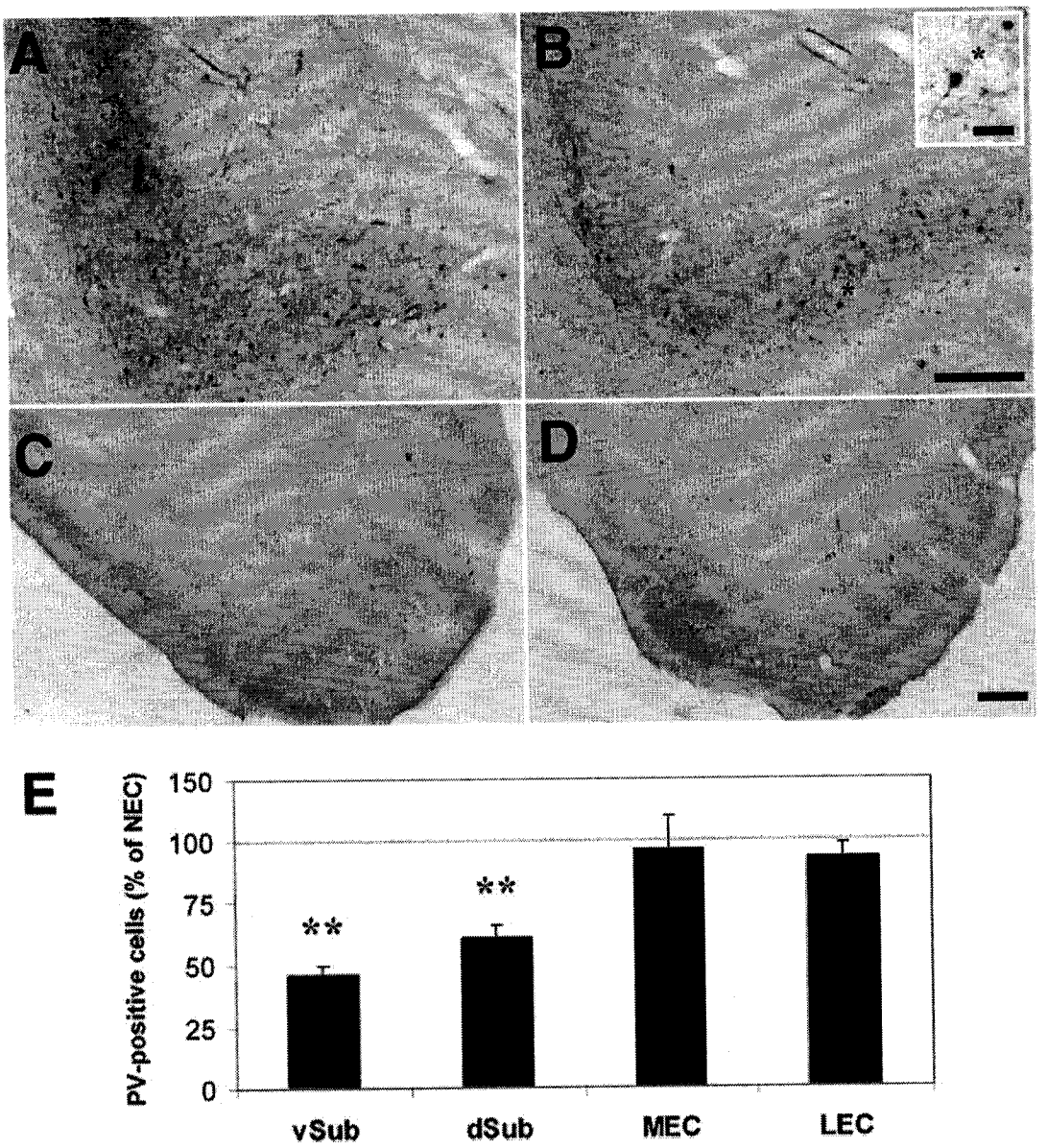

FIGURE 10. Parvalbumin immunoreactivity in the subiculum and EC of age-matched NEC and pilocarpine-treated rats. A and B: Immunohistochemical staining in the ventral subiculum (7.6 mm from bregma) reveals a reduced number of paravalbumin-positive inhibitory interneurons in pilocarpine-treated rats (B). The inset in B magnifies a parvalbumin-positive interneuron. C and D: distribution of parvalbumin-positive cells in the EC of NEC (C) and epileptic rats (D). E: quantitative analysis reveals a significant reduction ($P < 0.01$, Mann–Whitney test) of inhibitory interneurons in the epileptic subiculum vs. NEC (saline-treated) both at ventral and dorsal (3.6 mm from bregma) levels. In contrast, parvalbumin cell number was unaltered in the superficial layers of the lateral and medial EC. Scale bar: 250 μm.

within the NEC subiculum following EC stimulation (Maccaferri and McBain, 1995; Behr et al., 1998). In contrast, subicular activation by EC inputs in pilocarpine tissue revealed increased network excitation as indicated by the enhanced duration of the response that was characterized by multiphasic PSPs. In addition, hyperpolarizing synaptic potentials could not be recorded in pilocarpine tissue, as opposed to the NEC, thus further suggesting a perturbation in inhibitory and excitatory properties of the epileptic subiculum. Interestingly, this EC-subiculum network interaction correlates with the data obtained by studying epileptiform synchronization induced by 4-aminopyridine in pilocarpine-treated, epileptic mice (D'Antuono et al., 2002). While we observed increased network hyperexcitability in the epileptic subiculum, we did not detect a correlation with the intrinsic properties of subicular neurons.

A characteristic that was also indicative of network hyperexcitability within the epileptic subiculum was the higher fre-

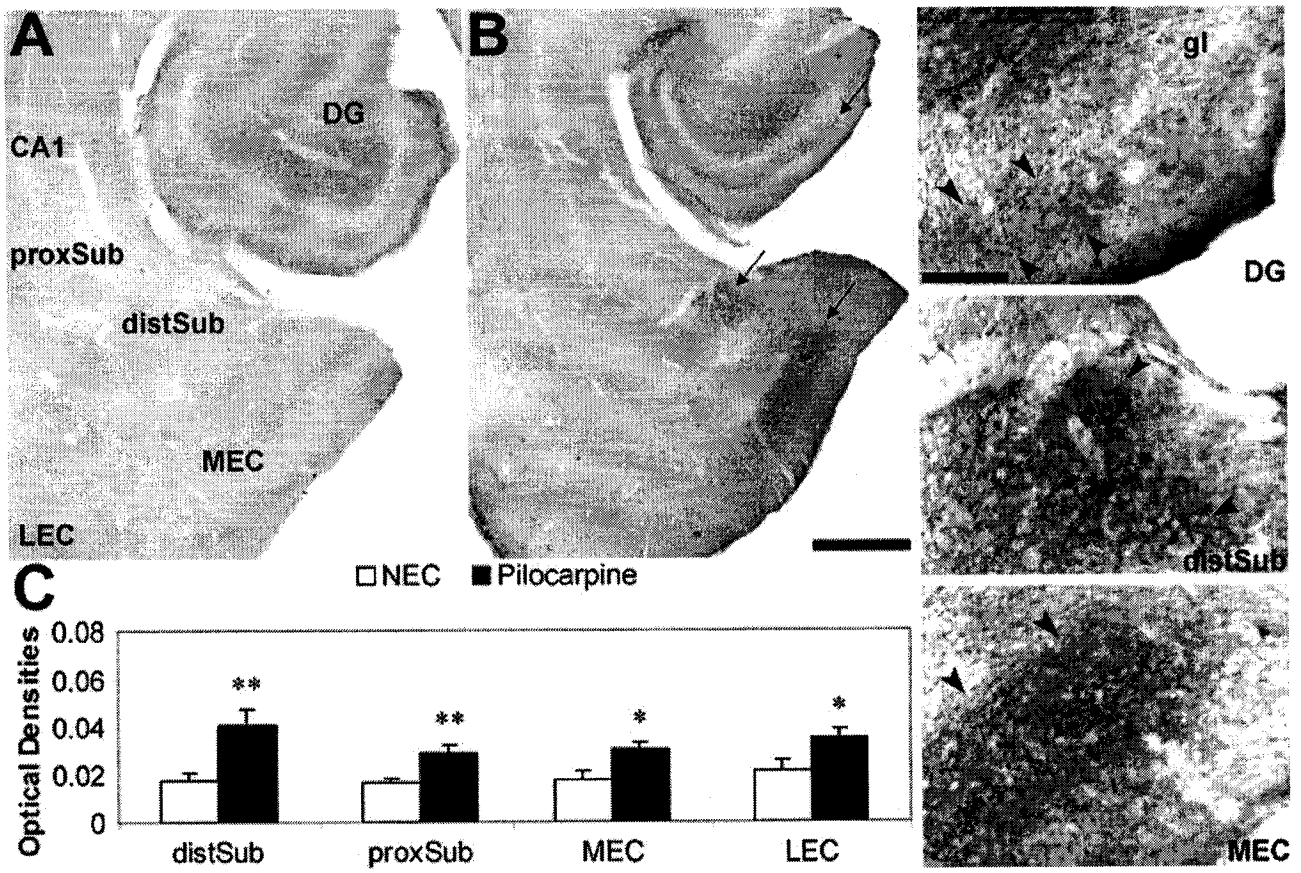

FIGURE 11. Changes in synaptophysin immunoreactive levels in NEC (A) and pilocarpine-treated epileptic rats (B). The arrows point to patches of highly dense synaptophysin immunoreactivity, respectively magnified in the insets on the right side (arrowheads), in the molecular layer of DG, the distal subiculum (distSub), and in the superficial layers of the medial EC (MEC). In panel C, densitometric analysis of synaptophysin immunoreactivity demonstrates higher levels in the subiculum and EC of pilocarpine-treated epileptic rats (see Fig. 1 for indications on the sampling procedure). Other abbreviations: CA1, cornu Ammonis 1; gl, granule layer; proxSub, proximal subiculum. * = $P < 0.05$, ** = $P < 0.01$, Mann–Whitney test. Scale bars, 500 μm for A and B, 100 mm for the insets.

quency of spontaneous PSPs when compared to NEC subicular cells. Previous in vitro studies in tissue obtained from epileptic patients (Cohen et al., 2002; Wozny et al., 2003) as well as kainic acid (Shah et al., 2005) or pilocarpine-treated rats (Sanabria et al., 2001; Kobayashi et al., 2003; Knopp et al., 2005) have shown the presence of network-driven phenomena.

Reduced GABAergic Inhibition Within the Pilocarpine-Treated Subiculum

We also discovered that the reversal potential of the spontaneous PSPs recorded in epileptic tissue was characterized by a positive shift suggesting decreased network inhibition. This aspect was further investigated by establishing the reversal potential of the stimulus-induced IPSPs generated by NEC and pilocarpine-treated epileptic subicular cells in the presence of glutamatergic antagonists. We found that the reversal potential of the $GABA_A$ receptor component of this IPSP was more positive in pilocarpine-treated neurons than in NEC cells. Such a decrease in reversal potential may account for attenuated inhibition and thus for the synaptic hyperexcitability documented following CA1 or EC stimulation. These data are also in keeping with the presence of depolarizing GABAergic events in the subiculum of human epileptic tissue (Cohen et al., 2002; Wozny et al., 2003).

Our results of a more positive fast IPSP reversal point can be attributed to an accumulation of intracellular Cl^- resulting from a reduced expression of the KCC2. Under normal physiological conditions, the classical hyperpolarzing GABAergic response relies upon a low intracellular Cl^- concentration due to Cl^- extrusion by KCC2. This mechanism, however, can become altered in conditions of network hyperexcitability. Accordingly, recent investigations have shown that KCC2 in the hippocampus is downregulated after kindling-induced seizures in vivo or by exogenous applications of BDNF or neurotrophin 4 in vitro (Rivera et al., 2002). In addition, Rivera et al. (2004) have reported that interictal epileptiform activity in hippocampal slices down-regulates KCC2 mRNA and protein expression in CA1 pyramidal neurons. Indeed, by utilizing RT-PCR and immunohistochemical analysis we found a significant reduction in KCC2 mRNA and protein expression in the pilocarpine-treated subicu-

lum vs. NEC. As such, the more depolarized $GABA_A$ receptor induced IPSP reversal potential identified in pilocarpine-treated neurons is most likely caused by a reduction in KCC2 expression and the functional consequence of increased intracellular Cl^-. Hence, our data reinforce the evidence that a reduction in KCC2 expression may contribute to epileptic hyperexcitability.

Pharmacologically isolated IPSPs generated by pilocarpine-treated epileptic subicular cells are also characterized by a decreased peak conductance when compared with similar events in NEC tissue. This change, which is expected to decrease the IPSP shunting action, may relate to decreased number of interneurons (see below), as well as to alterations in $GABA_A$ receptor subunits (Friedman et al., 1994; Houser and Escalpez, 2003; Olsen et al., 2004). These factors may also contribute toward reduced subicular network inhibition coupled with an augmented excitatory drive.

Structural Changes in Subicular and EC Networks

The perturbations of network inhibition observed in the subiculum of pilocarpine-treated rats also appear to be contributed by a decrease of interneurons along with synaptic reorganization. First, we have found that parvalbumin-positive cells, which represent about 50% of interneurons in the rodent cortex (Kawaguchi and Kubota, 1993; Kubota et al., 1994) are markedly decreased in ventral and dorsal subiculum but not in EC. Similar findings have been reported in different TLE animal models (Du et al., 1995; van Vliet et al., 2004). A reduction in the number of parvalbumin-positive interneurons has been also found in the CA1 subfield (André et al., 2001) and in the dentate hilus (Gorter et al., 2001) of epileptic animals, which correlated with the development of spontaneous seizures following SE. Interestingly, parvalbumin-positive cells are also decreased in the neocortex (de Felipe et al., 1993) and hippocampus (Arellano et al., 2004) of epileptic patients presenting with intractable seizures. It should be, however, mentioned that these studies failed in disclosing significant differences in parvalbumin-positive cells in the human epileptic subiculum, suggesting a possible inconsistency with the animal model. Alternatively, the decrease of parvalbumin-labeled interneurons may result from reduced expression of this calcium binding protein following repeated seizures (Sloviter et al., 1991; Vizi et al., 2004), thus depending on the frequency by which a certain neuronal area is recruited by seizures.

Subiculum hyperexcitability may also be contributed by neuronal sprouting, as recently evidenced by tracing studies in rats made epileptic with different procedures (Cavazos et al., 2004). Mossy fiber sprouting has been described in the DG and CA3 subfield of TLE patients (Sutula et al., 1989; Houser et al., 1990; Houser, 1999; Proper et al., 2000) and epileptic rats (Ben-Ari, 1985; Sutula et al., 1988; Gorter et al., 2001). We have investigated the possibility that neuronal sprouting took place in our rats by means of synaptophysin immunostaining. Synaptophysin is a synaptic vesicle-associated protein (Bahler et al., 1991) known to be upregulated by neuronal activity (Li et al., 2002; Valtorta et al., 2004) and lesion (Kadish and van Groen, 2003). Although it is not a classical marker of sprouting, changes in synaptophysin immunoreactivity have been taken as indirect index of increased nerve terminal density or activity in epileptic patients (Proper et al., 2000) as well as in animals (Chen et al., 1996; Li et al., 2002). Here, we have identified an increase in synaptophysin immunostaining in several limbic areas, possibly suggesting neuronal sprouting in pilocarpine-treated rats as reported in the kainic acid model (Chen et al., 1996), or indicating increased synaptic vesicle density. These changes appeared to be more evident in distal subiculum and medial EC, that are reciprocally interconnected (Naber et al., 2001). Increased synaptophysin immunoreactivity was also found in the hippocampus of pharmacoresistant TLE patients (Proper et al., 2000). Sprouting in the EC superficial layers has been reported to occur in human TLE tissue by analyzing the immunoreactivity of the highly polysialylated neural cell adhesion molecule (Mikkonen et al., 1998).

In conclusion, our findings highlight a change in subicular neuron excitability in epileptic rats that depends on multiple mechanisms. At the molecular level, KCC2 expression is downregulated, thus varying the neuronal response to GABAergic inputs. At the cellular level, parvalbumin interneurons are highly decreased, possibly hampering the control of neuronal excitability, while the upregulation of synaptophysin immunostaining, as also found in the DG and EC, favors the hypothesis of increased network coupling in the epileptic subiculum. This evidence along with findings from other laboratories (Cohen et al., 2002; Cavazos et al., 2004; Knopp et al., 2005) indicate in the subiculum a key region in the control of epileptic activity.

Acknowledgments

We thank Dr. M. D'Antuono for participating in the KCC2 experiments and Ms. T. Papadopoulos for secretarial assistance.

REFERENCES

Arellano JI, Munoz A, Ballesteros-Yanez I, Sola RG, DeFelipe J. 2004. Histopathology and reorganization of chandelier cells in the human epileptic sclerotic hippocampus. Brain 127:45–64.

Bahler M, Klein RL, Wang JK, Benfenati F, Greengard P. 1991. A novel synaptic vesicle-associated phosphoprotein: SVAPP-120. J Neurochem 57:423–430.

Behr J, Gloveli T, Heinemann U. 1998. The perforant path projection from the medial entorhinal cortex layer III to the subiculum in the rat combined hippocampal-entorhinal cortex slice. Eur J Neurosci 10:1011–1018.

Ben-Ari Y. 1985. Limbic seizure and brain damage produced by kainic acid: Mechanisms and relevance to human temporal lobe epilepsy. Neuroscience 14:375–403.

Biagini G, Babinski K, Avoli M, Marcinkiewicz M, Seguela P. 2001. Regional and subunit-specific downregulation of acid-sensing ion channels in the pilocarpine model of epilepsy. Neurobiol Dis 8:45–58.

Biagini G, D'Arcangelo G, Baldelli E, D'Antuono M, Tancredi V, Avoli M. 2005. Impaired activation of CA3 pyramidal neurons in the epileptic hippocampus. Neuromol Med 7:325–342.

Bragin A, Wilson CL, Staba RJ, Reddick M, Fried I, Engel J Jr. 2002. Interictal high-frequency oscillations (80–500 Hz) in the human epileptic brain: Entorhinal cortex. Ann Neurol 52:407–415.

Buhl EH, Otis TS, Mody I. 1996. Zinc-induced collapse of augmented inhibition by GABA in a temporal lobe epilepsy model. Science 271:369–373.

Cavalheiro EA, Leite JP, Bortolotto ZA, Turski WA, Ikonomidou C, Turski L. 1991. Long-term effects of pilocarpine in rats: Structural damage of the brain triggers kindling and spontaneous recurrent seizures. Epilepsia 32:778–782.

Cavazos JE, Jones SM, Cross DJ. 2004. Sprouting and synaptic reorganization in the subiculum and CA1 region of the hippocampus in acute and chronic models of partial-onset epilepsy. Neuroscience 126:677–688.

Chen LS, Wong JG, Banerjee PK, Snead OC. 1996. Kainic acid-induced focal cortical seizure is associated with an increase of synaptophysin immunoreactivity in the cortex. Exp Neurol 141:25–31.

Cohen I, Navarro V, Clemenceau S, Baulac M, Miles R. 2002. On the origin of interictal activity in human temporal lobe epilepsy in vitro. Science 298:1418–1421.

D'Antuono M, Benini R, Biagini G, D'Arcangelo G, Barbarosie M, Tancredi V, Avoli M. 2002. Limbic network interactions leading to hyperexcitability in a model of temporal lobe epilepsy. J Neurophysiol 87:634–639.

de Curtis M, Pare D. 2004. The rhinal cortices: A wall of inhibition between the neocortex and the hippocampus. Prog Neurobiol 74: 101–110.

de Felipe J, Garcia Sola R, Marco P, del Rio MR, Pulido P, Ramon y Cajal S. 1993. Selective changes in the microorganization of the human epileptogenic neocortex revealed by parvalbumin immunoreactivity. Cereb Cortex 3:39–48.

Doherty J, Dingledine R. 2001. Reduced excitatory drive onto interneurons in the dentate gyrus after status epilepticus. J Neurosci 21: 2048–2057.

Du F, Eid T, Lothman EW, Kohler C, Schwarcz R. 1995. Preferential neuronal loss in layer III of the medial entorhinal cortex in rat models of temporal lobe epilepsy. J Neurosci 15:6301–6313.

Friedman LK, Pellegrini-Giampietro DE, Sperber EF, Bennett MV, Moshe SL, Zukin RS. 1994. Kainate-induced status epilepticus alters glutamate and GABAA receptor gene expression in adult rat hippocampus: An in situ hybridization study. J Neurosci 14:2697–2707.

Gorter JA, van Vliet EA, Aronica E, Lopes da Silva FH. 2001. Progression of spontaneous seizures after status epilepticus is associated with mossy fibre sprouting and extensive bilateral loss of hilar parvalbumin and somatostatin-immunoreactive neurons. Eur J Neurosci 13:657–669.

Grob M, Mouginot D. 2005. Heterogeneous chloride homeostasis and GABA responses in the median preoptic nucleus of the rat. J Physiol 569:885–901.

Houser CR. 1999. Neuronal loss and synaptic reorganization in temporal lobe epilepsy. In: Delgado-Escuetta AV, Wilson WA, Olsen RW, Porter RJ, editors. Jasper's Basic Mechanisms of the Epilepsies, 3rd ed (Advances in Neurology, Vol 79). Philadelphia Lippincott Williams & Wilkins:.

Houser CR, Esclapez M. 2003. Downregulation of the α5 subunit of the GABA(A) receptor in the pilocarpine model of temporal lobe epilepsy. Hippocampus 13:633–645.

Houser CR, Miyashiro JE, Swartz BE, Walsh GO, Rich JR, Delgado-Escueta AV. 1990. Altered patterns of dynorphin immunoreactivity suggest mossy fiber reorganization in human hippocampal epilepsy. J Neurosci 10:267–282.

Kadish I, Van Groen T. 2003. Differences in lesion-induced hippocampal plasticity between mice and rats. Neuroscience 116:499–509.

Kawaguchi Y, Kubota Y. 1993. Correlation of physiological subgroupings of nonpyramidal cells with parvalbumin- and calbindin D28k-immunoreactive neurons in layer V of rat frontal cortex. J Neurophysiol 70:387–396.

Khalilov I, Holmes GL, Ben-Ari Y. 2003. In vitro formation of a secondary epileptogenic mirror focus by interhippocampal propagation of seizures. Nat Neurosci 6:1079–1085.

Knopp A, Kivi A, Wozny C, Heinemann U, Behr J. 2005. Cellular and network properties of the subiculum in the pilocarpine model of temporal lobe epilepsy. J Comp Neurol 483:476–488.

Kobayashi M, Wen X, Buckmaster PS. 2003. Reduced inhibition and increased output of layer II neurons in the medial entorhinal cortex in a model of temporal lobe epilepsy J Neurosci 23:8471–8479.

Kubota Y, Hattori R, Yui Y. 1994. Three distinct subpopulations of GABAergic neurons in rat frontal agranular cortex. Brain Res 649: 159–173.

Li S, Reinprecht I, Fahnestock M, Racine RJ. 2002. Activity-dependent changes in synaptophysin immunoreactivity in hippocampus, piriform cortex, and entorhinal cortex of the rat. Neuroscience 115: 1221–1229.

Lohrke S, Srinivasan G, Oberhofer M, Doncheva E, Friauf E. 2005. Shift from depolarizing to hyperpolarizing glycine action occurs at different perinatal ages in superior olivary complex nuclei. Eur J Neurosci 22:2708–2722.

Maccaferri G, McBain CJ. 1995. Passive propagation of LTD to stratum oriens-alveus inhibitory neurons modulates the temporoammonic input to the hippocampal CA1 region. Neuron 15:137–145.

Mathern GW, Pretorius JK, Babb TL. 1995. Quantified patterns of mossy fiber sprouting and neuron densities in hippocampal and lesional seizures. J Neurosurg 82:211–219.

Mattia D, Kawasaki H, Avoli M. 1997. In vitro electrophysiology of rat subicular bursting neurons Hippocampus 7:48–57.

Mikkonen M, Soininen H, Kalvianen R, Tapiola T, Ylinen A, Vapalahti M, Paljarvi L, Pitkanen A. 1998. Remodeling of neuronal circuitries in human temporal lobe epilepsy: Increased expression of highly polysialylated neural cell adhesion molecule in the hippocampus and the entorhinal cortex. Ann Neurol 44:923–934.

Naber PA, Lopes da Silva FH, Witter MP. 2001. Reciprocal connections between the entorhinal cortex and hippocampal fields CA1 and the subiculum are in register with the projections from CA1 to the subiculum. Hippocampus 11:99–104.

Nissinen J, Halonen T, Koivisto E, Pitkanen A. 2000. A new model of chronic temporal lobe epilepsy induced by electrical stimulation of the amygdala in rat. Epilepsy Res 38:177–205.

Olsen RW, Chang CS, Li G, Hanchar HJ, Wallner M. 2004. Fishing for allosteric sites on GABA(A) receptors. Biochem Pharmacol 68: 1675–1684.

Perez Y, Morin F, Beaulieu C, Lacaille JC. 1996. Axonal sprouting of CA1 pyramidal cells in hyperexcitable hippocampal slices of kainate-treated rats. Eur J Neurosci 8:736–748.

Priel MR, dos Santos NF, Cavalheiro EA. 1996. Developmental aspects of the pilocarpine model of epilepsy. Epilepsy Res 26:115–121.

Proper EA, Oestreicher AB, Jansen GH, Veelen CW, van Rijen PC, Gispen WH, de Graan PN. 2000. Immunohistochemical characterization of mossy fibre sprouting in the hippocampus of patients with pharmacoresistant temporal lobe epilepsy. Brain 123:19–30.

Racine RJ. 1972. Modification of seizure activity by electrical stimulation. II. Motor seizure. Electroencephalogr Clin Neurophysiol 32: 281–294.

Rivera C, Li H, Thomas-Crusells J, Lahtinen H, Viitanen T, Nanobashvili A, Kokaia Z, Airaksinen MS, Voipio J, Kaila K, Saarma M. 2002. BDNF-induced TrkB activation down-regulates the K^+-Cl^- cotransporter KCC2 and impairs neuronal Cl^- extrusion. J Cell Biol 159:747–752.

Rivera C, Voipio J, Thomas-Crusells J, Li H, Emri Z, Sipila S, Payne JA, Minichiello L, Saarma M, Kaila K. 2004. Mechanism of activity-dependent downregulation of the neuron-specific K-Cl cotransporter KCC2. J Neurosci 24:4683–4691.

Sanabria ER, Su H, Yaari Y. 2001. Initiation of network bursts by Ca^{2+}-dependent intrinsic bursting in the rat pilocarpine model of temporal lobe epilepsy. J Physiol 532:205–216.

Shah MM, Anderson AE, Leung V, Lin X, Johnston D. 2004. Seizure-induced plasticity of h channels in entorhinal cortical layer III pyramidal neurons. Neuron 44:495–508.

Sloviter RS. 1987. Decreased hippocampal inhibition and a selective loss of interneurons in experimental epilepsy. Science 235:73–76.

Sloviter RS, Sollas AL, Barbaro NM, Laxer KD. 1991. Calcium binding protein (calbindin-D28K) and parvalbumin immunocytochemistry in the normal and epileptic human hippocampus. J Comp Neurol 308:381–396.

Spencer SS, Spencer DD. 1994. Entorhinal-hippocampal interactions in medial temporal lobe epilepsy. Epilepsia 35:721–727.

Su H, Sochivko D, Becker A, Chen J, Jiang Y, Yaari Y, Beck H. 2002. Upregulation of a T-type Ca^{2+} channel causes a long-lasting modification of neuronal firing mode after status epilepticus. J Neurosci 22:3645–3655.

Sutula T, He XX, Cavazos J, Scott G. 1988. Synaptic reorganization in the hippocampus induced by abnormal functional activity. Science 239:1147–1150.

Sutula T, Cascino G, Cavazos J, Parada I, Ramirez L. 1989. Mossy fiber synaptic reorganization in the epileptic human temporal lobe. Ann Neurol 26:321–330.

Turski WA, Cavalheiro EA, Schwarz M, Czuczwar SJ, Kleinrok Z, Turski L. 1983. Limbic seizures produced by pilocarpine in rats: behavioral, electroencephalographic and neuropathological study. Behav. Brain Res 9:315–335.

Tuunanen J, Lukasiuk K, Halonen T, Pitkanen A. 1999. Status epilepticus-induced neuronal damage in the rat amygdaloid complex: distribution, time-course and mechanisms. Neuroscience 94:473–495.

Vale C, Schoorlemmer J, Sanes DH. 2003. Deafness disrupts chloride transporter function and inhibitory synaptic transmission. J Neurosci 23:7516–7524.

Vale C, Caminos E, Martinez-Galan JR, Juiz JM. 2005. Expression and developmental regulation of the K^+-Cl^- cotransporter KCC2 in the cochlear nucleus. Hear Res 206:107–115.

Valtorta F, Pennuto M, Bonanomi D, Benfenati F. 2004. Synaptophysin: Leading actor or walk-on role in synaptic vesicle exocytosis? Bioessays 26:445–453.

van Vliet EA, Aronica E, Tolner EA, Lopes da Silva FH, Gorter JA. 2003. Progression of temporal lobe epilepsy in the rat is associated with immunocytochemical changes in inhibitory interneurons in specific regions of the hippocampal formation. Exp Neurol 187:367–379.

Vizi S, Bagosi A, Krisztin-Peva B, Gulya K, Mihaly A. 2004. Repeated 4-aminopyridine seizures reduce parvalbumin content in the medial mammillary nucleus of the rat brain. Brain Res Mol Brain Res 131: 110–118.

Vreugdenhil M, Hoogland G, van Veelen CW, Wadman WJ. 2004. Persistent sodium current in subicular neurons isolated from patients with temporal lobe epilepsy. Eur J Neurosci 19:2769–2778.

Wellmer J, Su H, Beck H, Yaari Y. 2002. Long-lasting modification of intrinsic discharge properties in subicular neurons following status epilepticus. Eur J Neurosci 16:259–266.

Williams S, Vachon P, Lacaille JC. 1993. Monosynaptic GABA mediated inhibitory postsynaptic potentials in CA1 pyramidal of hyperexcitable hippocampal slices from kainic acid-treated rats. Neuroscience 52:541–554.

Williams JR, Sharp JW, Kumari VG, Wilson M, Payne JA. 1999. The neuron-specific K-Cl cotransporter, KCC2. Antibody development and initial characterization of the protein. J Biol Chem 274:12656–12664.

Witter MP. 1993. Organization of the entorhinal-hippocampal system: A review of current anatomical data. Hippocampus 3:33–44.

Wozny C, Kivi A, Lehmann TN, Dehnicke C, Heinemann U, Behr J. 2003. Comment on "On the origin of interictal activity in human temporal lobe epilepsy in vitro." Science 301:463.

APPENDIX B: Reprint of Chapter 3 and Waiver from the European Journal of Neuroscience

with internal bridge circuit for intracellular current injection. Resistance compensation was monitored throughout the experiment and adjusted as required. Electrophysiological recordings in IC were obtained from the agranular portion that was identified by using the perirhinal fissure at the level of the IC as a point of reference (Fig. 1A).

The IC cell passive membrane properties were measured as follows: (i) resting membrane potential (RMP) after cell withdrawal; (ii) apparent input resistance from the maximum voltage change in response to hyperpolarizing current pulses (< −0.5 nA); (iii) action potential amplitude from the baseline; and (iv) action potential duration at half-amplitude. The firing patterns of IC cells were established by injecting depolarizing current pulses. Extra- and intracellular signals were fed to a computer interface, acquired and stored using the pClamp 9 software and analysed with the Clampfit 9 software (both from Axon Instruments, Union City, CA, USA). Electrical stimuli (50–100 μs; < 200 μA) were delivered through bipolar, stainless steel electrodes. The recording and stimulating electrode location in the slice is shown in Fig. 1A. In some experiments the IC and PC were surgically isolated at the start of the experiment by a cut made under visual control with a razor blade (dotted line in Fig. 1A).

For intracellular labelling, electrodes were filled with 2% neurobiotin dissolved in 2 M K-acetate. Neurobiotin was applied by injecting depolarizing current pulses (0.5–1 nA, 3.3 Hz, 150 ms) for > 10 min. Only one cell was filled in each slice. At the end of the experiment, slices were processed as described by D'Antuono *et al.* (2001). Measurements are expressed as mean ± SEM, and *n* indicates the number of slices or neurons. Data were compared with the Student's *t*-test and were considered significant if $P < 0.05$.

Results

Neurons ($n = 27$) recorded in the IC at 400–1200 μm from the pia responded to intracellular depolarizing pulses by generating trains of action potentials with weak adaptation (Fig. 1, Ba), although a burst of two–three action potentials with intervals < 6 ms could occur at pulse onset (asterisk); these cells were therefore classified as regularly spiking (McCormick *et al.*, 1985). Neurobiotin-filled IC cells ($n = 14/27$) displayed pyramidal-like shape with a distinct apical dendrite directed towards the pia and extensive basal dendritic tree (Fig. 1, Bb). The fundamental electrophysiological properties of neurobiotin-filled and non-labelled cells were similar ($P > 0.21$), thus suggesting that the sampled neuronal populations exhibited comparable intrinsic physiological properties. By pooling the values obtained from labelled and unlabelled IC cells ($n = 27$), we found: (i) RMP = −74.2 ± 1.2 mV; (ii) apparent input resistance = 45.7 ± 2.5 MΩ; (iii) action potential amplitude = 94.6 ± 2.7 mV; and (iv) action potential duration = 1.7 ± 0.4 ms.

A striking characteristic of the brain slices analysed in this study was the presence of synchronous field discharges that occurred spontaneously in 22 of 52 slices (duration = 2.3 ± 0.25 s; intervals of occurrence = 44.9 ± 6.3 s) or following electrical stimuli delivered in PC (response duration = 1.3 ± 0.2 s, $n = 10$) or IC (duration = 1.4 ± 0.1 s, $n = 15$) in all experiments (Fig. 1C). Spontaneous events (duration = 1.7 ± 0.2 s; intervals of occurrence = 84.1 ± 10.9 s; $n = 6$) were still present in IC after surgical cut from PC (not shown). Spontaneous and stimulus-induced events corresponded in IC cells to sustained intracellular depolarizations leading to repetitive action potential discharges (Fig. 1C). Hyperpolarizing or depolarizing the neuron with steady current injection increased or decreased, respectively, the amplitude of these depolarizations (Figs 1C and 2A), thus suggesting that they were contributed by synaptic conductances. Moreover, bringing the membrane to depolarized levels disclosed hyperpolarizing potentials during the initial part of the response (Fig. 2A, arrows in −60 mV panel), while long-lasting (up to 4 s) hyperpolarizations terminated the intracellular events (Figs 1C and 2A, asterisks). The rate of occurrence of the spontaneous events was not influenced by changing the RMP (not shown), further indicating that this activity was network driven.

To determine the mechanisms underlying the occurrence of network discharges in the IC, we assessed the effects of the NMDA receptor antagonist CPP. As shown in Fig. 2B, CPP abolished the spontaneous activity in five experiments, while reducing the duration of the stimulus-induced events. This latter aspect was analysed in six additional slices that did not generate any spontaneous activity. Overall, the duration of the stimulus-induced responses was reduced by CPP to 18.3 ± 3.7% of that seen in control ($n = 7$), while only a depolarizing–hyperpolarizing potential sequence was observed in the remaining experiments ($n = 6$; Fig. 3A, +CPP). In addition, by changing the RMP we found that the polarity of the stimulus-induced intracellular response measured at a latency of about 50 ms inverted in polarity at −64.3 ± 2.9 mV ($n = 8$; Fig. 3, Bc), suggesting the participation of γ-aminobutyric acid $(GABA)_A$ receptor-mediated conductances (CPP + CGP 55845; Fig. 3, Ba).

To test this hypothesis, we bath-applied PHB, a drug that is known to enhance $GABA_A$ receptor-mediated mechanisms (Barker & McBurney, 1979; Twyman *et al.*, 1989). As illustrated in Fig. 3B, PHB produced a more negative reversal potential (from −64.5 ± 6.4 mV to −69.4 ± 4.2 mV, $n = 3$) of the response induced by PC stimuli, but also decreased synaptic responsiveness, presumably via an interaction with excitatory glutamatergic processes. Therefore, to firmly establish the presence of $GABA_A$ receptor-mediated activity within the IC network we used focal stimuli during bath application of glutamatergic (CPP + CNQX) and $GABA_B$ (CGP 55845) receptor antagonists. Under these conditions, stimuli delivered close (< 150 μm) to the recorded cell induced at RMP a short-lasting depolarization inverting in polarity at −71.6 ± 1.3 mV ($n = 8$; Fig. 3C). Moreover, further application of PHB caused a significant negative shift in its reversal potential (from −69.3 ± 0.6 to −78.9 ± 2.2; $n = 3$; $P < 0.05$) along with a prolongation of the response (Fig. 3C). Finally, we found that bath application of the $GABA_A$ receptor antagonist picrotoxin (50 μM; $n = 3$) abolished the synaptic response induced by close electrical stimuli during application of glutamatergic and $GABA_B$ receptor antagonists (not shown).

FIG. 1. (A) Drawing of the brain slice preparation used in this study, showing the position of recording and stimulating electrodes. Note that the agranular insular cortex (IC, arrow) was identified by taking the perirhinal fissure (asterisk) as point of reference. The dotted line highlights the location of the cut used to isolate the IC from the perirhinal cortex (PC). (B) Responses to the injection of pulses of hyperpolarizing (−0.6 and −0.2 nA) and depolarizing (0.2 nA) intracellular current (a) generated by an IC cell that was filled with neurobiotin (b); note that this cell generates rhythmic action potential firing while the asterisk identifies the first two action potentials that occurred at intervals < 6 ms. (C) Spontaneous and stimulus-induced activity recorded in the IC with intracellular and field potential recordings. The RMP of this neuron was −72 mV, while stimulation was delivered in the PC. Note that hyperpolarization of the neuronal membrane, through negative current injection, increases the amplitude of the depolarizing envelope and also terminates the intracellular discharge (asterisk) in the −72 mV sample. In this and following figures focal electrical stimuli are identified with triangles.

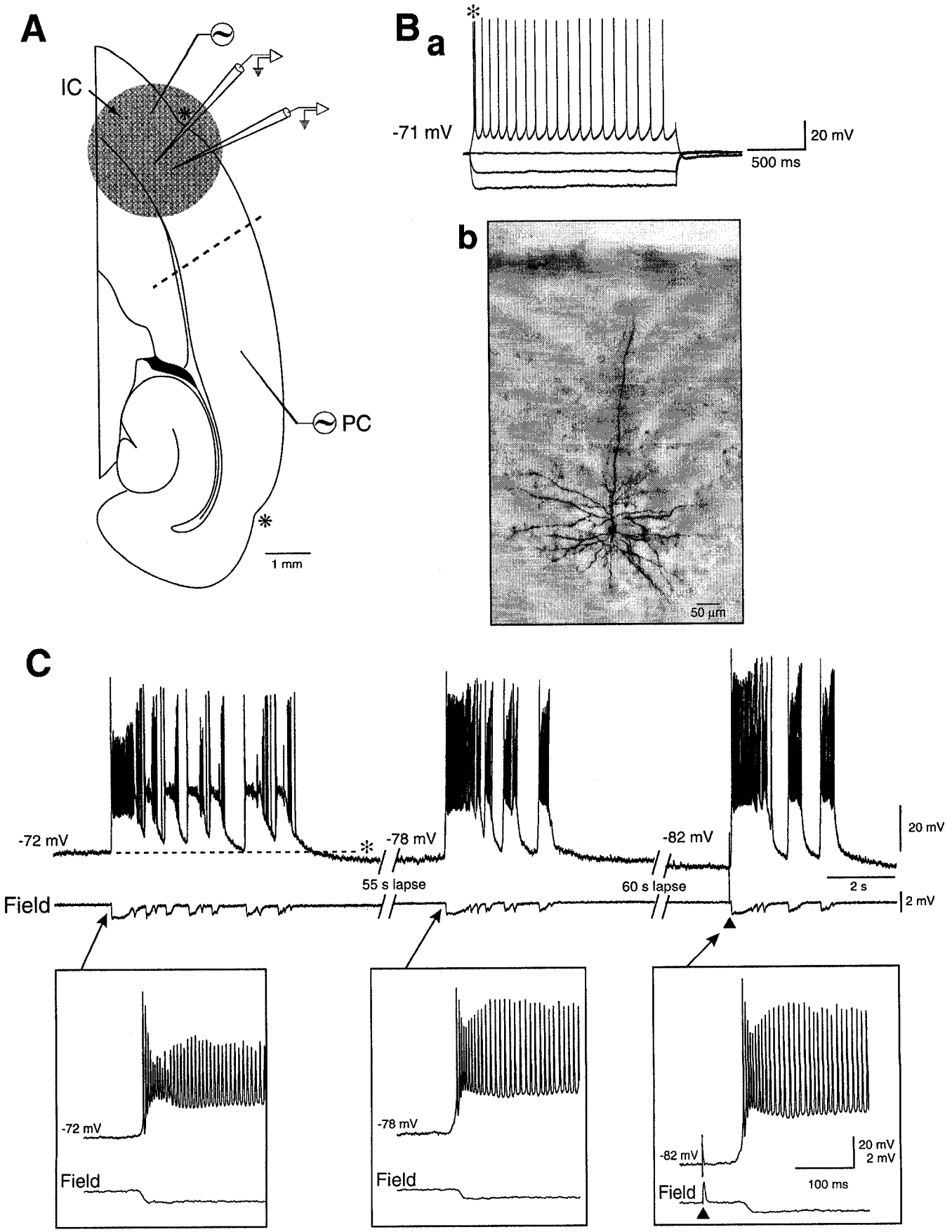

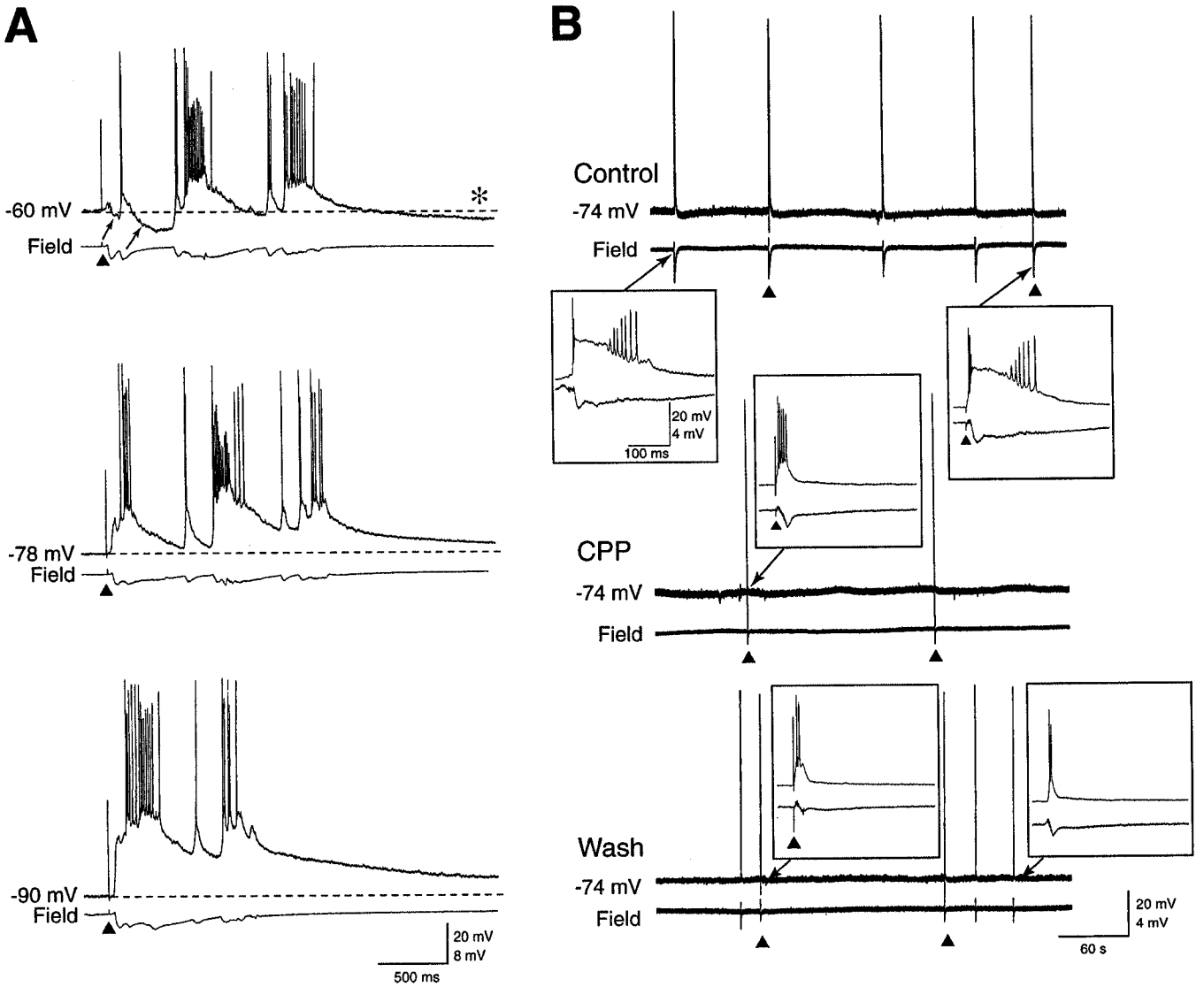

FIG. 2. (A) Field and intracellular characteristics of the responses recorded in the IC following single-shock stimuli delivered in the PC at RMP (−78 mV) and during injection of depolarizing (−60 mV) and hyperpolarizing (−90 mV) steady current. Note that hyperpolarizing or depolarizing the neuron with steady current injection increases or decreases, respectively, the amplitude of the stimulus-induced depolarizations. Note also in the −60 mV panel that depolarizing the neuron discloses hyperpolarizing potentials during the initial part of the intracellular response (arrows) as well as a slow post-discharge hyperpolarization (asterisk). (B) Effects induced by the NMDA receptor antagonist 3,3-(2-carboxypiperazin-4-yl)-propyl-1-phosphonate (CPP) on the spontaneous and stimulus-induced discharges recorded in the IC. Stimuli were delivered in the IC. Note that CPP reversibly abolishes the spontaneous activity and reduces the duration of the stimulus-induced discharge.

Discussion

We have found here that the rat agranular IC analysed with field potential and intracellular recordings in an *in vitro* slice preparation generates spontaneous or stimulus-induced synchronous events that are: (i) associated with synaptic depolarizations leading to sustained action potential firing; (ii) supported by NMDA receptor-mediated mechanisms; and (iii) accompanied by the activation of $GABA_A$ receptor-mediated, inhibitory conductances. These characteristics

FIG. 3. Stimulus-induced responses recorded in control ACSF and following bath application of NMDA and non-NMDA glutamatergic receptor antagonists. (A) 3,3-(2-carboxypiperazin-4-yl)-Propyl-1-phosphonate (CPP) blocks the stimulus-induced discharge, thus revealing a depolarizing postsynaptic response with latency similar to that seen under control. (B) Effects induced by changing the membrane potential (V_m) with current injection on the polarity of the synaptic responses induced by PC stimulation during CPP + (3-aminopropyl)(diethoxymethyl)phosphinic acid (CGP 55845) (Control) and CPP + CGP 55845 + phenobarbital (PHB). Raw data are shown in (a); note in (b) that the reversal points obtained by measuring the response amplitude (calculated at ~55 ms after the stimulus) were −64 mV (CPP + CGP 55845) and −70 mV (CPP + CGP 35348 + PHB). (C) Responses induced by focal IC stimulation during application of medium containing CPP + 6-cyano-7-nitroquinoxaline-2,3-dione (CNQX) + CGP 55845 (Control) and CPP + CNQX + CGP 55845 + PHB. Raw data are illustrated in (a), while in (b) normalized intracellular traces obtained under both conditions are superimposed; note that PHB (red traces) causes an increase in response duration. A plot of the amplitude of the stimulus-induced responses recorded at different membrane potentials (V_m) is shown in (c). Note that reversal points of −68 mV and −78 mV occur during control and PHB conditions, respectively. The amplitude of response was assessed at 17 ms after stimulus artefact.

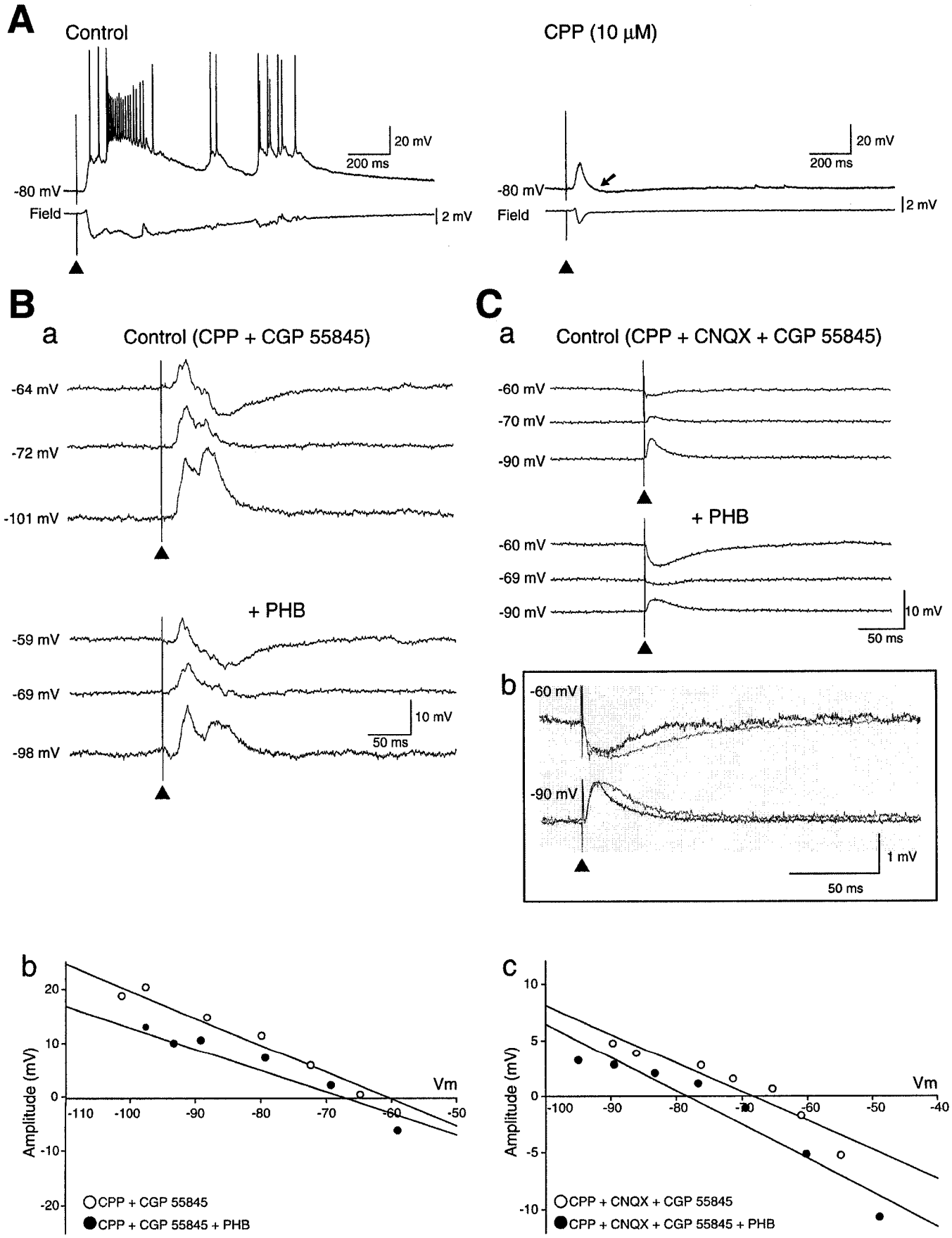

suggest that the agranular IC is 'hyperexcitable' as compared with limbic or neocortical networks maintained *in vitro* in normal ACSF, as cells in these structures rarely generate spontaneous activity and respond to stimuli with excitatory postsynaptic potentials–single action potentials (Jones & Lambert, 1990; Schwartzkroin, 1975; Connors *et al.*, 1982; Martina *et al.*, 2001). We have also established that the IC cells recorded intracellularly were regularly firing and pyramidal in shape when labelled with neurobiotin.

NMDA receptors play a unique role in the occurrence of spontaneous and stimulus-induced discharges in the IC. Indeed, at the best of our knowledge, these data are the first to identify an essential role for NMDA receptors in the generation of spontaneous network activity in brain slices bathed in normal ACSF. This evidence may imply that Mg^{2+} exerts a reduced control on NMDA receptor channels in the agranular IC. NMDA receptors are indeed known to contribute to epileptogenesis and represent a target for antiepileptic drug therapy (Rogawski, 1998). In addition, the trigger for the NMDA receptor-mediated events identified in IC may result from mixed non-NMDA and $GABA_A$ receptor-mediated conductances. The latter view is further reinforced by the sensitivity of the stimulus-induced response to application of the barbituate PHB (Nicoll *et al.*, 1975; Barker & McBurney, 1979; Twyman *et al.*, 1989). The presence of inhibitory conductances during the activity recorded in IC slices is in line with evidence obtained from epileptic human brain tissue indicating that spontaneous inhibitory potentials can be sufficiently synchronous to support field potential discharges (Köhling *et al.*, 1998; Cohen *et al.*, 2002).

In conclusion, our data point at a powerful NMDA receptor-mediated mechanism implementing network hyperexcitability in rat agranular IC. These findings may be relevant for understanding the role of the IC in epileptic disorders (Ferland *et al.*, 1998; Isnard *et al.*, 2000, 2004; Kodama *et al.*, 2001; Bouilleret *et al.*, 2002) and in central pain (Frot & Mauguière, 2003; Jasmin *et al.*, 2003, 2004).

Acknowledgements

This study was supported by grants from the Canadian Institutes of Health Research (CIHR; grant 8109) and the Savoy Foundation.

Abbreviations

ACSF, artificial cerebrospinal fluid; CGP 55845, (3-aminopropyl)(diethoxymethyl)phosphinic acid; CNQX, 6-cyano-7-nitroquinoxaline-2,3-dione; CPP, 3,3-(2-carboxypiperazin-4-yl)-propyl-1-phosphonate; GABA, γ-aminobutyric acid; IC, insular cortex; NMDA, *N*-methyl-D-aspartate; PC, perirhinal cortex; PHB, phenobarbital; RMP, resting membrane potential.

References

Allen, G.V., Saper, C.B., Hurley, K.M. & Cechetto, D.F. (1991) Organization of visceral and limbic connections in the insular cortex of the rat. *J. Comp. Neurol.*, **311**, 1–16.

Augustine, J.R. (1996) Circuitry and functional aspects of the insular lobe in primates including humans. *Brain Res. Rev.*, **22**, 229–244.

Barker, J.L. & McBurney, R.N. (1979) Phenobarbitone modulation of postsynaptic GABA receptor function on cultured mammalian neurons. *Proc. R. Soc. Lond. B. Biol. Sci.*, **206**, 319–327.

Bouilleret, V., Dupont, S., Spelle, L., Baulac, M., Samson, Y. & Semah, F. (2002) Insular cortex involvement in mesiotemporal lobe epilepsy: a positron emission tomography study. *Ann. Neurol.*, **51**, 202–208.

Cohen, I., Navarro, V., Clemenceau, S., Baulac, M. & Miles, R. (2002) On the origin of interictal activity in human temporal lobe epilepsy in vitro. *Science*, **298**, 1418–1421.

Connors, B.W., Gutnick, M.J. & Prince, D.A. (1982) Electrophysiological properties of neocortical neurons in vitro. *J. Neurophysiol.*, **48**, 1302–1320.

D'Antuono, M., Biagini, G., Tancredi, V. & Avoli, M. (2001) Electrophysiology of regular firing cells in the rat perirhinal cortex. *Hippocampus*, **11**, 662–672.

Ferland, R.J., Nierenberg, J. & Applegate, C.D. (1998) A role for the bilateral involvement of perirhinal cortex in generalized kindled seizure expression. *Exp. Neurol.*, **151**, 124–137.

Frot, M. & Mauguiere, F. (2003) Dual representation of pain in the operculo-insular cortex in humans. *Brain*, **126**, 438–450.

Isnard, J., Guenot, M., Ostrowsky, K., Sindou, M. & Mauguiere, F. (2000) The role of the insular cortex in temporal lobe epilepsy. *Ann. Neurol.*, **48**, 614–623.

Isnard, J., Guenot, M., Sindou, M. & Mauguiere, F. (2004) Clinical manifestations of insular lobe seizures: a stereo-electroencephalographic study. *Epilepsia*, **45**, 1079–1090.

Jasmin, L., Burkey, A.R., Granato, A. & Ohara, P.T. (2004) Rostral agranular insular cortex and pain areas of the central nervous system: a tract-tracing study in the rat. *J. Comp. Neurol.*, **468**, 425–440.

Jasmin, L., Rabkin, S.D., Granato, A., Boudah, A. & Ohara, P.T. (2003) Analgesia and hyperalgesia from GABA-mediated modulation of the cerebral cortex. *Nature*, **424**, 316–320.

Jones, R.S. & Lambert, J.D. (1990) Synchronous discharges in the rat entorhinal cortex in vitro: site of initiation and the role of excitatory amino acid receptors. *Neuroscience*, **34**, 657–670.

Kano, T., Inaba, Y. & Avoli, M. (2005) Periodic oscillatory activity in parahippocampal slices maintained in vitro. *Neuroscience*, **130**, 1041–1053.

Kodama, M., Yamada, N., Sato, K., Sato, T., Morimoto, K. & Kuroda, S. (2001) The insular but not the perirhinal cortex is involved in the expression of fully-kindled amygdaloid seizures in rats. *Epilepsy Res.*, **46**, 169–178.

Köhling, R., Lucke, A., Straub, H., Speckmann, E.J., Tuxhorn, I., Wolf, P., Pannek, H. & Oppel, F. (1998) Spontaneous sharp waves in human neocortical slices excised from epileptic patients. *Brain*, **121**, 1073–1087.

Martina, M., Royer, S. & Pare, D. (2001) Propagation of neocortical inputs in the perirhinal cortex. *J. Neurosci.*, **21**, 2878–2888.

McCormick, D.A., Connors, B.W., Lighthall, J.W. & Prince, D.A. (1985) Comparative electrophysiology of pyramidal and sparsely spiny stellate neurons of the neocortex. *J. Neurophysiol.*, **54**, 782–806.

Nicoll, R.A., Eccles, J.C., Oshima, T. & Rubia, F. (1975) Prolongation of hippocampal inhibitory postsynaptic potentials by barbiturates. *Nature*, **258**, 625–627.

Paxinos, G. & Watson, C. (1998) *The Rat Brain in Stereotaxic Coordinates*, 4th Edn. Academic Press, San Diego, CA.

Rogawski, M.A. (1998) Mechanism-specific pathways for new antiepileptic drug discovery. *Adv. Neurol.*, **76**, 11–27.

Schwartzkroin, P.A. (1975) Characteristics of CA1 neurons recorded intracellularly in the hippocampal in vitro slice preparation. *Brain Res.*, **85**, 423–436.

Silfvenius, H., Gloor, P. & Rasmussen, T. (1964) Evaluation of insular ablation in surgical treatment of temporal lobe epilepsy. *Epilepsia*, **5**, 307–320.

Twyman, R.E., Rogers, C.J. & Macdonald, R.L. (1989) Differential regulation of gamma aminobutyric acid receptor channels by diazepam and phenobarbital. *Ann. Neurol.*, **25**, 213–220.

APPENDIX C: Animal Subject Use Approval